UNIVERSITY OF SOUTHAMPTON

FACULTY OF MEDICINE

Clinical and Experimental Sciences

The role of T cells in cutaneous squamous cell carcinoma

by

Chester Lai

Thesis for the degree of Doctor of Philosophy

October 2016

UNIVERSITY OF SOUTHAMPTON

ABSTRACT

FACULTY OF MEDICINE

Clinical and Experimental Sciences

Thesis for the degree of Doctor of Philosophy

THE ROLE OF T CELLS IN CUTANEOUS SQUAMOUS CELL CARCINOMA

Chester Lai

Cutaneous squamous cell carcinoma (cSCC) is the most common form of human cancer with metastatic potential. Despite T cells accumulating around cSCCs, these tumours continue to grow and persist. To investigate reasons for the failure of T cells to mount a protective response in cSCC, tumoral T cells were characterised to determine factors responsible for cSCC T cell dysfunction. This thesis focused primarily on regulatory T cells (Tregs, which are considered immunosuppressive) and $CD8^+$ T cells (thought to be responsible for destroying cancer cells) within the population of T cells surrounding cSCCs.

Human primary cSCCs contained increased $FOXP3^+$ Treg and $CD8^+$ T cell frequencies compared with corresponding peripheral blood and normal skin. Most tumoral T cells expressed the skin addressin CLA and E-selectin was detected in the majority of peritumoral blood vessels. Functional studies showed that tumoral Tregs suppressed tumoral effector $CD4^+$ and $CD8^+$T cell proliferation and effector T cell interferon-γ secretion *in vitro*. OX40 was expressed by higher proportions of tumoral Tregs than other T cells (including $CD4^+FOXP3^-$ and $CD8^+$ T cells) and increased $OX40^+$ lymphocyte frequencies were observed in primary cSCCs which metastasised compared with primary cSCCs which had not metastasised. Furthermore, *in vitro* OX40 activation of Treg/$CD4^+$ effector T cell co-cultures enhanced tumoral $CD4^+$ T cell proliferation, thus overcoming Treg suppression.

Functional data demonstrated that $CD8^+$ T cells from cSCC were less able to proliferate and produce granzyme B and perforin *in vitro* than $CD8^+$ T cells from peripheral blood. In addition, IL-2 was produced by fewer T cells in cSCC than in normal skin. The inhibitory receptor PD-1 was expressed by higher proportions of

T cells in cSCC than peripheral blood and PD-1 inhibition augmented *in vitro* tumoral $CD8^+$ T cell proliferation.

The results in this thesis highlight that dysfunctional T cell responses are present in cSCC, potentially contributing to ineffective anti-tumour immunity and permitting the development and growth of cSCC. Furthermore, the data in this thesis show that T cells from cSCC can be used for functional assessment of T cell costimulatory/inhibitory antibodies, suggesting this system might be useful as a preclinical tool for investigation of anti-tumour immunotherapies.

Table of contents

List of tables

List of figures

DECLARATION OF AUTHORSHIP

I, Chester Lai, declare that this thesis and the work presented in it are my own and have been generated by me as the result of my own original research.

The role of T cells in cutaneous squamous cell carcinoma

I confirm that:

1. This work was done wholly or mainly while in candidature for a research degree at this University;
2. Where any part of this thesis has previously been submitted for a degree or any other qualification at this University or any other institution, this has been clearly stated;
3. Where I have consulted the published work of others, this is always clearly attributed;
4. Where I have quoted from the work of others, the source is always given. With the exception of such quotations, this thesis is entirely my own work;
5. I have acknowledged all main sources of help;
6. Where the thesis is based on work done by myself jointly with others, I have made clear exactly what was done by others and what I have contributed myself;
7. Part of this work that I have conducted has been published in the following journal article:

   Lai C., August S., Albibas A., Behar R., Cho S-Y., Polak M.E., Theaker J., MacLeod A.S., French R.R., Glennie M.J., Al-Shamkhani A., Healy E. 2016. $OX40^+$ regulatory T cells in cutaneous squamous cell carcinoma suppress effector T-cell responses and associate with metastatic potential. *Clin Cancer Res,* 22, 4236-48.

Signed:.....

Date: 1st October 2016

Acknowledgements

I would like to thank my supervisor, Eugene Healy for his constant support during the project and over the course of my career in Dermatology. I will always be grateful for his helpful guidance on careers and life in general. I would also like to thank Aymen Al-Shamkhani, who has been an excellent co-supervisor and a great source of advice. It has been a pleasure and a great learning experience to work in the Dermatopharmacology Unit at the Faculty of Medicine, University of Southampton, and I am thankful to the Dermatopharmacology laboratory researchers who have contributed to this study, including Suzannah August, Amel Albibas, Ramnik Behar, Shinny Cho, Kim Lim, Conor Healy, Claire Reid, Andy Shapanis and Marta Polak. In addition, I would also like to thank Jeff Theaker for helping in the procurement of tissue samples and advice on skin histology, as well as Ruth French and Martin Glennie, who kindly provided functional antibodies used in this study. In addition, I would like to thank Richard Jewell and Carolann McGuire in Dermatopharmacology, University of Southampton; Ian Mockridge in Cancer Sciences, University of Southampton; Susan Wilson and Jon Ward from the Histochemistry Research Unit, University of Southampton; and Dave Johnston from the Biomedical Imaging Unit, University of Southampton for their technical support. I am also grateful to Trevor Bryant and Scott Harris, Medical Statistics, University of Southampton, for providing statistical advice. Furthermore, I would like to thank the staff in the Dermatology Department, University Hospital Southampton NHS Foundation Trust, including Margaret Wheeler, Linda Baker, Jason Brynes, Jane Jones, Petra McMillan, Pete Langham, Dot Handley, Angela Maunder, Adam Fityan, Birgit Pees, Helen Lotery, Andrew Sherley-Dale and Sarah Macfarlane, for assistance with procurement of samples, and I am grateful to all the patients who participated in this study. I would also like to acknowledge the Wellcome Trust for funding my Clinical Research Training Fellowship; I have learned so much over the course of this PhD and have thoroughly enjoyed it. Lastly, I wish to thank my wife, Whitney, and my parents, Chermy and Chris, for their unwavering support.

Abbreviations

A	adenine
α4-1BB	anti-41BB
αCTLA-4	anti-cytotoxic T lymphocyte antigen-4
AJCC	American Joint Committee on Cancer
AK	actinic keratosis
AMP	adenosine monophosphate
ANOVA	analysis of variance
αOX40	anti-OX40
αPD-1	anti-programmed cell death-1
APES	3-aminopropyltriethoxysilane
APC	allophycocyanin
Arg151Cys	arginine to cysteine at position 151
Arg160Trp	arginine to tryptophan at position 160
Asp294His	aspartate to histidine at position 294
ATP	adenosine triphosphate
BACH2	broad complex-tramtrack-bric a brac and cap'n'collar homology 1 bZip transcription factor 2
BATF	basic leucine zipper transcription factor, activating transcription factor-like
BCC	basal cell carcinoma
BCIP	5-bromo-4-chloro-3-indolyphosphate
BCL-2	B cell lymphoma-2
Blimp-1	B lymphocyte-induced maturation protein-1
BRAF	v-raf murine sarcoma viral oncogene homolog B

BSA	bovine serum albumin
BTLA	B and T lymphocyte attenuator
BV421	Brilliant Violet 421
C	cytosine
CAF	cancer associated fibroblast
cAMP	cyclic adenosine monophosphate
CARD11	caspase recruitment domain-containing protein 11 gene
CCL	chemokine (C-C motif) ligand
CCR	CC-chemokine receptor
CD	cluster of differentiation
CDKN2A	cyclin-dependent kinase inhibitor 2A gene
CDR3	complementarity determining region 3
CK	cytokeratin
CLA	cutaneous lymphocyte-associated antigen
CNS	conserved non-coding deoxyribonucleic acid sequence
CPD	cyclobutane pyrimidine dimer
cpm	counts per minute
cSCC	cutaneous squamous cell carcinoma
CSL	C protein binding factor 1, suppressor of hairless, longevity assurance gene-1
CTLA-4	cytotoxic T lymphocyte antigen -4
CXCR	CXC chemokine receptor
Cy	cyanine
CYLD	cylindromatosis gene
DAB	3,3′-diaminobenzidine

DAPI	4',6-diamidino-2-phenylindol dihydrochloride
DC	dendritic cell
DMBA	dimethyl-1,2-benzathracene
DMEM	Dulbecco's Modified Eagle's Medium
DNA	deoxyribonucleic acid
DNase	deoxyribonuclease
DSS1	deletion of suppressor of var-1 suppressor 1 gene
DPX	distyrene-plasticizer-xylene
EDTA	ethylenediaminetetraacetic acid
EGFR	epidermal growth factor receptor
ELISPOT	enzyme-linked immunosorbent spot
ERK	extracellular signal-regulated kinase
EXOC2	exocyst complex component 2 gene
FACS	fluorescence activated cell sorting
FAK	focal adhesion kinase
FasL	Fas ligand
FAT1	FAT atypical cadherin 1 gene
FBS	foetal bovine serum
Fc	fragment, crystallisable
FFPE	formalin fixed paraffin embedded
FITC	fluorescein isothiocyanate
FOS	Finkel-Biskis-Jinkins murine osteosarcoma viral oncogene homolog
FoxO1	forkhead box protein O1
FOXP3	forkhead box P3
FRMD4A	4.1 protein, ezrin, radizin, moesin domain containing 4A

FZD	WNT receptor frizzled homolog gene
Gadd45	growth arrest and deoxyribonucleic acid damage 45
GM-CSF	granulocyte macrophage colony-stimulating factor
H & E	haematoxylin and eosin
HH	hedgehog gene
HIV	human immunodeficiency virus
HMGB1	high-mobility group box 1 protein
HRAS	Harvey rat sarcoma gene
Hsp90	heat shock protein 90
HSV	herpes simplex virus
HPV	human papilloma virus
HVEM	herpes virus entry mediator
ICAM1	intercellular adhesion molecule 1
IDO	indoleamine 2,3 dioxygenase
IFN-γ	interferon-gamma
Ig	immunoglobulin
IL	interleukin
iNOS	inducible nitric oxide synthase
IQR	interquartile range
IRF	interferon regulatory factor
K14-HPV16	keratin 14 – human papilloma virus 16
KA	keratoacanthoma
KLRG1	killer cell lectin-like receptor G1
KNSTRN	kinetochore-localized astrin/sperm associated antigen 5 binding protein gene

Kras	Kirsten rat sarcoma gene
LAG-3	lymphocyte-activation gene 3
LAMP-1	lysosome-associated glycoprotein 1
LCK	lymphocyte-specific protein tyrosine kinase
LFA1	lymphocyte function-associated antigen 1
MAPK	mitogen-activated protein kinase
MC1R	melanocortin-1 receptor
MCA	methylcholanthrene
MDSC	myeloid derived suppressor cell
MEK	mitogen-activated and extracellular signal-regulated kinase kinase
MFI	mean fluorescence intensity
MHC	major histocompability complex
miR	microribonucleic acid
MMP	matrix metallopeptidase
mRNA	messenger ribonucleic acid
mTOR	mammalian target of rapamycin
MUC1	mucin 1
NBT	nitroblue tetrazolium
NFAT	nuclear factor of activated T cells
NF-κB	nuclear factor kappa-light-chain-enhancer of activated B cells
NHS	National Health Service
NK	natural killer
NKG2D	natural killer group 2, member D
NKT	natural killer T
NMSC	non-melanoma skin cancer

OCT	optimum cutting temperature
PBMC	peripheral blood mononuclear cell
PBS	phosphate buffered saline
PD-1	programmed cell death-1
PD-L1 / 2	programmed cell death ligand-1 / 2
PDCD1	programmed cell death-1 gene
PE	phycoerythrin
PerCP	peridinin chlorphyll protein
PHA	phytohaemagglutinin
PI3K	phosphoinositide-3-kinase
PKC	protein kinase C
PMA	phorbol 12-myristate 13-acetate
PTEN	phosphatase and tensin homolog gene
PTN	pleiotrophin gene
pTreg	peripherally induced Treg
PUVA	psoralen with ultraviolet A
Rag2	recombinant activating gene 2
RANKL	receptor activator of nuclear factor-κB ligand
RAS	rat sarcoma
RBM10	ribonucleic acid-binding protein 10 gene
RORγt	retinoic acid receptor-related orphan receptor-γt
RPMI	Roswell Park Memorial Institute
RRas2	related rat sarcoma 2 gene
S1P	sphingosine-1-phospate
S1PR	sphingosine-1-phosphate receptor

SHP2	Src homology 2 domain-containing tyrosine phosphatase 2
SLC45A2	solute carrier family 45, member 2
Src	sarcoma
STAT	signal transducer and activator of transcription
Stub1	stress induced phosphoprotein 1 homology and U-box containing protein 1
T	thymidine
T-bet	T-box expressed in T cells
TBS	Tris buffered saline
TCM	central memory T cell
TCR	T cell receptor
Teff	effector T cell
TEM	effector memory T cell
TFH	T follicular helper cell
TGF-β	transforming growth factor-beta
TGFBR1	transforming growth factor-beta receptor 1 gene
TH	T helper cell
TIGIT	T cell immunoglobulin and immunoreceptor tyrosine-based inhibitory motif domains
Tim-3	T cell immunoglobulin and mucin domains-3
TLR	toll-like receptor
TNF	tumour necrosis factor
TP53	tumour protein p53 gene
TPA	tetradecanoyl-phorbol acetate
Treg	regulatory T cell

TRM	resident memory T cell
tTreg	thymically derived Treg
Tweak	tumour necrosis factor-like weak inducer of apoptosis
UBAC2	ubiquitin-associated domain-containing protein 2 gene
Ubc13	ubiquitin-conjugating enzyme 13
UK	United Kingdom
USA	United States of America
UV	ultraviolet
UVB	ultraviolet B
UVR	ultraviolet radiation
VEGF	vascular endothelial growth factor
WNT	wingless-type mouse mammary tumour virus integration site
XP	xeroderma pigmentosum
ZMIZ1	zinc finger muscle segment homeobox 1-interacting zinc finger type containing 1 gene

Chapter 1: Introduction

1.1 Structure and function of skin

The structure of skin allows it to undertake numerous vital homeostatic functions despite being constantly subjected to stresses from the external environment. The skin is composed of the epidermis, which is situated on the surface and separated by a basement membrane from the dermis, which is situated deeper in the skin (Di Meglio et al., 2011). The epidermis consists of terminally differentiating keratinocytes which grow out from the basal layer before dying to form the stratum corneum on the epidermal surface. Other major cells in the epidermis include melanocytes, which produce melanin pigment, and Langerhans cells, which are antigen presenting cells. The dermis contains elastin and collagen fibres which form a mechanical barrier and structural framework for blood vessels and various cells, including fibroblasts and immune cells as well as those in blood vessels, hair follicles and sweat glands/ducts.

The skin forms a first line of defence to prevent injury, provide impermeability against toxins, resist penetration by microbes and protect against damage from ultraviolet radiation (UVR) (Vandergriff, 2012). The barrier function of skin also prevents loss of water and heat, thereby regulating body hydration and temperature. In addition, skin can sense the external environment, repair wounds, allow synthesis of vitamin D, and serve as an immunological organ to protect against infections whilst preventing allergy and autoimmunity (Vandergriff, 2012).

Failure of the skin to protect against the harmful effects of UVR, defective repair mechanisms and impaired skin immunity contribute to cancers forming and developing within skin. Skin cancer can be subtyped into non-melanoma skin cancer (NMSC), which is derived from keratinocytes, and melanoma, derived from melanocytes (National Cancer Institute, 2016). NMSC predominantly consists of cutaneous squamous cell carcinoma (cSCC) and basal cell carcinoma (BCC); rarer types of NMSC include Merkel cell carcinoma, cutaneous lymphomas and adnexal tumours (Madan et al., 2010).

1.2 Skin cancer epidemiology

Skin cancer is the most common type of malignancy worldwide and accounts for one in every three cancers diagnosed (World Health Organization, 2015). The estimated annual global incidences of the three most common types of skin cancer are approximately 10.5 million for BCC, 2.9 million for cSCC and 0.21 million for melanoma (Lucas et al., 2006). Skin cancer is especially prevalent in Australia where 80% of all newly diagnosed cancers are skin cancer and it is estimated that two in three Australians will have skin cancer by the age of 70 (Cancer Council Australia, 2015). The reported incidence of NMSC in the UK was 98,368 in 2012, making it the most frequent type of cancer, whereas melanoma is the fifth most common malignancy, with an annual incidence of 13,497 (Cancer Research UK, 2015). This NMSC incidence is likely to be an underestimate of the true incidence because many cancer registries record only the first NMSC and NMSCs treated by general practitioners in the community or private practitioners are not routinely recorded (Cancer Research UK, 2015). In addition, a study by Lavell and colleagues in 2013 suggested a more accurate UK incidence of approximately 250,000 for BCC, thus the annual numbers of NMSC are likely to be higher than this (Levell et al., 2013). The two most common types of NMSCs are BCCs, which comprise 74% of NMSCs, and cSCCs, accounting for 23% (Cancer Research UK, 2015). High NMSC incidence is also an issue of concern in the USA, with 3.5 million NMSCs diagnosed each year (American Cancer Society, 2015). Skin cancer incidence is continuing to rise (Madan et al., 2010, Lomas et al., 2012) and has been predicted to increase two to three-fold in the UK over the next 15-20 years (All Party Parliamentary Group on Skin, 2008). Indeed, cSCC incidence in the UK has more than doubled over the last decade (Goon et al., 2015). Potential reasons for the increasing incidence of skin cancer include better detection by patients and physicians, increasing exposure to UVR due to ozone depletion (Norval et al., 2011) and an ageing population (80% occurring in individuals aged over 60) (Diffey and Langtry, 2005).

NMSC is associated with a significant economic burden for healthcare services and is one of the most costly of all cancers to treat in the USA (Housman et al., 2003). The direct financial cost of NMSC to the USA in 2004 was $1.4 billion, excluding the indirect costs due to lost productivity which amounted to $961 million and the intangible costs estimated at $130 million due to impact on quality of life (Bickers et al., 2006). The total economic cost of NMSC to the NHS

in England was over £90 million in 2008 (Vallejo-Torres et al., 2014), and £346 million in Australia in 2010 (Fransen et al., 2012).

1.3 cSCC

cSCC most commonly presents as a hyperkeratotic enlarging plaque, nodule or ulcer in sun exposed areas of the body. cSCCs are characterised by spread of malignant keratinocytes arising from the epidermis into the dermis, either *de novo* or from transformation of precursor lesions such as actinic keratosis (AK) and Bowen's disease (Lansbury et al., 2013). cSCCs have the potential to metastasise to regional lymph nodes and distant organs; metastasis carries a poor prognosis and leads to significant mortality (Clayman et al., 2005).

1.4 cSCC precursor skin lesions

AKs are the most common keratinocyte-derived precancerous lesion in humans, and are found predominantly in fair-skinned individuals on sun-exposed surfaces (Ratushny et al., 2012). AKs are characterised by disorganised growth of dysplastic keratinocytes that contain atypical enlarged, irregular and hyperchromatic nuclei. Epidermal keratinocyte differentiation is disrupted, resulting in a thickened stratum corneum (hyperkeratosis) and retained nuclei (parakeratosis) (Ratushny et al., 2012). Complete disruption of keratinocyte differentiation with atypical keratinocytes throughout the full thickness of the epidermis is associated with cSCC *in situ*, also termed Bowen's disease, which manifests as slow growing reddish scaly/crusty patches on the skin. 60 to 82% of cSCCs arise from AKs (Criscione et al., 2009, Czarnecki et al., 2002, Mittelbronn et al., 1998, Marks et al., 1988). Progression rates of AK to cSCC range from 0 – 0.075% per lesion per year, whereas regression rates for AKs are 15 - 63% after 1 year (Werner et al., 2013). Bowen's disease is usually persistent and progressive. The risk of progression to cSCC is estimated to be 3%, and approximately one-third of cSCCs arising from Bowen's disease may metastasise (Bath-Hextall et al., 2013). Figure 1.1 (page 4) shows the clinical and histological appearances of the precancerous skin lesions.

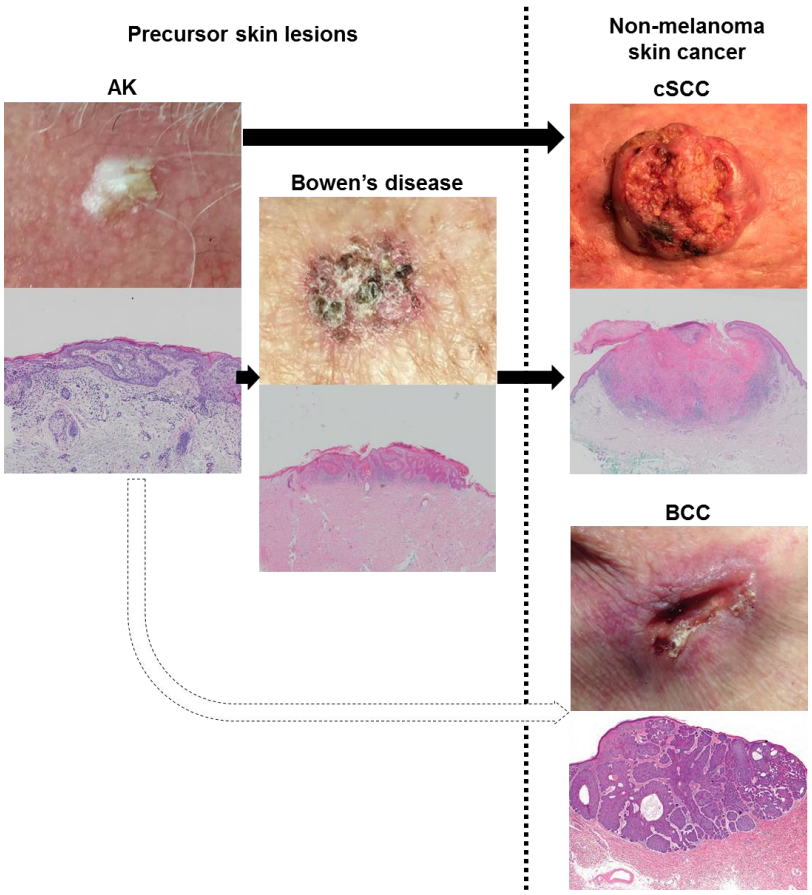

Figure 1.1 Non-melanoma skin cancers and precursor lesions.

Clinical appearance and histology of precursor skin lesions (AK and Bowen's disease) and NMSCs (cSCC and BCC). cSCCs often develop from AKs and Bowen's disease, whereas BCCs have less frequently been described as developing from AKs.

1.5 Role of UVR in cSCC

Solar UVR exposure has long been known to be associated with the development of skin cancer; in 1928, Findlay demonstrated that UVR-irradiated epilated albino mice developed skin 'papillomata' and 'epitheliomata', indicating that 'exposure to ultra-violet light plays an important part in the aetiology of cancer of the skin of the face, neck and hands' (Findlay, 1928). Increased rates of skin cancer were noted in individuals with prolonged exposure to sunlight (such as sailors, fishermen, farmers as opposed to town-dwellers) and highlighted a case series demonstrating higher skin cancer frequencies in those with fair skin or blond hair (Findlay, 1928). Further evidence for the crucial role of UVR exposure in cSCC development comes from these tumours developing predominantly on chronically sun exposed areas of skin, as well as epidemiological studies highlighting an

association between UVR levels (which increase with geographical proximity to the Earth's equator and at higher altitudes) and cSCC incidence (Schmitt et al., 2011, Xiang et al., 2014). Australia has the highest incidence of NMSC in the world (Lomas et al., 2012), and the BCC:cSCC ratio in Australia is 2.5:1 compared with 4:1 in the UK, which may reflect differences in the aetiology of BCC and cSCC, as cSCC is more associated with long-term chronic UVR exposure, whereas BCC is more linked to intermittent exposure (Rosso et al., 1996). The southwest of England has a sunnier climate than the rest of the country along with the highest rates of cSCC in the UK (Lomas et al., 2012), and the Channel Islands, situated farther south, has higher annual average sunshine hours and even greater age-standardised rates of NMSC than southwest England (Reilly et al., 2013). Lifestyle factors can also influence cSCC risk; occupational exposure to UVR is associated with a two-fold risk of cSCC (Schmitt et al., 2011). In addition, indoor tanning is attributed as a causal factor in 8.2% of cSCCs in the USA (Wehner et al., 2012). Therapeutic UVR also predisposes to cSCC development, for example, 7% of psoriasis patients exposed to fewer than 200 treatments with psoralen with ultraviolet A (PUVA) develop at least one cSCC after 25 years, whereas cSCCs develop in more than half of patients with ≥400 PUVA treatments (Nijsten and Stern, 2003). The use of photosensitising medications is also associated with enhanced cSCC risk (Robinson et al., 2013).

A randomised controlled trial investigating the effects of the daily use of sunscreen for 4.5 years showed no significant difference in the incidence of first new skin cancers, but sunscreen significantly reduced the incidence of subsequent cSCCs but not subsequent BCCs (Green et al., 1999). When the study participants were followed up for a further 8 years, sunscreen reduced cSCC rates by almost 40%, but there was still no effect on BCC (van der Pols et al., 2006). Furthermore, regular sunscreen use effectively reduces development of AKs (Thompson et al., 1993). Given the key role of UVR in skin cancer development, public health messages have recommended avoidance of excessive exposure to sunshine. However, potential beneficial health effects of UVR exposure include lowering of blood pressure through nitric oxide release from the skin (Liu et al., 2014), and cutaneous synthesis of vitamin D, which helps to maintain adequate vitamin D levels which are associated with superior health outcomes (Holick, 2008). Indeed, cSCC incidence tends to be lower in individuals with serum vitamin D concentrations above 75nmol/l (van der Pols et al., 2013), therefore, it remains unclear what the optimal levels of UVR exposure are for human health (Rice et al., 2015).

1.6 Risk factors for cSCC development

A number of phenotypic features have been found to lead to increased cSCC susceptibility. Skin sensitivity to sunlight, degree of freckling on the forearm, and increased number of AKs are strongly associated with increased risk of cSCC, whilst hair, eye and constitutive skin colour are weaker associations (English et al., 1998). A previous history of skin cancer is also a risk factor for subsequent primary cSCC development. The cumulative 3-year risk of a cSCC developing after an index cSCC ranges from 9-23% (Marcil and Stern, 2000), and a history of cSCC in the past 5 years increases the risk of further cSCCs by 5-fold (Xiong et al., 2013). Individuals with BCC have a 14% increased risk of developing a subsequent cSCC, whilst those with previous melanoma have a 150% increased risk of cSCC (Cantwell et al., 2009). A study on a cohort of veterans in the USA with a previous history of at least two NMSCs showed a 30% probability of developing a new cSCC within 5 years (Xiong et al., 2013). The most important risk factors for cSCC development were the number of cSCCs in the previous 5 years, number of AKs and total occupational time spent working outdoors (Xiong et al., 2013). A family history of cSCC also increases cSCC risk by two to three-fold (Hussain et al., 2009).

In addition to UVR exposure, other environmental factors influence susceptibility to cSCC. Immunosuppression strongly promotes cSCC development; cSCC is the most common cancer in organ transplant recipients who have up to a 200 times increased risk of cSCC (Euvrard et al., 2003) and cSCC affects up to 30% of kidney transplant recipients within 10 years of transplantation (Carroll et al., 2010). Immunosuppression promotes development of cSCC over BCC; in immunocompetent populations, BCC has a fourfold higher incidence than cSCC, whereas in organ transplant recipients,cSCC:BCC incidence ratios range from 0.7-3.6 (Mackintosh et al., 2013). Ionising radiation from radiotherapy has been associated with BCC but not cSCC development (Karagas et al., 1996), and exposure to cosmic radiation during flying may contribute to the higher NMSC risk in airline cockpit crew (Gundestrup and Storm, 1999). Smokers are also more likely to develop cSCC than non-smokers with a relative risk of 3.3 of developing cSCC after adjusting for age, sex and sun exposure (De Hertog et al., 2001). Other known predisposing factors for cSCC include arsenic exposure (Karagas et al., 2001) and chronic wounds - cSCCs arising in these are termed Marjolin's ulcers (Choa et al., 2015). Factors associated with reduced cSCC risk include the use of angiotensin converting enzyme inhibitors and angiotensin receptor

blockers (incidence rate ratio 0.67) (Christian et al., 2008), use of aspirin and non-steroidal anti-inflammatory drugs (relative risk 0.85 and 0.82 respectively) (Muranushi et al., 2015) and a history of warts on any part of the body (hazard risk ratio 0.7) (Xiong et al., 2013).

1.7 Clinical management of cSCC

A study based in the Australian city of Townsville showed that clinical examination alone for cSCC diagnosis by 202 GPs and 42 specialists (including one dermatologist) yielded a positive predictive value of 49.4% and sensitivity of 41.1% (Heal et al., 2008). Therefore, due to the inaccuracy of clinical examination, histological assessment is crucial for the accurate diagnosis of cSCC, as well as for staging and identification of "high risk" features (i.e. at high risk of metastasising). Histological analysis of the full excision biopsy is used for clinical staging as punch biopsies may not accurately identify high risk features and underestimate tumour stage (Westers-Attema et al., 2015). The mainstay of treatment for cSCC is surgical excision, which not only allows for histological examination of the excised specimen but also permits assessment of excision margins. Other treatments for cSCC include curettage and electrodessication, cryosurgery, radiotherapy and laser ablation/vaporisation (Madan et al., 2010). 95% of low risk cSCCs are adequately cleared with a predefined 4 mm surgical excision margin, (Madan et al., 2010). A systematic review reported incomplete excision rates of 8.8% following standard excision of cSCC, with those in the periorbital area having the highest rates (25%) (Lansbury et al., 2013). Although the majority of cSCCs can be treated adequately with standard surgical excision, there remains a high risk subset of cSCCs which carries a poor prognosis. For these high risk cSCCs, a 6 mm excision margin or Mohs micrographic surgery (histologically guided serial excision) is recommended, with adjuvant radiotherapy a commonly used option in narrowly excised tumours (O'Bryan et al., 2013). In general, evidence is lacking for optimal treatment of high risk cSCC, however, surgery combined with adjuvant cetuximab (a chimeric monoclonal antibody against the epidermal growth factor receptor, EGFR) may lead to improved outcomes in some patients with high risk cSCCs with perineural/lymphovascular invasion (O'Bryan et al., 2013).

1.8 Prognosis of cSCC

The primary goal of treatment of cSCC is prevention of recurrence and prevention of metastasis. Overall local recurrence rates following surgical excision of cSCC are 5.4%, and cSCCs in the ear region associated with the highest recurrence rates (14.1%) (Lansbury et al., 2013). Local recurrence rates for other modes of treatment are 3.0% after Mohs micrographic surgery, 6.4% after radiotherapy, 12.3% after photodynamic therapy, 0.8% after cryotherapy and 1.7% after electrodessication (Chren et al., 2013, Karia et al., 2014, Lansbury et al., 2013). Cryotherapy and electrodessication are associated with lowest recurrence rates presumably because they are only performed for low risk lesions (Lansbury et al., 2013).

Metastasis rates range widely and characteristics which determine 'high risk' cSCCs have not been consistently defined. Histological parameters may provide prognostic information, and the UK Royal College of Pathologists' minimum dataset for the histopathological reporting of cSCC includes the pathological pattern, morphological changes to cells, degree of differentiation, histological grade, depth, extent of dermal invasion and presence of perineural, vascular or lymphatic invasion (Madan et al., 2010). cSCCs are commonly stratified using the American Joint Committee on Cancer (AJCC) staging system to provide a guide for prognosis / treatment. In the AJCC staging system, prognosis is based on the following features: tumour diameter >2 cm, tumour depth >2 mm, Clarks' level ≥IV (signifying invasion into the deep dermis), location on the ear, lip and non-sun exposed sites, presence of perineural invasion and poorly differentiated histology (Lansbury et al., 2013). Stage T2 (>2 cm diameter or ≥2 other risk factors) confers a poor prognosis, and accounts for the majority of fatal cSCCs (Rose et al., 2013). Stages T3 and T4 are reserved for bone invasion which is rare.

A recent single centre study which included 1,818 primary cSCCs reported overall lymph node metastasis rates of 3.4% and disease specific death rates of 1.8% (Karia et al., 2014). In this study, cSCCs were staged according to the Brigham and Women's Hospital Tumour Staging System, based on the presence of the following risk factors - tumour diameter ≥2cm, poorly differentiated histology, depth of tumour invasion beyond fat and perineural invasion ≥0.1mm. Individuals with 0-1 risk factors (T1/2a) were associated with local recurrence rates of 1.4%, nodal metastasis rates of 0.6% and disease specific death rates of 0.2% whereas 2-4 risk factors (T2b/3) were associated with local recurrence rates of 24%, nodal

metastasis rates of 24% and disease specific death rates of 16%. Although this study is the largest study to date of cSCC outcomes, it was underpowered to evaluate the effect of immunosuppression.

In another cohort study of cSCC patients, 3% developed local recurrence and 4% developed metastases (Brantsch et al., 2008). Significant prognostic factors for metastasis were increased tumour thickness (e.g. metastasis occurred in 16% of cSCCs greater than 6mm in thickness), immunosuppression, localisation at the ear and increased horizontal size (Brantsch et al., 2008). Others have also reported on high risk parameters in cSCC, showing rates of metastasis of 30% - 42% for tumours greater than 2 cm in diameter, 25% for cSCCs of the lip and ear, and 28.6% for poorly differentiated tumours (Alam and Ratner, 2001, Rowe et al., 1992). Therefore, although most cSCCs are curable, there is a substantial subset of cSCCs that are associated with increased risk of metastasis and poor prognosis. Despite the risk of metastasis via lymphatic spread, there is still little evidence to justify routine sentinel lymph node biopsy in high risk cSCC (Madan et al., 2010). Given that early detection of metastases and subsequent appropriate treatment leads to high cure rates for cSCC (Karia et al., 2014), there remains a need to identify biomarkers that can accurately detect the high risk subset of cSCCs.

Another prognostic factor related to cSCC is the development of subsequent non-cutaneous malignancy and a study of 18,405 individuals, of whom 225 had a history of cSCC, demonstrated that cSCCs are associated with a multivariable-adjusted relative risk of 1.97 of subsequent cancer other than NMSC, and that the most frequently diagnosed cancers in these individuals were those that occur most commonly in the general population, such as lung, colorectal, breast and prostate cancer (Chen et al., 2008).

1.9 Pathogenesis of cSCC

A review by Hanahan and Weinberg (Hanahan and Weinberg, 2011) on the pathogenic hallmarks of cancer details the key biological capabilities that enable cancers to develop, see Figure 1.2. The processes which enable these hallmarks to develop in cSCC such as genetic mutations, signalling pathways and immune regulation will be described in this chapter.

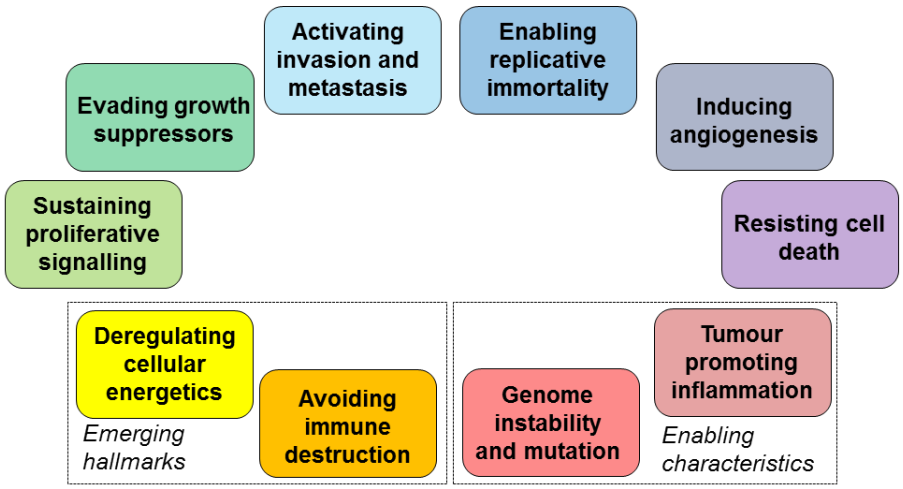

Figure 1.2 The hallmarks of cancer.

The hallmarks of cancer as detailed by Hanahan and Weinberg, 2011. The original six hallmarks were proposed in 2000 as distinctive and complementary capabilities that enable tumour growth and metastatic dissemination. More recently, there has been increasing evidence to suggest two additional emerging hallmarks ('deregulating cellular energetics' and 'avoiding immune destruction') are involved in the pathogenesis of cancer. Two further enabling characteristics ('genome instability and mutation' and 'tumour promoting inflammation') facilitate the acquisition of the core and emerging hallmarks.

1.9.1 Genetic susceptibility to cSCC

Skin pigmentation and tanning protect against the deleterious effects of UVR exposure and against the development of skin cancer, as can be seen by the lower incidence of skin cancer, including cSCC, in darker skinned populations (Kobayashi et al., 1998). One of the principal factors that influence the degree of skin pigmentation in Caucasians is the melanocortin-1 receptor (MC1R) and its ligand, alpha-melanocortin stimulating hormone, which govern the relative amounts of eumelanin and phaeomelanin in skin (Haddadeen et al., 2015). *MC1R* gene polymorphisms (e.g. Arg151Cys, Arg160Trp and Asp294His) are associated with higher phaeomelanin:eumelanin ratios, resulting in red hair, fair skin and reduced ability to tan (Valverde et al., 1995, Healy et al., 2000) as well as increased skin cancer susceptibility (Valverde et al., 1996, Kennedy et al., 2001, Bastiaens et al., 2001, Box et al., 2001, Chatzinasiou et al., 2011). In addition to reduced photoprotection due to lower levels of cutaneous eumelanin associated with variant *MC1R*, non-pigmentary mechanisms also play a role in skin cancer

susceptibility, such as inhibition of DNA repair and reduced apoptosis of UVR-damaged cells (Robinson et al., 2010, Bohm et al., 2005).

In addition to *MC1R*, other genes in which polymorphisms affect susceptibility to cSCC include *IRF4* (Han et al., 2011), *SLC45A2* (Stacey et al., 2009), *DSS1* (Venza et al., 2010b), *EXOC2* and *UBAC2* (Nan et al., 2011) and *IL10* (Welsh et al., 2011). Furthermore, certain genetic conditions have been noted to predispose to cSCC development, these include xeroderma pigmentosum (due to defective nucleotide excision repair), oculocutaneous albinism (characterised by lack of melanin and hence reduced photoprotection in skin) (Mabula et al., 2012), other hypopigmentary disorders including Hermansky-Pudlak syndrome (Toro et al., 1999), dystrophic and junctional epidermolysis bullosa (resulting in disordered type VII collagen and laminin 332 respectively, which are key structural proteins in skin) (Ortiz-Urda et al., 2005, Ng et al., 2012), epidermodysplasia verruciformis (leading to increased susceptibility to human papilloma virus) (Patel et al., 2008), dyskeratosis congenita (resulting in disordered telomere biology) (Alter et al., 2009), other syndromes characterised by genomic instability such as Rothmund-Thomson syndrome (Petkovic et al., 2005), Bloom syndrome (Ellis et al., 1995) and Werner syndrome (Crabbe et al., 2007). Another genetic syndrome, multiple self-healing squamous epitheliomata or Fergusson-Smith syndrome, caused by a mutation in *TGFBR1*, is characterised by the development of cSCC-like lesions which resolve spontaneously; some dermatologists consider the skin lesions in this condition to be similar to keratoacanthomas (Goudie et al., 2011).

1.9.2 **UVR-induced DNA damage**

UVR-induced DNA damage enables mutations in keratinocytes to occur and thus initiate skin cancer development. In the 1960s, it was discovered that UVR exposure leads to biological alteration of DNA (Setlow and Setlow, 1962) due to the formation of DNA photoproducts, which include cyclobutane pyrimidine dimers (CPDs, T=T and T=C) (Setlow and Setlow, 1962) and (6-4) photoproducts (Varghese and Wang, 1967), but that these DNA photoproducts could undergo repair under certain circumstances (Setlow and Carrier, 1964). In 1969, Setlow et al. (Setlow et al., 1969) highlighted the role for DNA photoproducts in causing skin cancer in xeroderma pigmentosum (XP), an autosomal recessive condition characterised by photosensitivity and 10,000-fold increased risk of NMSC (Bradford et al., 2011). XP skin is characterised by the inability to excise CPDs from DNA and failure to undertake/complete the nucleotide excision repair

process (Setlow et al., 1969). *In vivo* evidence that CPDs in DNA could give rise to tumours was first shown in 1977 (Hart et al., 1977). Since then, the nucleotide excision repair system has been characterised more comprehensively (Volker et al., 2001). More recently, XP group A protein and nucleotide excision repair rates have been demonstrated to exhibit a circadian rhythm, suggesting that UVR exposure in the evenings may have an increased carcinogenic effect in human skin (Gaddameedhi et al., 2011). Further evidence for the role of UVR-induced DNA damage in skin carcinogenesis comes from the presence of UV signature mutations in cSCCs; these mutations frequently occur following UVR exposure, are not attributable to other mutagens, and consist of cytosine to thymidine (C to T) and CC to TT transitions at sites of adjacent pyrimidines on the same DNA strand (Brash et al., 1991).

1.9.3 Genetic mutations in cancer

The accepted model of cancer development suggests that tumours evolve over time (e.g. 20-30 years) from benign to malignant lesions through a series of genetic mutations, termed 'driver' mutations which confer selective growth advantages to allow clonal expansion of mutated cells (Vogelstein et al., 2013). In this model, a typical tumour contains two to eight driver mutations as well as 'passenger' mutations which have no effect on the neoplastic process. A significant degree of genetic heterogeneity is present within the same tumour as well as between different tumours and different patients. Analysis of mutations in oncogenes and tumour suppressor genes from numerous cancers have demonstrated 138 driver genes which can be classified into pathways with belong to three core cellular processes: cell fate (e.g. *NOTCH*, *HH*), cell survival (e.g. *EGFR*, *TGFBR2*, *RAS*, *RAF*, *PTEN*, *CDKN2A*) and genome maintenance (e.g. *TP53*) (Vogelstein et al., 2013).

1.9.3.1 Gene mutations in normal skin

UVR is potently mutagenic and sun exposed normal skin can be considered as a polyclonal field of precancerous mutations (Martincorena et al., 2015). Driver mutations are frequent in normal skin, as up to 32% of keratinocytes from sun-exposed normal skin contain UV signature mutations in driver genes important in the pathogenesis of cSCC / AK / Bowen's disease (including in *TP53*, *NOTCH1/2/3, FAT1* and *RBM10*), with a high burden of somatic mutations (2-6 mutations per megabase per cell) (Martincorena et al., 2015). Apparently normal skin containing clones of keratinocytes with UV signature mutations in the *TP53*

gene, are termed p53 patches, which range from 60 – 3000 cells in size, and may involve as much as 4% of the epidermis (Jonason et al., 1996). The rate of progression of p53 patches to carcinoma is estimated at 1 in 8,300 - 40,000 per individual (Rebel et al., 2005).

1.9.3.2 cSCC gene mutations

1.9.3.2.1 TP53

Whole exome sequencing on human primary cSCCs has demonstrated that cSCCs are among the most highly mutated human malignancies with mutation rates up to 50 mutations per megabase pair (Durinck et al., 2011). C to T UV signature substitutions account for over 85% of mutations. It has recently been shown that the key genomic changes in cSCC development occur in the transition from normal skin to AK, and that AKs are also highly mutated with 18.5 mutations per megabase pair (Chitsazzadeh et al., 2016).

Mutations in the tumour suppressor gene *TP53* are present in 50-90% of cSCCs (Brash et al., 1991, Durinck et al., 2011, South et al., 2014), and loss of the second copy of *TP53* precedes a vast increase of mutations and chromosomal aberrations, therefore suggesting UVR-induced inactivation of *TP53* is an early event in cSCC development (Durinck et al., 2011). Sun-exposed skin and precursor skin lesions also contain mutations in *TP53* (Jonason et al., 1996, Ziegler et al., 1994, Martincorena et al., 2015) which likely lead to impaired genomic maintenance in affected skin cells (Brash et al., 1991, Jiang et al., 1999). Pharmacologically restoring the tumour suppressor function of mutant p53 can inhibit UVR-induced skin carcinogenesis in mice (Tang et al., 2007). In addition to mutations in *TP53*, reduced p53 activity in cSCCs can result from aberrant activation of Src family kinases (Zhao et al., 2009) and FOS (Guinea-Viniegra et al., 2012). In contrast to p53, the expression of p53-related transcription factor p63 is increased in cSCCs which inhibits apoptosis through its association with histone deacetylases 1/2 to repress *Bcl-2* (Ramsey et al., 2011) and activation of *p63*-regulated fibroblast growth factor receptor 2 signalling (Ramsey et al., 2013).

1.9.3.2.2 NOTCH

Loss of function mutations in *NOTCH-1/2* have been identified in up to 82% of human cSCCs, and NOTCH mutations have also been documented in AKs (Wang et al., 2011, South et al., 2014). NOTCH-1 is a tumour suppressor in skin, and can be induced by p53 in cSCC via tumour necrosis factor-α (TNF-α) converting

enzyme (Guinea-Viniegra et al., 2012). Aberrant NOTCH signalling leading to β-catenin activation is an early event in cSCC (Nicolas et al., 2003, Ratushny et al., 2012, South et al., 2014). Mice with deletion of CSL, a key Notch effector, develop cSCCs via upregulation of c-Jun and c-Fos (Hu et al., 2012). *NOTCH-1* transcription can be controlled by EGFR signalling which negatively regulates *NOTCH-1* in keratinocytes and cSCCs by suppressing p53 (Kolev et al., 2008).

1.9.3.2.3 RAS

Whole exome sequencing performed on murine cSCCs generated by topical application of dimethyl-1,2-benzathracene (DMBA), which induces DNA alterations, and tetradecanoyl-phorbol acetate (TPA), which stimulates inflammation and epidermal proliferation, has demonstrated that *Hras*, *Kras* and *Rras2* mutations are present in 90% of murine cSCCs (Nassar et al., 2015). However, only 11% of human cSCCs contain mutations in *RAS* (South et al., 2014). Oncogenic *RAS* combined with alterations in cellular pathways, e.g. NF-κ B blockade (Dajee et al., 2003) and *CDK4* (Lazarov et al., 2002, Ridky et al., 2010), leads to cSCC development in experimental models. In addition, melanoma patients treated with BRAF inhibitors (for mutations in BRAF, a molecule downstream of RAS) develop cSCCs containing *RAS* mutations, due to paradoxical activation of mitogen-activated protein kinase (MAPK) in BRAF wild type keratinocytes (Su et al., 2012). However, this mechanism does not explain why 40% of cSCCs in patients on BRAF inhibitors have wild type *RAS* (Su et al., 2012).

1.9.3.2.4 Other gene mutations

CDKN2A mutations have been detected in 28% of human cSCCs (South et al., 2014, Pacifico et al., 2008, Gray et al., 2006). In addition, 19% of cSCCs contain mutations in *KNSTRN* which disrupts chromatid cohesion, driving cells towards aneuploidy and in tumour development (Lee et al., 2014). Mutations in the *ZMIZ1* oncogene (Rogers et al., 2013), *CYLD* tumour suppressor gene (Alameda et al., 2010) and *CARD11* (Watt et al., 2015) which regulates NF-κ B signalling, may also induce cSCC development. In addition to somatic mutations, epigenetic changes (Venza et al., 2010a) and mitochondrial mutations (Prior et al., 2009) have been demonstrated in cSCC.

1.9.3.2.5 Gene mutations in aggressive / metastatic cSCCs

Whole exome sequencing of aggressive cSCCs (Pickering et al., 2014) and targeted sequencing of lymph node metastases from cSCCs (Li et al., 2015) have

confirmed mutations in various genes including *TP53*, *HRAS*, *NOTCH1/2* and *CDKN2A* as well as demonstrating alterations in numerous novel driver genes. In murine cSCC, lymph node and lung metastases involved very few additional mutations compared to the primary tumours, suggesting that epigenetic, transcriptional and environmental changes could be the major determinants of the metastatic process (Nassar et al., 2015).

1.9.4 **Molecular mechanisms involved in cSCC development**

The aberrant expression of genes resulting from UVR-induced mutations results in clonal expansion, defective apoptosis and increased replicative potential of tumour initiating cells. To demonstrate the cell of origin of cSCC, Lapouge et al. (Lapouge et al., 2011) showed that *p53* deletion in *KRas* mutant mice induced cSCC development from various epidermal cell lineages, including hair follicle bulge stem cells and their immediate progeny, as well as interfollicular keratinocytes (the BCC cell of origin (Youssef et al., 2010)). Stem cell quiescence acts as a tumour suppressor in cSCC: hair follicle stem cells are unable to initiate DMBA/TPA tumours during the quiescent phase of the hair cycle via phosphatase and tensin homolog (*Pten*) and remain despite activating *Ras* or loss of *p53* (White et al., 2014).

Haider et al. (Haider et al., 2006) showed a unique gene expression signature for human cSCC in comparison to psoriasis, another cutaneous disorder characterised by epidermal hyperproliferation, demonstrating potential roles of *WNT*, *FZD* (WNT receptor frizzled homolog) and *PTN* (pleiotrophin) in the pathogenesis of cSCC. Transcriptome profiling of AKs and cSCCs has identified certain differentially expressed genes, and highlighted a key role for the MAPK pathway in cSCC compared with AK (Lambert et al., 2014). The transcription factor interferon regulatory factor 6 (IRF6) is downregulated in cSCCs, leading to dysregulation of genes involved in differentiation and cell adhesion (Botti et al., 2011). Tumour initiating cells in cSCC (but not normal skin) express the transcription factor Sox2, which enhances neuropilin-1/ vascular endothelial growth factor (VEGF) signalling and promotes expansion of the tumour initiating cells along the tumour-stroma interface (Siegle et al., 2014). Heat shock protein 90 (Hsp90) stabilises and activates proteins essential for UVR-induced signal transduction pathways involved in cSCC development such as protein kinase C ε , and treatment of mice with a Hsp90 inhibitor reduces UVR-induced cSCC development (Singh et al., 2015). Gene expression profiling of the leading edge

of cSCC has shown increased matrix metallopeptidase 7 (MMP7) and IL-24 in areas of invasive cSCC, and IL-24 induces MMP7 expression in cSCC cells, which plays a crucial role in invasion (Mitsui et al., 2014). Altered microRNA expression has been demonstrated in cSCC and in response to UV irradiation (Dziunycz et al., 2010). Indeed, microRNA-9 (miR-9) increases invasiveness of cSCC cells and miR-9 has been detected in metastatic human primary cSCCs and cSCC metastases (White et al., 2013). Other recently reported mechanisms that promote cSCC growth and invasion include activation of focal adhesion kinase (FAK) and Src, leading to degradation of the cell adhesion molecule E-cadherin (Alt-Holland et al., 2011), loss of T-cadherin, which facilitates EGFR activation (Kyriakakis et al., 2012), upregulation of FRMD4A, an epidermal stem cell marker (Goldie et al., 2012), Axl, a receptor tyrosine kinase which regulates cell-cell adhesion and stemness in cSCC cells (Cichon et al., 2014), glyoxalase I (Zou et al., 2015), desmoglein 3 (Brown et al., 2014), the erythropoietin-producing hepatocellular receptor EphB2 (Farshchian et al., 2015) and the complement inhibitors Complement factor H and Complement factor I, which can be upregulated by interferon-γ (Riihila et al., 2015, Riihila et al., 2014). In addition, a role for the transcription factor c-Jun was recently highlighted in cSCC and that a DNAzyme engineered to destroy *c-jun* mRNA blocked murine cSCC growth by reducing growth factor expression, angiogenesis and metastasis while inducing T cell mediated anti-tumour immunity (Khachigian et al., 2012).

1.9.5 **Human papilloma virus**

Although a history of warts seems to reduce the risk of developing cSCC, certain genotypes of the human papilloma virus (HPV) are associated with increased cSCC risk (Bouwes Bavinck et al., 2010, Karagas et al., 2010), and HPV can induce cSCCs in mouse models (Holderfield et al., 2014). However, most normal human skin harbours HPV DNA from infancy and the relevance of HPV to cSCC pathogenesis in humans is unclear. Transcriptomic analysis of cSCCs has not detected HPV mRNA transcripts (Arron et al., 2011), and viral DNA is absent in the exome and whole genome sequence of cSCCs (Dimon et al., 2014). Therefore, it is possible that HPV has no role in cSCC or that HPV contributes to cSCC development via an unknown hit-and-run mechanism.

1.10 Skin immunology

cSCCs are characterised by a considerable mutational burden, and many driver mutations are present throughout the progression from sun-exposed skin to precancerous skin lesion to cSCC to invasion/metastasis. This suggests that mutant cells are tolerated in 'normal skin' and the mechanisms that determine whether these potentially dysplastic cells expand and invade to become cancerous may depend on non-genetic factors which include immunity. Indeed, a recent study which classified the genomic landscape in melanoma found that the only correlation with clinical outcome was associated with the lymphocytic infiltrate and that high expression of LCK, a T cell marker, was associated with improved patient survival (Cancer Genome Atlas Network, 2015). There is increasing knowledge that mutations in cancer lead to antigens recognised by the immune system (Schumacher and Schreiber, 2015) and that the high mutational loads in skin cancers frequently lead to the formation of neoepitopes that can activate host immune responses (Linnemann et al., 2015). In addition, recent developments in cancer immunotherapy have highlighted a role for immune checkpoint inhibitors that enhance anti-tumour immunity, and that these immunotherapies target T cells that are specific for tumour antigens (Gubin et al., 2014), with two separate studies showing that increased mutational burdens are associated with improved clinical responses to pembrolizumab, a programmed cell death-1 (PD-1) inhibitor (Rizvi et al., 2015, Le et al., 2015). Furthermore, given that immunosuppression substantially increases cSCC development (Euvrard et al., 2003), it is highly likely that aberrations in cutaneous immunity influence cSCC development and form potential therapeutic targets.

Skin forms a critical juncture with the external environment and is repeatedly exposed to pathogens, toxins, allergens and mutagens (including UVR). Immune cells in the skin (either resident or recruited) can respond to these insults to facilitate clearance of damaged cells and pathogens in order to maintain tissue homeostasis. Immune responses are generally categorised into 'innate' and 'adaptive' responses whereby innate immunity acts in a rapid and less specific manner to adaptive immunity, which is characterised by specificity and immunologic memory. The skin immune response can be initiated by the innate immune system, where dendritic cells (DCs), mast cells, macrophages and γδ T cells in the skin respond to damage-associated molecular patterns, Toll-like receptor (TLR) ligands, cytokines and chemokines released from 'damaged' epidermis. Keratinocytes also express TLRs and function as immune sensors

themselves. Activation of innate immune cells leads to secretion of chemical mediators which subsequently activate resident mesenchymal cells such as fibroblasts and endothelial cells, and promote recruitment of peripheral blood leucocytes to the tissue. Furthermore, antigen presenting cells, particularly DCs, activate the adaptive immune response via T and B cells, which mount antigen-specific responses (Nestle et al., 2009). It is becoming increasingly recognised that immunocytes that reside in the skin play a key role in cutaneous disease (Gaide et al., 2015, Ariotti et al., 2014, Mueller et al., 2013). Thus, the concept of skin as an immunological organ has been proposed, where memory T cells and antigen presenting cells reside and interact in sites in the skin termed 'skin associated lymphoid tissues' (Egawa and Kabashima, 2011). Figure 1.3 shows the common immune cells present in the skin.

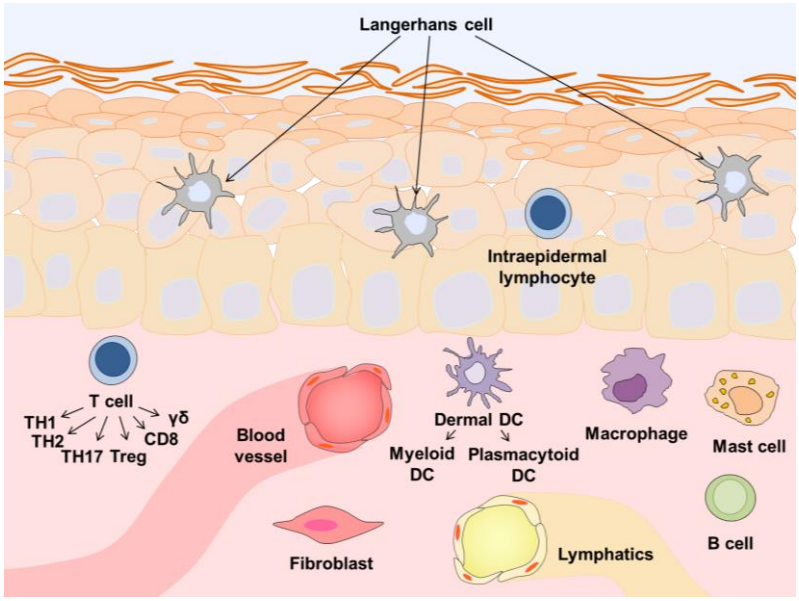

Figure 1.3 Skin immune cells.

Immunocytes in the epidermis mainly consist of Langerhans cells, which function as antigen presenting cells and intraepidermal lymphocytes. The dermis contains T cells, fibroblasts, dermal DCs, macrophages, mast cells and B cells, as well as a network of blood and lymphatic vessels. Figure adapted from Nestle et al. (2009).

1.10.1 Antigen presenting cells

DCs are professional antigen-presenting cells that mediate innate and adaptive immunity. In addition to being central orchestrators of cutaneous immune responses, DCs play a major role in the pathogenesis of many inflammatory skin

diseases. DCs are a heterogeneous cell population defined by their capacity for potent antigen presentation and naive T cell activation. There are three major subsets of cutaneous DCs in humans: Langerhans cells, myeloid DCs and plasmacytoid DCs (Zaba et al., 2009). Langerhans cells reside in the epidermis and use their dendrites which elongate to penetrate keratinocyte tight junctions to survey the environment, taking up antigens that have penetrated through the stratum corneum (Kubo et al., 2009). Myeloid and plasmacytoid DCs reside in the dermis and are collectively known as dermal DCs. Both Langerhans cells and dermal DCs are important for antigen presentation in the skin, where following encounter with antigen, they become activated and traffic via dermal lymphatics to the draining lymph nodes to present antigen via the major histocompatibility complex (MHC) to T cells (Heath and Carbone, 2013). However, recent work has also identified that rapid and efficient antigen presentation also occurs in the skin within dermal perivascular clusters of DCs and effector T cells in mice (Natsuaki et al., 2014), and that dermal $CD141^{high}$ DCs in humans constitute a distinct migratory cross-presenting DC subset (Haniffa et al., 2012) In addition to presenting the antigen, the nature of the interaction between the antigen presenting cell and T cell determines the characteristics of the subsequent effector immune response (Morris and Allen, 2012).

1.10.2 **T cells**

T cell precursors are produced in the bone marrow and migrate to the thymus, where they are subject to selection so that the T cells are able to recognise self MHC molecules and detect foreign antigen (Klein et al., 2014). In addition, T cells may differentiate into $CD4^+$ T cells, which function as helper T cells and $CD8^+$ T cells which are usually cytotoxic. The recognition of antigens occurs via the T cell receptor (TCR), a transmembrane molecule which forms a complex with the CD3 coreceptor and consists of heterodimers that are mostly $\alpha\beta$ or less frequently, $\gamma\delta$ (Dustin and Depoil, 2011). The $\alpha\beta$ TCR recognises a specific peptide which is presented bound to MHC by the antigen presenting cell, with $CD4^+$ T cells recognising peptides associated with MHC class II, and $CD8^+$ T cells with MHC class I. The specificity of each T cell clone is governed by how the TCR interacts with the MHC-peptide complex; the amino acid sequences in the variable regions of the α and β chains come into contact with the MHC helices in an orientation which allows the highly variable complementarity determining region 3 (CDR3) to interact with the presented peptide (Morris and Allen, 2012). In addition to peptide recognition by the TCR which complexes with the coreceptors CD4 or

CD8 to enable TCR signalling, a second costimulatory signal is required to enable activation, clonal expansion and differentiation into effector memory cells. An example of a T cell costimulatory receptor is CD28, which binds CD80 and CD86 on antigen presenting cells, whereas the inhibitory receptor cytotoxic T lymphocyte antigen-4 (CTLA-4) has affinity for the same ligands and negatively regulates T cell function (Chen and Flies, 2013, Pentcheva-Hoang et al., 2004). Other costimulatory receptors (and their ligands in italics) include CD27 (*CD70*), CD40 (*CD40L*), OX40 (*OX40L*) and 4-1BB (*4-1BBL*), see Figure 1.4. Examples of inhibitory receptors (and their ligands) include PD-1 (*PD-L1, PD-L2*), T cell immunoglobulin and mucin domains-3 (Tim-3) (*galectin-9, HMGB1*), B and T lymphocyte attenuator (BTLA) (*herpes virus entry mediator (HVEM)*), lymphocyte activation gene-3 (*LAG-3*) (MHCII) and T cell immunoglobulin and immunoreceptor tyrosine-based inhibitory motif domains (TIGIT) (*CD155, CD112*) (Chen and Flies, 2013), see Figure 1.4.

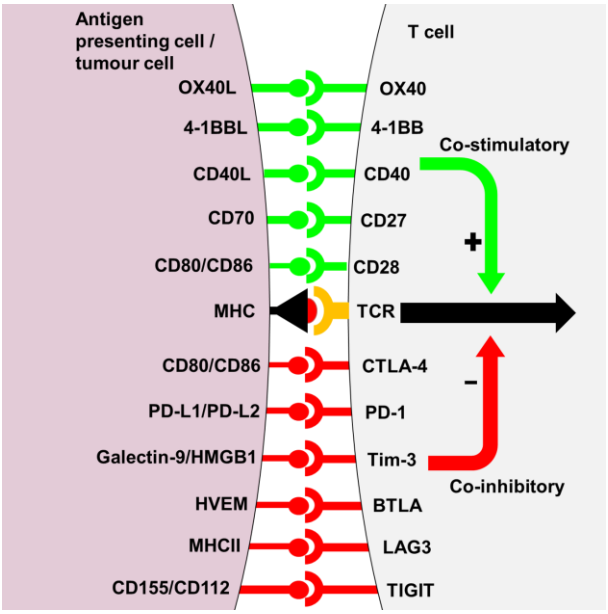

Figure 1.4 The immune synapse and costimulatory/inhibitory receptors.
Peptide antigens bound to MHC on antigen presenting cells or tumour cells are presented to the T cell receptor on T cells. A second signal provided by costimulatory or inhibitory receptors is required for a T cell response. Engagement of T cell costimulatory receptors with their respective ligands promotes T cell activation, leading to survival and proliferation of the T cell clone, whereas T cell inhibitory receptor binding leads to cell anergy and deletion.

Naive T cells recirculate to secondary lymphoid organs to maximise their opportunities for antigen detection before exiting via the lymphatics and thoracic duct back into the bloodstream. Naive T cell homing is mediated via L-selectin on T cells which interacts with ligands on endothelial cells in post-capillary venules to tether the T cells, allowing CC-chemokine ligand 21 (CCL21) to be recognised by CC-chemokine receptor 7 (CCR7), which activates lymphocyte function associated antigen 1 (LFA1) to bind to intercellular adhesion molecule 1 (ICAM1) that arrests the T cells to enable transmigration to the lymph nodes (Masopust and Schenkel, 2013). When a naive T cell encounters its cognate antigen, the T cell becomes activated and CD69 is upregulated which prevents cell surface expression of the sphingosine-1-phosphate receptor (S1PR), thereby stopping egress of the T cells from the lymph node (Shiow et al., 2006). Consequently, the presence of costimulation and cytokines in the lymph node promotes expansion of the T cell clone. Activated effector T cells disseminate to non-lymphoid tissues of the body to seek their cognate antigen and exert their functions. Downregulation of L-selectin and CCR7 with upregulation of homing molecules enables T cells to be targeted to specific tissues based on the site of priming. For example, T cells activated within the skin draining lymph nodes preferentially upregulate the E -selectin ligand cutaneous lymphocyte antigen (CLA) (Fuhlbrigge et al., 1997) as well as CCR4 (Campbell et al., 1999), CCR6 (Fitzhugh et al., 2000), CCR8 (Islam et al., 2011) and CCR10 (McCully et al., 2012). After antigen clearance, most effector T cells die, but a small proportion of surviving T cells differentiate into long lived memory T cells, which can be classified as central memory (TCM), which recirculate through secondary lymphoid organs where they proliferate upon TCR activation, producing effector T cells which migrate to the relevant tissues; and effector memory (TEM), which recirculate through non-lymphoid tissues and maintain effector functions that can be rapidly induced (Sallusto et al., 1999). Circulating T cells are characterised by expression of CCR7 which allows T cells to exit the skin and enter the afferent lymphatics (Debes et al., 2005). T cells which reside in non-lymphoid tissues following resolution of inflammation lack CCR7 and downregulate the sphingosine-1-phosphate receptor, thereby remaining *in situ* without recirculating to the blood, establishing a population of resident memory T cells (TRM) (Skon et al., 2013). Figure 1.5 (page 22) illustrates how naive T cells migrate and differentiate into memory T cells.

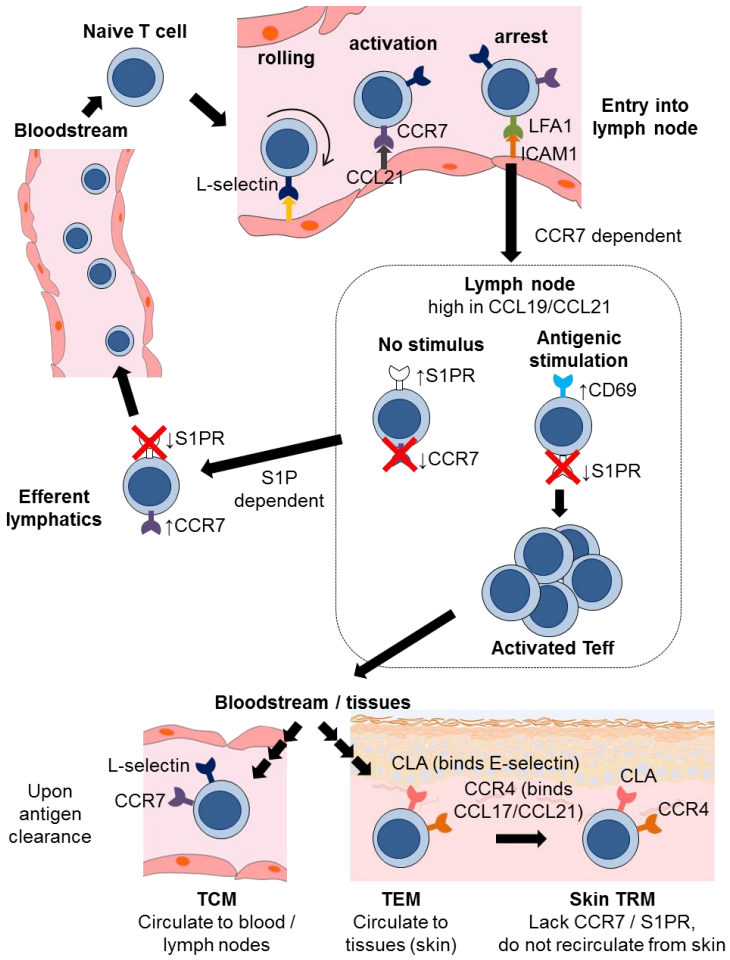

Figure 1.5 Migration and differentiation of T cells.

Naive T cells recirculate from the bloodstream to secondary lymphoid organs to maximise their opportunities for making contact with antigen. They enter lymph nodes from the bloodstream dependent on homing molecules that allow rolling, activation and arrest of the T cells. T cell migration to the lymph node occurs in a CCR7 dependent manner, as the CCR7 ligands CCL19 and CCL21 are highly expressed in the lymph node T cell zones. Naive T cells exit lymph nodes through downregulation of CCR7 and upregulation of sphingosine-1-phosphate receptor (S1PR), which enables homing to the efferent lymphatics and bloodstream. However, following antigenic stimulation and TCR activation, CD69 is upregulated which prevents S1PR expression at the cell surface, thereby causing the T cells to remain in the lymph node where the environment promotes proliferation of the activated effector T cells, which differentiate and migrate to the bloodstream and tissues based of their expression of homing molecules. Effector T cells exert their functions when they find their cognate antigen, and following antigen clearance, some memory T cells remain in the bloodstream / lymphatics (TCM) and in the tissues (TEM) where they provide a network for immunosurveillance. Skin resident TRM, which express the skin homing molecules CLA and CCR4, differentiate from TEM and lose the capability to recirculate into the bloodstream due to downregulation of CCR7 and S1PR. Figure adapted from Masopust

and Schenkel (2013).

1.10.2.1 Skin TRM cells

Over the last decade, the role of resident T cells in tissue immunosurveillance has become increasingly recognised. Approximately one million T cells are present per square centimetre of adult normal skin, and the total number of T cells in the whole of the skin is double of that in the entire blood volume (Clark et al., 2006a). TRM cells that remain in skin following herpes simplex virus (HSV) infection are autonomous from the circulating pool and these sessile T cells provide protection against HSV re-infection for over 100 days after the first infection (Zhu et al., 2013, Gebhardt et al., 2009). On resolution of inflammation, $CD8^+$ T cells are slow moving, resident in the epidermis and confined to the site of infection, whereas $CD4^+$ T cells can traffic rapidly through the dermis (Gebhardt et al., 2011). $CD8^+$ TRM in skin are potent effector memory cells and are superior to circulating TCM at providing rapid long term protection against cutaneous re-infection (Jiang et al., 2012). Following skin immunisation, TRM and TCM originate from a common naive T cell clone, and TRM, which are preferentially expanded following repetitive antigenic challenge, mediate rapid responses, whereas TCM elicit delayed and attenuated responses (Gaide et al., 2015). In addition, TRM cells can also augment innate rapid responses in the tissue (Schenkel et al., 2014).

1.10.2.2 $CD4^+$ helper T cells

Following TCR activation, naive T cells can differentiate into $CD4^+$ helper T (TH) cells depending on the strength of TCR stimulation and the cytokine environment which guide the development of functionally distinct TH cell subsets (Man and Kallies, 2015, Yamane and Paul, 2012). Activated cytokine receptors phosphorylate signal transducer and activator of transcription (STAT) transcription factors which reside in the cytoplasm and translocate to the nucleus to modulate gene expression and drive the expression of lineage specific factors. For example, TH1 cells require T-bet, TH2 require GATA3 and TH17 require the retinoic acid receptor-related orphan receptor-γ t (RORγ t). TH cells are essential for producing cytokines which can activate $CD8^+$ T cells as well as innate immune cells. T follicular helper (TFH) cells also provide help to B cells to undergo immunoglobulin class switching and to differentiate into plasma cells to produce

high-affinity antibodies. Another $CD4^+$ cell subset, the regulatory T cell (Treg) requires expression of forkhead box P3 (FOXP3) and regulates immune responses; Tregs will be discussed in greater detail later in this chapter.

TH cell subsets produce different cytokines, for example, the signature cytokine for TH1 cells is interferon-γ , whereas TH2 cells produce IL-4 and IL-13. The classical model of terminally differentiated TH cell lineages determined that memory T cells would not only remember the specific antigen but also mount a distinctive response. Selective cytokines produced by TH1 cells are thought to be important for elimination of intracellular microbes, whereas TH2 responses are activated in helminthic infection. Aberrant TH1 responses are implicated in autoimmune/delayed type hypersensitivity, while TH2 responses are associated with allergy. Figure 1.6 (page 25) summarises the main $CD4^+$ TH cell subsets.

The discovery of newer TH cell subtypes such as TH17 cells, a pro-inflammatory cell type characterised by production of IL-17, has furthered understanding about TH cell differentiation and led to the current view that TH cell phenotype / cytokine production can be plastic (O'Shea and Paul, 2010). For example, IL-10, initially thought to be a TH2 cytokine, is now recognised to be produced by all TH subsets (Zhou et al., 2009), interferon-γ can be produced by TH17 cells (Wilson et al., 2007), TGF-β can induce naive T cells in the periphery to become Tregs (Curotto de Lafaille and Lafaille, 2009) and that there is flexibility in the differentiation between Treg and TH17 cells (Zhou et al., 2008).

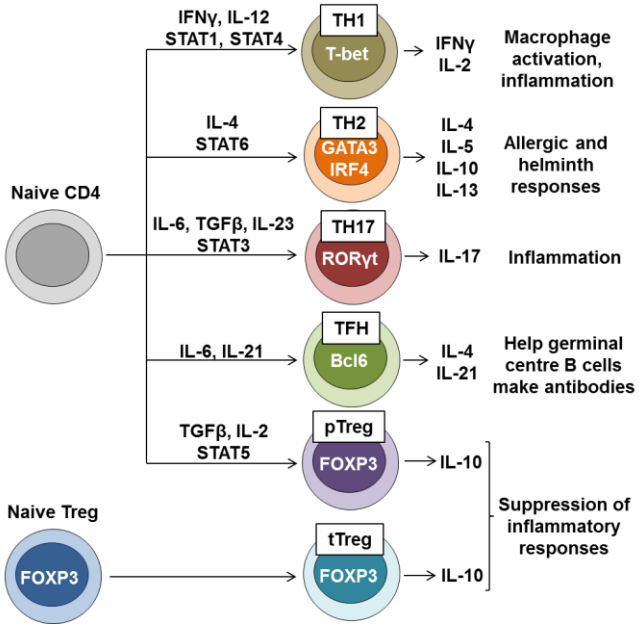

Figure 1.6 CD4⁺ T cell subsets.

Naive CD4⁺ T cells can differentiate into TH1, TH2, TH17, T follicular helper (TFH) and peripheral Treg (pTreg) cells. Thymic Tregs (tTregs) are derived from naive Treg precursors. Each of the CD4⁺ T cell subtypes is induced by different cytokines/STAT transcription factors which enable TH differentiation. Each subset is defined by a signature transcription factor and produces a distinct cytokine profile, which enables each subset to perform different immunological functions.

1.10.2.3 CD8⁺ cytotoxic T cells

CD8⁺ T cells are crucial for mediating pathogen clearance during viral and bacterial infections (Kaech and Cui, 2012). Full activation of CD8⁺ T cells requires the help of CD4⁺ T cells and the appropriate cytokine environment to mediate responses. Upon activation, CD8⁺ T cells can differentiate into effector cytotoxic T lymphocytes which kill infected cells by secreting perforin, which forms large transmembrane pores in the target cell, and granzymes which diffuse into the target cell cytosol and initiate apoptosis (Voskoboinik et al., 2015). Lysosome-associated glycoprotein-1 (LAMP-1) is required to safely transport toxic perforin to from the endoplasmic reticulum to lytic granules in cytotoxic cells (Krzewski et al., 2013), and expression of LAMP-1 on the cell surface might protect the cytotoxic cell from degranulation-associated damage (Cohnen et al., 2013). CD8⁺ T cells can also directly kill tumour cells, with intravital imaging showing that an individual CD8⁺ T cell takes 6 hours to kill a target cell (Breart et al., 2008). In

addition, $CD8^+$ effector T cells can secrete cytokines such as interferon-γ and TNF-α (Giordano et al., 2014).

A single naive $CD8^+$ T cell can give rise to both effector and memory T cell populations (Stemberger et al., 2007). In addition, $CD8^+$ T cells display functional heterogeneity in their ability to produce certain cytokines, perforin and various granzymes (Chang et al., 2014). Further diversity in $CD8^+$ T cell function is controlled by cytokine receptor signalling and transcription factors which guide $CD8^+$ effector and memory T cell development. Examples of transcription factors that influence T cell differentiation include T-bet, which is induced by inflammatory signals such as IL-12, and high levels of T-bet promote differentiation of $CD8^+$ effector T cells towards a terminally differentiated fate (Joshi et al., 2007), and eomesodermin, which fosters development of memory T cells (Intlekofer et al., 2005). Other markers of differentiation include IL-7 receptor subunit-α (IL-7Rα / CD127), which marks an intermediate stage of memory differentiation, killer cell lectin-like receptor G1 (KLRG1), which represents terminally differentiated effector T cells destined for apoptosis, and IL-2Rα (CD25), of which high expression levels during activation increase the likelihood of apoptosis (Chang et al., 2014). However, TRM cells show distinct transcriptional profiles as $CD8^+$ TRM cells in skin lack KLRG1 (Mackay et al., 2013), suggesting that TRMs may not be terminally differentiated T cells derived from TEMs.

1.10.2.4 Tregs

Tregs have a physiological role in maintaining immunological self-tolerance and homeostasis. In mouse models, depletion of $CD4^+CD25^+$ Tregs results in development of autoimmune disease which can be prevented by reconstitution of $CD4^+CD25^+$ Tregs (Sakaguchi et al., 1995). The suppressive function of Tregs is directed by the transcription factor FOXP3 (Liston and Gray, 2014), which is stably expressed under physiological and inflammatory conditions (Rubtsov et al., 2010). FOXP3 is essential for regulating immunity as mutations in the *FOXP3* gene cause fatal autoimmunity. However, activated conventional T cells also express FOXP3 transiently at low levels without being functionally immunosuppressive (Miyara et al., 2009). FOXP3 cooperates with other nuclear factors to establish the molecular signature and function of Tregs (Sakaguchi et al., 2013), and FOXP3 binds to pre-existing enhancers in a late cellular differentiation process (Samstein et al., 2012a). The binding of FOXP3 to the demethylated conserved non-coding DNA sequence 2 (CNS2) element at the

FOXP3 locus is required for Treg lineage stability (Zheng et al., 2010). In addition, the ubiquitin-conjugating enzyme Ubc13 maintains Treg function and stability (Chang et al., 2012).

Treg differentiation occurs at a late stage of thymocyte maturation, and $FOXP3^+$ Tregs are selected based on self-reactivity so that unlike conventional T cells, Tregs have a memory of self-antigen which is required for Treg maintenance in peripheral tissues (Hsieh et al., 2012). The transcription factor BACH2 is required for effective Treg formation and represses effector T cell differentiation (Roychoudhuri et al., 2013). TCR activation with appropriate costimulation leads to differentiation of 'central' Tregs which circulate through lymphoid tissues into 'effector' Tregs which can further be induced to migrate to sites of inflammation (Liston and Gray, 2014). This process can occur early in life, as a wave of highly activated Tregs influxes into the skin during a defined developmental window of neonatal life in response to commensal microbial colonisation of skin to mediate tolerance (Scharschmidt et al., 2015). During infection, antigen-specific memory Tregs are generated which become activated and differentiate into more potent suppressors. Upon reinfection, memory Tregs rapidly expand and control specific responses by $CD4^+$ and $CD8^+$ T cells in the tissue (Brincks et al., 2013). The localisation of Tregs to non-lymphoid organs occurs in a tissue specific manner (Sather et al., 2007). The skin appears to be an important site for immune regulation by Tregs, as up to 80% of peripheral blood Tregs express the skin homing markers (Hirahara et al., 2006). Skin Tregs, which comprise 5-10% of total skin T cells, express homing markers such as CLA, CCR4 and CCR6, as well as other phenotypic markers including the memory cell marker CD45RO and intracellular CTLA-4 (Clark and Kupper, 2007). These skin resident memory Tregs are maintained in the target tissue after inflammation and are primed to attenuate subsequent immune reactions when antigen is re-expressed, thereby conferring regulatory memory to the target tissue (Rosenblum et al., 2011). Cutaneous Tregs reside preferentially in the epidermis, where Langerhans cells induce Treg proliferation in resting state, but in the presence of pathogen, the same Langerhans cells promote expansion of effector memory T cells and limit Treg activation (Seneschal et al., 2012). Upon antigenic rechallenge, effector memory T cells and memory Tregs expand at the same rate, therefore suggesting that they arise from the same memory T cell pool (Vukmanovic-Stejic et al., 2008). Tregs are highly susceptible to apoptosis and have critically short telomeres and low telomerase activity, which is likely to be balanced by the high proliferative capacity of Tregs, which have a doubling time of 8 days compared

with conventional memory T cells (24 days) and naive T cells (199 days) (Vukmanovic-Stejic et al., 2006).

Homeostatic maintenance of the Treg population is controlled by production of IL-2 by activated conventional T cells which promotes survival and inhibits apoptosis of Tregs which express the IL-2 high affinity receptor subunit CD25, and quenching of IL-2 during conditions of Treg surplus leads to Treg apoptosis and contraction (Liston and Gray, 2014). In addition, the transient upregulation of CD25 by effector T cells during inflammation allows these activated T cells which consume IL-2 to expand and deprive Tregs of IL-2, which forces the Treg population to contract. Indeed, expression of high levels of CD25 cannot necessarily be used to identify Tregs from activated T cells, and low levels of the IL-7 receptor α chain (CD127) may distinguish Tregs within the $CD4^+CD25^+$ populations within peripheral blood and lymph nodes (Seddiki et al., 2006). However, skin resident memory Tregs in mice express high levels of CD25 and CD127, and that these Tregs may not require IL-2 but instead need IL-7 for their maintenance in skin (Gratz et al., 2013), allowing specialised resident memory Tregs to expand without affecting the central Treg pool, which would raise the overall burden of immunosuppression. In addition, other pathways of tissue-specific homeostatic Treg pathways have been described, for example, neuropilin-1 expressed by Tregs can bind to semaphorin 4A expressed by inflammatory tissues to upregulate the pro-survival protein BCL-2 thereby decreasing apoptosis of Tregs (Delgoffe et al., 2013).

The functional diversity of Tregs enables control of specific responses. For example, Tregs which express the TH1 transcription factor T-bet accumulate and suppress immune responses at sites of TH1 mediated inflammation (Koch et al., 2009). In addition, Tregs that express the transcription factor interferon regulatory factor 4 (IRF4), which is essential for TH2 effector cell differentiation, suppress TH2 responses (Zheng et al., 2009). Furthermore, Tregs can control TH17 responses in a STAT3 dependent manner (Chaudhry et al., 2009). This suggests that the shared use of the transcriptional and homing machinery of effector TH cells matches Tregs to the appropriate inflammatory milieu. Additionally, loss of the transcription factor Eos (Sharma et al., 2013) and upregulation of the ubiquitin ligase Stub1 (Chen et al., 2013) can convert Tregs into TH cells at sites of inflammation.

1.10.2.4.1 Peripherally-induced Tregs

Tregs can be classified into thymically-derived (t)Tregs, otherwise known as natural (n)Tregs, which develop in the thymus, and peripherally-induced (p)Tregs, also termed adaptive or induced (i)Tregs, which are converted from mature non-regulatory $CD4^+$ T cells in the secondary lymphoid organs or inflamed tissues in response to various stimuli (Bilate and Lafaille, 2012). TGF-β can induce naive $CD4^+CD25^-$ T cells into $CD4^+CD25^+FOXP3^+$ Tregs in experimental settings (Chen et al., 2003). In environments such as the intestinal tract which require tolerance to microbiota and in models of inflammation, Tregs can be induced through interactions with DCs (Belkaid and Oldenhove, 2008), for example, via TGF-β and retinoic acid (Coombes et al., 2007) or IL-18 (Oertli et al., 2012). Gene expression profiling has highlighted differences between tTregs and pTregs, showing that the genes for Helios, neuropilin-1 and granzyme B are upregulated by tTregs whereas *IL10* is differentially expressed by pTregs (Haribhai et al., 2011). Conserved non-coding sequence element 1 (CNS1), a *FOXP3* enhancer, is essential for pTregs, and is only present in placental mammals which probably evolved this mechanism to enforce maternal foetal tolerance (Samstein et al., 2012b). In addition, experimental models of inflammation have shown that tTregs play a crucial role in protecting from inflammatory disease (Haribhai et al., 2011). More recently, Josefowicz et al. (Josefowicz et al., 2012) demonstrated distinct homeostatic roles for tTregs and pTregs, with tTregs controlling systemic and tissue-specific immunity, whereas pTregs affect the composition of the commensal microbiota to restrain allergic inflammation at mucosal surfaces, although single cell sequencing has shown that tTregs and not pTregs dominantly mediate tolerance to intestinal commensals (Cebula et al., 2013).

No markers exclusively identify pTregs, although pTregs retain expression of genes more typical of conventional T cells than tTregs. The transcription factor Helios has been proposed as a marker of tTregs (Thornton et al., 2010), however, Helios can be upregulated on activated T cells and pTregs (Gottschalk et al., 2012). Furthermore, neuropilin-1 may distinguish tTregs from pTregs in mice but its usefulness as a marker in humans remains unclear (Bilate and Lafaille, 2012, Milpied et al., 2009). Other regulatory T cell populations have also been described, including T regulatory 1 cells and T helper 3 cells, which do not express FOXP3 and can be generated by and mediate their suppressive activity through IL-10 and TGF-β respectively.

1.10.2.4.2 Mechanisms of suppression by Tregs

Tregs can suppress the activation, proliferation and effector functions of a wide range of immune cells including $CD4^+$ and $CD8^+$ T cells, natural killer (NK) and natural killer T (NKT) cells, B cells and professional antigen presenting cells (Sakaguchi et al., 2010). Whilst Tregs optimally suppress in an antigen-specific manner, Tregs can also suppress T cells that recognise a different antigenic epitope (Sakaguchi et al., 2013). Numerous mechanisms for Treg-mediated immunosuppression have been described (see Figure 1.7, page 31), and different modes of suppression can be employed depending on the context of the response.

Tregs residing in normal human skin are immunosuppressive, and *in vitro* assays suggest suppression can be mediated via a cell-cell contact dependent mechanism (Clark and Kupper, 2007). Tregs can use perforin and granzyme-based cytotoxicity to directly kill activated $CD4^+$ T cells, $CD8^+$ T cells and monocytes (Grossman et al., 2004). In addition, Tregs can exert suppression by directly interacting with antigen presenting cells, forming stable and persistent associations which inhibit TH cell activation (Tang et al., 2006). This interaction can also lead to death of the DCs in a perforin-dependent manner (Boissonnas et al., 2010). CTLA-4 is constitutively expressed by Tregs (as well as activated effector T cells), and mediates suppression by downregulating CD80 / CD86 on antigen presenting cells, thereby providing co-inhibitory signalling with TCR engagement (Wing et al., 2008), as well as inducing expression of the immunosuppressive enzyme indoleamine 2,3 dioxygenase (IDO) (Fallarino et al., 2003). LAG-3 expressed by Tregs contributes to their suppressive function and may block DC maturation by binding MHC class II molecules (Huang et al., 2004). cAMP can transfer via gap junctions from Tregs to responder T cells which inhibits proliferation and IL-2 synthesis (Bopp et al., 2007). Furthermore, cell surface TGF-β has also been implicated in cell contact dependent immunosuppression by Tregs (Nakamura et al., 2001). Tregs can also cause metabolic disruption to effector T cells by consuming IL-2 through CD25 which is required for Treg survival, which 'starves' actively dividing effector T cells of IL-2 (Thornton and Shevach, 1998). Adenosine generation catalysed by the ectoenzymes CD39, also known as ectonucleoside triphosphate diphosphohydrolase-1, and CD73 expressed by Tregs can also mediate immune suppression (Deaglio et al., 2007).

Tregs can suppress immunity in non-contact dependent mechanisms by producing IL-10 (Belkaid et al., 2002, Rubtsov et al., 2008), TGF-β (Strauss et al., 2007) and IL-35 which is upregulated by Tregs and required for their suppressive function (Collison et al., 2007). In addition, binding of semaphorin-4a on effector cells/DCs to neuropilin-1 on Tregs mediates immunosuppression by inducing transcriptional changes that promote Treg stability by enhancing quiescence and survival factors and inhibiting programmes that promote differentiation (Delgoffe et al., 2013).

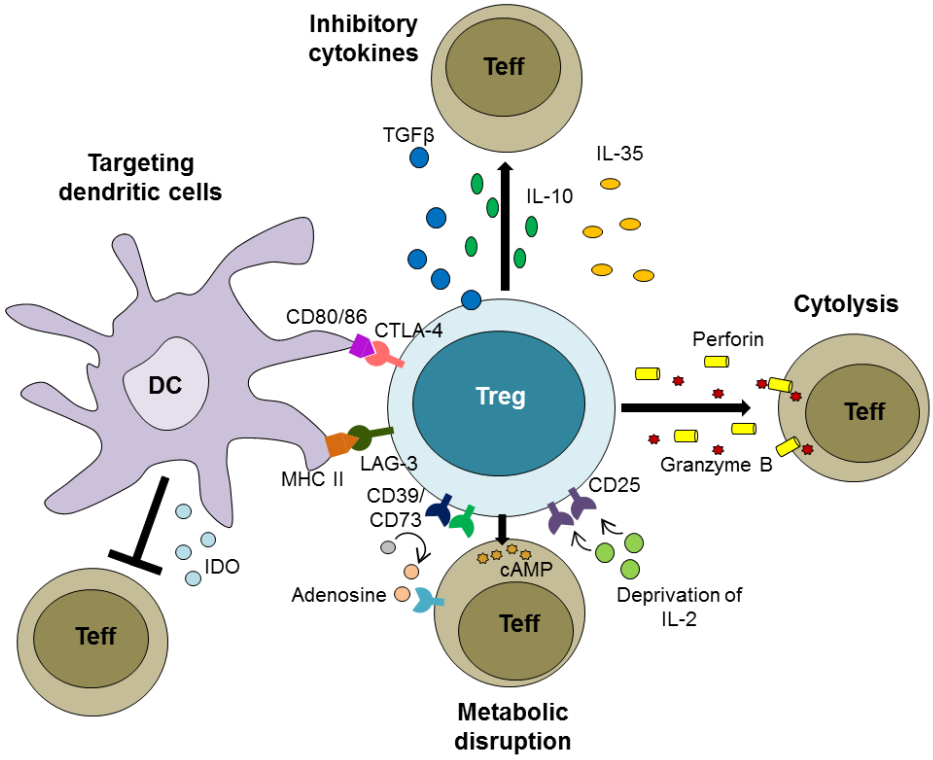

Figure 1.7 Mechanisms of suppression by Tregs.

Tregs can exert suppressive functions through four basic mechanisms, which include 'inhibitory cytokines', 'cytolysis', 'metabolic disruption' and 'targeting dendritic cells'. Inhibitory cytokines produced by Tregs include IL-10, TGF-β and IL-35. Tregs can kill effector cells via a perforin and granzyme B dependent mechanism. Tregs can cause metabolic disruption to effector T cells by CD25-dependent IL-2 deprivation, cAMP-mediated inhibition and generation of immunosuppressive adenosine by CD39/CD73. Treg mechanisms that modulate DC maturation and function include LAG-3 and CTLA-4, which can induce immunosuppressive IDO. Figure adapted from (Vignali et al., 2008).

1.10.3 **Changes in skin immunity during ageing**

Ageing is associated with defective cutaneous immunity resulting in increased susceptibility to cutaneous infections and malignancy. Decreased TNF-α synthesis during ageing results in defective activation of dermal blood vessels, thereby preventing memory T cell entry into the skin after antigen challenge (Agius et al., 2009). In addition, ageing is associated with increased CD45RA expression by $CD8^+$ effector memory T cells with lower antigen binding avidity (Griffiths et al., 2013). Memory Tregs continue to proliferate throughout life and increase with age in skin, as well as expression inhibitory receptor PD-1 on $CD4^+$ T cells (Booth et al., 2010, Vukmanovic-Stejic et al., 2015).

1.10.4 **Skin immune response to UVR**

UVR has long been understood to cause immunosuppression. In the late 1970s, it was noted that UV-irradiated mice are unable to reject tumours due to the presence of 'suppressor T lymphocytes' (Greene et al., 1979). Subsequently, it was found that mice irradiated with UVR, which depletes epidermal Langerhans cells, are unable to be sensitised to dinitrofluorobenzene (Toews et al., 1980). The effect of UVR in impairing contact hypersensitivity was demonstrated in patients receiving phototherapy for psoriasis, who exhibit reduced responses to dinitrochlorobenzene (Strauss et al., 1980). A decade later, it was found that UVR-induced CPDs initiate systemic immunosuppression in mice (Kripke et al., 1992). UVR-induced Tregs are known to inhibit the induction and effector phases of contact hypersensitivity (Shreedhar et al., 1998, Schwarz et al., 2004). The induction of Tregs by UVR is dependent on Langerhans cells which play an important role in downregulating immune responses in skin (Schwarz et al., 2010) and can be mediated via activation of the aryl hydrocarbon receptor (Navid et al., 2013).

Whilst much of the literature emphasises a significant role for Langerhans cells in mediating the immunosuppressive effects of UVR, some reports have suggested a role for dermal DCs. For example, in mice, dermal $langerin^+$ DCs but not epidermal Langerhans cells are essential for $CD8^+$ T cell responses following immunisation with ovalbumin or exposure to dinitrofluorobenzene, and that these responses can be suppressed following UV irradiation in the absence of epidermal Langerhans cells (Wang et al., 2009). Following UVR exposure to human skin, monocytes and DCs with T cell activating properties are recruited to the epidermis, compensating for the loss of Langerhans cells (Achachi et al.,

2015). UVR exposure also causes monocytes/macrophages to infiltrate into murine skin, where they can migrate to draining lymph nodes and produce IL-10 after exposure to dinitrofluorobenzene, therefore suggesting a role for macrophages as a suppressive mediator of UVR-induced tolerance in skin (Toichi et al., 2008).

Other mechanisms for UVR-induced immunosuppression include the *cis*-isomerisation of urocanic acid (McLoone et al., 2005), the production of cytokines such as IL-10 (Ullrich, 1994), IL-12 (Schmitt et al., 1995), IL-18 (Schwarz et al., 2006) and IL-33 (Byrne et al., 2011) by keratinocytes, suppressive IL-10 producing mast cells (Chacon-Salinas et al., 2011), and depletion of nicotinamide adenine dinucleotide (Yiasemides et al., 2009). In relation to the latter, oral nicotinamide reverses UVR-induced immunosuppression in humans (Yiasemides et al., 2009) and nicotinamide 500mg twice daily in patients with a history of multiple NMSCs in the past 5 years reduces rates of NMSCs by 23% and AKs by 13% after 12 months (Chen et al., 2015). In addition to causing immunosuppression, UVR might also have immunostimulatory effects in the skin; mouse skin exposed to UVR and treated with the TLR7/8 agonist imiquimod activates dermal DCs and boosts specific cytotoxic T lymphocyte responses leading to memory formation and enhanced tumour protection (Stein et al., 2011).

1.11 Immunology of cSCC

1.11.1 Chronic inflammation

Tumour-promoting chronic inflammation has been identified as an enabling characteristic in cancer (Hanahan and Weinberg, 2011). Chronic inflammation arising from the infiltration of tumours by innate and adaptive immune cells, which originally appear as an attempt by the immune system to eradicate the tumour, may contribute to paradoxically enhance tumour progression. For example, chronic inflammation can lead to production of growth factors that promote tumour development, survival factors that limit cell death, proangiogenic factors, and extracellular matrix modifying enzymes which facilitate angiogenesis, invasion and metastasis (Grivennikov et al., 2010). The role of chronic inflammation in allowing cSCC to develop is evident in Marjolin's ulcers, which can develop in response to chronic allergic contact dermatitis (Demehri et al., 2014, Choa et al., 2015).

1.11.2 **Cancer immunosurveillance and immunoediting**

The theory of cancer immunosurveillance and immunoediting (Schreiber et al., 2011), which integrates the immune system's dual host-protective and tumour-promoting roles, proposes three phases – elimination, equilibrium and escape (see Figure 1.8, page 35). In the 'elimination' phase, immune cells attempt to recognise and eliminate any early tumour cells. One of the emerging hallmarks of cancer described by Hanahan and Weinberg (Hanahan and Weinberg, 2011) is 'evading immune destruction', where cancers disable components of the anti-tumour immune response, leading to immune latency after incomplete elimination of the tumour which characterises the 'equilibrium' phase. It is during this period that chronic inflammation allows 'editing' of the tumour cells to produce new populations of tumour variants. The 'escape' phase refers to the final outgrowth of tumours that have outstripped the immunological restraints of the equilibrium phase. Thus according to this model of immunoediting, highly immunogenic cancer cell clones are eliminated in an immunocompetent host, therefore leaving only weakly immunogenic tumour cells which grow and develop. A study that supports the theory of immunoediting in cSCC shows that although most cSCCs express MHC class I, in contrast to BCCs where MHCI appears to be downregulated, cSCCs express comparatively low levels of cancer-testis antigens, suggesting that when cSCC develops from sub-clinically pre-existing areas of neoplasia, high immunologic pressure leads to immunoediting, resulting in the outgrowth of tumours that express fewer tumour antigens (Walter et al., 2010).

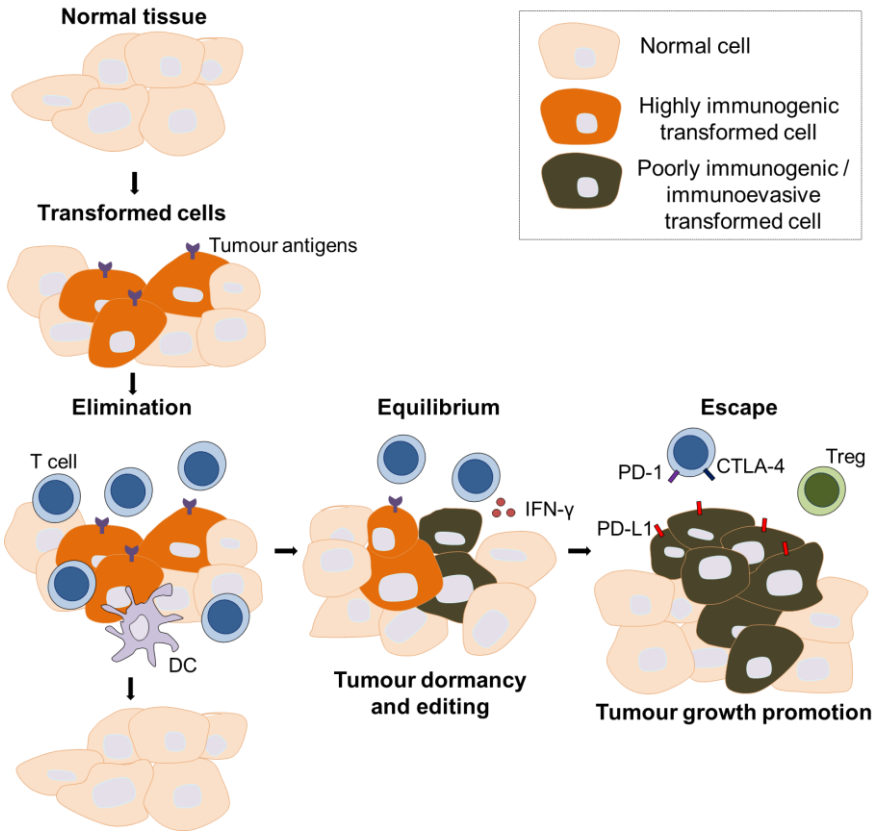

Figure 1.8 Cancer immunoediting.

Cancer immunoediting occurs after cellular transformation to suppress tumour growth, and consists of three sequential phases: elimination, equilibrium and escape. In the elimination phase, the immune system destroys developing tumours before they become clinically apparent. Cells not destroyed by the elimination phase may enter the equilibrium phase where T cells and interferon-γ maintain tumour dormancy and cancer immunoediting occurs due to the constant immune selection pressure placed on genetically unstable tumour cells. When tumour cell variants emerge that are no longer recognised by adaptive immunity (e.g. tumour antigen downregulation), become insensitive to immune effector mechanisms (e.g. express inhibitory ligands), and induce an immunosuppressive tumour microenvironment (e.g. induce Tregs), these cells enter the escape phase, in which their growth is not restrained by immunity, and cause clinically apparent disease. Figure adapted from (Schreiber et al., 2011).

1.11.3 Evidence for impaired immunity in cancer

The role of immunity in regulating tumour development has become increasingly evident. Since the late 1990s, mouse models of immunodeficiency have shown a crucial role of adaptive immunity in cancer development, and that interferon-γ receptor knockout and recombinant activating gene 2 (*Rag2*) knockout mice are

more susceptible to methylcholanthrene (MCA)-induced tumour formation, and when these tumours are transplanted into immunocompetent mice they are rejected by an intact host immune system (Shankaran et al., 2001). Subsequently, prognostic studies in many types of human cancers have determined that tumour-infiltrating T lymphocytes, particularly $CD8^+$ T cells and Tregs are critical determinants of prognosis (Sato et al., 2005, Pages et al., 2005, Galon et al., 2006, Fridman et al., 2012). Furthermore, it has long been observed that immunosuppression in organ transplant recipients to prevent rejection greatly promotes skin cancer, particularly cSCC, which occurs 65 to 250 times more frequently in organ transplant recipients than the general population (Euvrard et al., 2003). Pharmacological immunosuppression also increases incidence of BCC by 10-fold (Hartevelt et al., 1990) and melanoma by up to 8-fold (Vajdic et al., 2006, Le Mire et al., 2006). Admittedly, azathioprine may promote carcinogenesis by non-immune mediated mechanisms by causing UVR-induced mutations via incorporation of 6-thioguanine into DNA in *TP53* (O'Donovan et al., 2005). However, immunosuppression as a result of HIV increases cSCC risk, which correlates with lower $CD4^+$ T cell counts (Silverberg et al., 2013). A case report that highlights the role of the immune system in restricting cancer development showed that when two kidneys from a cadaveric organ donor with a history of successfully treated melanoma 16 years previously were transplanted into two separate immunosuppressed recipients, melanoma developed in the recipients, suggesting that in the immunocompetent donor, occult tumour cells were kept dormant by intact immunity, but transfer of these tumour cells to naive immunosuppressed recipients allowed the tumour cells to grow into clinically apparent cancers (MacKie et al., 2003). cSCC but not BCC patients have impaired contact hypersensitivity responses, suggesting impaired cutaneous immunity preferentially permits cSCC development (de Berker et al., 1995).

More recently, a study which used massively parallel exome sequencing and MHC class I affinity prediction algorithms on methylcholanthrene induced tumours in *Rag2-/-* immunodeficient mice which were then transplanted into wild type recipients has determined that a T cell-dependent immunoediting process occurs which allows tumour clones with reduced antigenicity to grow and evade detection by the immune system (Matsushita et al., 2012). In addition, tumours may adopt strategies to prevent T cell mediated anti-tumour immunity; for example, in melanoma, activation of the WNT/β-catenin signalling pathway is associated with absence of T cell infiltration (Spranger et al., 2015), and tumour cyclooxygenase production induces prostaglandin E2 to inhibit myeloid DC

function and suppress type I immunity (Zelenay et al., 2015). Furthermore, immunotherapy in melanoma, such as antibodies that block the T cell co-inhibitory receptors CTLA-4 (Hodi et al., 2010) and PD-1 (Topalian et al., 2012), and topical imiquimod in AK, Bowen's disease and superficial BCC (Kerr, 2002) demonstrate that enhancing immunity is an effective approach for the treatment of skin cancer.

1.11.4 T cell exhaustion in cancer

A key mechanism for T cell dysfunction in cancer is T cell exhaustion, a T cell differentiation state resulting from persistent antigen exposure and inflammation which was initially described in chronic infection (e.g. HIV and hepatitis C) (Wherry and Kurachi, 2015). Characteristic features of T cell exhaustion include progressive and hierarchical loss of effector functions (e.g. loss of IL-2 production, proliferative capacity and cytotoxicity followed by TNF-α and then interferon-γ), sustained upregulation of inhibitory receptors (e.g. PD-1, CTLA-4, Tim-3, BTLA, LAG-3, TIGIT, CD160 and CD244), and unlike functional memory T cells, poor responsiveness to IL-7 and IL-15 and the need for continual presence of antigen to proliferate and persist long term (Wherry and Kurachi, 2015). As a result of these changes, exhausted T cells are unable to effectively eliminate tumour cells, resulting in a stalemate between the immune system and tumour. The tumour microenvironment promotes T cell exhaustion due to a number of factors: tumour antigens are weakly immunogenic due to host immunoediting, tumour T cells have low TCR avidity for self-antigens because T cells with TCRs with high avidity for self-antigens are deleted during the thymic selection process, and insufficient priming of T cells results from impaired antigen presentation in the tumour microenvironment. In autoimmune and inflammatory disease, CD8 T cell exhaustion can reduce CD4 T cell costimulation, leading to poorer outcomes in autoimmune diseases such as type 1 diabetes, autoimmune vasculitis, systemic lupus erythematosus and idiopathic pulmonary fibrosis (McKinney et al., 2015). In psoriasis, PD-1 expressing IL-17A-producing T cells have been documented, although it is not known whether these represent exhausted T cells (Kim et al., 2016).

Inhibitory receptors can be transiently upregulated in functional activated effector T cells, however higher and sustained inhibitory receptor expression dependent on continued epitope recognition, and co-expression of multiple inhibitory receptors are characteristic of T cell exhaustion. The normal physiological

function of PD-1 is thought to be in limiting immunopathology and preventing autoimmunity (Keir et al., 2008). Expression of PD-1 alone is not a selective marker for exhausted T cells, as PD-1$^+$ T cells are found in healthy individuals which do not share the same transcriptional programme with exhausted T cells in viral infections (Duraiswamy et al., 2011). PD-1 expression is regulated by the transcription factors nuclear factor of activated T cells (NFAT) (Oestreich et al., 2008), T-bet (Kao et al., 2011), B lymphocyte-induced maturation protein-1 (Blimp-1) (Shin et al., 2009) and Forkhead box protein O1 (FoxO1) (Staron et al., 2014). Furthermore, epigenetic regulation of PD-1 expression is altered in exhausted T cells in which the locus of the PD-1 gene *PDCD1* remains unmethylated (Youngblood et al., 2011). Inhibitory receptors can regulate T cell function by competing with and sequestering costimulatory receptors and ligands (Pentcheva-Hoang et al., 2004), modulation of intracellular mediators such as Src homology 2 domain-containing tyrosine phosphatase 2 (SHP2) thereby attenuating TCR and costimulatory receptor signalling (Yokosuka et al., 2012), inhibition of cell cycle progression, suppressing signalling pathways such as phosphoinositide 3-kinase (PI3K)-AKT and Ras-mitogen-activated and extracellular signal-regulated kinase kinase (MEK)/extracellular signal-regulated kinase (ERK) (Patsoukis et al., 2012), inducing T cell motility paralysis (Zinselmeyer et al., 2013) and through the induction of inhibitory genes such as *BATF* (Quigley et al., 2010). More recently, the ectonucleotidase CD39 has been identified as a marker of exhausted T cells, implicating the purinergic pathway in the regulation of T cell exhaustion (Gupta et al., 2015). In addition, T cell function can be affected by the metabolic balance in the tumour microenvironment, as PD-L1 promotes AKT/mTOR activation and glycolysis in tumour cells leading to increased glucose consumption by tumours which metabolically restricts T cell function, thereby allowing tumour progression (Chang et al., 2015).

Baitsch et al. (Baitsch et al., 2011) used microarray gene expression profiling to demonstrate CD8$^+$ T cell exhaustion in human melanoma metastases. Other studies have also shown upregulation of inhibitory receptors in CD8$^+$ T cells and T cell dysfunction in cancer. PD-1 expression can be used to identify the tumour-reactive and mutation-specific CD8$^+$T cells infiltrating human tumours (Gros et al., 2014). Combined PD-1 and Tim-3 co-expression is associated with failure of T cells to proliferate and produce IL-2, TNF and interferon-γ in murine tumours (Sakuishi et al., 2010) and human melanoma (Fourcade et al., 2010). Dysfunctional CD8$^+$ T cells in melanoma can also express BTLA (Derre et al., 2010, Fourcade et al., 2012). Ovarian tumour specific CD8$^+$ T cells are negatively

regulated by LAG-3 and PD-1 (Matsuzaki et al., 2010). More recently, TIGIT has been detected in tumoral $CD8^+$ T cells in melanoma (Chauvin et al., 2015). In the above studies, combined inhibitory receptor blockade additively reversed exhausted T cells.

PD-L1 is abundant in human cancers and can be upregulated by interferon-γ (Dong et al., 2002) as well as loss of the tumour suppressor gene *PTEN* with activation of the PI3K pathway (Parsa et al., 2007). In addition to its effects in inhibiting $PD\text{-}1^+$ effector T cell function, PD-L1 also regulates the development, maintenance and function of pTregs (Francisco et al., 2009). PD-L1 expression is a prognostic factor in ovarian cancer (Hamanishi et al., 2007) and melanoma (Hino et al., 2010).

To date, the role of PD-1/PD-L1 in human cSCC remains undescribed. In murine skin, PD-L1 expressed by keratinocytes directly downregulates effector $CD8^+$ T cell function resulting in impaired contact hypersensitivity responses (Ritprajak et al., 2010). In Bowen's disease, PD-L1 has been shown to be expressed by neoplastic cells and infiltrating leucocytes (Furudate et al., 2014). In squamous cancer, PD-L1 promotes markers of epithelial-mesenchymal transition in chemical-induced murine cSCCs (Cao et al., 2011) and impairs T cell anti-tumour responses in human head and neck squamous cell carcinoma (Strome et al., 2003, Herbst et al., 2014).

1.11.5 **T cells in cSCC**

T cells in cSCC, which comprise up to 68% of the immune cell infiltrate (Krynitz et al., 2010), have been described as Th1 biased non-cutaneous central memory T cells which lack skin-homing receptors CLA and CCR4 and express L-selectin and CCR7 (Clark et al., 2008). Blood vessels in cSCCs seemingly lack E-selectin (a CLA ligand), suggesting that cSCCs are associated with impaired T cell recruitment. Increased expression of immunosuppressive cytokines such as TGF-β and IL-10 is also present in cSCC (Bluth et al., 2009, Clark et al., 2008), and expression of these cytokines is increased in moderately and poorly differentiated cSCCs compared with well differentiated cSCCs (Azzimonti et al., 2015). Treatment of cSCCs with imiquimod induces E-selectin on cSCC blood vessels, increases production of interferon-γ , granzyme and perforin by effector T cells whilst reducing production of and TGF-β and IL-10 (Clark et al., 2008, Huang et al., 2009).

cSCCs contain greater numbers of $CD3^+$ T cells and $CD8^+$ T cells compared to normal skin (Zhang et al., 2013). $CD8^+$ T cells have a protective role against cSCC, e.g. interferon-γ^+ $CD8^+$ T cells inhibit MCA-induced cSCC growth (Wakita et al., 2009). Indeed, patients with cSCC have elevated frequencies of p53-specific $CD8^+$ T cells in their peripheral blood, and the frequency of p53-specific $CD8^+$ T cells correlates with the degree of tumour lymphocytic infiltration (Black et al., 2005).

$CD4^+$ T cells also play a role in cSCC immunity. Depletion of $CD4^+$ T cells in a mouse model of UVB-induced cSCC increases UVB-induced inflammation, $p53^+$ keratinocytes and tumour development, suggesting that $CD4^+$ T cells play a role in tumour immunosurveillance and regulating UVR-induced cutaneous inflammation (Hatton et al., 2007). However, in a mouse model of cSCC induced by HPV oncogenes, tumour-infiltrating $CD4^+$ T cells are predominantly reactive towards staphylococcal bacterial antigens; these $CD4^+$ T cells promote tumour development and increase neutrophil infiltration and MMP-9 activity, suggesting that $CD4^+$ T cells apparently responding to bacterial infection of the cSCCs can enhance neoplastic progression (Daniel et al., 2003).

Human cSCCs contain IL-17 and IL-22-expressing T cells which may play pathogenic roles. IL-17 and IL-22 can increase proliferation and migration of cSCC cells and IL-22^+ $CD8^+$ T cells are increased in cSCCs from immunosuppressed patients (Nardinocchi et al., 2015, Zhang et al., 2013). In addition, the chemokine receptor CXCR3 on T cells induces keratinocyte proliferation in a DMBA/TPA mouse model of cSCC and $CXCR3^+$ lymphocytes have been identified in the immune infiltrate in human cSCC (Winkler et al., 2011).

1.11.6 **Role of Tregs in cancer**

The importance of Tregs in permitting tumour growth was highlighted by Shimizu et al. (Shimizu et al., 1999), who found that upon removal of Tregs, tumours in mice can be eliminated by cytotoxic T cells. Regulatory T cells (Tregs) play a role in the pathogenesis of numerous human cancers, and increased numbers of tumour-infiltrating Tregs are associated with poorer clinical outcomes in ovarian, gastric, oesophageal, breast and pancreatic cancers (Curiel et al., 2004, deLeeuw et al., 2012, Bates et al., 2006, Ichihara et al., 2003, Hiraoka et al., 2006), although increased Tregs in colon cancer is associated with better prognosis (Salama et al., 2009). Tumour-infiltrating Tregs may lead to tumour metastasis and poorer outcomes by producing receptor activator of nuclear factor-κ B ligand (RANKL) (Tan et al., 2011).

Cytokines produced within the tumour microenvironment can promote the accumulation of Tregs. For example, the chemokine ligand CCL22 is secreted by tumour cells and macrophages, which attracts Tregs that express the chemokine CCR4 (Curiel et al., 2004). In breast cancer, loss of type III TGF-β receptors in the tumour enhances TGF-β signalling in myeloid DCs, which upregulates CCL22 production, leading to Treg infiltration and suppression of anti-tumour immunity (Hanks et al., 2013). Anti-CCR4 monoclonal antibodies which selectively deplete Tregs augment anti-tumour immunity in melanoma and T cell leukaemia (Sugiyama et al., 2013). Tumour hypoxia can also induce CCL28 expression, which promotes recruitment of $CCR10^+$ Tregs which promote angiogenesis by enhancing tumour VEGF-A expression (Facciabene et al., 2011). In addition, eosinophils are associated with tumoral Treg depletion and secrete chemoattractants that guide $CD8^+$ T cell infiltration, promote an inflammatory macrophage phenotype and normalise tumour vasculature to promote tumour rejection (Carretero et al., 2015). Tumoral Treg accumulation is also caused by Fas ligand upregulation in tumour vessel endothelial cells which kills $CD8^+$ effector T cells but not Tregs (Motz et al., 2014).

Cancers induce Tregs to kill DCs in a tumour antigen and perforin-dependent manner in tumour-draining lymph nodes (Boissonnas et al., 2010). Exosomes produced by tumours skew IL-2 responsiveness away from cytotoxic T cells in favour of enhancing Treg function (Clayton et al., 2007). Furthermore, cancers in thymectomised mice convert naive $CD4^+CD25^-$ T cells into *bona fide* $FOXP3^+$ Tregs which suppress *in vitro* effector cell responses (Valzasina et al., 2006). Tumour-derived TGF-β increases pTregs and treatment of mice with a neutralising antibody against TGF-β reduces induction of Tregs and tumour burden (Liu et al., 2007). It is uncertain whether pTregs play a biologically significant role in tumour immunity given the presence of tTregs. In a mouse lymphoma model, both tTregs and *de novo* generation of pTregs independently contribute to anti-tumour immunity, with pTregs induced by the presence of tumour antigen (Zhou and Levitsky, 2007). However, another study which analysed TCR repertoires of infiltrating T cells in carcinogen-induced mouse tumours showed that conversion from conventional T cells does not contribute significantly to the accumulation of tumour-infiltrating Tregs, and that the Tregs and conventional T cells arise from different populations with unique TCR repertoires (Hindley et al., 2011). In addition to induction of pTregs by cytokines, tumours can convert naive $CD4^+$ T cells into pTregs through coinhibitory signalling via PD-L1 on DCs (Wang et al., 2008).

1.11.7 **Tregs in cSCC**

Nearly 50% of T cells infiltrating cSCCs are FOXP3$^+$ Treg cells (Clark et al., 2008), which is higher than frequencies of Tregs observed in colorectal cancer (Saito et al., 2016) and breast cancer (Plitas et al., 2016). Tregs are present in higher frequencies in cSCCs compared with normal skin and precursor skin lesions, and Ki-67, a marker expressed by dividing cells, is not detected in cSCC Tregs, suggesting that recruitment from the blood is the predominant mechanism for the accumulation of Tregs in cSCCs (Clark et al., 2008, Jang, 2008). FAK, which is expressed in the nucleus of cSCC cells but not normal keratinocytes, regulates the transcription of CCL5, which is required for recruitment of Tregs that inhibit CD8$^+$ T cell activity, thereby permitting tumour growth (Serrels et al., 2015). In addition, Tregs can suppress anti-tumour immunity via IL-10 during photocarcinogenesis (Loser et al., 2007). Other studies investigating Tregs in cSCC have found upregulation of *FOXP3*-mRNA in cSCCs compared with normal skin (Schipmann et al., 2014), and increased intratumoral Treg frequencies and a higher Treg/CD8$^+$ T cell ratio are present in moderately differentiated and poorly differentiated cSCCs compared to well differentiated cSCCs (Azzimonti et al., 2015).

1.11.8 **cSCC T cells in immunosuppressed individuals**

A recent study which used NanoString technology to analyse gene expression by T cells in human cSCCs also reinforced a role for Tregs in cSCC immunity, showing FOXP3 and other transcription factors for Tregs are highly expressed, especially in cSCCs from organ transplant recipients, as well as strong upregulation of gene expression signatures associated with T cell exhaustion (Feldmeyer et al., 2016). It remains unclear whether Treg frequencies differ in cSCCs of organ transplant recipients and those from immunocompetent subjects: two separate studies have shown transplant-associated cSCCs contain higher Treg to CD8$^+$ T cell ratios (Zhang et al., 2013, Carroll et al., 2010), whereas another study demonstrated increased FOXP3$^+$ Tregs in organ transplant recipient cSCCs (Muhleisen et al., 2009). Other differences in the composition of the cSCC immune infiltrate of transplant recipients also include reduced immunocyte infiltration and decreased frequencies of CD3$^+$ T cells, interferon-γ producing CD4$^+$ T cells, monocytes and plasmacytoid DCs compared with those in immunocompetent subjects (Krynitz et al., 2010, Muhleisen et al., 2009, Zhang et al., 2013).

1.11.9 T cells in progression from precancerous skin lesions

There also seem to be differences in the immune infiltrates between cSCCs and precancerous skin lesions. For example, cSCC tumours have increased depth and density of infiltrating immunocytes and contain higher $CD4^+$ T cell but lower $CD8^+$ T cell frequencies than premalignant lesions (Freeman et al., 2014, Muhleisen et al., 2009, Berhane et al., 2002). Unexpectedly, Tregs are reduced in invasive Bowen's disease compared with non-invasive Bowen's disease (Furudate et al., 2014). However, gene expression profile analysis of papillomas in a DMBA/TPA murine cSCC model showed reduced expression of immune function genes in cSCCs and high risk papillomas versus low risk papillomas, with immunohistochemistry confirming reduced T cell numbers in the high risk papillomas, suggesting that reduced adaptive immunity defines papillomas that progress to cSCC (Darwiche et al., 2007). The Fas/FasL pathway may play a role in the progression of AK to cSCC. cSCCs contain greater numbers of Fas ligand ($FasL^+$) T cells than AKs, whereas cSCC keratinocytes have reduced Fas but increased FasL expression compared with AK keratinocytes, suggesting that during progression from AK to cSCC, tumours downregulate Fas, thereby resisting attack by FasL-expressing cytotoxic T cells, and the upregulation FasL on the tumour cells enables the tumour to 'counterattack' the T cells by inducing Fas/FasL mediated apoptosis (Satchell et al., 2004).

1.11.10 T cells in keratoacanthomas

Keratoacanthomas (KAs) are cutaneous neoplasms that are closely related to cSCCs as they share clinical similarities, develop on sun exposed sites and display cytological atypia on histology. Although some regard KAs as a subset of cSCCs, unlike cSCCs, KAs are characterised by a tendency to spontaneously regress after 3-6 months, and array-based comparative genomic hybridisation studies suggest they represent biologically separate entities (Li et al., 2012). It has been hypothesised that an immune-mediated mechanism might be responsible for the ability of KAs to regress. KAs contain higher $CD3^+$ and granzyme B^+ T cell frequencies and fewer Tregs, $CD163^+$ macrophages and $MMP\text{-}9^+$ cells than cSCC, suggesting increased cytotoxic T cells and reduced immunomodulating cells in KA compared to cSCC (Kambayashi et al., 2013, Batinac et al., 2006). In addition, KAs are associated with increased numbers of cells which produce IL-27, which activates STAT1 and STAT3, leading to T cell proliferation, Th1 differentiation and induction of the anti-tumour response (Kambayashi et al., 2013). However, KAs

contain increased IL-10, an immunosuppressive cytokine, and decreased granulocyte macrophage colony-stimulating factor (GM-CSF) compared with cSCC, suggesting that an immunosuppressive microenvironment also permits KA development (Lowes et al., 1999).

1.11.11 Other immune cells in cSCC

1.11.11.1 B cells

B lymphocytes function as the central component of humoral immunity by producing antibodies, presenting antigen and secreting pro-inflammatory cytokines. In a K14-HPV16 cSCC mouse model, B cells promote a chronic inflammatory state by activating Fcγ receptors on myeloid cells which potentiate inflammation, angiogenesis and squamous carcinogenesis (Andreu et al., 2010, de Visser et al., 2005). In a separate murine cSCC model, depletion of B cells with anti-CD20 monoclonal antibodies improves responses to chemotherapy due to altered chemokine expression by macrophages that promote tumour infiltration of $CD8^+$ lymphocytes (Affara et al., 2014). There may also be a role for IL-10-secreting regulatory B cells in suppressing anti-tumour immunity in murine cSCCs (Schioppa et al., 2011). However, despite evidence from animal models regarding B cells in squamous carcinogenesis, and that $CD20^+$ B cells comprise 6.9 – 15% of the immune infiltrate in human cSCCs (Krynitz et al., 2010), little is known about their role in human cSCCs.

1.11.11.2 DCs

$CD1a^+$ and $Langerin^+$ Langerhans cells infiltrate human cSCC tumour nests at lower densities than their presence in normal epidermis (Bluth et al., 2009). Langerhans cells can present tumour antigens, leading to protective immunity to tumour growth in mice (Grabbe et al., 1991), and Langerhans cells in human cSCC can induce T cell proliferation, interferon-γ production and induce type 1 immunity more potently than Langerhans cells from normal skin, suggesting that cSCC Langerhans cells may form a suitable target for cancer immunotherapy (Fujita et al., 2012). However, a pro-tumorigenic role for Langerhans cells has also been reported in models of chemical carcinogenesis, for example, Langerhans cells facilitate epithelial DNA damage and cSCC development in a DMBA mouse model of cSCC (Modi et al., 2012).

$CD11c^+$ myeloid DCs and TNF-α / inducible nitric oxide synthase (iNOS) producing myeloid DCs are abundant around human cSCC tumours (Bluth et al., 2009). cSCC

myeloid DCs are poor stimulators of allogeneic T cell proliferation compared with DCs from adjacent non-lesional skin, and treatment with maturation cytokines enhanced stimulatory potential of DCs from normal skin but had less effect on DCs from cSCC. Plasmacytoid DCs have also been detected in cSCCs, with higher frequencies in cSCCs compared with AKs (Muhleisen et al., 2009), but reduced numbers in moderately to poorly differentiated tumours compared with well differentiated cSCCs (Azzimonti et al., 2015).

1.11.11.3 Macrophages

Tumour-associated macrophages (TAMs) in human cSCCs express CD163, produce the pro-tumoral factors MMP9 and MMP11, and are heterogeneously activated with classical M1 and alternative M2 phenotypes (Pettersen et al., 2011). M1 macrophages are induced by interferon-γ and have a high capacity to present antigen, reflecting a TH1-type immune environment, thereby preventing tumour progression, whereas M2 macrophages are induced by IL-4, which promotes type 2 responses which are less effective at controlling tumour growth.

1.11.11.4 Myeloid derived suppressor cells

Myeloid derived suppressor cells (MDSCs) are a heterogeneous group of myeloid progenitor cells and immature myeloid cells that inhibit T cell function (Nagaraj et al., 2010). Human cSCCs are infiltrated by MDSCs that express inducible iNOS and produce nitric oxide, which has a number of anti-inflammatory effects, including the impairment of vascular E-selectin expression which can be restored by iNOS inhibition (Gehad et al., 2012). As E-selectin is important for infiltration of skin-homing T cells into skin, and that E-selectin is downregulated in cSCC (Clark et al., 2008), MDSCs appear to play an important role in maintaining an immunosuppressive tumour environment in cSCC. Furthermore, CD200, an immunosuppressive molecule expressed by metastatic murine cSCC keratinocytes, can interact with and alter immune responses in MDSCs which express the CD200 receptor to promote tumour metastasis (Stumpfova et al., 2010).

1.11.11.5 Mast cells

Although mast cells have been reported in human cSCCs, their role remains undefined (Biswas et al., 2014). Treatment of mice with UVR-induced cSCCs with a C-X-C motif chemokine receptor 4 (CXCR4) antagonist inhibits cSCC development and blocks UVR-induced mast cell recruitment to the tumour (Sarchio et al.,

2014). To investigate whether dermal mast cells influenced susceptibility to cSCC, a study which quantified dermal mast cell prevalence in non-lesional non-sun exposed buttock skin showed no difference in mast cell numbers in patients with a history of cSCC and age matched control subjects (Grimbaldeston et al., 2002), however, a history of BCC was associated with increased dermal mast cell prevalence compared with controls (Grimbaldeston et al., 2000).

1.11.11.6 Fibroblasts

Changes in the tissue / stroma surrounding tumours may promote tumour development. Cancer associated fibroblasts (CAFs) are fibroblasts residing in tumour stroma with myofibroblastic properties and are considered responsible for extracellular matrix deposition and remodelling which support tumour progression and invasion (Dotto, 2014, Commandeur et al., 2011). CAFs isolated from human cSCCs have different morphology and functions to fibroblasts from normal skin, and culture of cSCC CAFs in a human skin equivalent model increases dermal invasion of cSCC cells (Commandeur et al., 2011). It is clinically evident that UVR causes dermal alterations which may promote cancer development: solar elastosis, a condition commonly observed in individuals with a history of chronic UVR exposure and is characterised by dermal atrophy and extracellular matrix alterations, predisposes to cutaneous field cancerisation and skin cancer. Actinic field cancerisation can be mediated through impaired NOTCH signalling in dermal fibroblasts. Reduced NOTCH signalling is seen in areas of actinic field change in human skin, and causes development of multifocal keratinocyte tumours in mice through upregulation of c-Jun and c-Fos, leading to increased diffusible growth factors, inflammatory cytokines and matrix remodelling enzymes which result in dermal atrophy and inflammation (Hu et al., 2012).

1.11.11.7 Lymphoid stress surveillance in cSCC

The natural killer group 2, member D (NKG2D) ligands are often expressed after exposure to cellular stress (e.g. in tumour cells or virus-infected cells), and binding to the NKG2D receptor stimulates the activation of natural killer cells and γ δ T cells (Jamieson et al., 2002). The process whereby lymphocytes instead of myeloid cells are activated by stress ligands has been termed ‘lymphoid stress surveillance’ which can occur rapidly in synchrony with innate responses and can affect downstream adaptive immunity (Hayday, 2009). Mice lacking γ δ cells are highly susceptible to chemical-induced cutaneous carcinogenesis, which

upregulates NKG2D ligands, and NKG2D^{+} γ δ cells can kill cSCC cells by a NKG2D-dependent mechanism (Girardi et al., 2001). In addition, NKG2D is downregulated in murine cSCC and correlates with cSCC incidence and progression, suggesting NKG2D as a marker of tumour resistance (Oppenheim et al., 2005). Strid et al. (Strid et al., 2008) showed that Intraepidermal γ δ T cells protect against DMBA/TPA-induced cSCC development, whereas Langerhans cells promote tumorigenesis, and that upregulation of NKG2D ligands alone is sufficient to initiate immune surveillance in skin, demonstrating a novel pathway in activation of cutaneous immune responses which was previously hypothesised to require lymphocyte stimulation via cell necrosis and/or activation of antigen-presenting cells e.g. via TLRs. In addition to reacting to stress ligands resulting from chemical carcinogens, dendritic epidermal γ δ T cells in mice and skin resident T cells in humans can sense UVR-induced injury by increasing CD69 expression, cell proliferation and IL-17 production via release of adenosine triphosphate (ATP) from keratinocytes, and can limit DNA damage in keratinocytes by inducing growth arrest and DNA damage 45 (Gadd45) and TNF-like weak inducer of apoptosis (Tweak), molecules involved in the DNA repair response (MacLeod et al., 2014). Activin, a growth and differentiation factor important in wound repair, is increased in human cSCCs (Antsiferova et al., 2011). Activin causes accumulation of Langerhans cells and Tregs whilst inhibiting proliferation of epidermal γ δ T cells thereby promoting cSCCs in mice (Antsiferova et al., 2011). However, despite evidence from mouse studies, the relevance of lymphoid stress surveillance in human cSCCs remains unclear, and although NK cells have been detected in human cSCCs, accounting for <2% of the immune infiltrate (Freeman et al., 2014, Carroll et al., 2010, Krynitz et al., 2010), γ δ T cells in human cSCCs have yet to be described in detail.

1.11.12 **Lymphatics**

The growth of lymphatic vessels, lymphangiogenesis, is activated in cancer and inflammation, and tumour cells may invade into the lymphatics and subsequently metastasise (Alitalo et al., 2013). VEGF-C and VEGF-D are critical for mediating lymphangiogenesis in DMBA/TPA murine models of cSCC (Hirakawa et al., 2007, Alitalo et al., 2013). Human cSCCs are surrounded by increased lymphatic densities and tumour-associated macrophage-derived VEGF-C (Moussai et al., 2011).

1.12 T cell immunotherapy

An early description on the treatment of cancer by manipulating the immune system is detailed in Coley's work entitled 'Contribution to the Knowledge of Sarcoma' (Coley, 1891). In this paper, Coley noted that patients with sarcoma and other cancers had tumour regression following 'erysipelas', a streptococcal infection of the skin, leading him to treat cases of sarcoma by repeated inoculations with this bacteria, either into the skin or intratumorally. Although no mechanism is uncovered in this work, the author noted that after inoculation, patients developed a high temperature which was proposed as a factor to 'destroy cells of lower vitality'. In 1985, administration of IL-2 was shown to lead to tumour regression in patients with metastatic melanoma (Atkins et al., 1999). In the late 1980s, adoptive cell therapy using tumour-infiltrating lymphocytes was demonstrated to mediate tumour rejection (Rosenberg et al., 1986). Subsequent identification of tumour antigens, followed by increased understanding of mechanisms for dysfunctional T cell immunity has led to the development of various immunotherapeutic approaches for cancer, which have primarily focused on amplification of tumour-specific immune responses by T cell costimulatory receptor agonism and inhibitory receptor antagonism based on the capacity of T cells for selective recognition of peptides in all cellular compartments, killing target cells and orchestrating adaptive and innate immune responses.

1.12.1.1 Costimulatory receptors

As a result of the increasing evidence for the role of Tregs and dysfunctional $CD8^+$ T cells in cancer, there has been considerable interest in developing immunotherapeutic strategies that target tumoral Tregs and boost effector immune responses (Simpson et al., 2013, Taraban et al., 2002, Piconese et al., 2008, Marabelle et al., 2013, Bulliard et al., 2014). One such approach involves the provision of costimulatory signals through receptors that belong to the tumour necrosis receptor superfamily, including OX40 and 4-1BB. Engagement of these receptors promotes T cell activation through effects on different subpopulations of T cells, for example by promoting proliferation and survival of effector memory T cells following antigenic activation, as well as by suppressing regulatory T cell activity (Piconese et al., 2008, Marabelle et al., 2013, Bulliard et al., 2014, Voo et al., 2013).

In vitro studies of human peripheral blood T cells have demonstrated that anti-OX40 monoclonal antibodies can be agonistic which can enhance the resistance

of effector T cells to suppression and reduce the suppressive activity of Tregs (Voo et al., 2013). In addition, anti-OX40 monoclonal antibodies can stimulate anti-tumour immunity by preferential depletion of Tregs, as shown in pre-clinical studies (Marabelle et al., 2013, Bulliard et al., 2014). Furthermore, a phase I clinical trial using an anti-OX40 agonistic monoclonal antibody has demonstrated an acceptable safety/toxicity profile and some evidence of tumour regression in cases of melanoma, renal cancer, urethral squamous cell carcinoma, prostate cancer and cholangiocarcinoma (Curti et al., 2013), highlighting OX40 as a promising target for tumour therapy.

4-1BB may be upregulated on activated T cells in tumours due to hypoxia (Palazon et al., 2012) and 4-1BB expression in tumoral T cells may accurately identify the tumour reactive T cell population (Ye et al., 2014). 4-1BB signalling induces a cytotoxic T cell phenotype (driven by high eomesodermin expression (Curran et al., 2013)), generates memory T cells (Willoughby et al., 2014), and increases effector function, leading to tumour regression in mouse models as monotherapy (Melero et al., 1997), or combined with other treatments such as cetuximab (Kohrt et al., 2014), peptide vaccines (Bartkowiak et al., 2015, Williams et al., 2013), anti-PD-1 (Duraiswamy et al., 2013), anti-CTLA-4 (Curran et al., 2011) and adoptive T cell therapy in human melanoma (Chacon et al., 2013). The role of 4-1BB stimulation on Tregs is still unclear; 4-1BB agonism can inhibit Treg mediated suppression (Choi et al., 2004, Akhmetzyanova et al., 2016) or maintain Treg expansion in different settings (Madireddi et al., 2014, Elpek et al., 2007).

1.12.1.2 Inhibitory receptors

Antibodies targeting inhibitory pathways (e.g. anti-CTLA-4 (ipilimumab and tremelimumab) and anti-PD-1 (pembrolizumab and nivolumab)) which reverse the suppressive mechanisms that restrain tumour-infiltrating T cells have recently been introduced into clinical use (Hamid et al., 2013, Topalian et al., 2012, Hodi et al., 2010). Clinical trials have shown enhanced tumour immunity in various cancer types including melanoma, non-small cell lung cancer, renal cell carcinoma and bladder cancer.

Anti-CTLA-4 antibodies were initially thought to block inhibitory signals to effector T cells, and when Tregs were found to express high levels of CTLA-4, initial studies suggested Tregs could be expanded with anti-CTLA-4 treatment (Quezada et al., 2006). Subsequently, it was demonstrated that the effect of CTLA-4 blockade in augmenting immune responses against cancer involves both

direct enhancement of effector T cell function and concomitant inhibition of Treg activity (Peggs et al., 2009). In a later study, whereas anti-CTLA-4 increased both effector T cell and Treg numbers in the lymph nodes, the effect of anti-CTLA-4 in the tumour environment was to increase effector T cells and reduce Tregs; this was due to Fcγ R-expressing tumour macrophages which deplete Tregs, leading to an increase in the effector T cell / Treg ratio within the tumour (Simpson et al., 2013). Indeed, melanoma patients who responded to ipilimumab were associated with increased frequencies of Fcγ RIIIA-expressing peripheral monocytes and tumour infiltrating macrophages than non-responders (Romano et al., 2015). Ipilimumab prolongs overall median survival in metastatic melanoma by 10 months (Hodi et al., 2010), and ipilimumab plus dacarbazine improves survival compared to dacarbazine plus placebo (Robert et al., 2011). As a result of the evidence for its benefit, ipilimumab is currently an approved first line treatment for advanced/metastatic *BRAF* wild type melanoma. Two whole exome sequencing studies performed on patients with melanoma treated with CTLA-4 blockade showed that mutational load, neoantigen load and expression of cytolytic markers in the immune microenvironment are significantly associated with the degree of clinical benefit, however it is not clear whether specific neoantigen peptide sequences can predict response to CTLA-4 blockade (Snyder et al., 2014, Van Allen et al., 2015). Another study identified tumour-specific mutant antigens that activated T cells in mice with tumours treated with PD-1 and/or CTLA-4 inhibition, and that peptide vaccines incorporating these mutant epitopes could mediate tumour rejection (Gubin et al., 2014). Anti-CTLA-4 therapy is associated with immune related adverse events in 60% of patients which include diarrhoea / colitis, pruritus, vitiligo, hypothyroidism and hypopituitarism (Hodi et al., 2010). The longer term effects of reduced CTLA-4 activity in humans is described in two recent reports of germline mutations in the CTLA-4 gene in humans, demonstrating impaired Treg function, hyperactivation of effector T cells and decreased circulating B cell numbers, and manifesting as a severe immunoregulatory disorder termed CTLA-4 haploinsufficiency with autoimmune infiltration (CHAI) disease (Kuehn et al., 2014, Schubert et al., 2014).

PD-1 inhibitors have demonstrated encouraging results for the treatments of various types of cancer since their introduction into clinical trials. Initially, objective and durable responses were reported in up to 27% of cancer patients (Topalian et al., 2012). Subsequently, a clinical trial in melanoma showed response rates of 38%, with an overall median progression-free survival of 7 months (Hamid et al., 2013). Further studies have compared responses to anti-

PD-1 with other modes of therapy, demonstrating improved overall survival with nivolumab over docetaxel in non-small cell lung cancer (Borghaei et al., 2015, Brahmer et al., 2015) and everolimus in renal cell carcinoma (Motzer et al., 2015). More recently, improved survival in melanoma was observed with pembrolizumab versus ipilimumab (Robert et al., 2015), and nivolumab plus ipilimumab in combination or nivolumab alone was associated with longer progression-free survival than ipilimumab alone (Larkin et al., 2015). Numerous studies have examined factors which predict efficacy of PD-1/PD-L1 inhibition in cancer. In melanoma, positive clinical responses with PD-1 inhibition correlate with higher numbers of $CD8^+$, $PD\text{-}1^+$ and $PD\text{-}L1^+$ cells in the invasive tumour margins before treatment, suggesting that tumours which upregulate the PD-1/PD-L1 immune inhibitory axis are those most responsive to treatment (Tumeh et al., 2014). Similarly, responses to PD-L1 blockade also correlate with tumour PD-L1 expression and presence of infiltrating immune cells (Herbst et al., 2014, Powles et al., 2014). Distinct Fcγ R dependency and mechanisms may be responsible for differing *in vivo* activity of anti-PD1 and anti-PD-L1 antibodies; although anti-PD-1 antibodies are Fcγ R independent, engagement of activating Fcγ Rs by anti-PD-L1 antibodies augments anti-tumour activity (Dahan et al., 2015). The relatively mild phenotypes of *Pd1*, *Pdl1* and *Pdl2* knockout mice initially suggested less immune toxicity with anti-PD-1 therapy than with CTLA-4 blockade, which was indeed confirmed in clinical trials (Topalian et al., 2012, Hamid et al., 2013, Robert et al., 2015).

1.13 cSCC as a model for studying cancer immunity

cSCC offers an excellent opportunity for studying human cancer immunity because of the prevalence and ease of access to samples from human primary tumours and the visible presence of clinically identifiable precancerous lesions. In addition, cSCCs can be considered to be the most common human cancer with metastatic potential, and a recent study has highlighted a clinical need for research into cSCC (Healy et al., 2015). That immunosuppression greatly increases cSCC incidence and aggressiveness, and that cSCCs in immunocompetent subjects are usually infiltrated by T cells suggests that immune mechanisms play a key role in the pathogenesis of cSCC.

1.14 Hypothesis

The hypothesis investigated in this study is that the insufficient immune response in cSCCs results from phenotypic and functional alterations in the tumoral Treg and $CD8^+$ T cell populations.

1.15 Aims of the study

This study will investigate the mechanisms for insufficient tumoral T cell responses in cSCC. Specifically, the project will:

1. Investigate the phenotype and function of Tregs in cSCC to determine whether they inhibit tumoral T cell immune responses;
2. Characterise the effector T cell population to determine the role of T cell exhaustion in cSCC;
3. Examine whether the cSCC *in vitro* T cell culture system provides useful information regarding potential therapeutic targets for future clinical studies.

Chapter 2: Materials and methods

2.1 Ethical approval

Ethical approval for the study was provided by the South Central Hampshire B National Research Ethics Service Committee (reference number 07/H0504/187). All participants recruited to the study provided informed consent for blood, non-lesional skin and tumour samples to be used for research purposes.

2.2 Procurement of samples

Fresh tissue samples were obtained from patients following surgical excision at the Dermatology Department, University Hospital Southampton NHS Foundation Trust (see Figure 2.1, page 54). Patients with tumours less than 8 mm in diameter were excluded as the tumours needed to be of sufficient size to allow a fresh section to be obtained for the study whilst leaving enough material for histological processing and analysis for clinical purposes. For lesions ≥8 mm in diameter, an off-centre, 2 mm full thickness vertical section was obtained from each lesion for the study, with the rest of the specimen fixed in formalin for processing and use by the Histopathology department as per normal clinical care, and as agreed by Dr Jeff Theaker, Consultant Histopathologist (see Figure 2.2, page 60). This portion of lesional skin was obtained from an area of the lesion which would not compromise the histological assessment of tumour excision margins, and was not taken from the centre of the lesion (usually the deepest part) which would therefore not affect the assessment of the maximum depth of invasion, which is required for tumour staging. Peripheral blood and non-lesional 'normal' skin were also obtained from the cSCC patients when feasible. The non-lesional 'normal' skin obtained from patients during cSCC surgery was excess skin which was excised during surgery to enable apposition of wound edges for optimal wound closure and would otherwise be discarded. All 'normal skin' used in this study was normal in appearance and was at least 6 mm in distance away from the tumour. Archived formalin-fixed paraffin-embedded (FFPE) cSCC samples were also obtained from the Histopathology department, University Hospital Southampton NHS Foundation Trust.

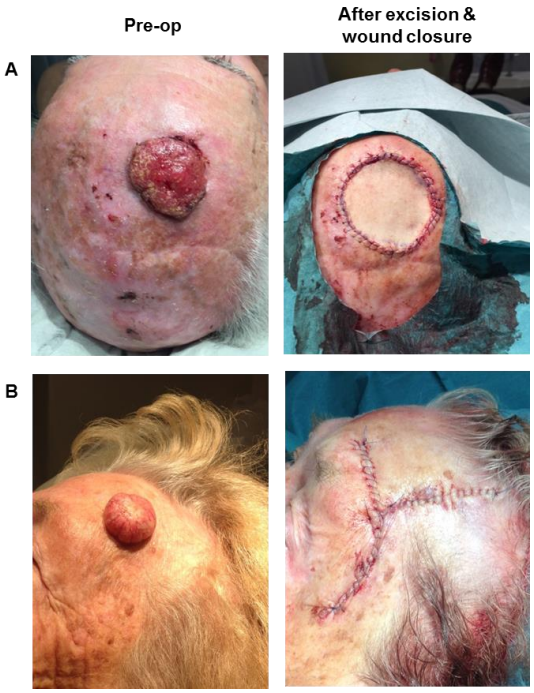

Figure 2.1 Surgical excision of cSCCs.

cSCC samples were obtained from patients undergoing surgery performed by the author of this thesis at the Dermatology Department, University Hospital Southampton NHS Foundation Trust. Photos show appearances of cSCCs before excision and following (A) full thickness skin graft and (B) local flap wound repair.

2.3 Immunohistochemistry

2.3.1 Buffers and antibodies

Tris buffered saline (TBS): 5mM Tris (ThermoFisher Scientific) and 137mM sodium chloride (ThermoFisher Scientific) dissolved in water and adjusted to pH 7.6 with hydrochloric acid (BDH Laboratory Supplies). Citrate buffer: 10mM citrate (ThermoFisher Scientific) dissolved in water and adjusted to pH 6 with sodium hydroxide solution (BDH Laboratory Supplies). Ethylenediaminetetraacetic acid (EDTA) buffer: 1.6µM EDTA (BDH Laboratory Supplies) dissolved in water and adjusted to pH 8 with sodium hydroxide solution (BDH Laboratory Supplies). Blocking medium: 1% bovine serum albumin (BSA, Sigma-Aldrich) and 20% foetal bovine serum (FBS, Life Technologies) in Dulbecco's Modified Eagle's Medium (DMEM, Life Technologies). Antibodies used are listed in Table 2.1 (page 55) and biotinylated secondary antibodies in Table 2.2 (page 55). Initial titration experiments were performed on some cSCC sections and tonsil tissues using at

least three doubling dilutions to establish the optimal dilutions of primary antibody which resulted in specific staining with good intensity with minimal background staining.

Table 2.1 Primary antibodies for immunohistochemistry

Marker	Host	Isotype	Clone	Manufacturer	Antigen retrieval buffer	Dilution used
CD3	rabbit	polyclonal		Dako	Citrate	1:200
CD4	mouse	IgG1	4B12	Dako	EDTA	1:100
CD8	mouse	IgG1	144B	Abcam	Citrate	1:20
FOXP3	mouse	IgG1	236A/E7	Abcam	Citrate	1:50
OX40	mouse	IgG1	ACT35	BD Biosciences	Citrate	1:50
PD-1	mouse	IgG1	NAT105	Abcam	EDTA	1:100
CD39	rabbit	polyclonal		Abcam	Citrate	1:1000
γ δ TCR	mouse	IgG1	B1.1	eBioscience	Citrate	1:20

Table 2.2 Biotinylated secondary antibodies

Target	Host	Manufacturer	Dilution used
mouse IgG	rabbit	Dako	1:100
mouse IgG	rabbit	Jackson	1:400
rabbit IgG	swine	Dako	1:400

2.3.2 **Methods**

FFPE specimens were cut with a microtome (Leica Microsystems) into 5μm sections onto 3-aminopropyltriethoxysilane (APES)-coated microscope slides (CellPath). Sections were deparaffinised in xylene (ThermoFisher Scientific) and rehydrated through graded alcohols. Endogenous peroxidase was exhausted with 0.5% hydrogen peroxide (Sigma-Aldrich) in methanol (ThermoFisher Scientific). Formalin fixation enables preservation of tissue structure, but poor antigen availability may result from strong cross-linking of tissue proteins. Therefore, sections were microwaved in citrate or EDTA buffer to enable antigens to be revealed. Endogenous avidin and biotin were blocked (Vector Labs), before addition of blocking medium, which reduces non-specific hydrophobic and electrostatic interactions by occupying binding sites in the tissue, but allows stronger antibody-antigen binding to occur. Primary antibodies specific for the

marker of interest were left on the immunohistochemistry sections for 16 hours at 4˚C before being washed three times with TBS. This was followed by incubation with the relevant biotinylated secondary antibodies which are of very high avidity to the γ -globulin of the species that donated the primary antibody. Multiple anti-Ig molecules can bind one primary antibody, which increases sensitivity. The secondary antibodies were washed off after 30 minutes with 3 TBS washes. As the secondary antibody is coupled to biotin which has a very high affinity for streptavidin, which can further bind multiple biotin molecules, sensitivity is further improved and addition of biotinylated peroxidase forms a streptavidin-biotin-peroxidase complex, meaning a large number of peroxidase molecules attaches to each primary antigen site. Therefore, streptavidin-biotin-peroxidase complexes (Vector Labs) were added to the sections, before being washed with TBS x 3 and 3,3'-diaminobenzidine (DAB, Dako) applied, which produces a brown colour when oxidised by peroxidase. After this was washed off with TBS, the sections were counterstained with Mayer's Haematoxylin (Sigma-Aldrich) and dehydrated through graded alcohols and xylene. Sections were mounted in distyrene-plasticizer-xylene (DPX) mountant (Sigma-Aldrich) and coverslips (BDH Laboratory Supplies) were applied. For haematoxylin and eosin staining, slides were sequentially dewaxed in xylene, rehydrated through graded alcohols, immersed in Mayer's haematoxylin for 5 minutes, rinsed in water, then immersed in eosin (TCS Biosciences) for 5 minutes, rinsed in tap water before dehydrating and mounting with coverslips. For cell quantification, 5 representative images at 40x magnification were taken from each immunostained cSCC section and analysed using ImageJ software, which was used to threshold positive staining (brown DAB for identification of markers, blue haematoxylin for nuclei), thereby converting images into binary format for automated counting of positively stained cells.

2.4 Immunofluorescence / confocal microscopy

2.4.1 Buffers and antibodies

Phosphate buffered saline (PBS) was made up by dissolving 10 PBS tablets (Oxoid, containing 8g sodium chloride, 0.2g potassium chloride, 1.15g disodium hydrogen phosphate, 0.2g potassium dihydrogen phosphate) per litre of water. Blocking solution consisted of 1% BSA and 10% FBS in PBS. Primary antibodies are listed in Table 2.3 and fluorophore-conjugated secondary antibodies in Table 2.4 (page 57). Antibody dilutions were established through initial titration

experiments which were performed using at least three doubling dilutions, and the optimal dilution which produced the clearest specific staining with minimal background was selected for use in further experiments.

Table 2.3 Primary antibodies for immunofluorescence microscopy

Marker	Host	Isotype	Clone	Manufacturer	Dilution used
CD3	rabbit	polyclonal		Dako	1:200
	mouse	IgG1	F7.2.38	Dako	1:100
CD4	rabbit	IgG	EPR6855	Abcam	1:50
	mouse	IgG1	mAB51312	Abcam	1:20
CD8	mouse	IgG2a	3B5	ThermoFisher Scientific	1:20
FOXP3	mouse	IgG1	236A/E7	Abcam	1:100
	rat	IgG2a	PCH101	eBioscience	1:20
4-1BB	mouse	IgG1κ	BBK-2	ThermoFisher Scientific	1:50
CD31	mouse	IgG1	WM-59	eBioscience	1:200
CLA	rat	IgM	HECA-452	Biolegend	1:200
Cytokeratin 16	mouse	IgG1	LL025	ThermoFisher Scientific	1:200
Cytokeratin 17	mouse	IgG2b	E3	Dako	1:20
E-selectin	mouse	IgG1	BBIG-E4	R & D Systems	1:20
MUC1	mouse	IgG1	GP1.4	Leica Biosystems	1:200
Multi-cytokeratin (4/5/6/8/10/16/18)	mouse	IgG1	C11	Leica Biosystems	1:50
OX40	mouse	IgG1	ACT35	BD Biosciences	1:200
PD-1	mouse	IgG1	NAT105	Abcam	1:100
PD-L1	rabbit	polyclonal		Abcam	1:400

Table 2.4 Fluorophore-conjugated secondary antibodies.

All fluorophore-conjugated secondary antibodies were obtained from ThermoFisher Scientific.

Target	Host	Alexa Fluor conjugate	Dilution used
Mouse IgG1	goat	488	1:500
	goat	555	1:500
Mouse IgG2a	goat	488	1:100
	goat	633	1:200
Mouse IgG2b	goat	568	1:500
Rabbit IgG	goat	555	1:500
	goat	633	1:2000
Rat IgG	goat	555	1:500
Rat IgM	goat	488	1:500

2.4.2 **Methods**

Immunofluorescence microscopy was performed in order to enable detection of multiple target antigens in the same section of tissue. Tissue samples were snap frozen in liquid nitrogen, embedded in optimum cutting temperature (OCT) medium (CellPath) and cut into 5-10μm sections onto APES-coated glass slides. Sections were fixed in 4% paraformaldehyde (Sigma-Aldrich) before blocking solution was added. Primary antibodies were applied and left for 1 hour at room temperature or 16 hours at 4˚C. After 3 washes with phosphate buffered saline (PBS), fluorophore-conjugated secondary antibodies were added. Sections were washed in PBS x 3 and counterstained with 4',6-diamidino-2-phenylindol dihydrochloride (DAPI, Sigma-Aldrich), a fluorophore that binds to AT regions of DNA. Mowiol 4-88 (Harco) was used to mount the sections and coverslips were applied. The principle of immunofluorescence microscopy relies on a light source (e.g. mercury lamp or laser) which passes to the sample via a dichroic mirror which reflects light shorter than a certain wavelength, resulting in detection of longer wavelength light emitted by the fluorophore, rather than scattered light from the source. A Zeiss Axioskop 2 fluorescence microscope was used, with Neofluar 10x, 20x and 40x lenses and three channels (filter sets 2, 10 and 15) to detect DAPI (filter set 2: excitation 300-400 nm, dichroic mirror 395 nm, emission 400-750 nm), Alexa Fluor 488 (filter set 10: excitation 450-500 nm, dichroic mirror 510 nm, emission 500-580 nm) and Alexa Fluor 555/568 (filter set 15: excitation 550-580 nm, dichroic mirror 580 nm, emission 590-750 nm). Confocal microscopy enables clearer detection of fluorescence by using a pinhole which focuses emitted light from the sample, thereby reducing background fluorescence, and enabling fluorescence from different z-planes to be detected, thus building a three-dimensional image of the sample. Only one point of the sample can be visualised at a time, and therefore a computer scans the sample to build up the image. The confocal microscopy was conducted using a Leica TCS SP5 laser scanning confocal microscope on a Leica DMI 6000 inverted microscope frame, controlled by Leica LAS AF software. A true spectral detection system was used, which was tuneable to nanometer precision on bandwith, allowing four non-overlapping colour ranges to be detected simulataneously, and more with sequential imaging. The lasers used for detection of the fluorophores used in this study were 405 nm (for DAPI), argon 488 nm (for Alexa Fluor 488), 561 nm (for Alexa Fluor 555/568) and 633 nm (for Alexa Fluor 633). The objectives used were HC plan apochromat lambda blue 20x 0.70 immersion (with 8 parts glycerol, 2 parts water), HC plan apochromat CS 40x 1.25 oil immersion and HC plan

apochromat CS 63x 1.30 glycerol immersion. Images were captured at 1024 x 1024 pixel resolution with optical zoom and z spacing as approriate. Secondary antibody only controls were imaged to determine levels of non-specific binding and autofluorescence in each detection range and the maximum PMT gains to detect no fluorescence signal in control samples were recorded; experimental samples were then imaged at lower/equal gain settings to controls. Image J and Leica LAS AF Lite software were used for overlaying immunofluorescence and confocal microscopy images respectively.

2.5 Lymphocyte isolation

2.5.1 Media

Roswell Park Memorial Medium 1640 (RPMI, Life Technologies) was supplemented with 100 U/ml penicillin + 100 µg/ml streptomycin (Life Technologies) and 1mM sodium pyruvate (Life Technologies).

2.5.2 Methods

Immunocytes were isolated from cSCC and non-lesional skin samples as illustrated in Figure 2.2 (page 60). Tissue samples were cut into small pieces and treated with 1 mg/ml collagenase I-A (Sigma-Aldrich) and 10 µg/ml DNAse I (Sigma-Aldrich) in Roswell Park Memorial Institute (RPMI) medium at 37˚C for 1.5 hours. The resulting digest was passed through a 70µm cell strainer (BD) and washed with RPMI medium containing 10% FBS. The lymphocyte population was enriched amongst the other cells in the tumour suspension by centrifugation over density gradients provided by Optiprep (60% iodixanol in water, Sigma-Aldrich), which is considered less toxic than other density gradient media (Polak, 2011). The cell pellet was suspended in RPMI containing 14% iodixanol (density of 1.077g/ml), layered underneath a 9% iodixanol gradient and centrifuged at 600 x *g* for 20 minutes at 4˚C and without applying the brake for deceleration following centrifugation in order to preserve cell viability as much as possible. Lymphocytes form a band at the interface between the 14% and 9% iodixanol gradients, whereas erythrocytes, granulocytes and cellular debris have higher densities and therefore sink to the bottom. Dendritic cells, monocytes, macrophages and tumour cells have lower densities than lymphocytes and rise to the top of the 9% gradient. Lymphocytes were extracted and washed with PBS before use in experiments. Peripheral blood mononuclear cells (PBMCs) were separated from

whole blood by centrifugation over Lymphoprep (Axis-Shield), which consists of sodium diatrizoate and polysaccharide and has a density of 1.077g/ml. Following centrifugation at 600 x *g* for 30 minutes, erythrocytes and granulocytes pass down through the Lymphoprep, leaving a layer of mononuclear cells above the interface, which was collected and washed with PBS before use.

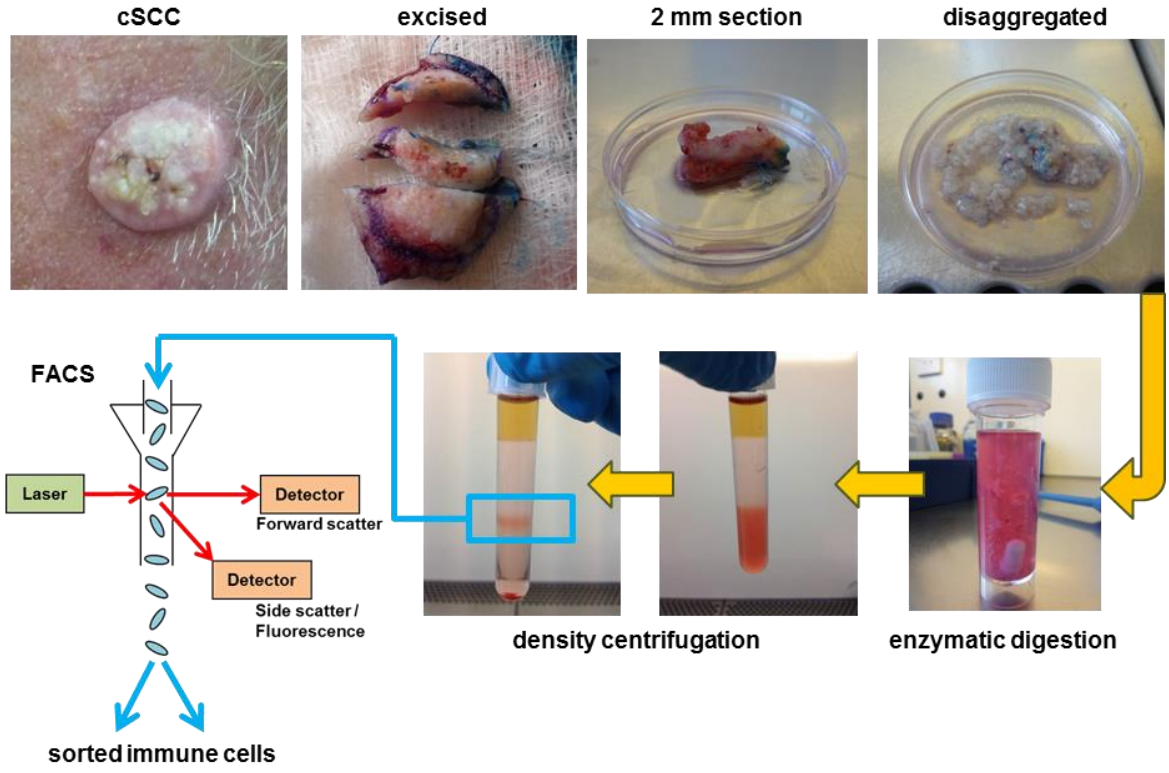

Figure 2.2 Schematic diagram showing method for isolation of tumour-infiltrating immunocytes.

Following excision of the cSCC, a 2 mm section was obtained for research, with the rest of the excised specimen processed by the Histopathology department as per normal clinical procedure for diagnostic purposes and assessment of staging / excision margins. The portion of the cSCC used for research was finely disaggregated with scalpels and incubated with collagenase I-A and DNAse I for 1.5 hours. The resulting suspension was passed through a cell strainer and centrifuged over Optiprep density gradients. The lymphocyte band was obtained for flow cytometry, details for staining for flow cytometry are provided in Section 2.6. The total time taken for isolation of immunocytes from skin tumours was normally up to 4 hours.

2.6 Flow cytometry

2.6.1 Buffers and antibodies

FACS buffer contained 1% BSA in PBS. Blocking medium consisted of 10% FBS and 1% BSA in PBS. Antibodies and isotype controls are detailed in Table 2.5 and Table 2.6 (page 62) respectively. Flow cytometry panels were worked up in this study and are listed in Appendix B Table 7.2, page 241.

Table 2.5 Primary antibodies for flow cytometry

Marker	Host	Isotype	Clone	Fluorophore	Manufacturer	Dilution used
CD1a	mouse	IgG1	HI149	APC	BD Biosciences	1:10
CD3	mouse	IgG1	UCHT1	APC Cy7	Biolegend	1:50
CD4	mouse	IgG2b	OKT4	PerCP Cy5.5	Biolegend	1:50
				FITC	Biolegend	1:50
CD8	mouse	IgG1	SK1	PE Cy7	Biolegend / eBioscience	1:50
CD11c	mouse	IgG1	3.9	APC	Biolegend	1:50
				PE Cy7	Biolegend	1:50
CD14	mouse	IgG1	HCD14	APC Cy7	Biolegend	1:50
				Pacific Blue	Biolegend	1:50
CD15	mouse	IgM	HI98	PE	Biolegend	1:50
CD16	mouse	IgG1	3G8	PE Cy7	Biolegend	1:50
CD19	mouse	IgG1	HIB19	APC	Biolegend	1:50
CD25	mouse	IgG1	CD25-3G10	PE	ThermoFisher Scientific	1:20
				FITC	ThermoFisher Scientific	1:20
CD39	mouse	IgG1	A1	PE	Biolegend	1:50
CD45	mouse	IgG1	2D1	PerCP Cy5.5	Biolegend	1:50
CD45RO	mouse	IgG2a	UCHL1	PerCP Cy5.5	Biolegend	1:50
				PE	BD Biosciences	1:10
CD56	mouse	IgG1	B159	APC	BD Biosciences	1:10
CD68	mouse	IgG2b	eBioY1/82A	FITC	eBioscience	1:50
CD73	mouse	IgG1	AD2	Brilliant Violet 421	Biolegend	1:20
CD117	rat	IgG2b	2B8	APC	Biolegend	1:50
CD123	mouse	IgG1	6H6	FITC	Biolegend	1:50
CD127	mouse	IgG1	eBioRDR5	PE Cy7	eBioscience	1:20
	mouse	IgG1	A019D5	Brilliant Violet 421	Biolegend	1:20
CD141	mouse	IgG1	1A4	PE	BD Biosciences	1:10
CD160	mouse	IgM	BY55	PE	eBioscience	1:20

Marker	Host	Isotype	Clone	Fluorophore	Manufacturer	Dilution used
CD203c	mouse	IgG1	NP4D6	PE Cy7	Biolegend	1:50
CD244	mouse	IgG1	eBioC1.7	PE	eBioscience	1:20
2D7	mouse	IgG1	2D7	PE	Biolegend	1:50
4-1BB	mouse	IgG1	4B4-1	PE	Biolegend	1:50
BTLA	mouse	IgG2a	MIH26	APC	Biolegend	1:20
CCR4	mouse	IgG2b	205410	FITC	R & D Systems	1:20
	mouse	IgG1	L291H4	PerCP Cy5.5	Biolegend	1:20
CCR7	mouse	IgG2a	G043H7	PE	Biolegend	1:20
CLA	rat	IgM	HECA-452	Brilliant Violet 421	BD Biosciences	1:10
				FITC	BD Biosciences	1:10
CTLA-4	mouse	IgG2a	14D3	PE	eBioscience	1:20
DC-LAMP	mouse	IgG1	I10-1112	APC	BD Biosciences	1:10
DC-SIGN	mouse	IgG2b	DCN46	FITC	BD Biosciences	1:10
Fcε RI	mouse	IgG2b	AER-37	FITC	Biolegend	1:50
FOXP3	rat	IgG2a	PCH101	APC	eBioscience	1:10
Helios	Armenian hamster	IgG	22F6	PerCP Cy5.5	Biolegend	1:20
L-selectin	mouse	IgG1	DREG-56	Brilliant Violet 421	Biolegend	1:20
LAG-3	mouse	IgG1	874501	PE	R & D Systems	1:20
NKG2D	mouse	IgG1	1D11	FITC	Biolegend	1:50
OX40	mouse	IgG1	ACT35	PE	eBioscience	1:50
				Brilliant Violet 421	Biolegend	1:50
PD-1	mouse	IgG1	EH12.2H7	PerCP Cy5.5	Biolegend	1:50
				APC	Biolegend	1:50
PD-L1	mouse	IgG2b	29E.2A3	Brilliant Violet 421	Biolegend	1:20
TIGIT	mouse	IgG1	MBSA43	PE	Biolegend	1:20
TIM-3	rat	IgG2a	344823	PE	R & D Systems	1:20
γ δ TCR	mouse	IgG1	B1	PE	Biolegend	1:50

Table 2.6 Isotype control antibodies for flow cytometry

Host	Isotype	Clone	Fluorophore	Manufacturer
mouse	IgG1	MOPC-21	APC Cy7	Biolegend
			PerCP Cy5.5	Biolegend
			PE-Cy7	Biolegend
			Brilliant Violet 421	Biolegend
mouse	IgG1	P3.6.2.8.1	PE	eBioscience
			PE-Cy7	eBioscience
			APC	eBioscience
			FITC	eBioscience
mouse	IgG2a	G155-178	PerCP Cy5.5	BD Biosciences
		MOPC-173	APC	Biolegend

Host	Isotype	Clone	Fluorophore	Manufacturer
mouse	IgG2a	MOPC-173	Brilliant Violet 421	Biolegend
			PE	Biolegend
mouse	IgG2b	eBMG2b	PerCP Cy5.5	eBioscience
			PE	eBioscience
			FITC	eBioscience
mouse	IgG2b	MPC-11	Brilliant Violet 421	Biolegend
mouse	IgM	MM-30	PE	Biolegend
rat	IgG1	RTK2071	PerCP Cy5.5	Biolegend
			PE	Biolegend
rat	IgG2a	54447	PE	R & D Systems
		RTK2758	Brilliant Violet 421	Biolegend
		eBR2a	APC	eBioscience
rat	IgM	R4-22	Brilliant Violet 421	Biolegend
Armenian hamster	IgG	HTK888	PerCP Cy5.5	Biolegend

2.6.2 Cell surface staining

Cells were incubated in 100µl blocking medium with the relevant antibodies (up to 5 x 10^6 cells per tube) for 30 minutes in the dark at 4˚C, then washed and resuspended in FACS buffer. To determine cell viability, an aqua or violet fixable live/dead viability stain (ThermoFisher Scientific) was used, which binds with intracellular free amines in cells with compromised membranes. Flow cytometry was performed using a FACSAria cell sorter (BD Biosciences) containing a red laser (wavelength 633nm), blue laser (488nm) and violet laser (405nm). To minimise issues with overlapping emission spectra with multi-colour staining, automated compensation was performed based on the emission spectra detected from compensation beads (OneComp eBeads, eBioscience) stained with the fluorophores of interest. Following data acquisition, analysis was performed using FlowJo software. Staining was considered positive if fluorescence intensity was above that of isotype control staining.

2.6.3 Intracellular markers

To enable detection of cytoplasmic or nuclear markers, cells must be fixed and cell membranes permeabilised to allow antibodies into the cells. For staining of intracellular Helios, CTLA-4 and FOXP3, cells were first stained as in the preceding paragraph with the cell surface markers of interest, and then fixed for 30 minutes in Fixation/Permeabilisation buffer (eBioscience), which contains formaldehyde,

and washed with Permeabilisation buffer (eBioscience), which contains 0.1% saponin. For FOXP3 staining, cells were incubated with anti-FOXP3 antibody in Permeabilisation buffer with 2% rat serum (eBioscience) for 30 minutes in the dark at 4˚C. For other markers, cells were incubated with antibodies in Permeabilisation buffer with 10% FBS. Cells were then washed twice with Permeabilisation buffer prior to flow cytometry.

2.6.4 UVR irradiation

PBMCs were irradiated with UVB in a unit containing UVB TL20W/12RS lamps (Philips) in PBS in 12 well plates with the lid removed. Cells were irradiated for 30, 60, 120, 240 and 480 s which provide the doses of 37.9, 75.8, 151.7, 303.4 and 606.7 mJ/cm^2 respectively. Cells were then washed with PBS before staining for flow cytometry.

2.7 T cell functional assays

2.7.1 Intracellular cytokines and markers of degranulation

Cells were cultured with cell stimulation cocktail (eBioscience, containing 81nM phorbol 12-myristate 13-acetate, a protein kinase C (PKC) activator and 1.34μM ionomycin, which can also induce PKC, hydrolyse phosphoinositides and activate calcium-dependent signalling pathways) for 5 hours in RPMI + 10% heat inactivated FBS at 37˚C, 5% CO_2. Brefeldin A 3μg/ml (eBioscience) was added during the last 4 hours of culture to block transport of synthesised proteins from the endoplasmic reticulum to the Golgi complex. At the end of culture, cells were washed and stained for cell surface markers (including LAMP-1) as before, followed by fixation with Intracellular Fixation buffer (eBioscience), which contains 4% formaldehyde, and permeabilisation with Permeabilisation buffer. Cells were then incubated with the relevant antibodies for cytokines (Table 2.7) and markers of degranulation for 30 minutes (Table 2.8, page 65) in the dark at 4˚C and then washed twice with Permeabilisation buffer prior to flow cytometry.

Table 2.7 Flow cytometry antibodies for intracellular cytokines

Marker	Host	Isotype	Clone	Fluorophore	Manufacturer	Dilution used
IFN-γ	mouse	IgG1	4S.B3	PE	Biolegend	1:20

				PerCP Cy5.5	Biolegend	1:20
TNF-α	mouse	IgG1	Mab11	PerCP Cy5.5	Biolegend	1:20
IL-2	rat	IgG2a	MQI-17H12	Brilliant Violet 421	Biolegend	1:20
IL-4	mouse	IgG1	8D4-8	PE	Biolegend	1:20
IL-13	rat	IgG1	JES10-5A2	PerCP Cy5.5	Biolegend	1:20
IL-17	mouse	IgG1	eBio64CAP17	PE	eBioscience	1:20

Table 2.8 Flow cytometry antibodies for degranulation markers

Marker	Host	Isotype	Clone	Fluorophore	Manufacturer	Dilution used
Granzyme B	mouse	IgG1	GB11	FITC	BD Biosciences	1:10
LAMP-1	mouse	IgG1	H4A3	Brilliant Violet 421	Biolegend	1:20
Perforin	mouse	IgG2b	dG9	PE	Biolegend	1:20

2.7.2 Co-culture experiments

Tumoral $CD3^+CD4^+CD25^{high}CD127^{low}$ Tregs and $CD3^+CD4^+CD25^{low}$ or $CD3^+CD8^+$ effector T cells were sorted by FACS using the "purity" setting, which enables up to 99% purity. During sorting, cells are passed into a stream of regularly spaced electrically charged droplets which are deflected by electrostatic plates into collection tubes. 96 well U-bottomed plates (Cellstar) were used for co-culture assays and all functional experiments were performed using triplicate wells. Tumoral effector T cells (2,500 per well) were co-cultured with/without tumoral Tregs (1,250 per well) in the presence of irradiated (46.5 Gy) autologous PBMCs (25,000 per well), stimulated with 1 µg/ml phytohaemagglutinin (PHA, Sigma) or anti-CD3 (eBioscience) with/without other antibodies (see Table 2.9)/isotype controls (see Table 2.10, page 66) and cultured in RPMI + 10% heat inactivated FBS at 37˚C, 5% CO_2 for 72 hours before lymphocyte proliferation or interferon-γ production was measured. Concentrations of functional antibodies used were based on those recommended by the manufacturer, and for anti-CTLA-4, 50µg/ml was used as previously reported in the literature for *in vitro* Treg assays (Peggs et al., 2009).

Table 2.9 Functional antibodies

*Anti-OX40 and anti-4-1BB agonistic antibodies were provided by Dr Ruth French, Cancer Sciences, University of Southampton.

Target	Host	Isotype	Clone	Manufacturer	Concentration used (µg/ml)
CD3	mouse	IgG2a	OKT3	eBioscience	1
OX40	mouse	IgG1	SAP 25-29	in house*	5
4-1BB	mouse	IgG1	SAP 3-28	in house*	5
CTLA-4	mouse	IgG2a	14D3	eBioscience	50
PD-1	goat	IgG	polyclonal	R & D Systems	30

Table 2.10 Isotype control antibodies for functional experiments

Host	Isotype	Clone	Manufacturer
mouse	IgG1	P3	eBioscience
mouse	IgG2a	eBM2a	eBioscience
goat	Polyclonal IgG		Abcam

2.7.3 Lymphocyte proliferation assay

To determine proliferation of T cells which were cultured in the presence of stimulus and/or Tregs and/or costimulatory/inhibitory antibodies, cells were pulsed with 1 µCi/ml tritiated thymidine (Perkin Elmer) in the last 16 hours of culture. Tritiated thymidine is incorporated into the DNA of dividing cells during S-phase, and therefore can be used as a marker of proliferation, this method of measuring cell proliferation was used because the limited numbers of lymphocytes isolated from the tumour samples meant that carboxyfluorescein succinimidyl ester dilution experiments were not feasible. A MicroBeta FilterMate-96 harvester (Perkin Elmer) was used to aspirate well contents and leave cells entrapped in a filter microplate (Perkin Elmer). Microscint 40 scintillation fluid (Perkin Elmer) was added to each well of the filter microplate which emits luminescence following β-particle emission which was detected with a Top Count liquid scintillation counter (Perkin Elmer).

2.7.4 Interferon-γ enzyme-linked immunosorbent spot (ELISPOT) assay

The ELISPOT assay is highly sensitive and measures the frequency of cytokine-secreting cells at the single cell level. Cells were incubated as before in 96 well ELISPOT plates (Merck Millipore), which were initially pre-blocked with RPMI + 10%

FBS and pre-coated with anti-interferon-γ antibody (ELISPOT assay for human interferon-γ kit, Mabtech), which captures interferon-γ immediately after secretion by the cell. After 72 hours of culture, the well contents were washed off with PBS + 0.1% Tween 20 (Amersham Life Sciences) and the biotinylated secondary antibody (Mabtech) was added. Following another wash with PBS + 0.1% Tween 20, streptavidin-alkaline phosphatase (Mabtech) was applied, which was detected using 5-bromo-4-chloro-3-indolyphosphate (BCIP, ThermoFisher Scientific) which forms dark spots when oxidised by nitroblue tetrazolium (NBT, ThermoFisher Scientific). Spots were counted automatically with an AID ELISPOT Reader (Autoimmun Diagnostika).

2.8 cSCC cell culture

cSCC samples were finely cut into small pieces, treated with collagenase I-A and DNAse I, and centrifuged with Optiprep as detailed in section 2.5, page 59. Following centrifugation, the cell layer above the 9% iodixanol Optiprep gradient was obtained, washed with sterile PBS, suspended in 5 ml warmed keratinocyte growth medium (containing 0.4% bovine pituitary extract, 0.125 ng/ml recombinant human epidermal growth factor, 5 µg/ml recombinant human insulin, 0.33 µg/ml hydrocortisone, 0.39 µg/ml epinephrine, 10 µg/ml transferrin and 0.06 mM calcium chloride, PromoCell) + 10% FBS + 100 U/ml penicillin + 100 µg/ml streptomycin, seeded into T25 culture flasks (Cellstar), and kept in culture at 37ºC, 5% CO_2. The culture medium was changed after 24 hours and then after every 2-3 days. Cells were passaged prior to reaching confluence. The cultures were washed with sterile PBS before warmed TrypLE Express (a solution containing cell dissociation enzymes, ThermoFisher Scientific) was added to the flask, which was then kept at 37ºC until all cells had detached. FBS was added to inactivate the cell dissociation process and the resultant suspension was washed in PBS and centrifuged at 310 x *g* for 5 minutes. The cell pellet was then resuspended in keratinocyte growth medium, seeded into T75 culture flasks (Cellstar), and cultured at 37ºC, 5% CO_2.

Cells were grown on coverslips for immunofluorescence microscopy; following passage, cells were seeded onto circular coverslips (CellPath) that had been precoated with 4 µg/ml collagen (Sigma-Aldrich) in sterile PBS for 30 minutes, the cells / coverslips were contained in 12-well plates (Cellstar) and incubated at 37ºC for 24 hours. The supernatant was discarded and the coverslips were used for immunofluorescence staining as described in section 2.4, page 56.

For cryopreservation, cell cultures were washed in PBS, centrifuged at 310 x *g* for 5 minutes and pelleted. The resulting cell pellet was suspended in FBS + 10% dimethyl sulfoxide (Sigma-Aldrich) in cryovials, which were initially stored in a Mr Frosty Freezing container (Sigma-Aldrich) at -80ºC before being kept in storage in liquid nitrogen.

2.9 Statistical analysis

Advice was provided by Trevor Bryant and Scott Harris, Medical Statisticians at the Faculty of Medicine, University of Southampton. Statistical analysis was conducted using GraphPad Prism software. For cell proliferation assays, paired Wilcoxon rank tests were used to assess significance, and for immunohistochemical and flow cytometric quantification of normally distributed data, paired T tests or one way ANOVA with Tukey's test for multiple comparisons were used.

Chapter 3: Development of methods

3.1 Introduction

Much of the previous work on the identification of immune cells in human cSCCs has relied on using immunohistochemistry and immunofluorescence of tissue samples (Clark et al., 2008, Jang, 2008). Whilst immunostaining provides information about the spatial distribution of the immune cells within the skin, only limited numbers of markers can be used simultaneously. Flow cytometry allows the analysis of multiple parameters simultaneously, and therefore multiple cell populations can be phenotyped at the same time. However, fresh tissue samples are needed for isolation of immune cells for flow cytometry, and therefore few studies have used this potentially powerful method for characterising immunocytes from human cSCCs (Clark et al., 2008, Huang et al., 2009, Freeman et al., 2014).

Various approaches have been tried to isolate immune cells from skin tissue for flow cytometry. Campbell et al. separated epidermis and superficial dermis from deeper dermis prior to incubation in solution containing the chelating agent EDTA for 120 minutes; this method for skin dissociation did not affect expression of cell surface markers on the isolated immunocytes as detected by flow cytometry (Campbell et al., 2001). Schaerli et al. used enzymatic digestion with collagenase D for 30-90 minutes at 37ºC prior to filtration and centrifugation on a density gradient; similarly, it was noted that enzymatic digestion did not reduce staining of cell surface markers (Schaerli et al., 2004, Schaerli et al., 2006). Freeman et al. also extracted immunocytes from fresh human skin cSCC and sun-exposed skin for flow cytometry using mechanical disaggregation and enzymatic digestion with collagenase D for 90 minutes at 37ºC (Freeman et al., 2014). Although a combination of mechanical methods and collagenase / EDTA treatment has been most commonly used for isolation of skin T cells for phenotypic analysis, this method yields relatively low numbers of cells, making functional studies difficult. Clark et al. devised a novel method for isolation of larger numbers of T cells from skin and cSCC by taking advantage of the tendency of skin resident T cells to migrate towards areas of wound healing and tissue repair (Clark et al., 2006b, Clark et al., 2008). In their experiments, skin samples were minced and placed in three-dimensional Cellfoam growth matrices and cultured for 3 weeks in the presence of IL-2 and/or IL-15 to expand the T cell population. This skin explant

culture system enables proliferation of dermal fibroblasts in the matrix which produce chemokines such as IL-8, monocyte chemotactic protein-1, macrophage-derived chemokines and interferon-inducible protein-10, which can induce migration of T cells out of the skin explants. Furthermore, although expression of the skin homing receptor CLA is lost upon culture of T cells in serum (Fuhlbrigge et al., 1997), the skin T cells cultured in matrices colonised with dermal fibroblasts maintained CLA expression for up to 4 weeks, suggesting that the presence of dermal fibroblasts supports the survival and differentiation state of the cutaneous T cells (Clark et al., 2006b). However, whilst this method of isolating T cells from cSCC provides a greater yield than a short period of enzymatic digestion *ex vivo*, it remains uncertain whether certain immune markers may be downregulated during three week culture in the matrices when removed from the tumour microenvironment.

As tumoral immunity plays a key role in cSCC pathogenesis, characterisation of the cSCC immune infiltrate is important in order to better understand the mechanisms for dysfunctional immunity in this cancer. Therefore, the aim of the current chapter was to determine whether isolation of immunocytes from human cSCC and flow cytometric characterisation of these cells was feasible and reliable.

3.2 Results

3.2.1 Flow cytometric characterisation of cSCC immunocytes

Flow cytometry was used to perform *ex vivo* characterisation of immunocytes from blood, normal skin and cSCC. Initially, experiments were performed on PBMCs to determine whether lymphocytes and T cells could be identified. A distinct population of lymphocytes was detected on the forward scatter / side scatter profile, and gating upon this lymphocyte population showed them all to be live cells, of which many were $CD3^+$ T cells (Figure 3.1, page 71). Immunocytes were then isolated from cSCCs following mechanical disaggregation and incubation with collagenase I-A and DNAse I for 1.5 hours at 37ºC (as per Methods section 2.5, page 59), based on studies showing that this method of immune cell extraction did not alter expression of T cell markers (Schaerli et al., 2004, Schaerli et al., 2006, Freeman et al., 2014). As the current study aims to characterise the *ex vivo* phenotype of the tumoral immunocytes, the cells were not expanded *in vitro* or kept in culture for long periods.

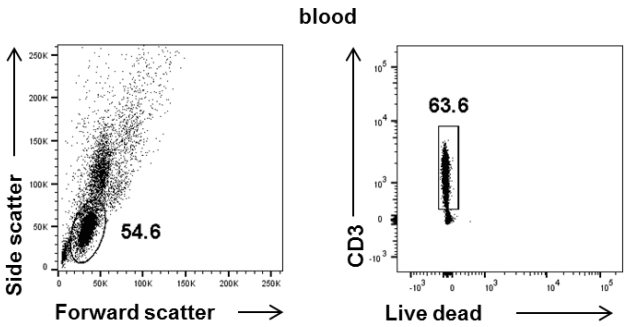

Figure 3.1 Flow cytometry of PBMCs.

PBMCs were isolated from patients with cSCC and stained with anti-CD3 antibody and a live / dead stain prior to flow cytometry. Representative forward scatter / side scatter plot with lymphocyte gate is shown on the left. The lymphocyte gate is subgated in the Live dead / CD3 plot on the right, with the subgate showing the live $CD3^+$ cell population.

Flow cytometry was then conducted on the immunocytes isolated from cSCCs, demonstrating that most were lymphocytes and that most of these were live $CD3^+$ T cells (Figure 3.2). Repeated experiments suggested that sufficient numbers of viable T cells (up to 500,000) were able to be consistently isolated from cSCC tissue for flow cytometric characterisation.

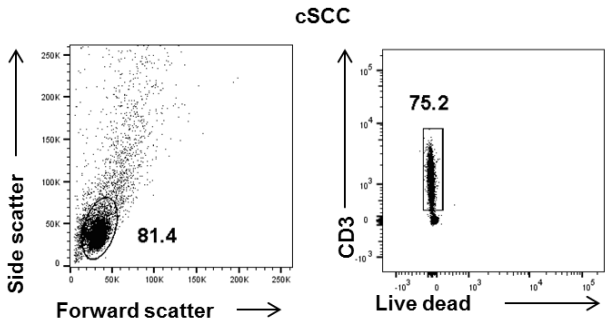

Figure 3.2 Flow cytometry of cSCC immunocytes.

Immunocytes isolated from cSCCs were stained with anti-CD3 antibody and a live / dead stain for flow cytometry. Representative FACS plots are shown, demonstrating that the majority of isolated cells were lymphocytes (left) and that most of the lymphocytes were live $CD3^+$ T cells (right).

Experiments were also performed on non-lesional 'normal skin' from the cSCC patients, these skin samples were excised from areas adjacent to the cSCC (> 6

mm away from the tumour) to enable closure / reconstruction of the wound from cSCC excision. Flow cytometry of immunocytes from normal skin confirmed the presence of lymphocytes and viable $CD3^+$ T cells (Figure 3.3), and although typically only approximately 50,000 T cells were able to be isolated from a 1 cm^2 area of non-inflamed normal skin, this suggests that the normal skin could be a source of T cells that can be used as a patient-matched control.

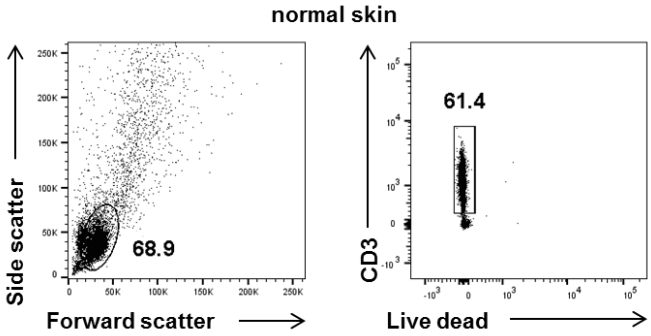

Figure 3.3 Flow cytometry of immunocytes from non-lesional normal skin.
Immunocytes were isolated from non-lesional normal skin from cSCC patients and stained for flow cytometry as per Figure 3.1 and Figure 3.2. Representative FACS plots are shown, demonstrating that lymphocytes and live $CD3^+$ T cell populations can be identified.

In order to determine whether the phenotypic differences in immunocytes isolated from blood and skin tissue were indeed real or due to the fact that immunocytes were isolated from skin but not blood by enzymatic digestion with collagenase and DNAse, experiments were performed to examine whether enzymatic treatment of PBMCs affected cell surface marker expression. Treatment of PBMCs with collagenase I-A and DNAse I for 1.5 hours at 37ºC did not affect cell viability or alter expression of CD3, CD4, CD8, CD25 and CD127 (Figure 3.4, page 73).

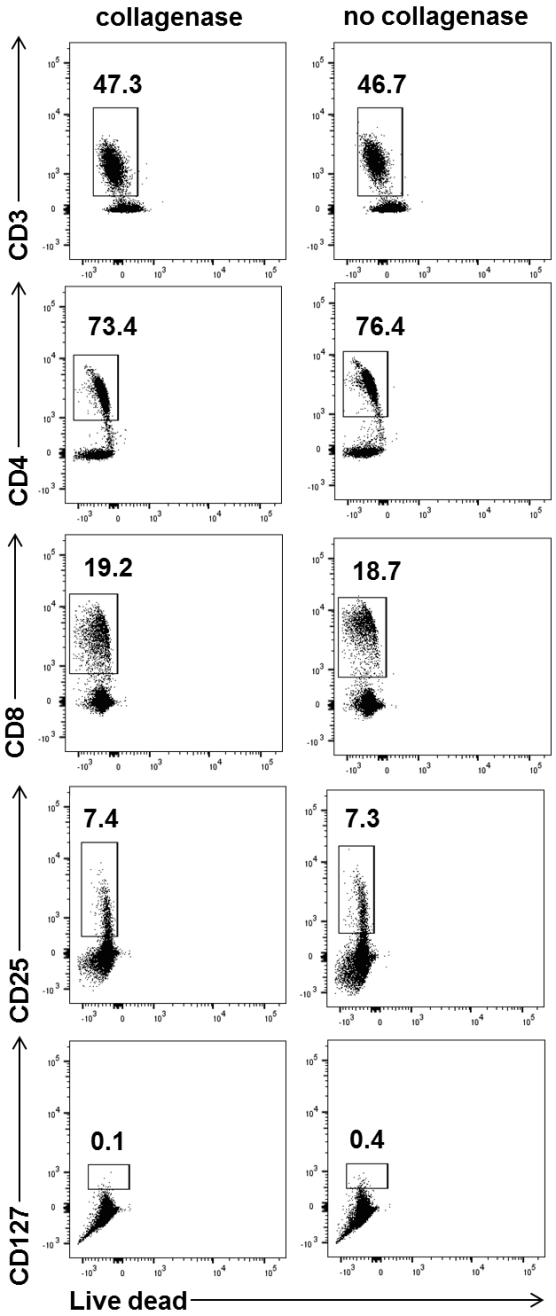

Figure 3.4 Effect of enzymatic treatment on PBMC cell surface marker expression
Representative FACS plots of PBMCs which were isolated from a single individual and either treated with 1 mg/ml collagenase I-A and 10 µg/ml DNAse I for 1.5 hours (left column) or not treated with enzymes (right treatment). Cells were stained with antibodies against CD3, CD4, CD8, CD25 and CD127, and a live dead stain, showing that collagenase and DNAse treatment did not affect cell surface expression of the T cell markers that were tested. Plots shown are representative of three experiments.

Further experiments were performed to assess whether flow cytometry could consistently detect viable $CD4^+$ and $CD8^+$ T cell populations in cSCC. These

experiments showed that many $CD3^+$ T cells were present in cSCC (ranging from 32.4 to 65.7% of the immune cell infiltrate), and that the $CD3^+$ T cells consisted of distinct $CD4^+$ and $CD8^+$ T cell populations, with small populations of double positive and double negative T cells (Figure 3.5, page 75). Given that the sizes of the $CD4^+$ and $CD8^+$ T cell populations determined by FACS meant that enough cells were available for further characterisation and functional analysis, this study focused on the T cell populations in cSCC rather than other immune cells. In addition, the proportions of $CD4^+$ T cells, $CD8^+$ T cells and Tregs in cSCCs determined using flow cytometry were consistent with the relative frequencies of these T cell subsets identified in previous immunohistochemistry experiments performed by the laboratory group (Lai et al., 2016), suggesting that flow cytometry of the isolated immune cells from cSCCs is a relatively accurate method of determining relative frequencies of tumoral immunocyte subtypes. Although experiments were not performed to assess what proportion of the absolute numbers of the different immunocyte cell subsets could be isolated from each tumour due to technical and time limitations, over the course of the study, which included 200 tumours, cell viability remained >99% for all of the cSCCs used for flow cytometry, indicating that the method used for isolating immune cells from cSCCs was not leading to cell death of any particular cell type.

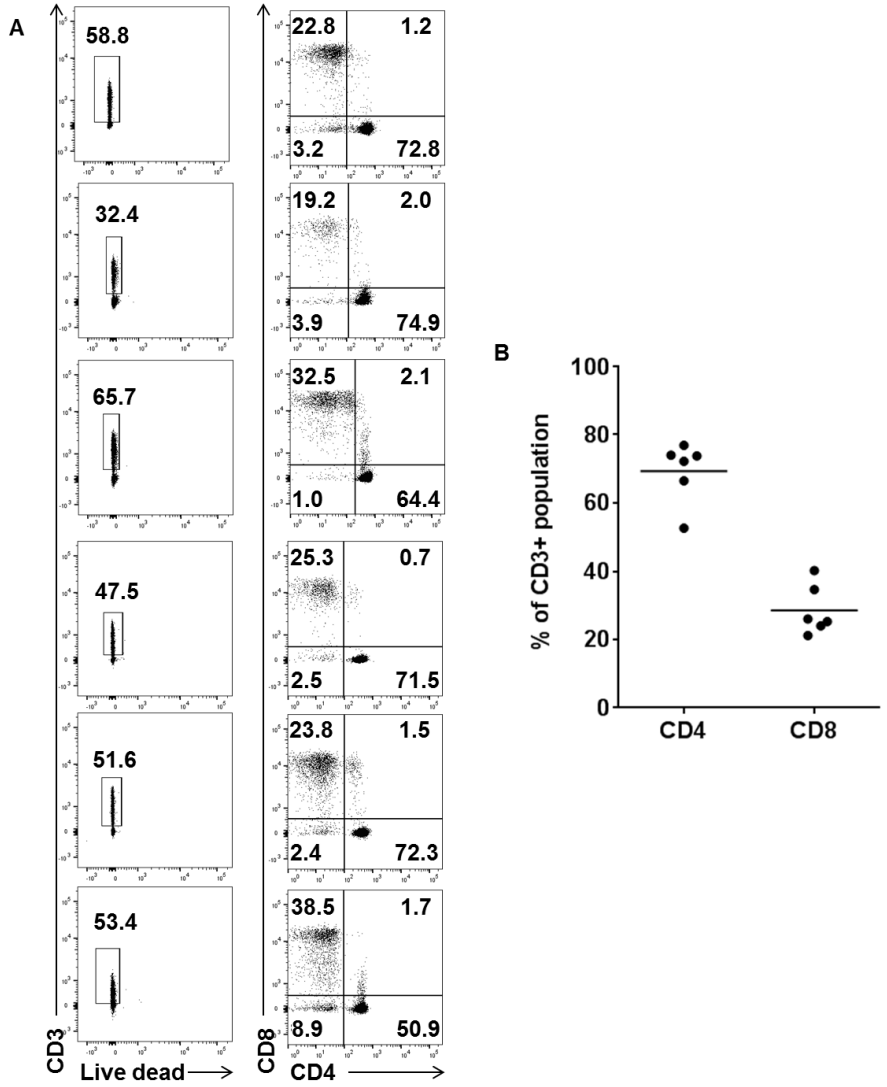

Figure 3.5 Flow cytometry analysis of CD4⁺ and CD8⁺ T cells from cSCC

(A) Immunocytes were isolated from six cSCCs and analysed using flow cytometry, showing that viable CD3⁺, CD4⁺ and CD8⁺ T cell populations could be consistently identified. (B) Graph showing CD4⁺ and CD8⁺ T cell frequencies as a percentage of the live CD3⁺ T cell population in the six cSCCs in (A). Horizontal bars = means.

Although the non-T cell population was not the focus in the current study, preliminary experiments were performed to identify the other immunocytes present in cSCC by FACS. Several flow cytometry panels were attempted in order to determine the feasibility of the panels, and to provide an initial observation of the cellular composition of the cSCC immune infiltrate. γ δ T cells, which are known to play a role in cutaneous carcinogenesis in mice (Girardi et al., 2001), accounted for 1.0-1.9%, 0.2-0.5% and 0.1-0.2% of the live CD45⁺ lymphocyte

populations in peripheral blood, normal skin and cSCC respectively (n=2 subjects), and did not appear to express the NKG2D receptor (Figure 3.6).

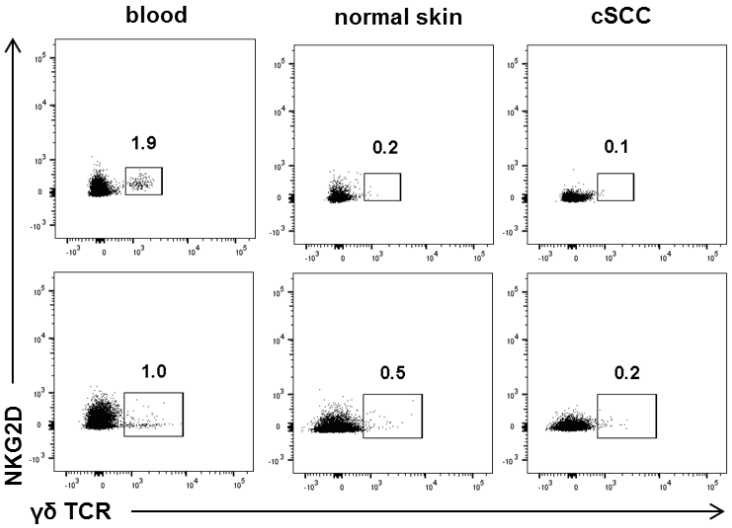

Figure 3.6 Flow cytometry shows few γ δ T cells in cSCC.

FACS plots from two subjects gated on live CD45$^+$ lymphocytes showing γ δ TCR and NKG2D expression in blood, normal skin and cSCC.

CD3$^-$CD56$^+$ NK cells were also scarcely present in cSCC; CD3$^-$CD56$^+$ cells comprised 0.0-0.6% of live lymphocytes in the tumour whereas 10.9-12.0% of live lymphocytes in blood were NK cells (n=2 subjects, Figure 3.7, page 77).

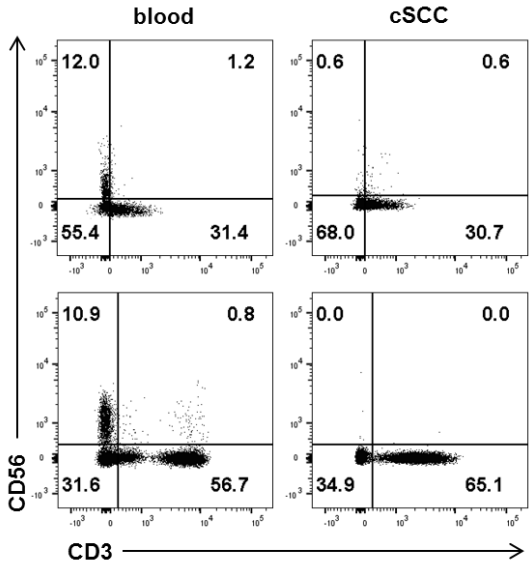

Figure 3.7 Flow cytometric detection of NK cells.

FACS plots from two subjects gated on live lymphocytes showing CD3 and CD56 expression in blood and cSCC. NK cells were considered to be $CD3^{-}CD56^{+}$.

$CD19^{+}$ B cells were also detected by FACS, comprising 2.5-3.8% of live lymphocytes in peripheral blood, 0.2-0.6% of those in normal skin, and 2.6-17.8% of those in cSCC (n=2 subjects, Figure 3.8).

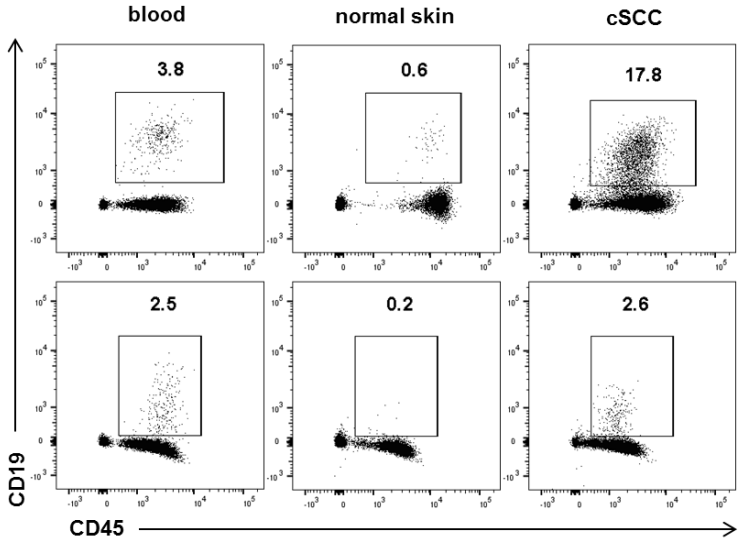

Figure 3.8 Flow cytometry for B cells.

FACS plots from two subjects gated on live lymphocytes showing CD45 and CD19 expression in blood, normal skin and cSCC. B cells were considered to be $CD45^{+}CD19^{+}$.

Expression of CD11c, a marker for monocytes, macrophages, neutrophils and myeloid DCs, and CD14, which is present on monocytes and macrophages, was examined. CD11c was expressed by 4.0% ± 5.2% (mean ± SD) of live cells in blood, 2.8% ± 2.1% of those in normal skin and 8.6% ± 12.9% of those in cSCC (n=6 tumours, Figure 3.9B). CD14 was expressed by 14.4% ± 8.4% of live cells in blood, 6.5% ± 5.0% of those in normal skin and 10.9% ± 7.4% of those in cSCC (n=11 tumours, Figure 3.9C).

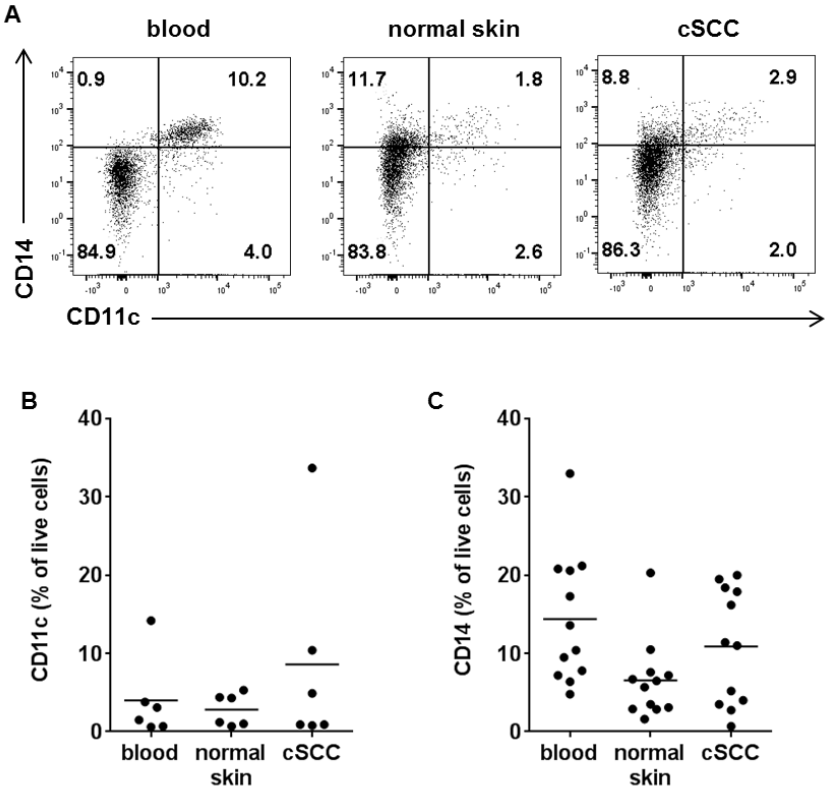

Figure 3.9 Flow cytometry for CD11c and CD14 expressing immunocytes.

(A) Representative FACS plots showing CD11c and CD14 expression in live cells from blood, normal skin and cSCC from the same patient. (B, C) Graphs showing expression of (B) CD11c and (C) CD14 as a percentage of the live cell population in blood, normal skin and cSCC ((B) n=6 tumours, (C) n=12 tumours), horizontal bars = means.

CD68, another marker of monocytes and macrophages, was present on 0.09% ± 0.09% of the live cell population in blood, 4.1% ± 4.2% of those in normal skin and 4.7% ± 7.4% of those in cSCC (n=5 tumours, Figure 3.10).

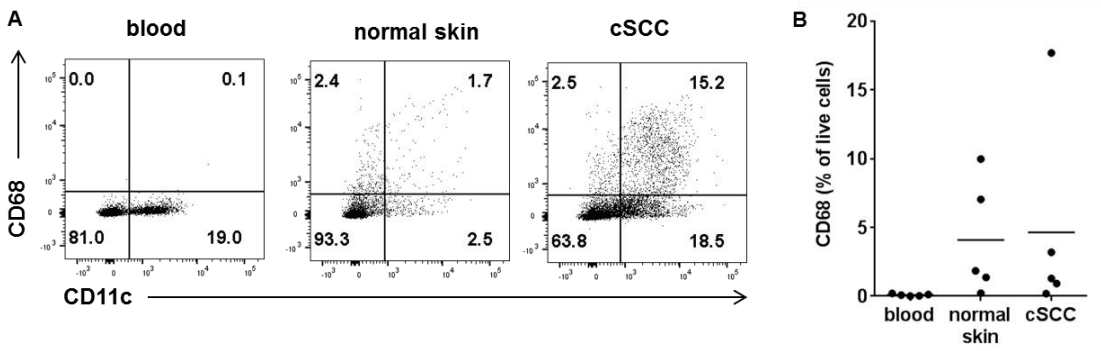

Figure 3.10 Flow cytometry for CD68⁺ immune cells.

Representative FACS plots showing CD11c and CD68 expression in live cells from blood, normal skin and cSCC from the same patient. (B) Graph showing expression of CD68 as a percentage of the live cell population in blood, normal skin and cSCC (n=5 tumours), horizontal bars = means.

CD15, which is present on mature neutrophils, monocytes and promyelocytes, and CD16, expressed by macrophages and NK cells, were also detected in subpopulations of cells in cSCC (Figure 3.11).

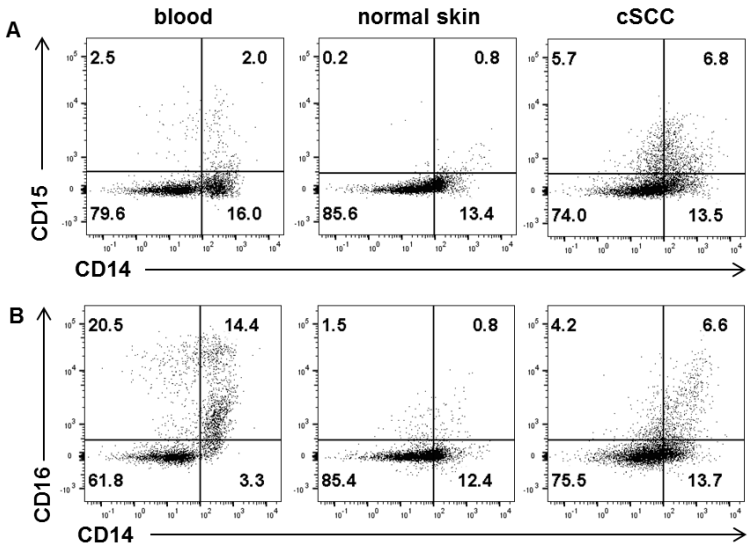

Figure 3.11 Flow cytometry for CD15 and CD16 expressing immunocytes.

(A) CD15 and (B) CD16 plotted against CD14 in live cells from blood, normal skin and cSCC from the same subject.

CD1a was used to identify Langerhans cells, showing that they accounted for 0.0% ± 0.0% of live immunocytes from blood, 2.1% ± 2.0% of those from normal skin, and 1.2% ± 0.9% of those from cSCC (n=6 tumours, Figure 3.12).

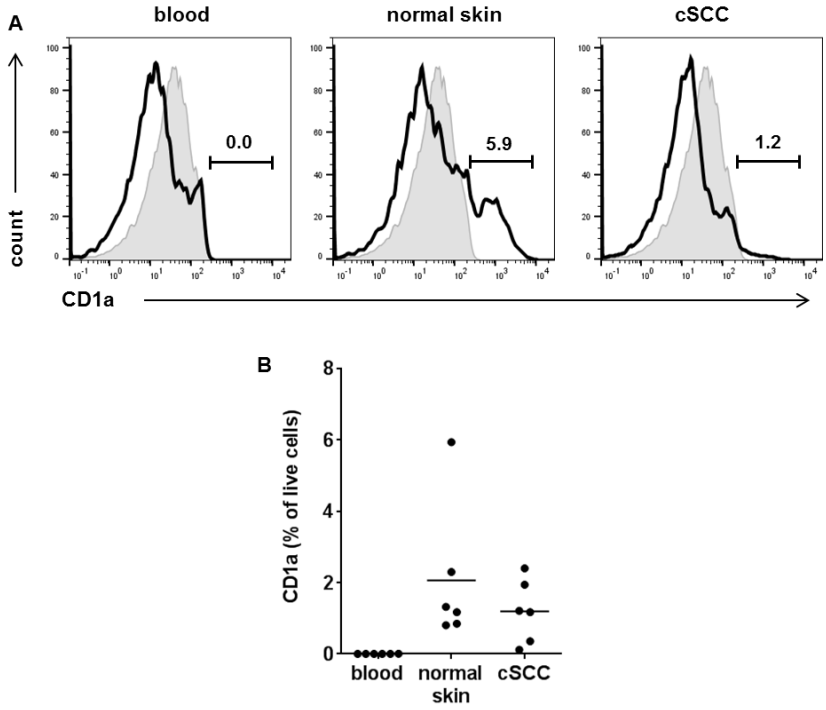

Figure 3.12 Flow cytometric detection of Langerhans cells.

(A) Representative FACS histograms showing CD1a expression in live immunocytes from blood, normal skin and cSCC from the same subject. Grey shaded areas = isotype control. (B) Graph showing $CD1a^+$ cell frequencies as a percentage of the live immune cell population in blood, normal skin and cSCC (n=6 tumours), horizontal bars = means.

The dermal dendritic cell markers, DC-LAMP and DC-SIGN, were also examined by FACS. DC-LAMP was expressed by 0.03% ± 0.06% of live cells from blood, 0.33% ± 0.06% of those from normal skin and 0.23% ± 0.06% of those from cSCC (n=3 tumours, Figure 3.13B). DC-SIGN was present in 0.03% ± 0.06% of live cells from blood, 4.80% ± 6.45% of those from normal skin, and 8.47% ± 8.0% of those from cSCC (n=3 tumours, Figure 3.13C).

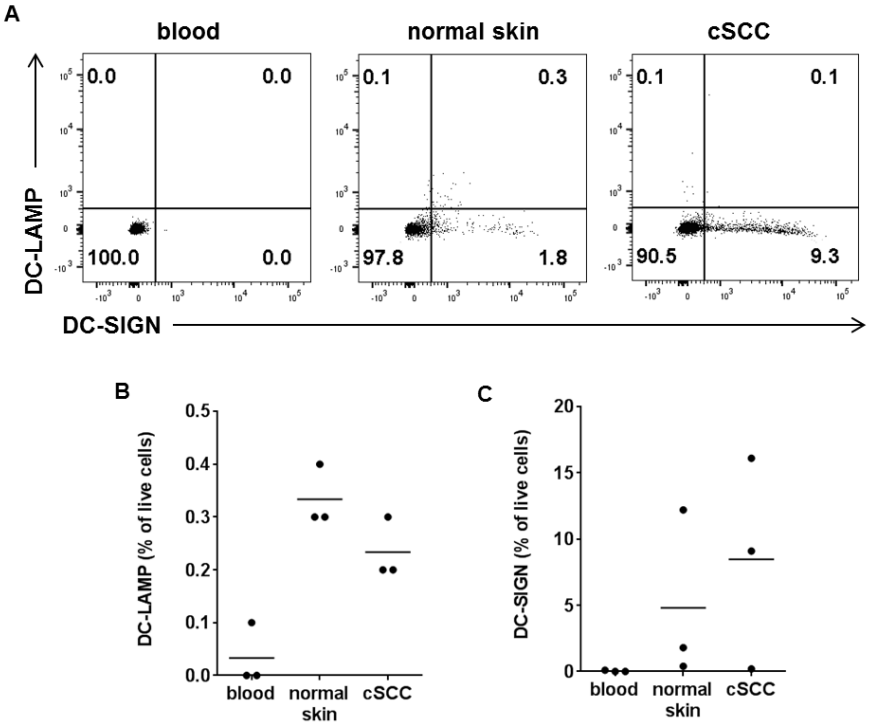

Figure 3.13 Flow cytometric detection of dermal dendritic cell markers.

(A) Representative FACS plots showing DC-LAMP and DC-SIGN expression in live cells isolated from blood, normal skin and cSCC of the same subject. (B, C) Graphs showing percentage of live cells that are (B) DC-LAMP$^+$ and (C) DC-SIGN$^+$ in blood, normal skin and cSCC (n=3 tumours), horizontal bars = means.

CD141$^+$ dermal DCs have been shown to have tolerogenic properties (Chu et al., 2012) and in the current study, CD141 was expressed by 1.7% ± 2.6% of the live immune cell population in blood, 3.8% ± 2.2% of those from normal skin and 13.8% ± 14.3% of those from cSCC (n=3 tumours, Figure 3.14).

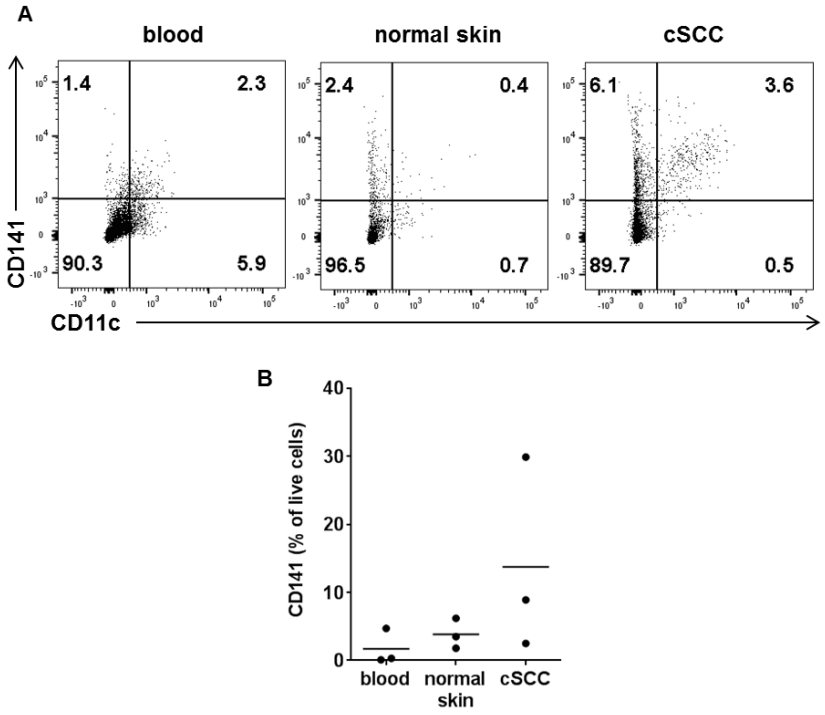

Figure 3.14 Flow cytometry for CD141 expressing immunocytes.

(A) Representative FACS plots gated on live cells demonstrating CD11c and CD141 expression in blood, normal skin and cSCC from the same subject. (B) Graph showing CD141$^+$ cell frequencies as a percentage of the live immune cell population in blood, normal skin and cSCC (n=3 tumours), horizontal bars = means.

CD123 is expressed by plasmacytoid DCs as well as some monocytes, neutrophils, basophils and eosinophils. In the current study, CD123 was detected in 1.1% ± 1.0%, 1.8% ± 1.8% and 5.1% ± 5.7% of the live cell population isolated from blood, normal skin and cSCC respectively (n=3 tumours, Figure 3.15).

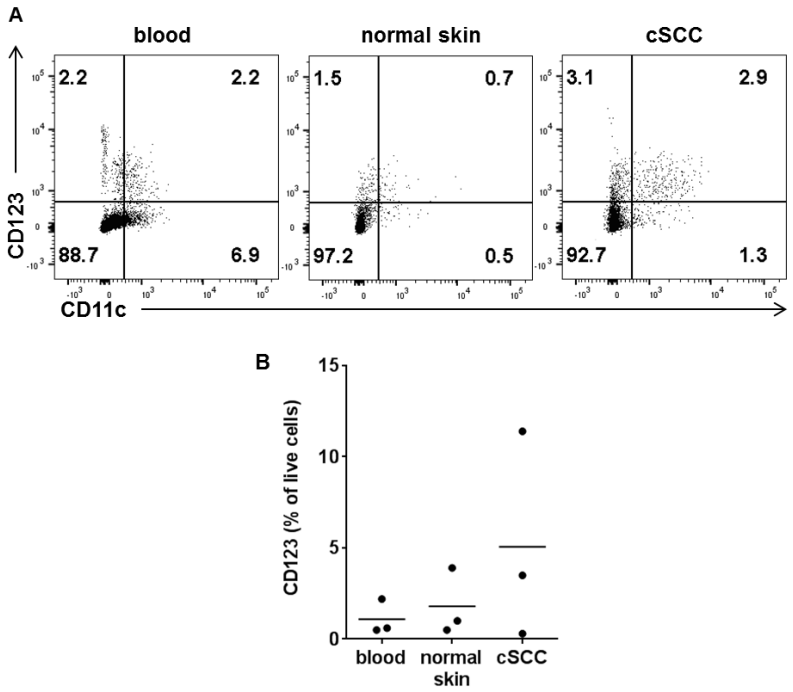

Figure 3.15 Flow cytometry for CD123⁺ cell populations.

(A) Representative FACS plots gated on live cells demonstrating CD11c and CD123 expression in blood, normal skin and cSCC from the same subject. (B) Graph showing CD123⁺ cell frequencies as a percentage of the live immune cell population in blood, normal skin and cSCC (n=3 tumours), horizontal bars = means.

Mast cells, identified as $CD45^+CD117^+$ cells, comprised 0.1% ± 0.1%, 3.7% ± 4.0% and 1.4% ± 2.9% of the live $CD45^+$ cell population from blood, normal skin and cSCC respectively (n=10 tumours), and also expressed Fcε RI and CD203c (Figure 3.16).

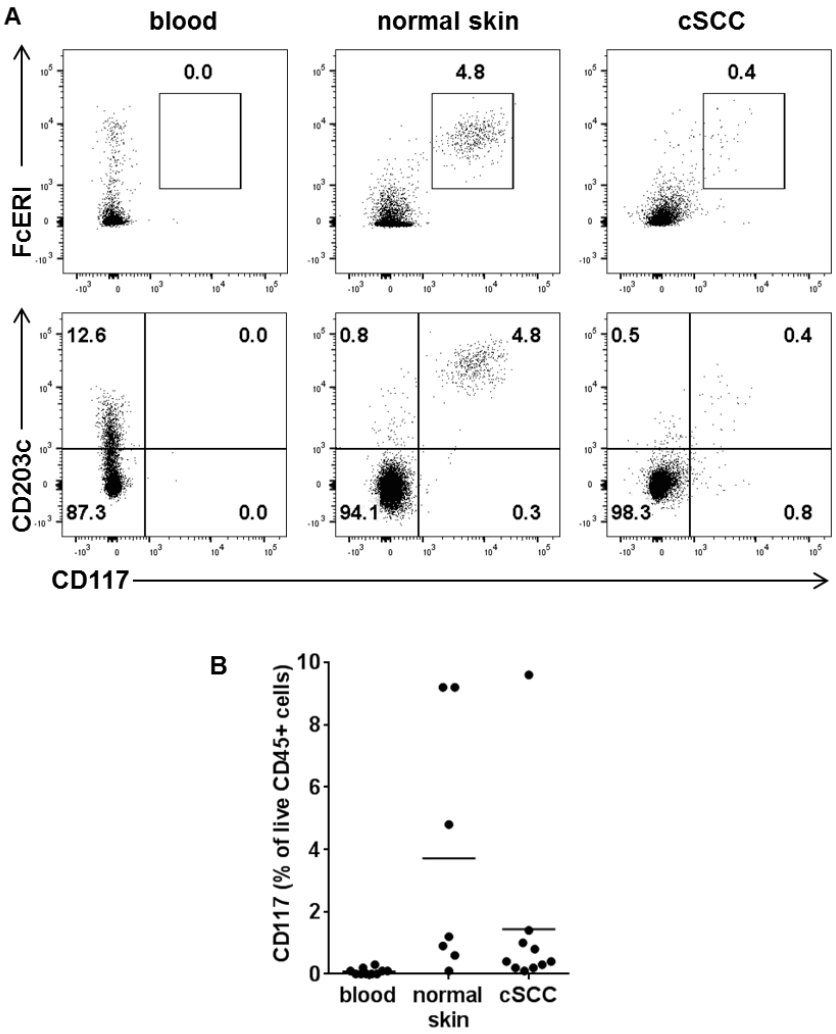

Figure 3.16 Flow cytometric detection of mast cells.

(A) Representative FACS plots showing CD117, Fcε RI and CD203c expression of live $CD45^+$ cells from blood, normal skin and cSCC from the same subject. Mast cells were considered to be $CD45^+CD117^+$. (B) Graph showing the percentage of live $CD45^+$ cells that were $CD117^+$ (n=10 tumours), horizontal bars = means.

Basophils were detected with flow cytometry using 2D7, an intracellular marker specific for basophils. Fcε RI expression appeared to be downregulated in 2D7$^+$ basophils from cSCC (Figure 3.17a), basophils comprised 0.69% ± 0.55%, 0.75% ± 0.63% and 0.31% ± 0.38% of live CD45$^+$ cells in blood, normal skin and cSCC respectively (n=9 tumours, Figure 3.17b).

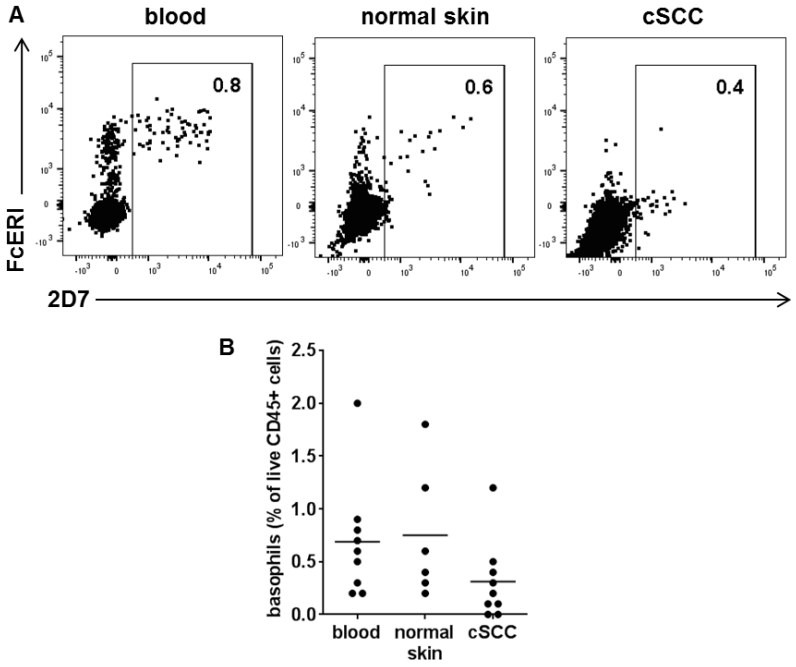

Figure 3.17 Flow cytometry for basophils.

(A) Representative FACS plots showing expression of the basophil marker 2D7 and Fcε RI in live CD45$^+$ cells from blood, normal skin and cSCC from the same subject. (B) Graph demonstrating frequencies of basophils in blood, normal skin and cSCC (n=9 tumours), horizontal bars = means.

3.2.2 *In vitro* cSCC culture

Preliminary experiments were conducted to attempt to culture cSCCs *in vitro*, with a long term aim to develop an *in vitro* cSCC system that would allow investigation into the effects of manipulation of tumoral immunity in this cancer. Initially, cSCC samples were cultured en bloc as whole tissue explants. cSCC tissue was washed and then cultured in a petri dish containing RPMI medium + 10% FBS + 100 U/ml penicillin + 100 µg/ml streptomycin + 1mM sodium pyruvate for 24 hours at 37ºC or 32ºC (to simulate the temperature of the surface of skin *in vivo*), prior to being snap frozen in liquid nitrogen and cryosectioned. H&E

staining demonstrated grossly oedematous tissue with marked epidermal spongiosis and splits appearing between the epidermis and dermis (seen in 2 tumours at each temperature, Figure 3.18). Due to the poor state of the tissues, this method of culturing cSCCs was not continued.

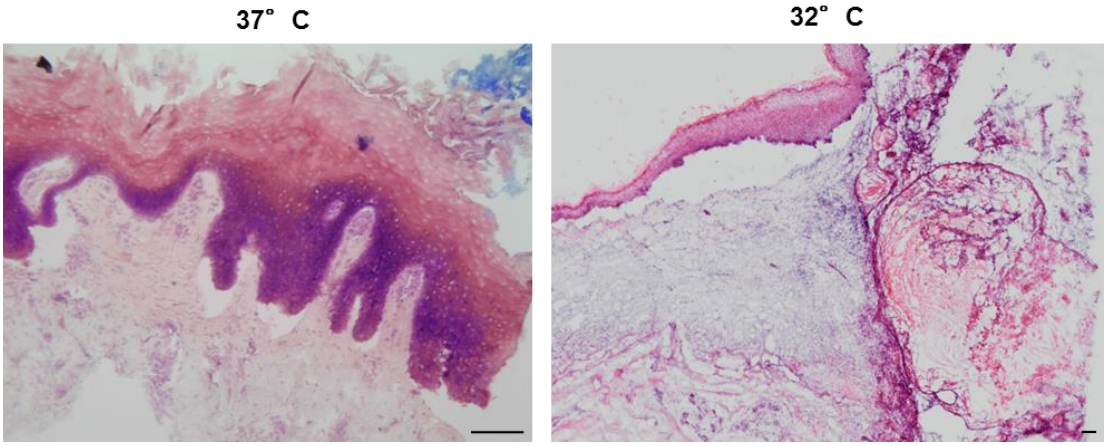

Figure 3.18 *In vitro* whole explant culture of cSCC for 24 hours leads to tissue damage.

cSCC samples were cultured as whole tissue explants in RPMI medium + 10% FBS + penicillin/streptomycin + sodium pyruvate for 24 hours at either 37ºC (left) or 32ºC (right). Samples were then snap frozen in liquid nitrogen, cryosectioned and stained with H&E. Representative images from 2 tumours are shown, scale bars = 100 µm.

Experiments were then performed to isolate cSCC keratinocytes from primary tumours for culture. Following enzymatic digestion of the tumour sample, cell filtration and density centrifugation, the band on top of the 9% iodixanol density layer was obtained (see Methods section 2.8, page 67); this band contained cells of lower density, which appeared larger than lymphocytes. These cells were cultured in keratinocyte growth medium, and proliferated without the requirement of feeder cells. The morphology of the cells appeared consistent with those of keratinocytes, but there was heterogeneity between different cells, with some cells appearing large with atypical nuclei (n=5 tumours, Figure 3.19, page 87). Cells were passaged prior to cultures reaching confluence, and cells from 3 tumours continued to proliferate even after at least 5 passages (4 weeks).

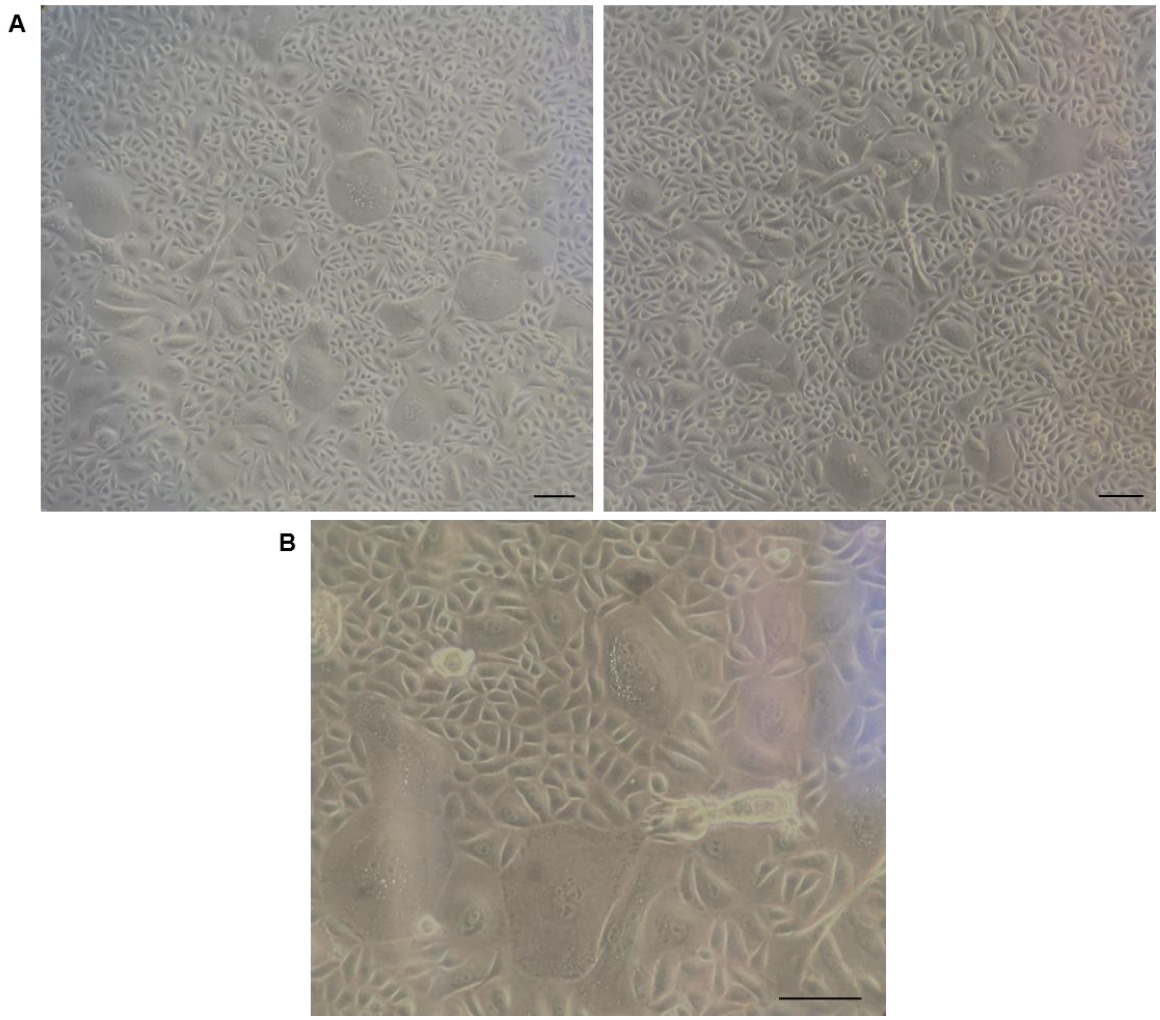

Figure 3.19 Culture of isolated primary cSCC cells.

(A, B) Representative (A) low magnification and (B) high magnification micrographs of isolated primary cSCC cells in culture. Photos are representative of cells isolated from 5 cSCCs, scale bars = 100 μm.

Immunofluorescence microscopy was performed to characterise the cultured primary cSCC cells. A multi-cytokeratin stain was used to determine expression of cytokeratins 4, 5, 6, 8, 10, 18 and 18, which are intermediate filament cytoskeletal proteins present in epithelial cells, and separate stains were also performed for cytokeratin 16, normally expressed in the skin by dividing suprabasal keratinocytes. The cSCC cells were then counterstained with DAPI, which shows nuclear DNA. Many of the cells expressed cytokeratin in the cytoplasm and cytokeratin 16 appeared to be present in the larger cells, suggesting that proliferating keratinocytes were present in the cSCC cell cultures (Figure 3.20, page 88).

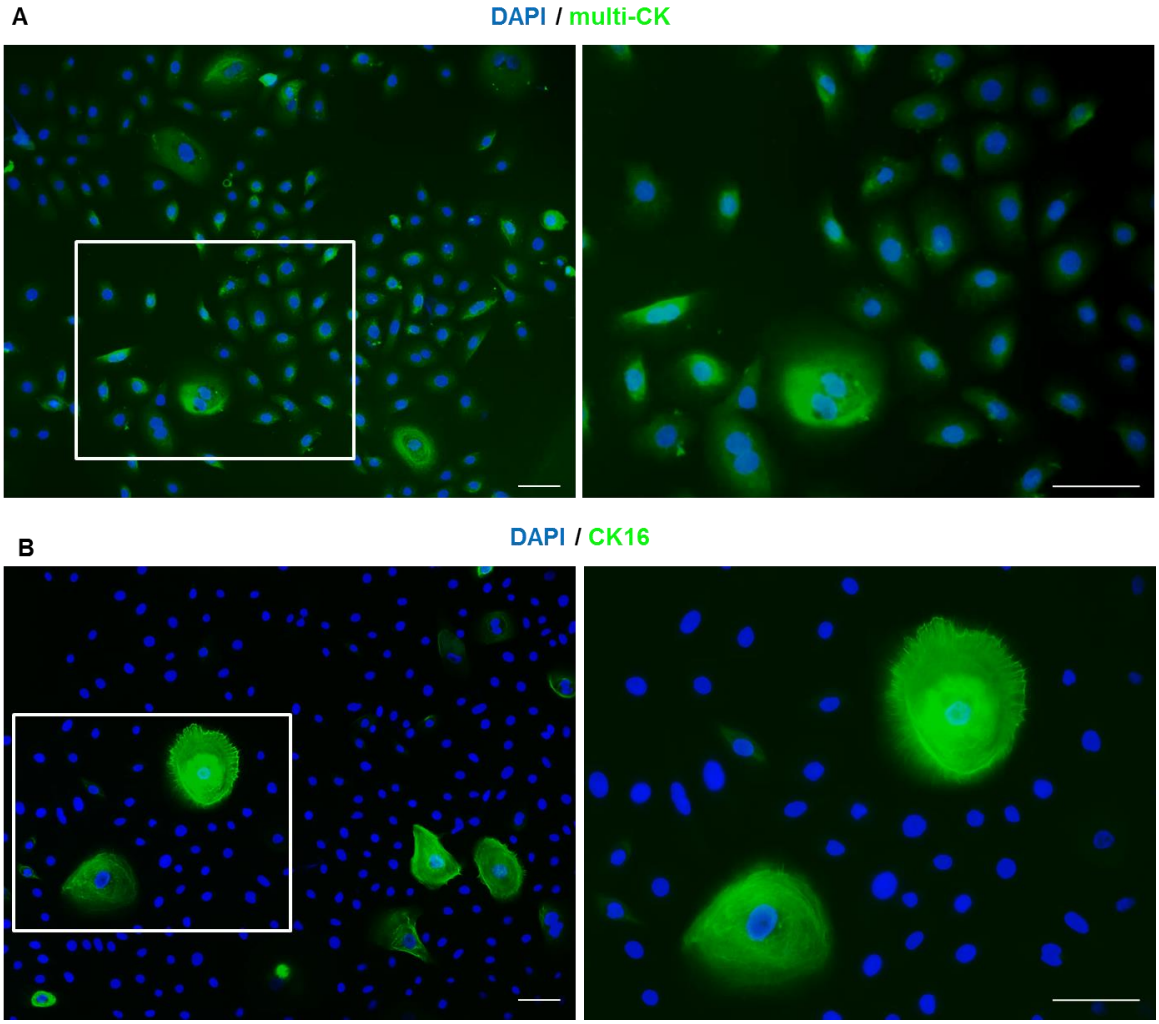

Figure 3.20 Expression of cytokeratins in cultured cSCC cells.

(A, B) Immunofluorescence microscopy images of cSCC cells stained with DAPI and (A) cytokeratins 4, 5, 6, 8, 10, 13 and 18 (multi-CK), and (B) cytokeratin 16 (CK16). Photos on the left show low magnification, high magnification images of the areas indicated by the white boxes are shown on the right. Images are representative of cells from 3 cSCCs.

Immunofluorescence microscopy was also performed to examine expression of mucin 1 (MUC1, also known as epithelial membrane antigen), a marker present in 95% of cSCCs (Cooper et al., 2004). MUC1 staining of the cSCC cells showed that some of the cells expressed this marker in the cytoplasm, suggesting that they could be cSCC keratinocytes (Figure 3.21, page 89).

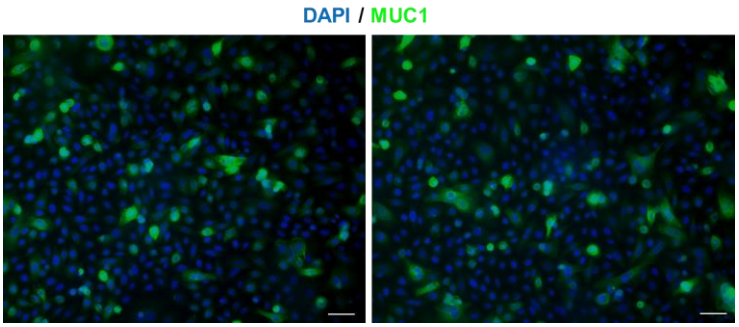

Figure 3.21 Expression of MUC1 in cultured cSCC cells.

Immunofluorescence microscopy images of cSCC cells stained with DAPI (blue) and MUC1 (green), images representative of cells from 3 cSCCs, scale bars = 50 μm.

cSCC cells were also examined for expression the inhibitory ligand PD-L1 and its receptor PD-1. PD-L1 staining was observed in the cytoplasm of many of the cSCC cells (Figure 3.22A), however, PD-1 was only scarcely present (Figure 3.22B).

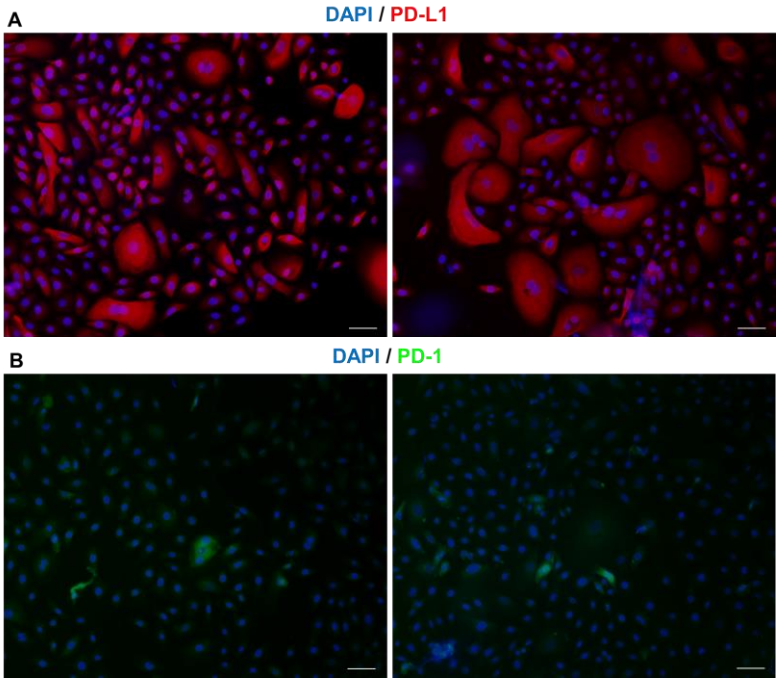

Figure 3.22 PD-L1 is expressed by cultured cSCC cells, whilst PD-1 expression is minimal.

(A, B) Immunofluorescence microscopy images of cSCC cells stained with DAPI (blue) and (A) PD-L1 (red), or (B) PD-1, green. Images representative of cells from 3 cSCCs, scale bars = 50 μm.

3.2.3 Confocal microscopy of cSCC

Confocal microscopy of frozen cSCC tissue sections was undertaken to enable multiple markers to be simultaneously visualised. Initially, single stains were performed to determine a working method for cSCC immunofluorescence staining / confocal microscopy, and staining was considered positive when fluorescence intensity was greater than the background fluorescence from control sections that were incubated with the relevant fluorophore-conjugated secondary antibody without prior incubation with any primary antibody. Single stains showed that $CD3^+$ cells (Figure 3.23A), $CD4^+$ cells (Figure 3.23B), $FOXP3^+$ cells (Figure 3.23C) and $CD8^+$ cells (Figure 3.23D) were abundant in cSCCs, with CD3, CD4 and CD8 present on cell membranes, whereas FOXP3 was nuclear.

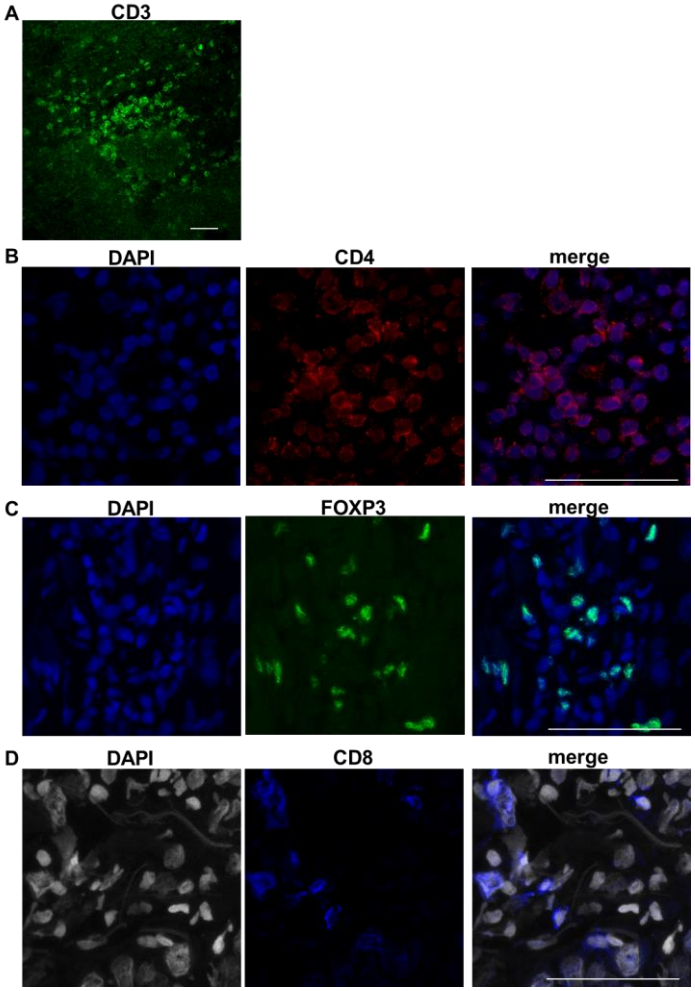

Figure 3.23 Development of single and double staining panels for confocal microscopy.

Representative confocal microscopy images showing staining for (A) CD3, (B) DAPI and CD4, (C) DAPI and FOXP3, and (D) DAPI and CD8 from separate cSCC sections. Images representative of at least 3 cSCCs, scale bars = 50 μm.

Staining for multiple markers simultaneously required the primary and secondary antibodies relevant for each marker not to cross-react, as well as minimally overlapping fluorophore emission spectra. Therefore, the design of the immunofluorescence staining panels needed careful consideration to ensure that the primary antibodies were of different isotypes/from different host species, and that each of the fluorophore-conjugated secondary antibodies were specific for a single primary antibody isotype and be derived from a different host species from the primary antibodies. CD4 and FOXP3 were co-stained with DAPI, showing that CD4 was present on the cell membranes of the T cells in cSCCs, and FOXP3 was present in the nuclei of some of the $CD4^+$ T cells, suggesting that they were Tregs (Figure 3.24).

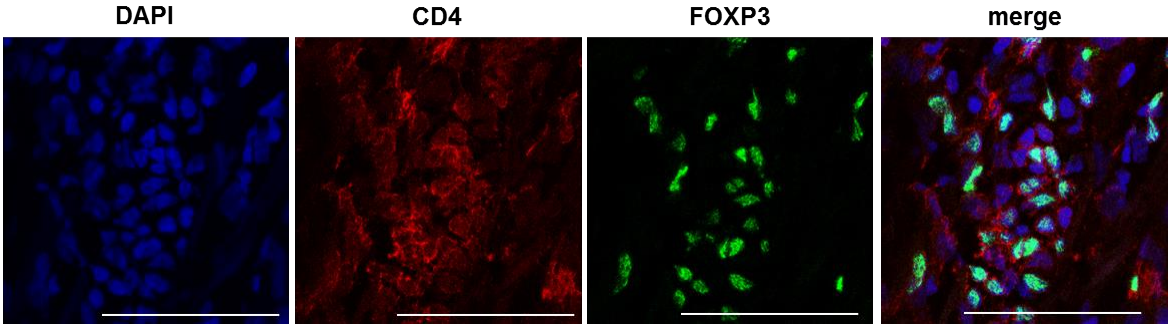

Figure 3.24 Development of three colour panel for confocal microscopy.

Representative confocal microscopy images showing staining for DAPI, CD4 and FOXP3. Images representative of 3 cSCCs, scale bars = 50 μm.

Further experiments were undertaken determine whether staining for 3 cell markers in addition to a DAPI nuclear counterstain was possible. Four-colour confocal microscopy for CD4, CD8, FOXP3 and DAPI demonstrated that $CD4^{+}FOXP3^{-}$, $CD4^{+}FOXP3^{+}$, and $CD8^{+}$ T cells could clearly be identified in the cSCC immune infiltrate (Figure 3.25, page 93).

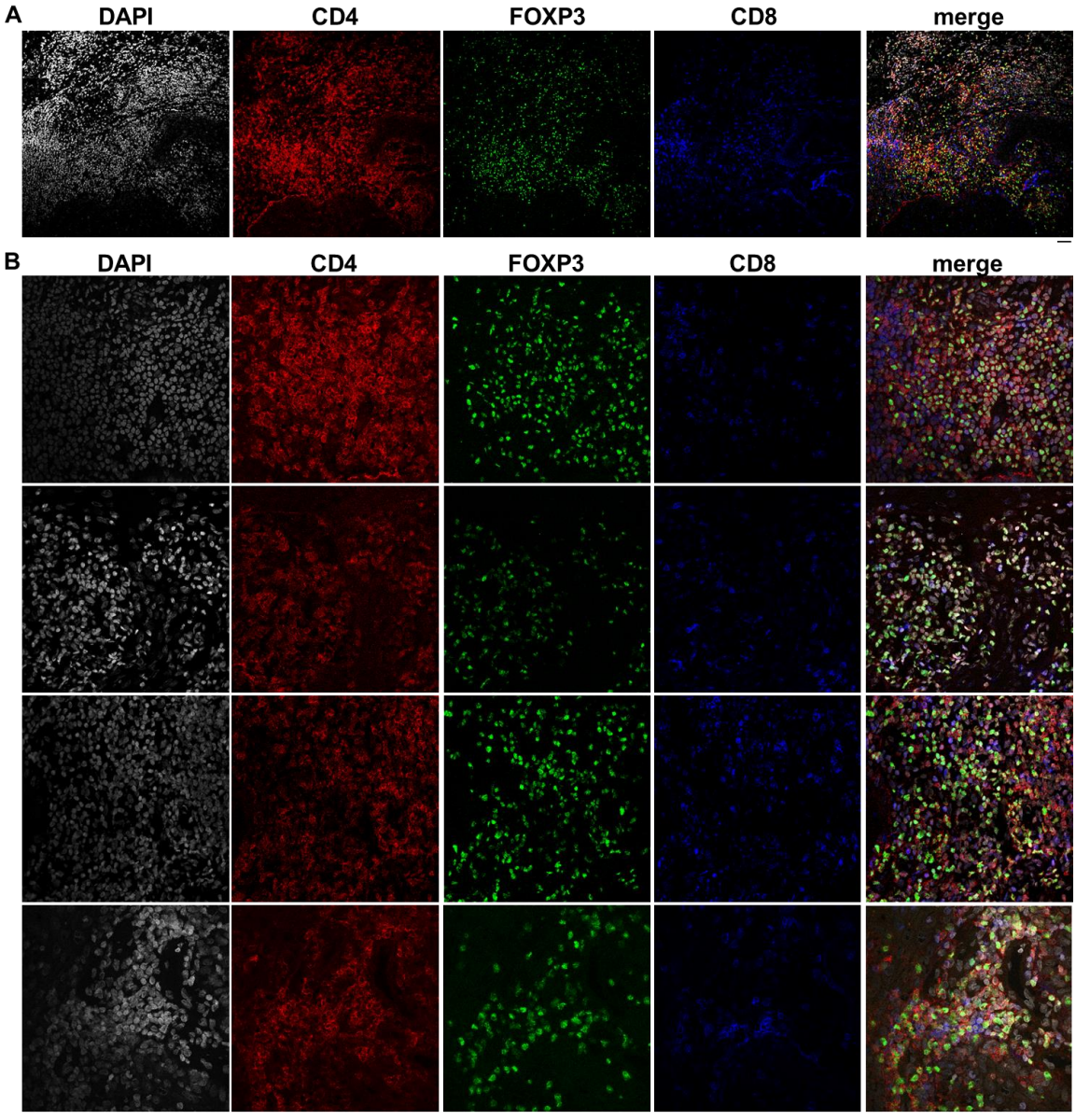

Figure 3.25 Development of four colour confocal microscopy panel.

(A) Low magnification and (B) high magnification images of cSCC sections stained for DAPI, CD4, FOXP3 and CD8. Images representative of at least 3 fields of view in 5 cSCCs. Scale bars = 50 μm.

3.3 Discussion

As it is recognised that host immune responses can restrict cancer development (Hanahan and Weinberg, 2011, Schreiber et al., 2011, Shankaran et al., 2001, Shimizu et al., 1999), that dysfunctional immunity is characteristic of many tumours (Euvrard et al., 2003, Baitsch et al., 2011, Curiel et al., 2004), and that therapies that enhance anti-tumour immunity can improve clinical outcomes in

cancer (Topalian et al., 2012, Hodi et al., 2010), investigating mechanisms that suppress anti-tumour immunity will likely identify new potential therapeutic targets. As the procurement of tumour tissue from human cSCCs is facilitated by the high incidence of these tumours in the UK and their accessible location on the skin, one of the benefits of using cSCCs for the study of cancer immunology is that large numbers of tumours can be obtained for research. In the current study, heterogeneity between different tumours was observed, highlighting the necessity of having sufficient sample numbers when studying patient-derived cSCCs to ensure validity of the results.

A variety of different immune cells have been implicated in anti-tumour immunity, and in this chapter, preliminary experiments were performed to determine the cellular composition of the cSCC immune infiltrate using flow cytometry, as this approach enables multiple parameters to be simultaneously analysed. In line with other flow cytometry studies analysing T cells in cSCC (Clark et al., 2008, Freeman et al., 2014), the current study identified T cells as the predominant cell type in this tumour. Nearly all T cells isolated were viable, and $CD4^+$ and $CD8^+$ cell subpopulations could consistently be identified, suggesting that these cells could be sorted and used for functional assays. In addition, treatment of PBMCs with collagenase and DNAse (in the same conditions as those used for isolating immunocytes from skin tissue samples) did not alter viability or T cell marker expression, confirming that the method used in this study for isolating immunocytes from skin enables reliable *ex vivo* phenotypic analysis to be undertaken. However, although the relative frequencies of the different T cell subsets determined by flow cytometry were in line with those ascertained previously using immunohistochemistry (Lai et al., 2016), further experiments would be helpful to establish what proportion of the absolute numbers of cells of each cell type can be isolated from each tumour and to optimise the cell yield. Confocal microscopy also indicated that T cells were the major immune cell type in cSCC, and confirmed the presence of $CD4^+$ T cells, $CD8^+$ T cells and $FOXP3^+$Tregs within the infiltrate. The use of confocal microscopy for examining the immune infiltrate in this study highlights the potential for future experiments to be performed which investigate the patterns of cell-cell interactions between different cell types in cSCCs by using image analysis to determine colocalisation coefficients. Other initial experiments undertaken for flow cytometry panel design helped to identify other immunocytes in cSCC, demonstrating that $\gamma\delta$ T cells, NK cells, basophils and mast cells appeared to be infrequent, whilst relatively larger proportions of B cells, macrophages and DCs were observed.

Pilot experiments were conducted to determine the feasibility of establishing a primary human cSCC *in vitro* model to enable future investigation into the effects of manipulating immune mechanisms in this tumour. Currently, human cSCC models that exist include primary cell lines (Purdie, 2011), three-dimensional *in vitro* organotypic models (Commandeur et al., 2009), and animal models where human cSCC cell lines, genetically modified human keratinocytes or fresh patient-derived tumour are injected or grafted onto the skin of nude mice (Belkin et al., 2013, Park et al., 2005, Dajee et al., 2003). In the current study, a 24 hour *ex vivo* cSCC whole tissue explant culture was attempted, which showed that the tissue did not remain viable after this duration of culture. Culture of the cells isolated from the low density band (non-lymphocyte portion) of cells isolated from cSCCs showed that these cells could proliferate readily and continuously *in vitro*. Many of these cells expressed cytokeratins and MUC1, providing support for them being cSCC keratinocytes. However, the purity of these cultures remains to be determined, as it is possible that other cell types (e.g. fibroblasts) and benign keratinocytes (which could undergo genomic/chromosomal alterations *in vitro*) may contaminate the cultures. Therefore, further experiments (e.g. genome sequencing) are required to ascertain whether these patient-derived primary cells from cSCCs are indeed truly malignant keratinocytes. However, the inhibitory ligand PD-L1 was found to be expressed by many of the cultured cSCC cells, particularly by the larger, differentiating and dysplastic cells (Figure 3.22, page 89). This may indicate that PD-L1 may have a role in the cSCC dysplastic process, and that these cells could be used in future experiments for the investigation of the PD-1 / PD-L1 axis in this tumour.

This results chapter establishes that immune cells, especially T cells, can be isolated from cSCCs for flow cytometry, which raises the potential for further experiments to be conducted in cSCC to investigate tumour immunity. T cells form an important component of the anti-tumour immune response in many cancers, and the abundance of T cells in cSCC suggests that they are likely to play a key role in the pathogenesis of this neoplasm. Therefore, further phenotypic and functional characterisation of the tumoral T cells, as undertaken in the subsequent chapters of this thesis, will be essential to identify the mechanisms for the inability of these T cells to mount an effective response in cSCC.

Chapter 4: Characterisation of regulatory T cells in cSCC

4.1 Introduction

Most cSCCs are surrounded by an immune cell infiltrate, yet this infiltrate is generally incapable of mounting a successful anti-tumour response, resulting in the growth and persistence of cSCCs. Tregs, which have a physiological function in maintaining immunological self-tolerance and homeostasis, may constitute a mechanism by which cancers can escape anti-tumour immunity. Increased numbers of tumour infiltrating Tregs are associated with poorer clinical outcome in various cancers, suggesting that Tregs suppress immune responses within the tumoral environment (Curiel et al., 2004, Deng et al., 2010, Bates et al., 2006, Ichihara et al., 2003).

Although Tregs have previously been reported in cSCCs (Clark et al., 2008), detailed characterisation of tumoral Tregs in cSCC remains lacking. Therefore, in the current study, tumoral Tregs were characterised to determine whether they inhibit tumoral effector T cell responses. Targeting T cell costimulatory receptors such as OX40 and 4-1BB (Simpson et al., 2013, Taraban et al., 2002, Piconese et al., 2008, Marabelle et al., 2013, Bulliard et al., 2014) and inhibitory receptors such as CTLA-4 (Peggs et al., 2009, Simpson et al., 2013, Hodi et al., 2010), which are present on Tregs, appear to be promising immunotherapeutic approaches for treating cancer. Therefore, investigating the role of Tregs in cSCC will help to determine whether tumoral Tregs form a suitable target for pharmacological treatment of this neoplasm.

The aims of this chapter are to:

1) examine the location and frequencies of tumoral Tregs in cSCC,

2) identify phenotypic markers expressed by the tumoral Tregs including the skin homing markers CLA and CCR4,

3) investigate the functional ability of tumoral Tregs to suppress effector responses, and

4) assess the ability of CTLA-4 inhibitors and 4-1BB and OX40 agonists in enhancing tumoral effector T cell function.

4.2 Results

4.2.1 Distribution of T cells in cSCC

cSCCs are infiltrated by immune cells, and immunohistochemistry conducted on archived FFPE cSCCs showed accumulation of $CD3^+$ T cells in the stroma around islands of tumour keratinocytes (i.e. peritumoral), whilst $CD3^+$ T cells within tumour cell nests (i.e. intratumoral) were found less frequently (Figure 4.1 and Appendix Figure 7.1, page 243). Immunohistochemistry also detected $CD4^+$ helper T cells, $CD8^+$ cytotoxic T cells and $FOXP3^+$ Tregs in the tumoral immune infiltrate (Figure 4.2, page 99 and Appendix Figure 7.2, page 243).

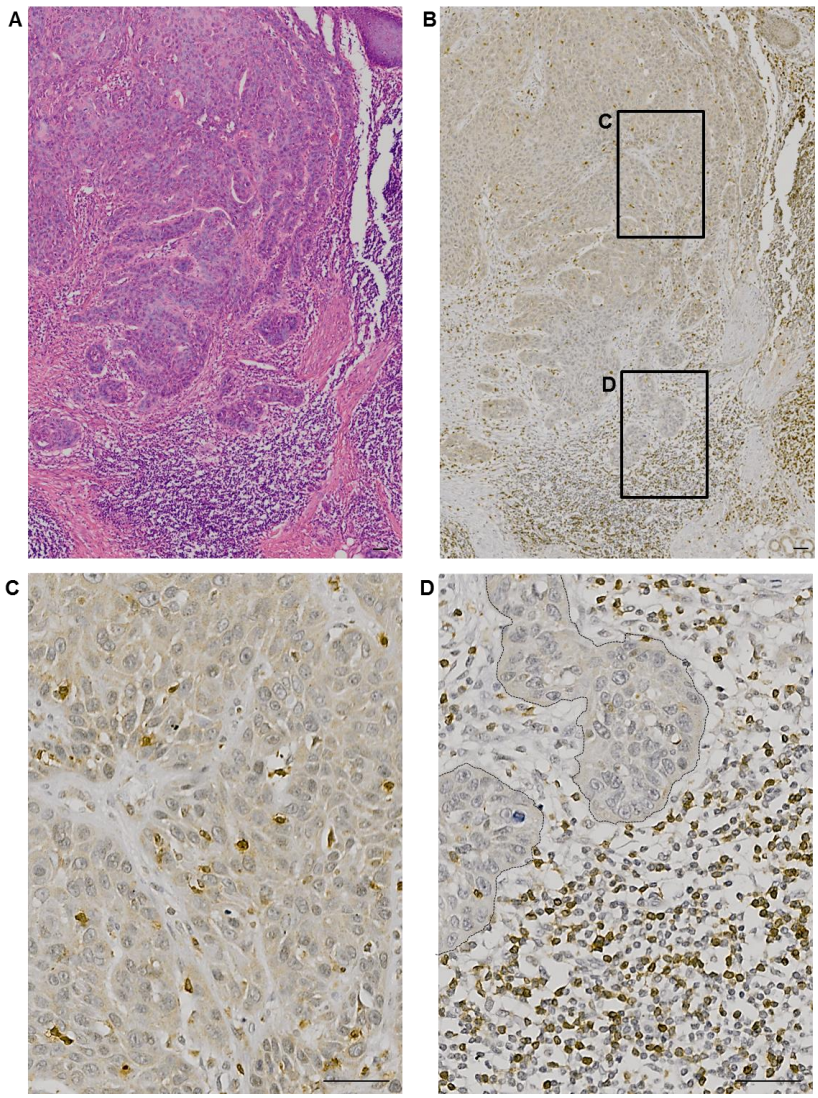

Figure 4.1 Distribution of T cells in cSCC.

(A) Haematoxylin and eosin stain of cSCC. (B) Sequential cSCC section showing immunohistochemical staining of CD3 in brown. (C & D) Higher magnification of $CD3^+$ T cells in (C) intratumoral and (D) peritumoral areas. Images representative

of 10 cSCCs, dashed line in (D) = tumour outline, scale bars = 50 μm.

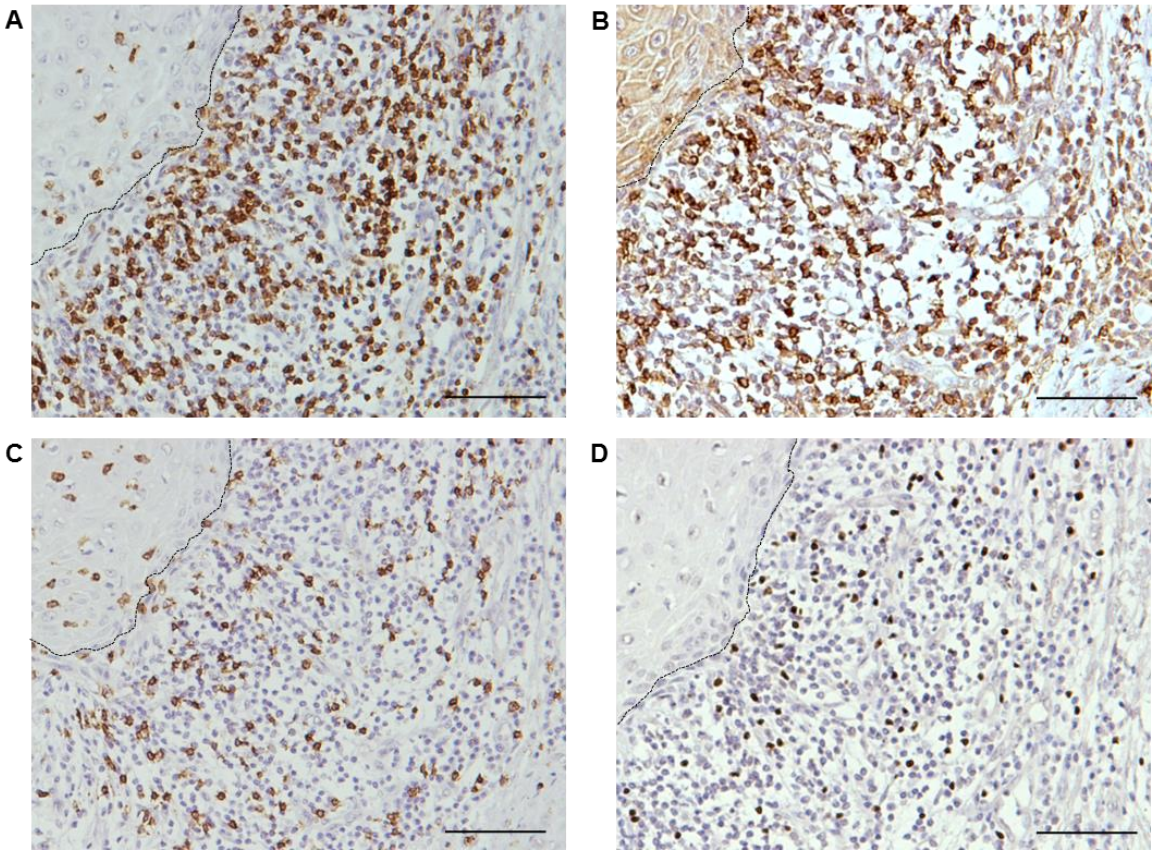

Figure 4.2 Immunohistochemistry of T cell subsets in cSCC.
Immunohistochemical staining of (A) CD3, (B) CD4, (C) CD8 and (D) FOXP3 in sequential cSCC sections. Images representative of 10 cSCCs. Dashed lines = tumour outlines, scale bars = 50 μm.

Using anti-cytokeratin (CK) 16 to delineate the tumour islands, $CD3^+$ T cells (Figure 4.3, page 100) and $FOXP3^+$ Tregs (Figure 4.4, page 101) were detected surrounding cSCCs with immunofluorescence microscopy. Confocal microscopy

of cSCCs indicated close approximation of tumoral Tregs (identified by nuclear FOXP3 and cell membrane CD4) and $CD4^{+}FOXP3^{-}$ T cells and, separately, $CD8^{+}$ T cells (Figure 4.5, page 102), suggesting contact dependent interactions between Tregs and effector T cells in this tumour.

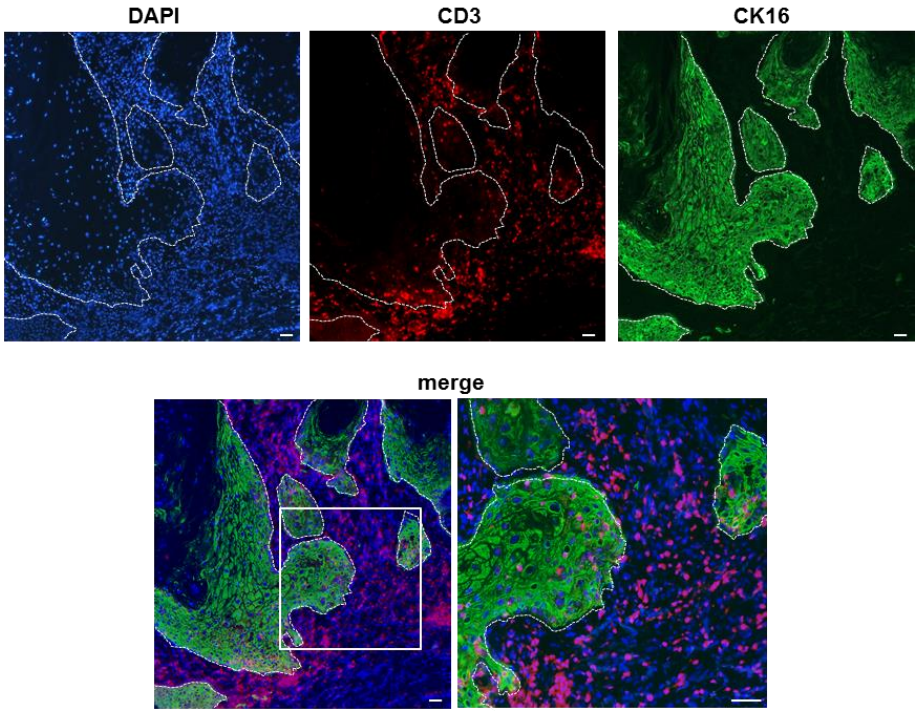

Figure 4.3 Immunofluorescence microscopy of tumoral $CD3^{+}$ T cells.

Immunofluorescence staining demonstrating $CD3^{+}$ T cells in cSCC. Cytokeratin (CK) 16 staining highlights tumour keratinocytes. Images representative of 5 cSCCs. Dashed lines = tumour outlines, scale bars = 50 μm.

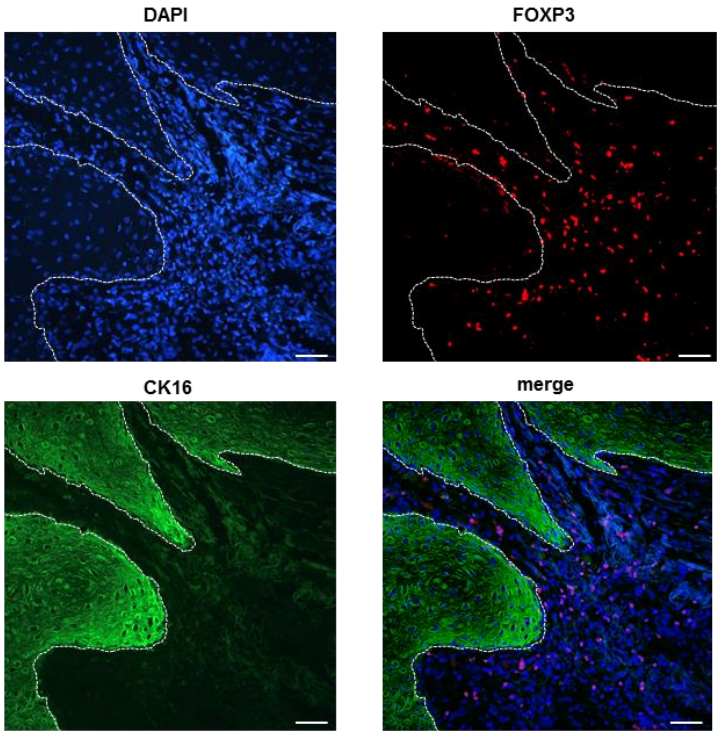

Figure 4.4 Immunofluorescence microscopy of FOXP3⁺ Tregs in cSCC.

Immunofluorescence microscopy of tumoral FOXP3⁺ Tregs. Cytokeratin (CK) 16 staining highlights tumour keratinocytes. Images representative of 5 cSCCs. Dashed lines = tumour outlines, scale bars = 50 μm.

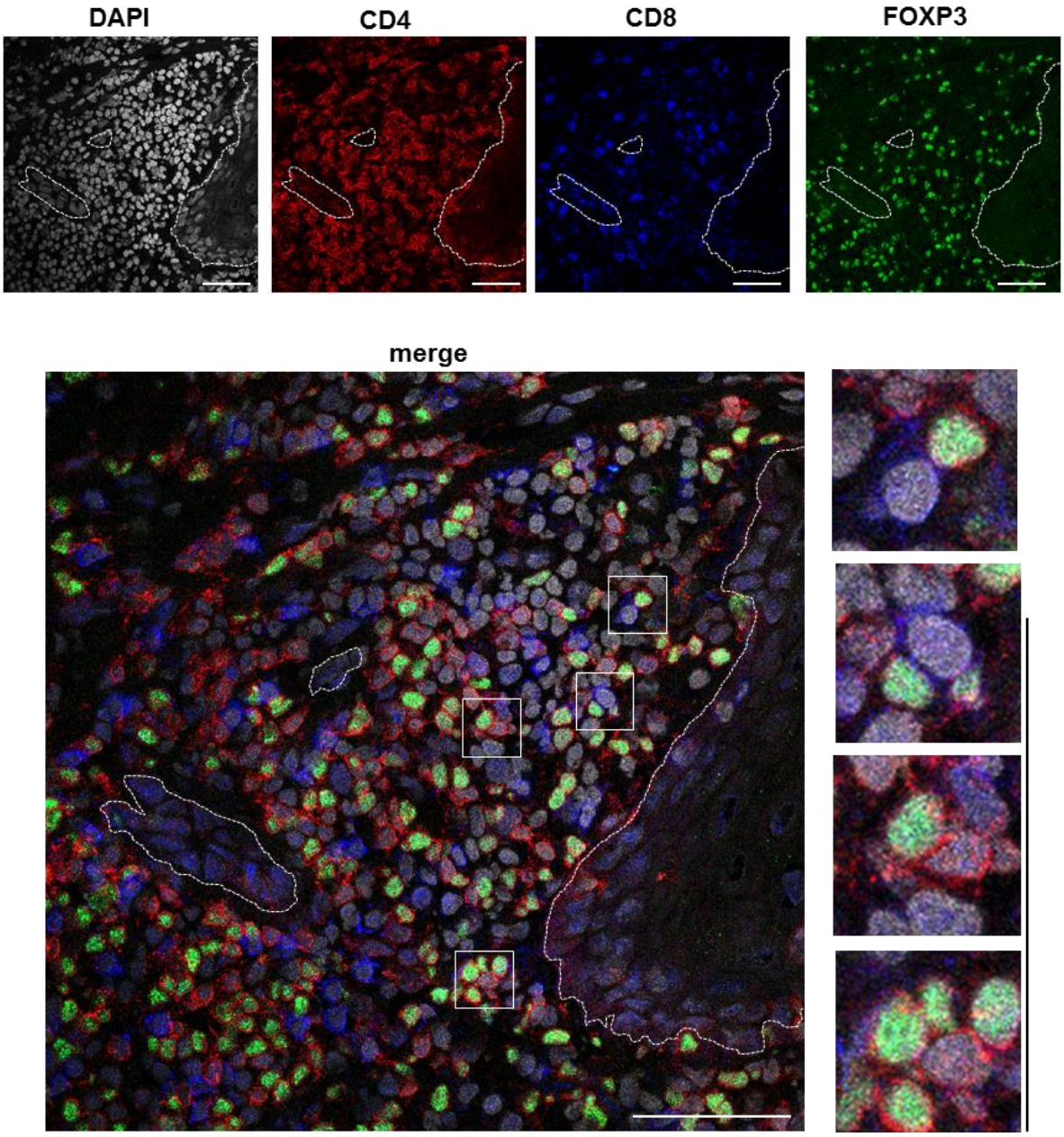

Figure 4.5 Confocal microscopy of T cell subsets in cSCC.

Confocal microscopy of $CD4^+$ T cells, $CD8^+$ T cells and $CD4^+FOXP3^+$ T cells in cSCC, boxes highlight examples of $CD4^+FOXP3^+$ Tregs (red membrane, green nucleus) in close contact with $CD8^+$ T cells (blue membrane, grey nucleus) and $CD4^+FOXP3^-$ T cells (red membrane, grey nucleus), higher magnification images on the right. Images representative of 5 cSCCs. Dashed lines indicate tumour outlines, scale bars = 50 μm.

4.2.2 Quantification of tumoral T cell subsets

Flow cytometry was conducted on tumoral immunocytes from cSCCs to examine the $CD4^+$ T cell, $CD8^+$ T cell and $CD4^+FOXP3^+$ Treg populations (Figure 4.6). cSCCs

contained lower $CD4^+$ T cell frequencies (63.3% ± 15.3% of the live $CD3^+$ lymphocyte population, n=81 tumours) than peripheral blood (67.9% ± 17.8%, p=0.0277) and non-lesional skin (73.6% ± 10.6%, p=0.0008) of the same individuals (Figure 4.7A, B, page 104). Conversely, $CD8^+$ T cell frequencies were higher in cSCC (28.8% ± 13.0% of the live $CD3^+$ lymphocyte population, n=76 tumours) compared with blood (22.4% ± 13.1%, p=0.0355) and normal skin (19.3% ± 9.0%, p=0.0008, Figure 4.7A, C).

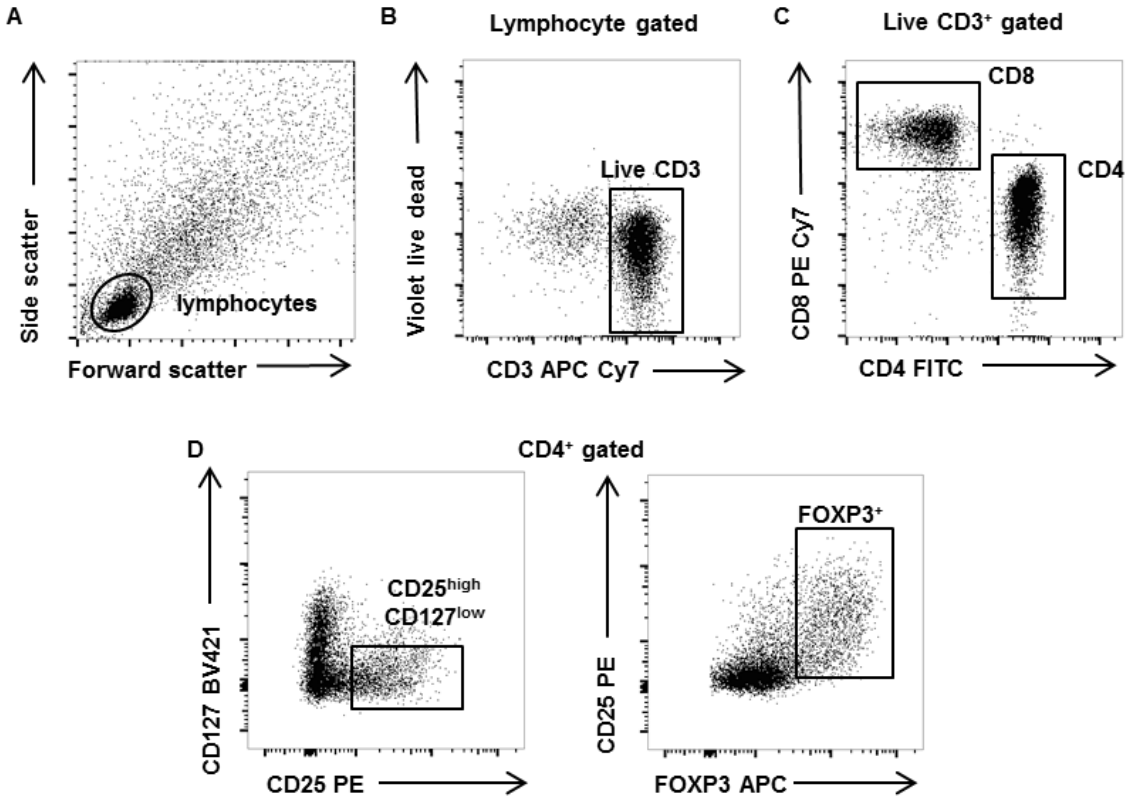

Figure 4.6 Flow cytometry panel for identification of Tregs.

(A) Forward and side scatter profile of immunocytes isolated from cSCC. Lymphocyte gate is shown. Gating for (B) live $CD3^+$ lymphocytes, (C) $CD4^+$ and $CD8^+$ T cell subsets, and (D) $CD4^+CD25^{high}CD127^{low}$ and $CD4^+FOXP3^+$ Tregs. The $CD25^{high}CD127^{low}$ gate as shown in (D) was used for experiments to isolate live Treg cells. As FOXP3 is an intracellular marker, cells were fixed and permeabilised prior to analysis of FOXP3 expression, and hence these cells were not able to be used for functional studies. In (B-D), axes are labelled with the cell marker and fluorophore used.

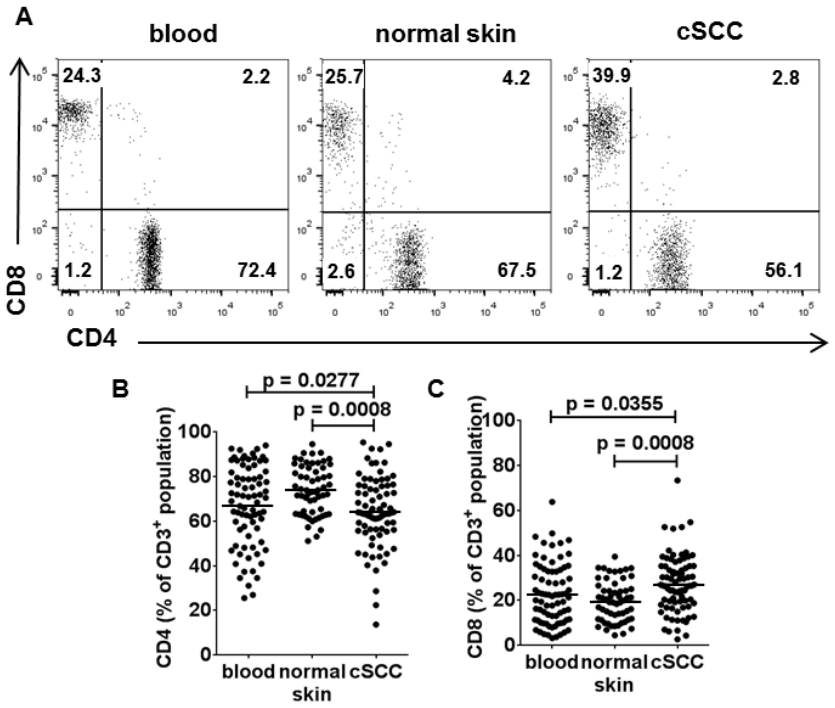

Figure 4.7 CD4⁺ and CD8⁺ T cell frequencies in cSCC.

(A) Representative dot plots of $CD3^+$ gated lymphocytes in blood, normal skin and cSCC on the same individual showing $CD4^+$ and $CD8^+$ T cell populations. (B, C) Aggregate data showing (B) $CD4^+$ and (C) $CD8^+$ T cell population frequencies in blood, normal skin and cSCC. (B) n=81 tumours, (C) n=76 tumours, horizontal bars = means, one-way ANOVA with Tukey's test for multiple comparisons.

Tregs were present in higher frequencies in cSCCs than the corresponding peripheral blood and non-lesional skin (19.8% ± 8.6% versus 5.5% ± 4.1% and 7.3% ± 4.1% of the $CD4^+$ population respectively expressed FOXP3, $p<0.0001$ for both comparisons, n=86 tumours, Figure 4.8, page 105), indicating that in cSCC there is an accumulation of tumoral Tregs, potentially contributing to the protumorigenic microenvironment. To determine whether Treg frequencies were associated with histological features of cSCC associated with poorer prognosis, Tregs were quantified according to depth of cSCC tumour invasion and histological differentiation (Figure 4.9, page 105). There was no significant correlation between $FOXP3^+$ Treg frequencies and depth of tumour invasion ($r^2=0.040$, $p=0.065$, Figure 4.9A) and there were no significant differences between Treg proportions in well differentiated (18.0% ± 7.5% of $CD4^+$ population), moderately differentiated (21.8% ± 7.9%) and poorly differentiated cSCC subgroups (20.4% ± 10.9%, Figure 4.9B).

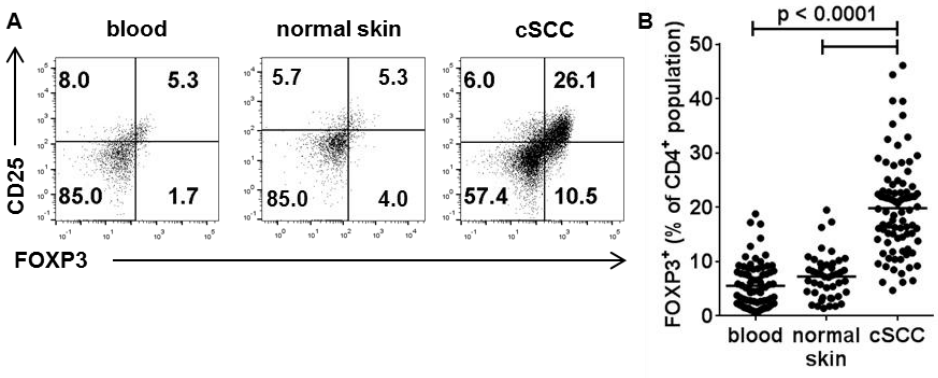

Figure 4.8 cSCCs contain increased FOXP3⁺ Treg frequencies than blood and normal skin.

(A) $CD3^+CD4^+$ gated lymphocyte populations in blood, normal skin and cSCC plotted for FOXP3 and CD25 expression. (B) Data from 86 cSCCs demonstrating higher $FOXP3^+$ Treg frequencies as a percentage of the $CD4^+$ T cell population in cSCC than blood and non-lesional skin. Horizontal bars = means. One-way ANOVA with Tukey's test for multiple comparisons.

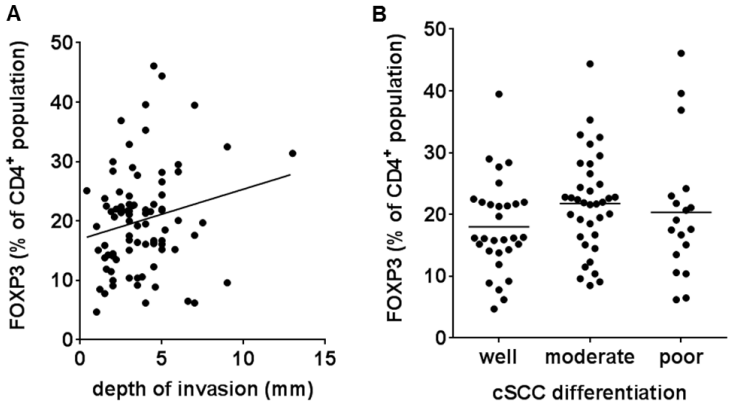

Figure 4.9 FOXP3⁺ Treg frequencies by depth of cSCC invasion and differentiation.

(A & B) Percentages of $CD4^+$ T cells expressing FOXP3 by (A) depth of tumour invasion and (B) histological differentiation of the cSCC tumour (n=86 tumours). In (A), best fit line = linear regression. In (B), horizontal bars = means.

Tregs were also significantly more frequent in KA and BCC than in corresponding peripheral blood (12.5% ± 3.6% versus 3.2% ± 2.8% of $CD4^+$ population for KA and blood respectively, p=0.0105, n=8 KAs; 15.0% ± 7.9% versus 3.5% ± 1.9%, p=0.0003, n=10 BCCs, Figure 4.10A, page 106). $FOXP3^+$ Tregs were also observed

in AKs (14.4% ± 5.6% of $CD4^+$ population, n=6), Bowen's disease (14.3% ± 7.3%, n=7) and seborrhoeic keratoses (8.6% ± 4.6%, n=3, Figure 4.10B).

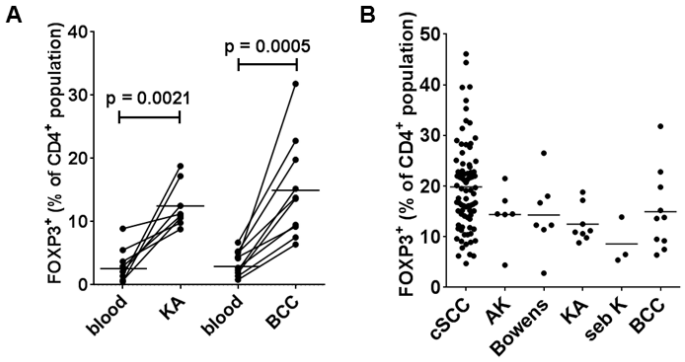

Figure 4.10 Analysis of $FOXP3^+$ Treg frequencies in other skin lesions.

(A) Flow cytometric quantification of $FOXP3^+$ Treg frequencies in blood and skin lesions in subjects with KA (n=8) and BCC (n=10), paired T tests. (B) $FOXP3^+$ Treg frequencies in AK (n=6), Bowen's disease (n=7), KA (n=8), seborrhoeic keratosis (seb K, n=3) and BCC (n=10). Horizontal bars = means.

4.2.3 Tumoral Tregs are memory T cells that express skin homing markers

Many of the T cells within normal skin are effector memory T cells which express CD45RO (Clark et al., 2008). In the current study the majority of $FOXP3^+$ Tregs (87.8% ± 11.7%, n=8, Figure 4.11A, B, page 107), $CD4^+FOXP3^-$ T cells (85.7% ± 7.3%, n=8, Figure 4.11A, C) and $CD8^+$ T cells (69.9% ± 11.5%, n=19, Figure 4.11A, D) in cSCCs were $CD45RO^+$. In the peripheral blood, 77.6% ± 16.7% of $FOXP3^+$ Tregs, 52.7% ± 19.3% of $CD4^+FOXP3^-$ T cells and 39.1% ± 18.5% of $CD8^+$ T cells were $CD45RO^+$, and in the non-lesional skin, CD45RO expressing cells comprised 90.6% ± 7.1% of Tregs, 89.3% ± 9.3% of $CD4^+FOXP3^-$ T cells and 71.0% ± 14.8% of $CD8^+$ T cells. $CD45RO^+$ memory T cells comprised a higher proportion of $CD4^+FOXP3^-$ T cells and $CD8^+$ T cells in cSCC and normal skin compared with peripheral blood ($p<0.001$ for all comparisons, Figure 4.11C, D).

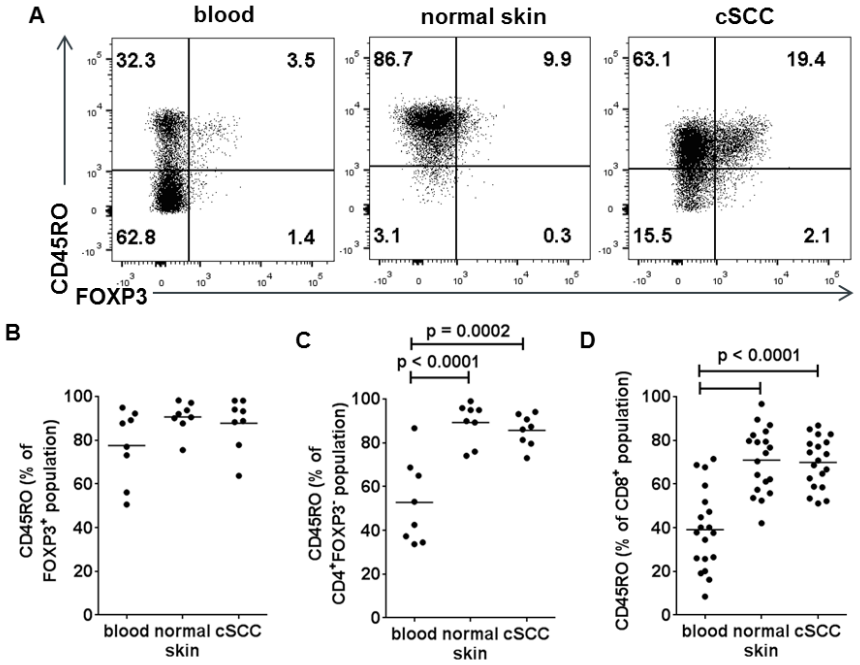

Figure 4.11 Tumoral T cells are predominantly memory phenotype.

(A) FACS plots showing CD45RO expression on $CD4^+$ gated lymphocyte populations from peripheral blood, normal skin and cSCC. CD45RO positivity as a percentage of (B) $FOXP3^+$ Treg, (C) $CD4^+FOXP3^-$ T cell and (D) $CD8^+$ T cell populations from blood and cSCC. Horizontal bars = means, one-way ANOVA with Tukey's test for multiple comparisons.

Clark et al. (Clark et al., 2008) reported that T cells, including Tregs, from cSCCs lack expression of the skin homing addressins, cutaneous lymphocyte antigen (CLA) and C-C chemokine receptor 4 (CCR4). In the current study, CLA was expressed by 78.8% ± 13.0% of the $FOXP3^+$ Treg population in cSCCs, which was similar to the proportion of $FOXP3^+$ Tregs in normal skin expressing CLA (80.6% ± 18.3%) and higher than that in peripheral blood (40.0% ± 13.7%, $p<0.0001$, n=19 tumours, Figure 4.12, Figure 4.13A, page 108). The latter is similar to that reported by Booth et al. in blood (Booth et al., 2010). Likewise, greater numbers of tumoral $CD4^+FOXP3^-$ T cells (58.2% ± 15.1%, Figure 4.13B) and $CD8^+$ T cells (41.6% ± 16.0%, Figure 4.13C) expressed CLA than those in peripheral blood ($p<0.0001$ for both comparisons, n=19 tumours), however, fewer tumoral $CD4^+FOXP3^-$ and $CD8^+$ T cells expressed CLA compared with $CD4^+FOXP3^-$ (74.1% ± 17.9%, $p= 0.0046$) and $CD8^+$ T cells (57.9% ± 18.4%, $p=0.0050$) in normal skin.

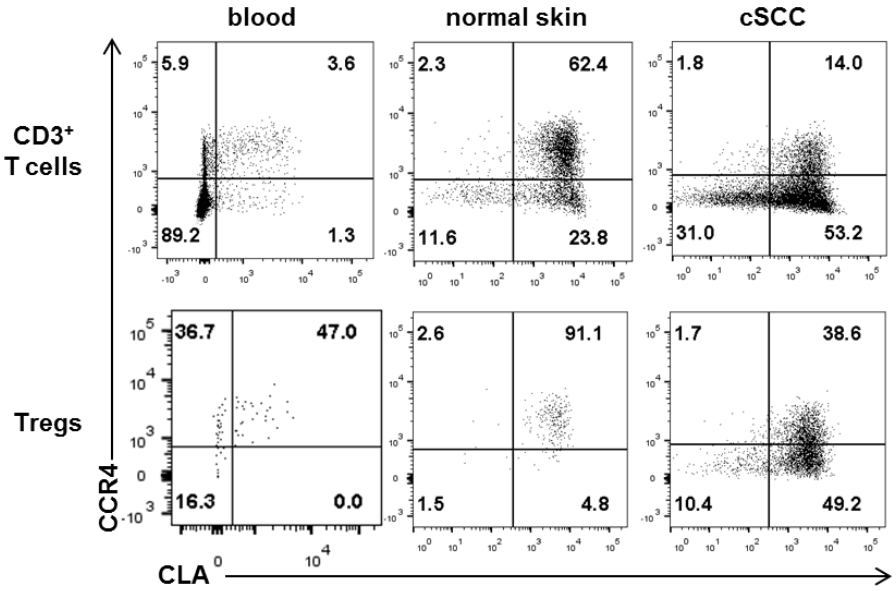

Figure 4.12 Flow cytometry of CLA and CCR4 expression in tumoral T cells.

Representative plots demonstrating CLA and CCR4 expression in $CD3^+$ T cells (top row) and $CD4^+FOXP3^+$ Tregs (bottom row) from peripheral blood, normal skin and cSCC from the same subject. Plots representative of samples from 17 cSCC subjects.

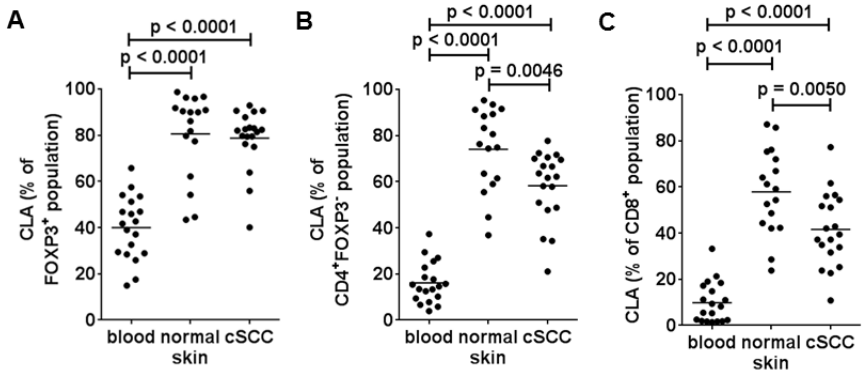

Figure 4.13 Tumoral T cells express CLA.

(A-C) Graphs showing aggregate data for CLA expression in peripheral blood, normal skin and tumoral (A) $FOXP3^+$ Tregs, (B) $CD4^+FOXP3^-$ T cells, and (C) $CD8^+$ T cells, n=19 tumours. Horizontal bars = means, one-way ANOVA with Tukey's test for multiple comparisons.

CCR4 expression was detected on 44.1% ± 32.7% of $FOXP3^+$ Tregs in cSCCs, although this was lower than the number of $FOXP3^+$ Tregs expressing CCR4 in peripheral blood (72.7% ± 17.8%, p=0.0139, n=17 tumours, Figure 4.14A, page 109) and normal skin (80.9% ± 15.9%, p<0.0001). Lower frequencies of tumoral

$CD4^+FOXP3^-$ T cells (25.4% ± 21.4% of $CD4^+FOXP3^-$ population, Figure 4.14B) and tumoral $CD8^+$ T cells expressed CCR4, 11.3% ± 11.6% of $CD8^+$ population, Figure 4.14C) compared with those in normal skin (59.7% ± 18.2% of $CD4^+FOXP3^-$ population, p<0.0001, 34.3% ± 22.6% of $CD8^+$ population, p=0.0014).

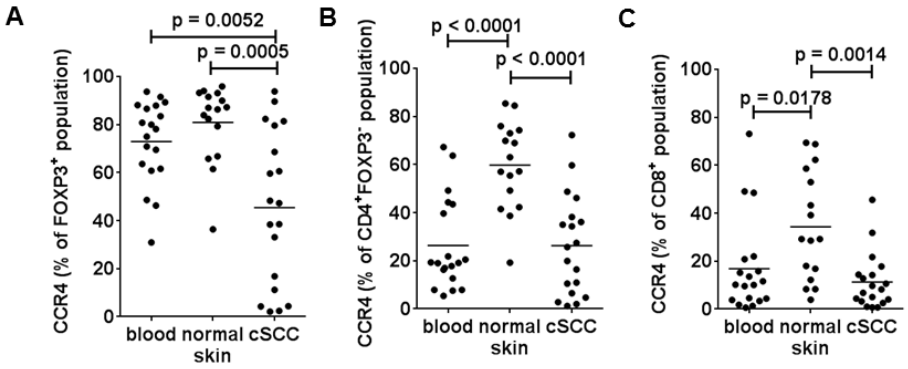

Figure 4.14 Expression of CCR4 by tumoral T cells.

(A-C) CCR4 expression in peripheral blood, normal skin and tumoral (A) $FOXP3^+$ Tregs, (B) $CD4^+FOXP3^-$ T cells, and (C) $CD8^+$ T cells, n=17 tumours. Horizontal bars = means, one-way ANOVA with Tukey's test for multiple comparisons.

Immunofluorescence microscopy was performed to examine CLA expression on tumour-infiltrating immunocytes. Indeed, CLA^+ immune cells were detected in cSCCs (Figure 4.15, page 110). Tumoral $FOXP3^+$ cells were demonstrated to express CLA by immunofluorescence microscopy (Figure 4.16A, page 110) and confocal microscopy (Figure 4.16B). Taken together with the flow cytometry data, these results indicate that tumoral Tregs in cSCC are of an effector memory T cell phenotype which expresses the skin homing marker CLA.

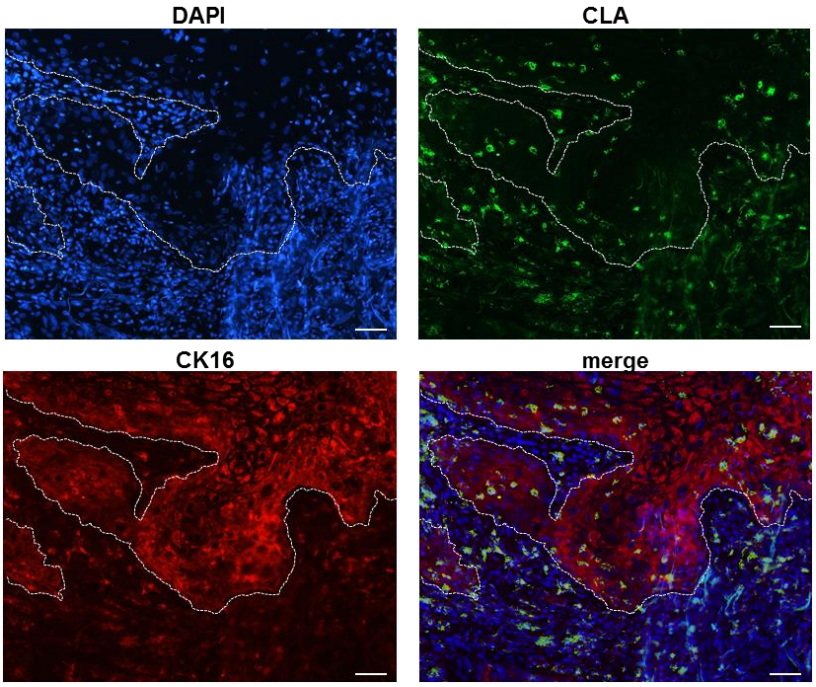

Figure 4.15 Immunofluorescence microscopy of CLA$^+$ immunocytes in cSCC.

Photomicrographs of a frozen cSCC section stained for CLA, CK16 and DAPI. Images representative of 5 cSCCs, dashed lines = tumour outlines, scale bars = 50 μm.

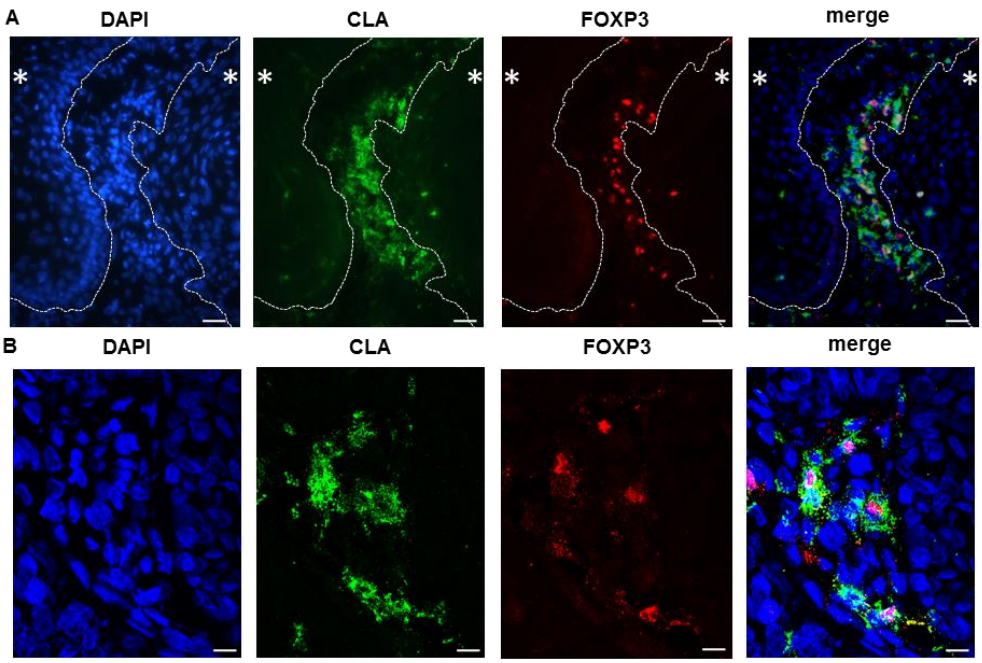

Figure 4.16 Tumoral Tregs express CLA.

(A) Immunofluorescence microscopy and (B) confocal microscopy demonstrating tumoral FOXP3$^+$ Tregs express CLA. In (A), asterisks (*) represent areas of tumour cells and dotted lines indicate tumour outlines. Images representative of 5 cSCCs, scale bars = 50 μm.

4.2.4 Peritumoral blood vessels express E-selectin

CLA permits lymphocyte trafficking to the skin through its binding to E-selectin on cutaneous endothelial cells (Clark et al., 2008). Immunofluorescence microscopy was performed using CK16 or 17 co-staining which allows the cSCC tumour cells to be visualized. Blood vessels (highlighted by $CD31^+$ endothelial cells) were detected in the peritumoral areas of cSCCs with no evidence of intratumoral vessels (Figure 4.17 and Figure 4.18, page 112). Fluorescence microscopy also showed most of the peritumoral vasculature expressed E-selectin (Figure 4.19, page 113 and Appendix Figure 7.3, page 244), suggesting that CLA^+ Tregs can readily be directed to the site of the tumour from the blood via interaction with E-selectin on these endothelial cells.

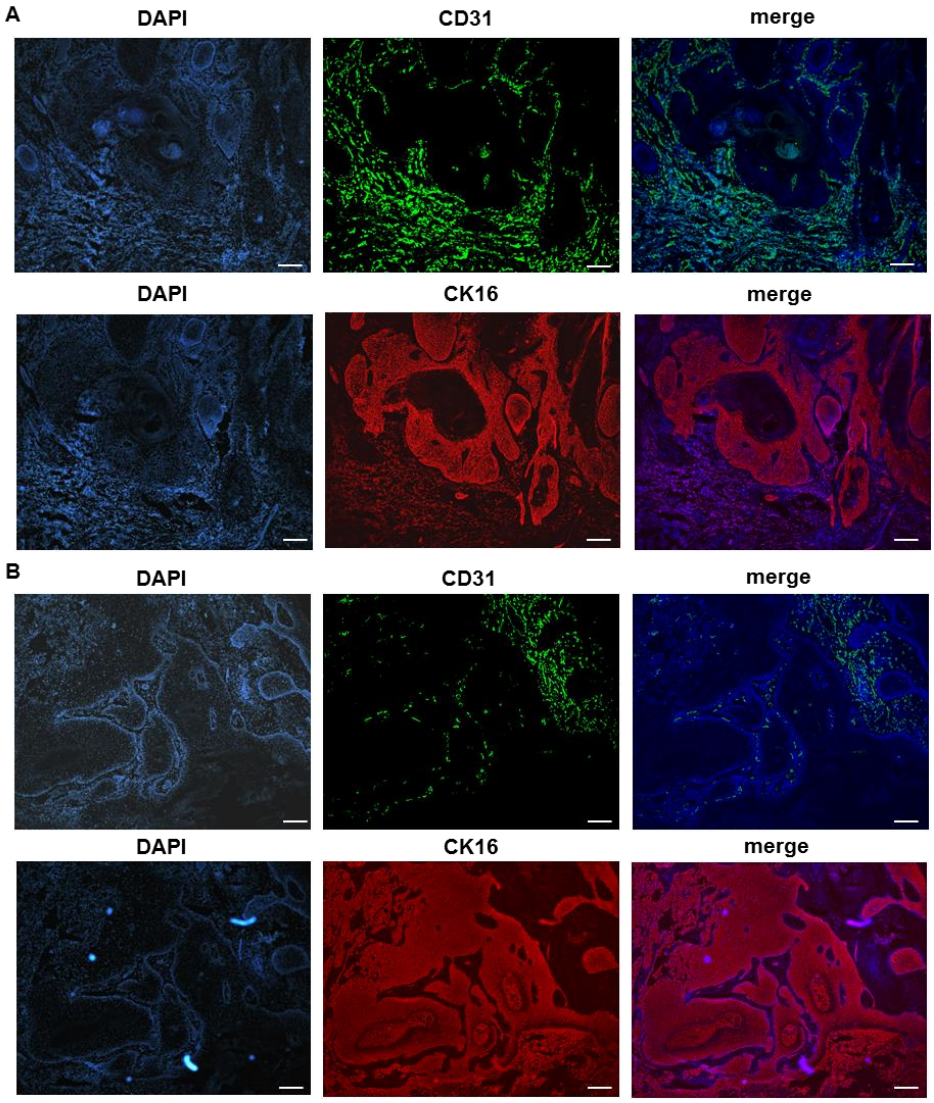

Figure 4.17 Distribution of blood vessels in cSCC.

(A & B) Representative fluorescence microscopy images from two cSCCs showing the distribution of $CD31^+$ blood vessels and tumour areas denoted by $CK16^+$ staining in

sequential sections. Images representative of 5 cSCCs, scale bars = 50 µm.

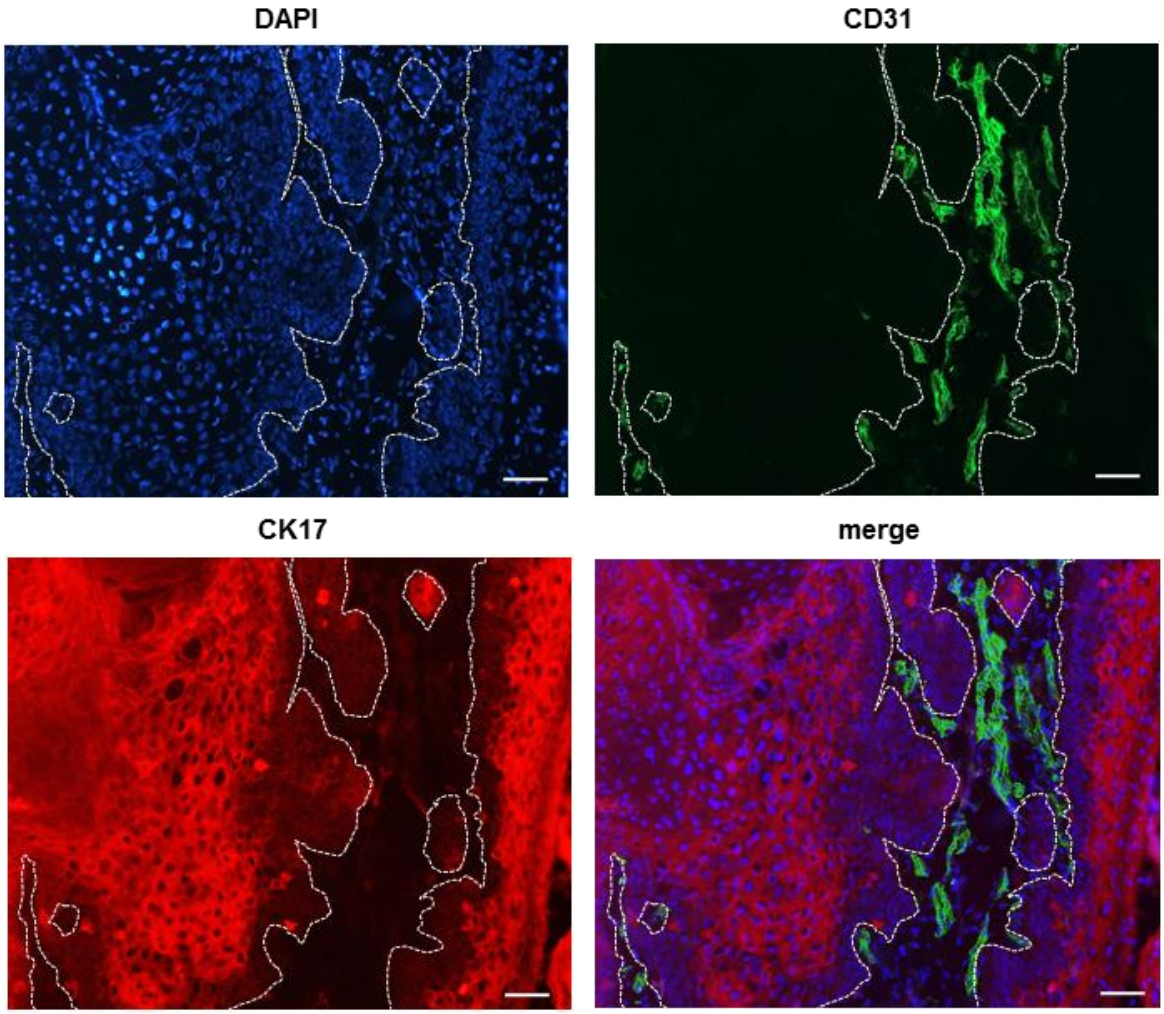

Figure 4.18 Peritumoral location of blood vessels in cSCC.

Fluorescence microscopy image showing $CD31^+$ blood vessels are situated in the peritumoral areas surrounding $CK17^+$ tumour nests. Images representative of 5 cSCCs. Dashed lines = tumour outlines, scale bars = 50 µm.

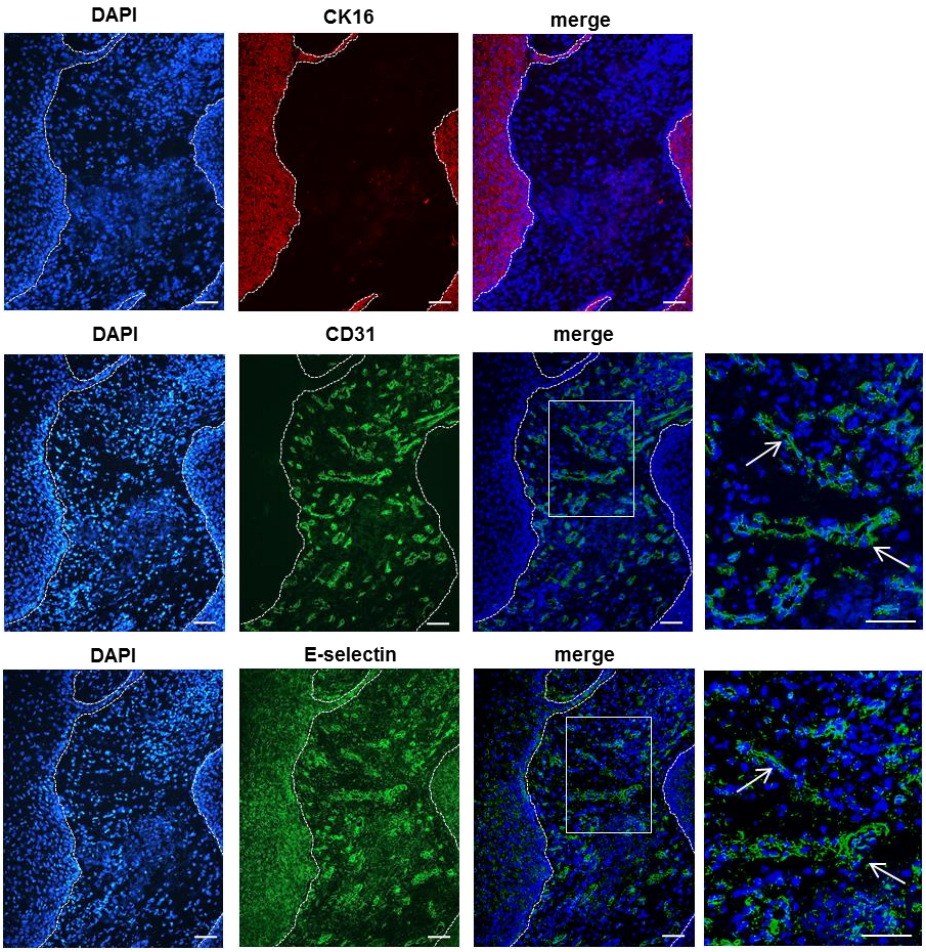

Figure 4.19 E-selectin is expressed by the cSCC vasculature.

Sequential cSCC sections showing e-selectin expression in the peritumoral vasculature (highlighted by CD31 straining) between $CK16^+$ tumour islands. Arrows in the right hand boxes, which depict higher power images of the merged images, indicate the same blood vessels in sequential sections. Images representative of 5 cSCCs. Dashed lines = tumour outlines, scale bars = 50 μm.

4.2.5 Tumoral Tregs express the transcription factor Helios

The T cell marker Helios may denote thymically derived natural Tregs (Thornton et al., 2010) but can also be upregulated on activated T cells (Gottschalk et al., 2012). Flow cytometry established that Helios was expressed at higher levels in tumoral $FOXP3^+$ Tregs (47.2% ± 7.9%, n=9 tumours) than peripheral blood $FOXP3^+$ Tregs (26.7% ± 8.5%, p=0.0002), normal skin $FOXP3^+$ Tregs (29.7% ± 11.7%, p=0.0022) and tumoral non-regulatory $CD4^+FOXP3^-$ T cells (9.6% ± 5.8%, p<0.0001) and $CD8^+$ T cells (8.3% ± 5.2%, p<0.0001) from the same subjects, (Figure 4.20, page 114).

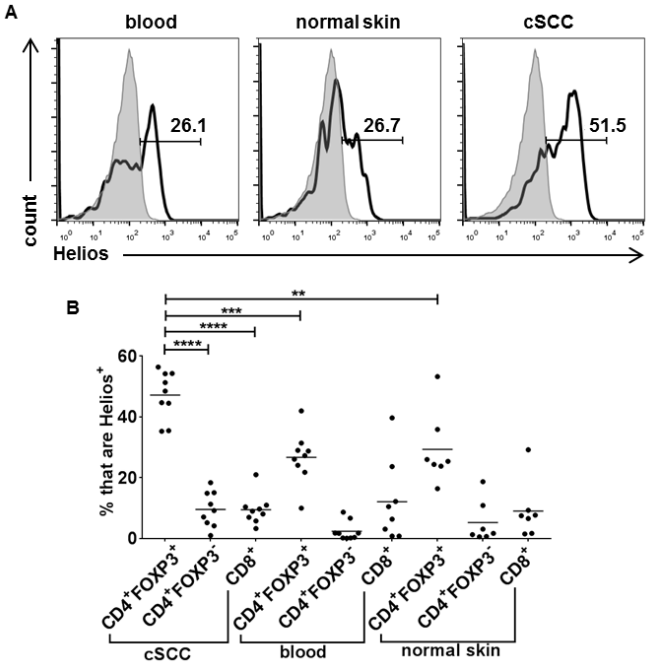

Figure 4.20 Helios is expressed by tumoral Tregs in cSCC.

(A) Representative histograms demonstrating Helios expression in fixed and permeabilised $CD4^+FOXP3^+$ gated lymphocytes from peripheral blood and corresponding cSCC. Grey shaded areas represent isotype control. (B) Percentage of $CD4^+FOXP3^+$ Tregs, $CD4^+FOXP3^-$ T cells and $CD8^+$ T cells from cSCC (n=9 tumours), peripheral blood and normal skin that are $Helios^+$. Horizontal bars = means, **p<0.01, ***p<0.001, ****p<0.0001, one-way ANOVA with Tukey's test for multiple comparisons.

4.2.6 Tumoral Tregs express the ectonucleotidase CD39

Extracellular ATP is hydrolysed in stepwise fashion into adenosine by the ectonucleotidases CD39, which is the rate-limiting enzyme and converts ATP to AMP, and CD73, which hydrolyses AMP to adenosine. CD39 can contribute to the immunosuppressive capacity of Tregs and may be overexpressed in cancer (Bastid et al., 2013, Mandapathil et al., 2009). $CD39^+$ tumoral immunocytes were observed in cSCC using immunohistochemistry (Figure 4.21A, page 115). Flow cytometry demonstrated that CD39 was expressed by higher frequencies of tumoral Tregs (86.9% ± 13.3%, n=14 tumours) than tumoral $CD4^+FOXP3^-$ T cells (38.5% ± 14.4%, p<0.0001), tumoral $CD8^+$ T cells (25.9% ± 16.5%, p<0.0001), Tregs from peripheral blood (67.6% ± 15.6%, p<0.0001) and Tregs from normal skin (73.4% ± 19.5%, p=0.0053, Figure 4.21B, C). CD73 expression was also

examined on immune cells in cSCC; the majority of tumoral CD73$^+$ immunocytes were found in the CD3$^-$ population (Figure 4.22A, page 116), and within the CD3$^+$ population, CD73 was present on small proportions of tumoral FOXP3$^+$ Tregs (6.3% ± 4.7%, n=6 tumours, Figure 4.22B), CD4$^+$FOXP3$^-$ T cells (3.3% ± 1.6%, Figure 4.22C) and CD8$^+$ T cells (9.3% ± 7.9% Figure 4.22D). This data indicates that the CD39, rate-determining ectonucleotidase for the hydrolysis of ATP, is highly upregulated by Tregs in cSCC with higher expression in the tumour compared to normal skin and blood, suggesting that CD39 contributes to the suppressive tumour microenvironment in cSCC.

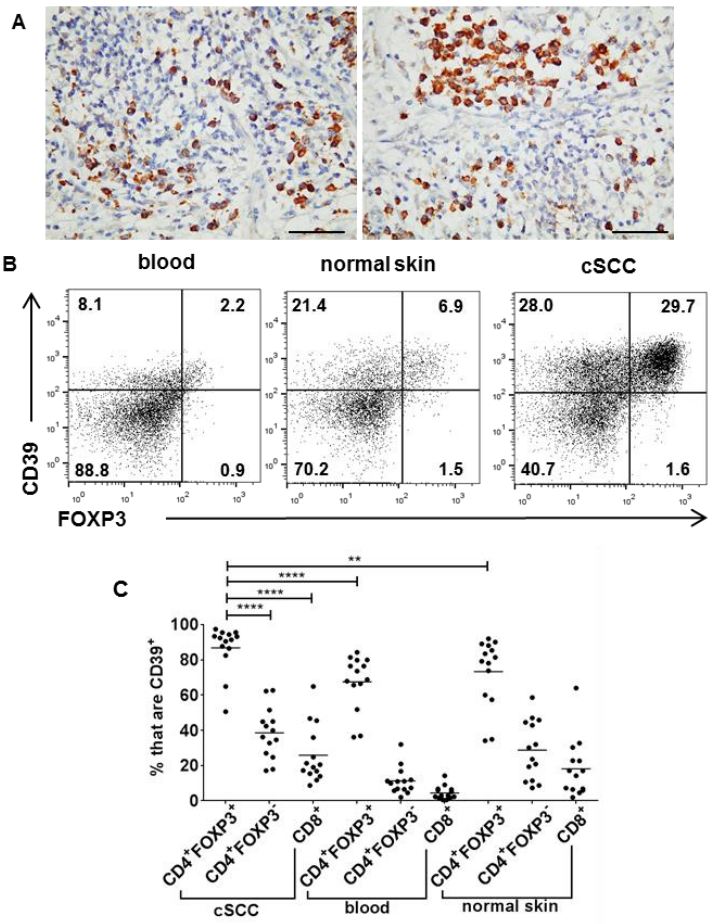

Figure 4.21 CD39 is expressed by tumoral Tregs in cSCC.

(A) Immunohistochemical staining of CD39$^+$ immune cells in two cSCCs, images representative of 33 cSCCs, scale bars = 50 μm. (B) Representative flow cytometry dot plots showing CD39 and FOXP3 expression in CD3$^+$ gated cells in peripheral blood, normal skin and cSCC from the same patient. (C) Graph showing CD39 positivity amongst CD4$^+$FOXP3$^+$ Tregs, CD4$^+$FOXP3$^-$ T cells and CD8$^+$ T cells in cSCC (n=14 tumours), peripheral blood and normal skin. Horizontal bars = means, **p<0.01, ****p<0.0001, repeated measures one-way ANOVA with Tukey's test for multiple

comparisons.

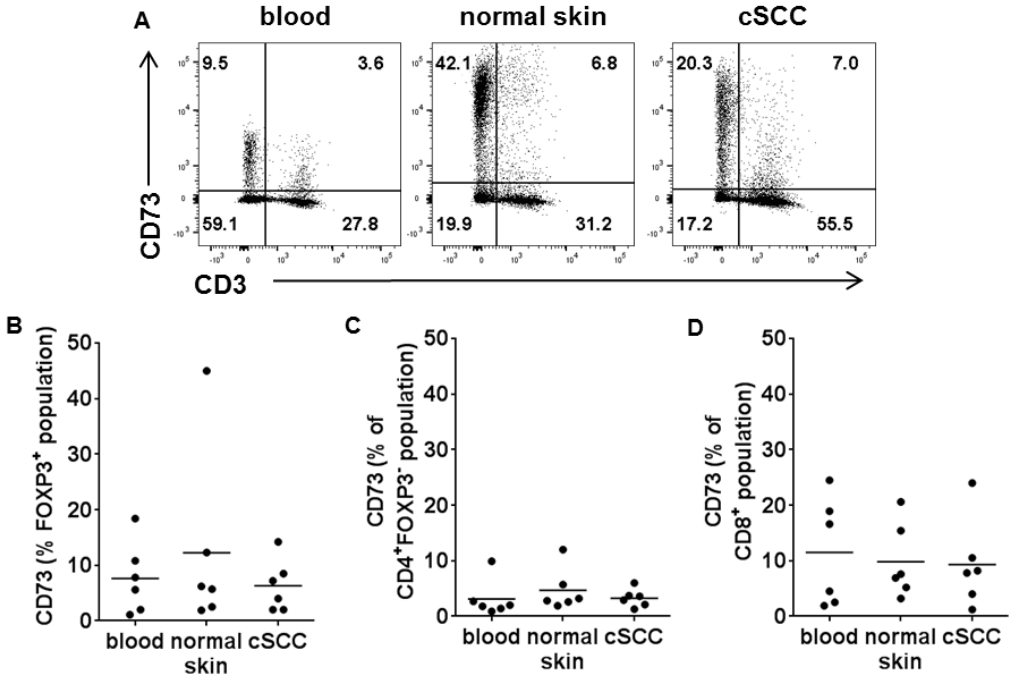

Figure 4.22 CD73 is expressed by a small proportion of T cells in cSCC.

(A) Representative flow cytometry dot plots showing expression of CD3 and CD73 in live cells from blood, normal skin and cSCC from the same patient. (B-D) Expression of CD73 by (A) Tregs, (B) $CD4^+FOXP3^-$ T cells and (C) $CD8^+$ T cells in blood, normal skin and cSCC (n=6 tumours). Horizontal bars = means.

4.2.7 cSCC Tregs suppress tumoral effector T cell responses

In vitro co-culture experiments with Tregs and effector T cells were performed to investigate cSCC Treg function. cSCC Tregs and effector T cells were co-cultured in a 1:2 ratio based on their relative frequencies observed in previous immunohistochemical quantification experiments performed within the laboratory group. Tumoral Tregs were identified by expression of CD3, CD4, high levels of CD25 and low levels of CD127 and isolated using fluorescence activated cell sorting (Figure 4.23A, page 117). Sorted tumoral $CD4^+$ effector T cells identified as $CD3^+CD4^+CD25^{low}$ and $CD8^+$ effector T cells were $CD3^+CD8^+$ (Figure 4.23A). After sorting, a sample of the cells were fixed and permeabilised for analysis of FOXP3 expression, confirming that most of the sorted $CD3^+CD4^+CD25^{high}CD127^{low}$ cells were Tregs (Figure 4.23B, C). In addition, interferon-γ was produced by <4%

of tumoral $CD3^+CD4^+CD25^{high}CD127^{low}$ cells following PMA and ionomycin stimulation, suggesting that this $CD3^+CD4^+CD25^{high}CD127^{low}$ population was minimally contaminated by effector T cells (Figure 4.23D).

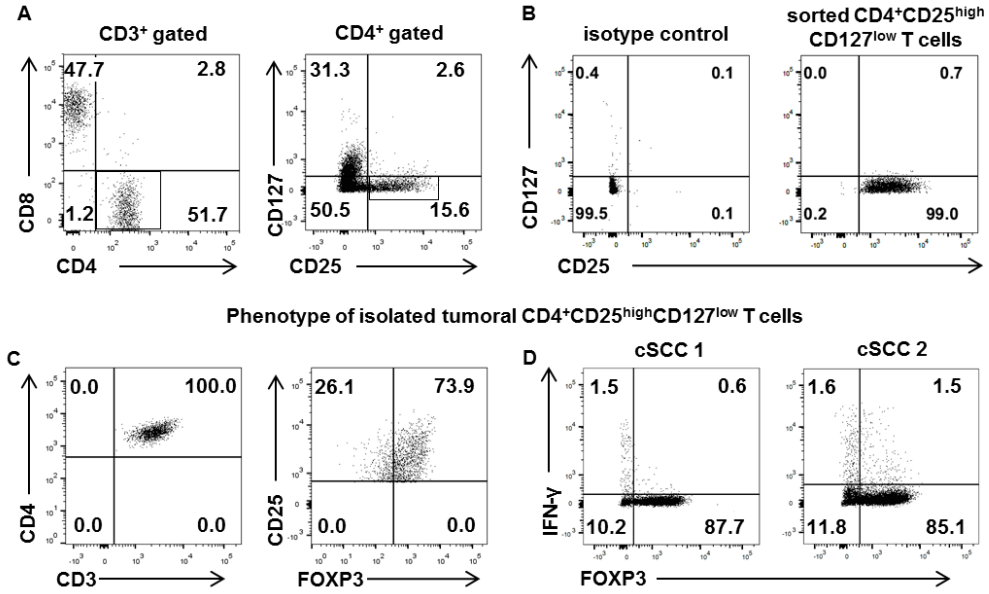

Figure 4.23 FACS sorting of tumoral Tregs.

(A) Representative flow cytometry gating strategy for isolating cSCC Tregs and effector T cells. Highlighted box in the top left FACS plot shows the $CD3^+CD4^+$ population, and sub-gating of this population is displayed in the top right FACS plot, where the sorted $CD25^{high}CD127^{low}$ Treg population is shown in the highlighted area. Effector T cells were $CD3^+CD4^+CD25^{low}$ or $CD3^+CD8^+$. (B) Expression of CD25 and CD127 in sorted tumoral Tregs, showing 99% purity of sorted $CD25^{high}CD127^{low}$ Tregs. (C) The majority of sorted $CD3^+CD4^+CD25^{high}CD127^{low}$ cells expressed FOXP3. (D) Sorted $CD3^+CD4^+CD25^{high}CD127^{low}$ T cells were stimulated with PMA and ionomycin for 5 hours and intracellular flow cytometry was performed for FOXP3 and interferon-γ .

Tritiated thymidine-based lymphocyte proliferation assays showed that tumoral $CD3^+CD4^+CD25^{high}CD127^{low}$ Tregs were able to suppress PHA-induced proliferation of tumoral $CD3^+CD4^+CD25^{low}$ effector T cells (median suppression 41.7%, n=10 tumours, Figure 4.24, page 118) and, to a lesser extent, $CD3^+CD8^+$ effector T cells (median suppression 12.6%, p=0.043, n=9 tumours, Figure 4.25, page 118). Tumoral Tregs cultured without effector T cells did not proliferate in response to PHA (median 108 counts per minute (cpm) without PHA versus 107 cpm with PHA, n=4 tumours). As there was a wide range in the percentage suppression of effector T cell proliferation by tumoral Tregs from different individuals, the sorted

Treg fractions were analysed for FOXP3 expression to determine whether FOXP3 expression correlated with the suppressive ability of the sorted $CD4^+CD25^{high}CD127^{low}$ cells, showing no significant correlation with percentage suppression of $CD4^+$ effector T cell proliferation (r^2=0.00, p=0.998, Figure 4.26A, page 119), and a small but non-significant correlation with percentage suppression of $CD8^+$ effector T cell proliferation (r^2=0.21, p=0.210, Figure 4.26B).

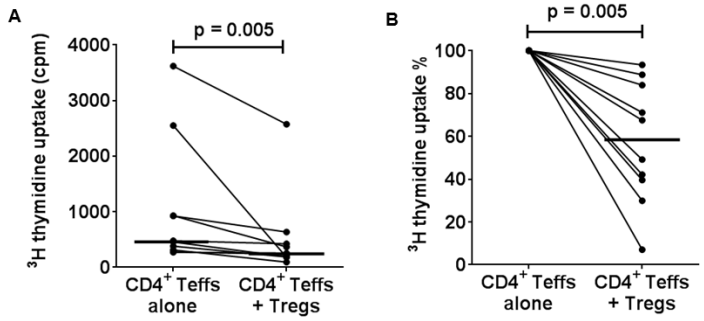

Figure 4.24 Tumoral Tregs suppress PHA-induced tumoral effector $CD4^+$ T cell proliferation.

(A & B) Tumoral effector T cells were co-cultured in the presence of autologous irradiated PBMCs and 1µg/ml PHA with/without the addition of tumoral Tregs. Tritiated thymidine uptake was used to assess tumoral $CD4^+$ T cell proliferation, results are displayed as raw cpms in (A) and normalised to 100% without Tregs in (B), n=10 tumours, dots = median values for each tumour from triplicate well experiments, horizontal bars = median values for all tumours, paired Wilcoxon rank test.

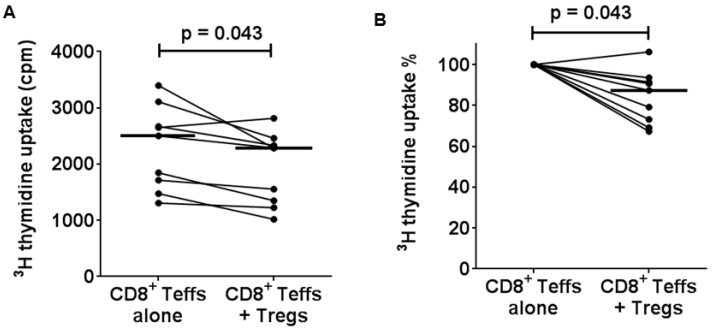

Figure 4.25 Tumoral Tregs suppress PHA-induced tumoral effector $CD8^+$ T cell proliferation.

(A & B) Tumoral effector T cells were co-cultured in the presence of autologous irradiated PBMCs and 1µg/ml PHA with/without the addition of tumoral Tregs. Tritiated thymidine uptake was used to assess tumoral $CD8^+$ T cell proliferation, results are displayed as raw cpms in (A) and normalised to 100% without Tregs in (B), n=9 tumours, dots = median values for each tumour from triplicate well experiments,

horizontal bars = median values for all tumours, paired Wilcoxon rank test.

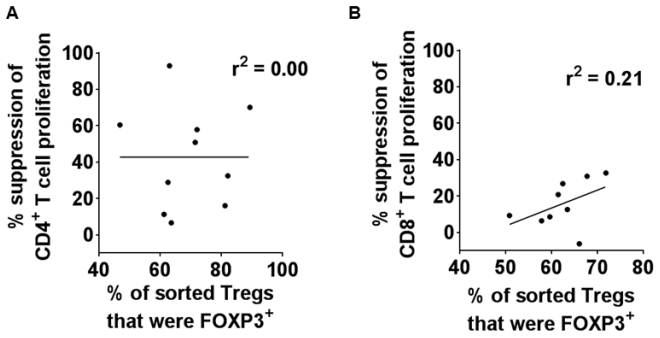

Figure 4.26 Suppressive capacity of FACS-sorted tumoral CD3$^+$CD4$^+$CD25^{high}CD127^{low} fraction by FOXP3 positivity.

(A & B) Results of Treg suppression assays in (A) Figure 4.24 and (B) Figure 4.25 by percentage of sorted CD4$^+$CD25^{high}CD127^{low} cells that expressed FOXP3. Best fit line = linear regression.

Treg suppression assays were also conducted on four cSCCs to confirm that tumoral Tregs could also suppress T cell responses to anti-CD3 antibody instead of PHA. Tumoral Tregs appeared to suppress proliferation of anti-CD3 stimulated tumoral CD4$^+$ effector T cells (median suppression 46.2%, n=4 tumours, Figure 4.27) and CD8$^+$ T cells (median suppression 40.2%, n=4 tumours, Figure 4.28, page 120). In addition, ELISPOT assays demonstrated that tumoral Tregs reduced effector T cell interferon-γ secretion in response to PHA (median inhibition 24.2%, p=0.0186, n=11 tumours, Figure 4.29, page 120). These results indicate that tumoral Tregs from cSCCs can suppress tumoral effector T cell function, and may therefore contribute to an immunosuppressive milieu that prevents immune-mediated destruction of the tumour.

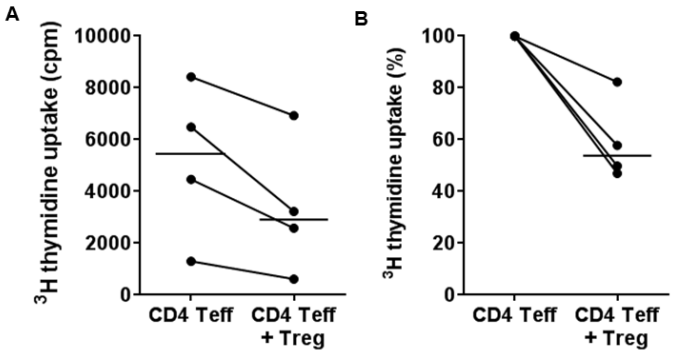

Figure 4.27 Tumoral Tregs suppress anti-CD3 induced tumoral effector CD4$^+$ T cell proliferation

(A & B) Tumoral effector T cells were co-cultured in the presence of autologous

irradiated PBMCs and 1µg/ml anti-CD3 with/without the addition of tumoral Tregs. Tritiated thymidine uptake was used to assess tumoral $CD4^+$ T cell proliferation, results are displayed as raw cpms in (A) and normalised to 100% without Tregs in (B), n=4 tumours. Dots = median values for each tumour from triplicate well experiments, horizontal bars = median values for all tumours.

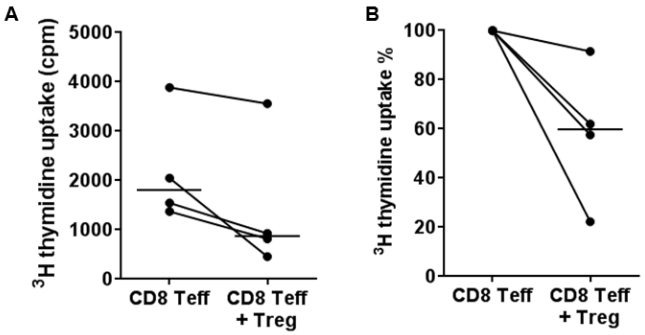

Figure 4.28 Tumoral Tregs suppress anti-CD3 induced tumoral effector $CD8^+$ T cell proliferation.

(A & B) Tumoral effector T cells were co-cultured in the presence of autologous irradiated PBMCs and 1µg/ml anti-CD3 with/without the addition of tumoral Tregs. Tritiated thymidine uptake was used to assess tumoral $CD8^+$ T cell proliferation, results are displayed as raw cpms in (A) and normalised to 100% without Tregs in (B), n=4 tumours. Dots = median values for each tumour from triplicate well experiments, horizontal bars = median values for all tumours.

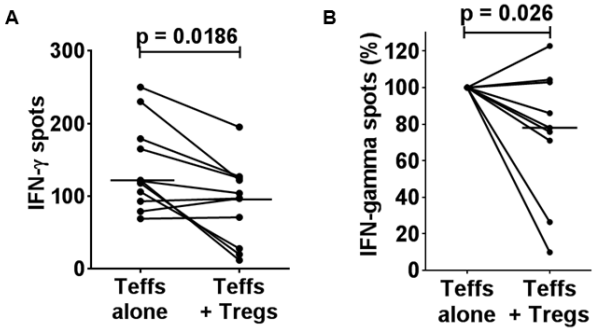

Figure 4.29 Tumoral Tregs suppress interferon-γ production by tumoral effector T cells.

(A & B) Tumoral effector T cells were co-cultured in the presence of autologous irradiated PBMCs and 1µg/ml PHA with/without the addition of tumoral Tregs. ELISPOT assays were used to assess tumoral effector T cell interferon-γ secretion, results are displayed as raw spots per well in (A) and normalised to 100% without Tregs in (B), n=11 tumours. Dots = median values for each tumour from triplicate well

experiments, horizontal bars = median values for all tumours, paired Wilcoxon rank tests.

4.2.8 CTLA-4 is expressed by tumoral Tregs intracellularly

Skin resident memory Tregs constitutively express CTLA-4 (Clark and Kupper, 2007), which plays a role in mediating suppression by competing with the costimulatory receptor CD28 for the ligands CD80 and CD86 on antigen presenting cells as well as providing co-inhibitory signalling (Walker and Sansom, 2011). Flow cytometry analysis of the presence of CTLA-4 on the cell membrane of T cells in cSCCs showed 18.3% ± 10.1% of tumoral Tregs expressed CTLA-4, which was a higher frequency compared with tumoral non-regulatory T cells and Tregs from peripheral blood and normal skin ($p<0.05$ for all comparisons, n=6 tumours, Figure 4.30).

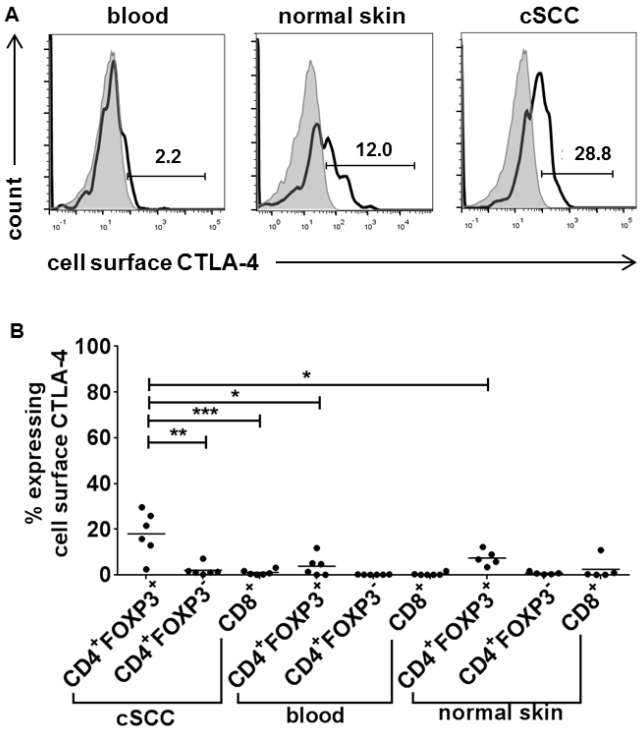

Figure 4.30 CTLA-4 is expressed by tumoral Tregs in low levels on the cell membrane.

T cells from blood, normal skin and cSCC were stained for CTLA-4 and other cell membrane markers prior to fixation and permeabilisation. (A) Representative flow cytometry histograms demonstrating cell membrane CTLA-4 expression in $CD4^+FOXP3^+$ gated lymphocytes from peripheral blood, normal skin and cSCC. Grey shaded areas represent isotype control. (B) Percentage of $CD4^+FOXP3^+$ Tregs, $CD4^+FOXP3^-$ T cells and $CD8^+$ T cells from cSCC (n=6 tumours), peripheral blood and normal skin that express CTLA-4 on the cell surface. Horizontal bars = means,

*p<0.05, **p<0.01, ***p<0.001, one-way ANOVA with Tukey's test for multiple comparisons.

CTLA-4 is mainly located in intracellular vesicles and is trafficked to the cell surface upon TCR stimulation where it is continually endocytosed (Walker and Sansom, 2011). In the current study, flow cytometry of fixed and permeabilised T cells from cSCCs which were then stained for CTLA-4 showed that the vast majority (88.0% ± 5.9%) of tumoral Tregs expressed intracellular CTLA-4, and at significantly higher frequencies than tumoral non-regulatory T cells and Tregs from peripheral blood and normal skin ($p<0.05$ for all comparisons, n=10 tumours, Figure 4.31).

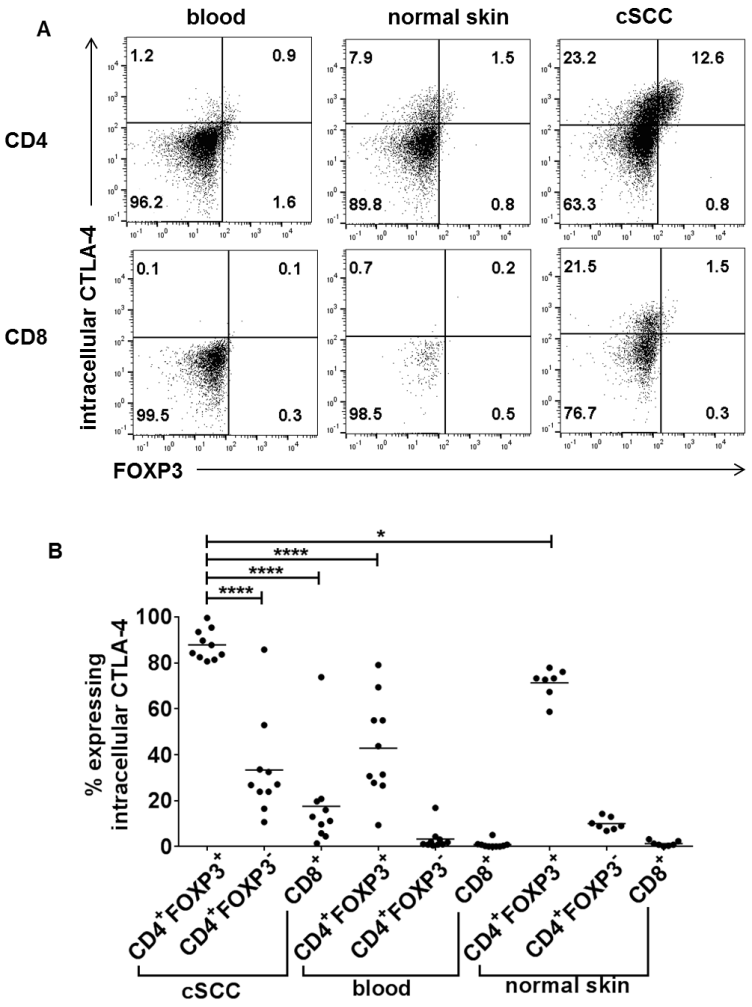

Figure 4.31 CTLA-4 is expressed by tumoral Tregs intracellularly.

T cells from blood, normal skin and cSCC were fixed and permeabilised prior to staining for CTLA-4. (A) Representative flow cytometry plots demonstrating intracellular CTLA-4 and FOXP3 expression in $CD4^+$ and $CD8^+$ gated lymphocytes from blood, normal skin and cSCC. (B) Percentage of $CD4^+FOXP3^+$ Tregs, $CD4^+FOXP3^-$ T cells

and CD8⁺ T cells from cSCC (n=10 tumours), peripheral blood and normal skin that express intracellular CTLA-4. Horizontal bars = means, *p<0.05, ****p<0.0001, one-way ANOVA with Tukey's test for multiple comparisons.

To determine whether CTLA-4 inhibition could enhance tumoral effector T cell function, tritiated thymidine uptake assays were performed to assess PHA-induced tumoral CD4⁺ T cell proliferation in the presence and absence of an inhibitory anti-CTLA-4 antibody, showing no significant difference in tumoral CD4⁺ T cell proliferation between anti-CTLA-4 and control (834.5 cpm versus 1074 cpm respectively, p=0.3750, n=10 tumours, Figure 4.32).

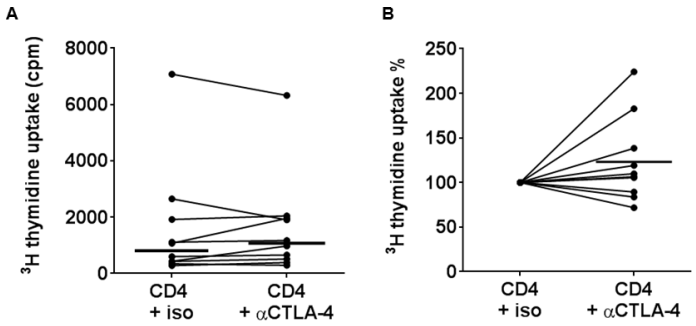

Figure 4.32 CTLA-4 inhibition does not enhance tumoral CD4⁺ T cell proliferation *in vitro*.

(A & B) Tumoral CD4⁺ T cells were co-cultured in the presence of autologous irradiated PBMCs and PHA with/without the addition of anti-CTLA-4. Tritiated thymidine uptake was used to assess tumoral CD4⁺ T cell proliferation, results are displayed as raw cpms in (A) and normalised to 100% without anti-CTLA-4 in (B), n=10 tumours, dots = median values for each tumour from triplicate well experiments, horizontal bars = median values for all tumours, paired Wilcoxon rank test.

4.2.9 4-1BB is expressed by cSCC Tregs and 4-1BB agonism enhances tumoral CD4⁺ T cell function

The costimulatory receptors 4-1BB and OX40 have been proposed as immunotherapeutic targets in cancer, and because the Faculty of Medicine at the University of Southampton, where this study was undertaken, is conducting a research programme investigating T cell costimulatory monoclonal antibodies for cancer immunotherapy, this study focused on examining 4-1BB and OX40 in cSCC. 4-1BB is present on tumoral T cells in certain cancers (Ye et al., 2014), and

4-1BB agonism has been shown to inhibit Treg suppressive ability (Akhmetzyanova et al., 2016) and increase tumoral effector T cell function (Melero et al., 1997). In the current study, 4-1BB$^+$ cells were detected in the cSCC immune infiltrate (Figure 4.33A). Flow cytometry showed tumoral Tregs expressed 4-1BB (12.7% ± 5.2%, n=9 tumours) at higher frequencies than tumoral CD4$^+$FOXP3$^-$ and CD8$^+$ T cells, as well as Tregs from peripheral blood and normal skin ($p<0.0001$ for all comparisons, Figure 4.33B, C). To determine whether 4-1BB agonism could augment tumoral effector T cell function, proliferation of tumoral CD4$^+$ T cells from cSCCs was assessed in the presence of an agonistic anti-4-1BB antibody (Curran et al., 2013). Culture with anti-4-1BB led to enhancement of PHA-induced CD4$^+$ T cell proliferation (median increase in proliferation 32.6%, $p=0.0029$, n=11 tumours, Figure 4.34, page 125), suggesting that 4-1BB agonism can augment effector responses by tumoral T cells in cSCC.

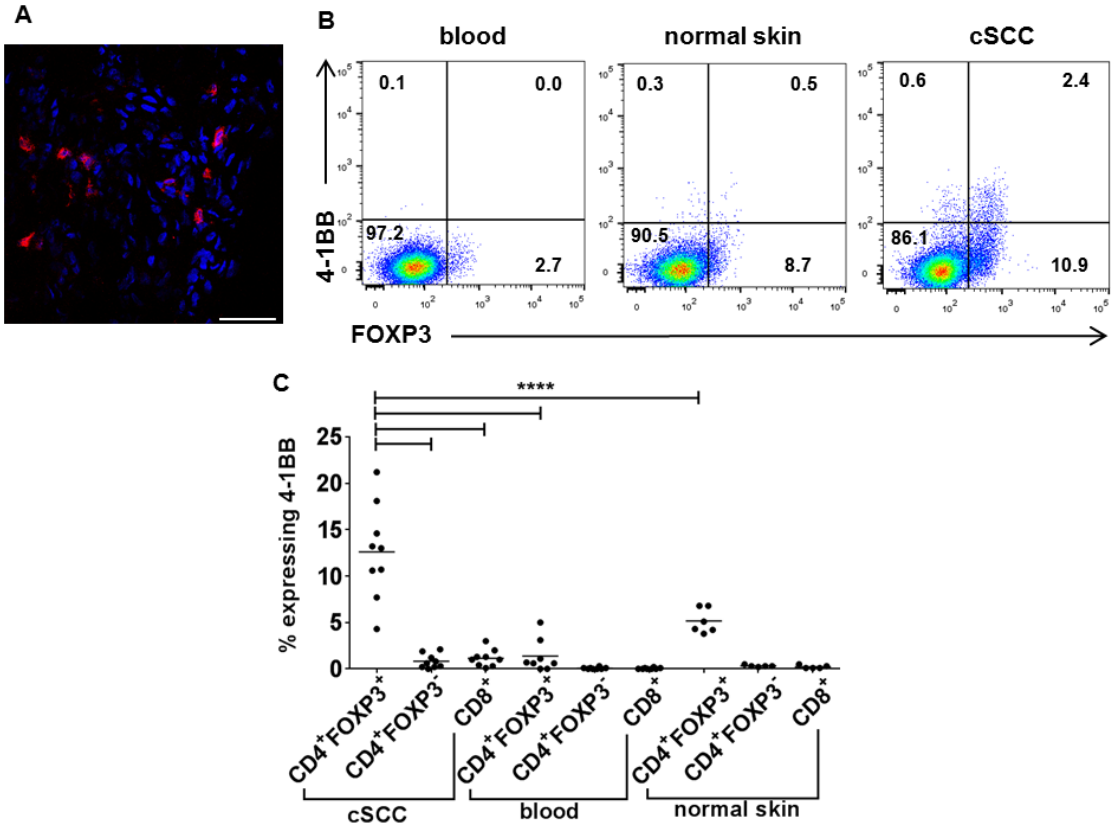

Figure 4.33 4-1BB is upregulated in cSCC Tregs.

(A) Confocal microscopy image of a representative high magnification field of the cSCC immune infiltrate, showing 4-1BB expression in red, DAPI in blue. Image representative of 5 cSCCs, scale bar = 50 μm. (B) Representative flow cytometry plots demonstrating 4-1BB and FOXP3 expression in CD3$^+$ gated cells in blood, normal skin and cSCC. (C) 4-1BB is present on higher proportions of tumoral Tregs than tumoral non-regulatory T cells and Tregs from peripheral blood and normal skin, n=9

tumours, ****p<0.0001, one-way ANOVA with Tukey's test for multiple comparisons. Horizontal bars = means.

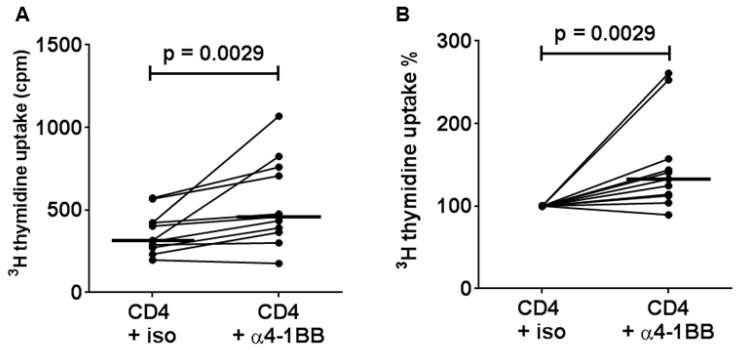

Figure 4.34 Agonistic anti-4-1BB antibody enhances tumoral CD4$^+$ effector T cell proliferation.

(A & B) Tumoral CD4$^+$ T cells isolated by flow cytometry from 11 fresh cSCCs were cultured with PHA + autologous irradiated CD3$^+$ cell depleted irradiated PBMCs ± agonistic anti-4-1BB antibody. Proliferation was assessed by tritiated thymidine uptake, results displayed in cpms in (A) and normalised to 100% without anti-4-1BB in (B), dots = median values from triplicate wells for each tumour, horizontal bar = median value from all tumours, paired Wilcoxon rank test.

4.2.10 OX40 is expressed by cSCC Tregs and OX40 agonism enhances tumoral CD4$^+$ T cell function

As the costimulatory receptor OX40 is expressed on effector and regulatory T cells and can augment T cell receptor signalling (Taraban et al., 2002, Piconese et al., 2008, Marabelle et al., 2013, Bulliard et al., 2014, Voo et al., 2013), the current study investigated whether OX40 was present on tumoral lymphocytes in cSCC. Immunofluorescence microscopy demonstrated the presence of OX40 predominantly on tumoral FOXP3$^+$ Tregs (Figure 4.35A, page 126). Flow cytometry confirmed FOXP3$^+$ Tregs in cSCC expressed OX40 (39.3% ± 13.6%), with significantly more tumoral Tregs expressing OX40 than CD4$^+$FOXP3$^-$ T cells and CD8$^+$ T cells in cSCCs, and FOXP3$^+$ Tregs in peripheral blood and normal skin ($p<0.0001$ for all comparisons, n=15 tumours, Figure 4.35C).

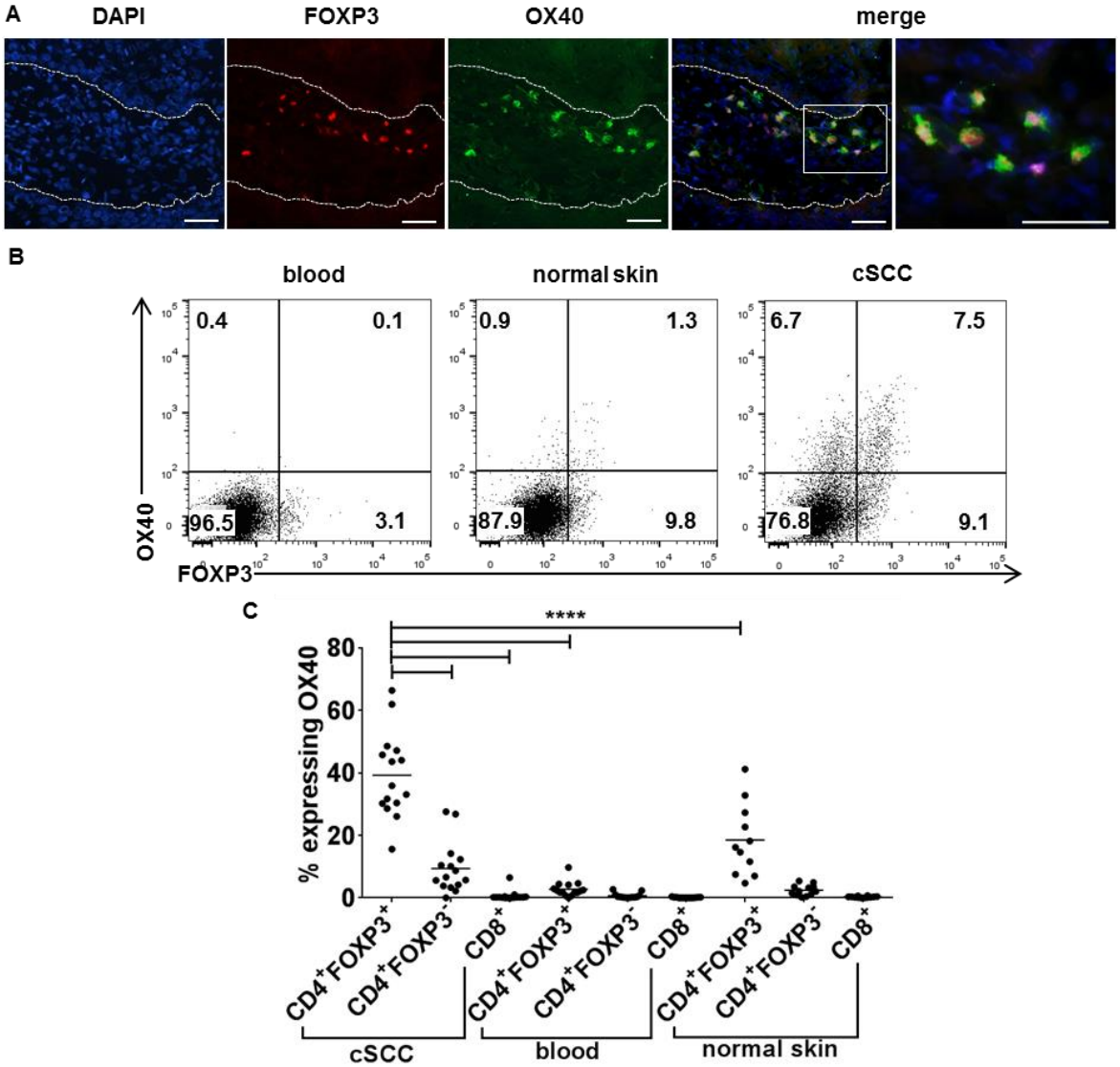

Figure 4.35 OX40 is upregulated on tumoral Tregs.

(A) Immunofluorescence microscopy showing OX40 on tumoral FOXP3⁺ Tregs. Dashed lines indicate the outline of the cSCC tumour islands. Images representative of 5 cSCCs, scale bars = 50 μm. (B) Flow cytometry plots of CD3⁺ gated lymphocytes from cSCC and corresponding peripheral blood showing OX40 and FOXP3 expression. (C) FACS quantification of OX40 expression in Tregs and effector T cells from cSCC, peripheral blood and normal skin, n=15 tumours, horizontal bars = means, ****p<0.0001, one-way ANOVA with Tukey's test for multiple comparisons.

To determine whether OX40 agonism attenuates the suppressive effects of Tregs in cSCC, proliferation of tumoral CD4⁺ T cells from cSCCs was assessed in the presence of an agonistic anti-OX40 antibody. The addition of anti-OX40, but not an isotype control antibody, led to enhancement of PHA-induced CD4⁺ T cell

proliferation (median increase in proliferation 45%, p=0.0098, n=10 tumours, Figure 4.36).

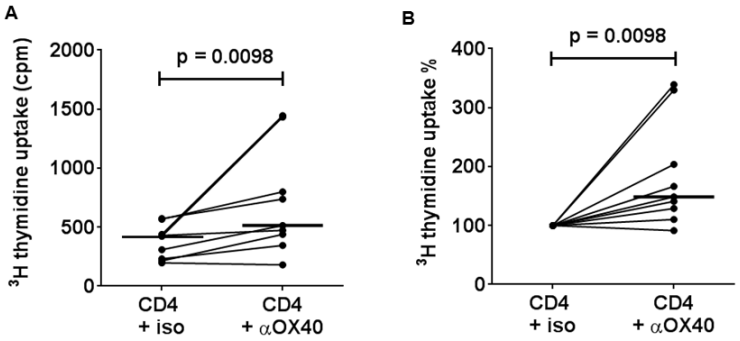

Figure 4.36 Agonistic anti-OX40 antibody enhances tumoral CD4$^+$ effector T cell proliferation *in vitro*.

(A & B) Tumoral CD4$^+$ T cells (which would have included CD4$^+$ Tregs and CD4$^+$ effector T cells) were isolated by flow cytometry from 10 fresh cSCCs and cultured with PHA + autologous irradiated CD3$^+$ cell depleted irradiated PBMCs ± agonistic anti-OX40 antibody. Proliferation was assessed by tritiated thymidine uptake, results displayed in cpms in (A) and normalised to 100% without anti-OX40 in (B), dots = median values from triplicate wells for each tumour, horizontal bar = median value from all tumours, paired Wilcoxon rank test.

Although OX40 was mainly found on tumoral Tregs *ex vivo* (Figure 4.35), to investigate whether PHA affected OX40 expression in tumoral T cells, tumoral T cells were cultured with PHA for 72 hours in the presence of accessory cells prior to flow cytometry analysis for OX40. Whereas the addition of PHA resulted in OX40 upregulation on Tregs and CD4$^+$FOXP3$^-$ T cells from peripheral blood (Figure 4.37A, B, page 128), this was not seen in Tregs and CD4$^+$FOXP3$^-$ T cells from the cSCCs (Figure 4.37C, D).

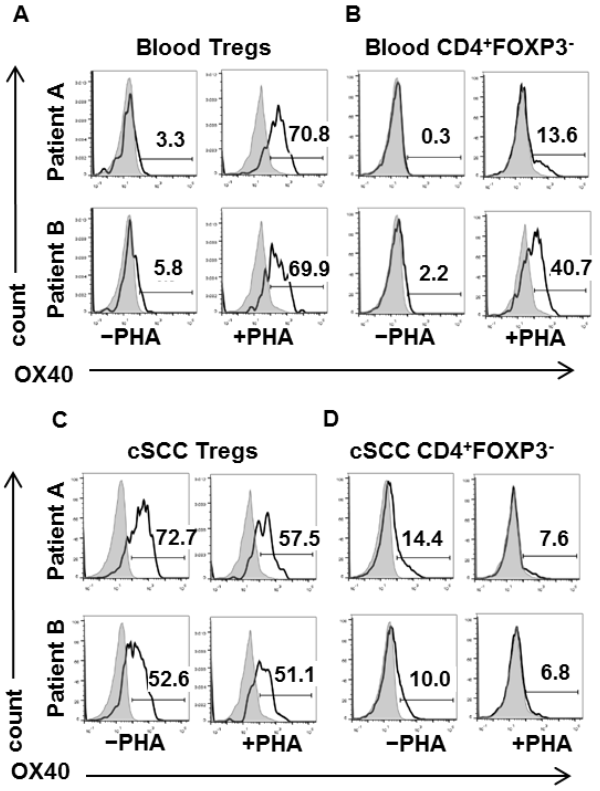

Figure 4.37 OX40 expression on Tregs and CD4$^+$ effector T cells following 72 hour culture with PHA.

(A-D) OX40 expression in (A) peripheral blood CD4$^+$FOXP3$^+$ Treg, (B) peripheral blood CD4$^+$FOXP3$^-$ T cells, (C) tumoral CD4$^+$FOXP3$^+$ Tregs and (D) tumoral CD4$^+$FOXP3$^-$ T cells prior to stimulation with PHA (-PHA) and after culture with PHA (+PHA) in the presence of autologous CD3$^+$ cell depleted irradiated PBMCs for 72 hours, demonstrating that PHA increases OX40 expression in Tregs and CD4$^+$FOXP3$^-$ T cells from peripheral blood but not from cSCCs. Grey areas = isotype control.

To determine whether anti-OX40 enhanced tumoral T cell function (Figure 4.36, page 127) through inhibition of Tregs or through direct stimulation of effector T cells, experiments were performed to assess the effect of anti-OX40 on tumoral CD4$^+$CD25^{high}CD127^{low} Tregs and CD4$^+$CD25^{low} effector T cells cultured separately and together. Proliferation of CD4$^+$CD25^{high}CD127^{low} Tregs was not increased by anti-OX40 when cultured with PHA in the presence of accessory cells alone (isotype control = 108.5 cpm (IQR 68.0-129.5 cpm), anti-OX40 = 107 cpm (IQR 73.3-135.5 cpm), n=4 tumours, Figure 4.38A, page 129). In cultures containing tumoral CD4$^+$CD25^{low} T cells without Tregs, median cell proliferation increased by 5.3% with the addition of anti-OX40 compared with isotype control, whereas in cultures containing tumoral CD4$^+$CD25^{low} T cells and Tregs, the improvement in

effector T cell function with the addition of anti-OX40 was more apparent (median increase in cell proliferation = 252.4% compared with isotype control, p=0.0313, n=5 tumours, Figure 4.38A, B). Similar results were also observed when anti-CD3 was used as a stimulus instead of PHA, with anti-OX40 increasing tumoral effector $CD4^+$ T cell proliferation from 5474 to 6572 cpm (by 20.1%) when Tregs were absent, and from 2906 to 5263 cpm (by 81.1%), when Tregs were present, n=4 tumours (Figure 4.39, page 130). Furthermore, increased interferon-γ spot production by tumoral $CD4^+$ effector T cells with the addition of anti-OX40 was more apparent in the presence of tumoral Tregs (53.5 with isotype versus 93.7 with anti-OX40) than in the absence of tumoral Tregs (114.2 with isotype to 131.5 with anti-OX40, Figure 4.40, page 130). Taken in combination with the fact that OX40 was found mainly on Tregs in cSCCs (Figure 4.41, page 131), these results suggest that OX40 agonism reduces Treg-mediated suppression of tumoral $CD4^+$ T cell responses.

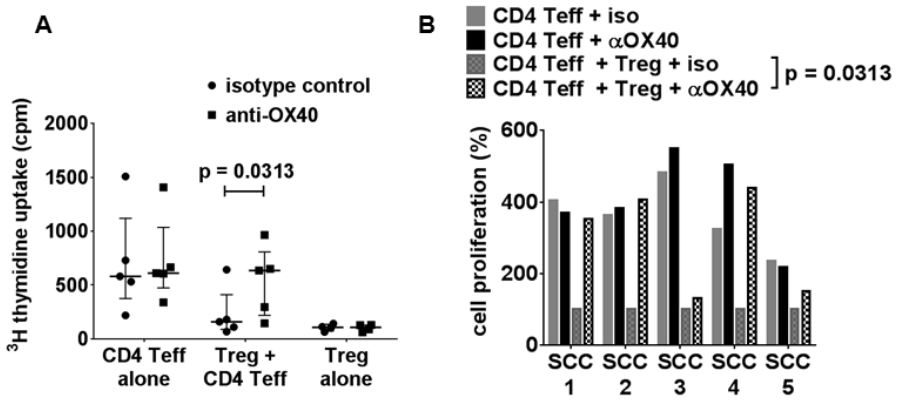

Figure 4.38 Effect of anti-OX40 on PHA-stimulated tumoral $CD4^+$ effector T cell proliferation in the presence and absence of tumoral Tregs.

(A & B) Tritiated thymidine uptake assays were performed where tumoral $CD4^+$ effector T cells were cultured ± tumoral Tregs ± agonistic anti-OX40 antibody. Median cpm values from triplicate wells are shown in (A), n=5 tumours. Median values for each tumour are displayed with circles for isotype control, squares for anti-OX40, horizontal bar = median for all tumours, error bars = IQR, paired Wilcoxon rank test. (B) Results for experiments performed in (A), represented as normalized to 100% of CD4 Teff + Treg + iso for each individual tumour.

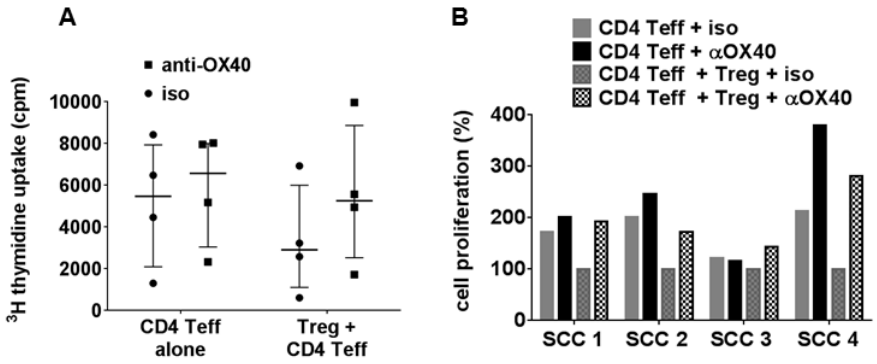

Figure 4.39 Effect of anti-OX40 on anti-CD3-stimulated tumoral CD4$^+$ effector T cell proliferation in the presence and absence of tumoral Tregs.

Tumoral CD4$^+$ effector T cells were cultured ± tumoral Tregs ± agonistic anti-OX40 antibody in the presence of anti-CD3, median cpm values from triplicate wells are shown in (A), n=4 tumours. Median values for each tumour are displayed with circles for isotype control, squares for anti-OX40, horizontal bar = median for all tumours, error bars = IQR, paired Wilcoxon rank test. (B) Results for experiments performed in (A), represented as normalized to 100% of CD4 Teff + Treg + iso for each individual tumour.

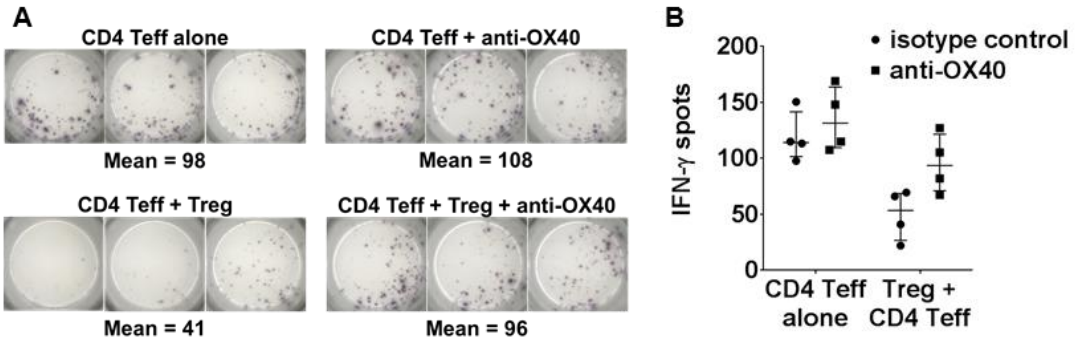

Figure 4.40 Effect of anti-OX40 on PHA-stimulated tumoral CD4$^+$ effector T cell interferon-γ secretion in the presence and absence of tumoral Tregs.

(A) Representative interferon-γ ELISPOT assay and (B) aggregate data from 4 tumours showing that the effect of the agonistic OX40 antibody is more apparent when tumoral Tregs are present in culture. Median values for each tumour are shown with circles for isotype control, squares for anti-OX40, horizontal bar = median for all tumours, error bars = IQR, n=4 tumours.

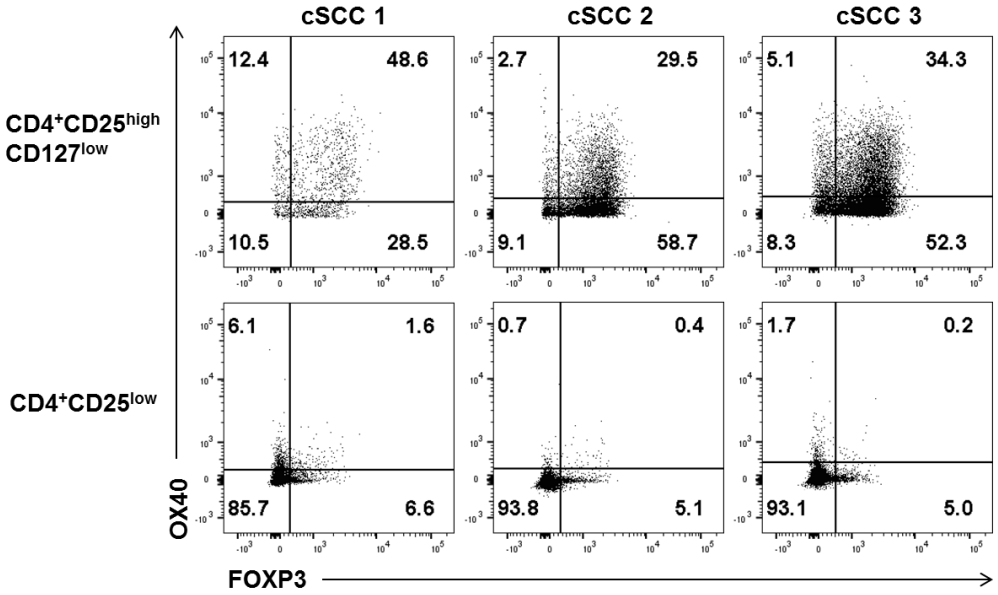

Figure 4.41 Expression of OX40 and FOXP3 in sorted tumoral $CD4^+CD25^{high}CD127^{low}$ and $CD4^+CD25^{low}$ lymphocyte populations.

Flow cytometry plots from 3 cSCCs showing OX40 and FOXP3 expression in $CD4^+CD25^{high}CD127^{low}$ (top row) and $CD4^+CD25^{low}$ (bottom row) cell populations.

4.2.11 Increased $OX40^+$ lymphocyte frequencies are associated with primary cSCCs which metastasise

In order to determine whether OX40 expression in cSCCs is associated with poorer clinical outcome, $OX40^+$ lymphocytes were quantified in archived FFPE primary cSCCs that had metastasised and in cSCCs that were known not to have metastasised after 5 years. OX40 was chosen as a marker to be investigated as the earlier experiments in this study suggested a functional role for OX40 on cSCC Tregs and previous work in the laboratory had shown that primary cSCCs which had metastasised were associated with Treg frequencies compared with primary cSCCs which had not metastasised (Lai et al., 2016). As expected, histological data demonstrated differences in known prognostic factors between the metastatic and non-metastatic groups, with primary metastatic cSCCs being larger, invading deeper and being more poorly differentiated than non-metastatic cSCCs (Table 4.1, page 132). Nevertheless, increased percentages of tumoral immunocytes expressing OX40 were observed in primary metastatic cSCCs (17.0% ± 10.7% of immune infiltrate, n=48 tumours) than in primary non-metastatic cSCCs (11.7% ± 6.9% of immune infiltrate, n=49 tumours, p=0.0041, Figure 4.42, page 132).

	Primary non-metastatic	Primary metastatic	P value
Age (years)	74.8 ± 10.3	80.0 ± 10.6	0.0159
Male	71.4%	77.1%	0.5244
Female	28.6%	22.9%	
Tumour diameter (mm)	13.4 ± 8.7	29.0 ± 30.5	0.0012
Tumour depth (mm)	4.1 ± 2.7	7.9 ± 5.9	0.0003
Well differentiated	34.7%	2.1%	<0.0001
Moderately differentiated	55.1%	29.2%	
Poorly differentiated	10.2%	68.8%	
Perivascular invasion	2.0%	20.1%	0.0039
Perineural invasion	4.1%	25.0%	0.0038
Immunosuppressed	8.2%	16.3%	0.2035
Fully excised	100%	87.5%	0.0204

Table 4.1 Details of primary non-metastatic and primary metastatic cSCCs.
Patient clinical and histological details of archived FFPE primary cSCCs that had not metastasised at 5 years post-excision (primary non-metastatic, n=48 tumours) and primary cSCCs which had metastasised (primary metastatic, n=49 tumours). T-tests for continuous variables, chi-squared tests for categorical variables.

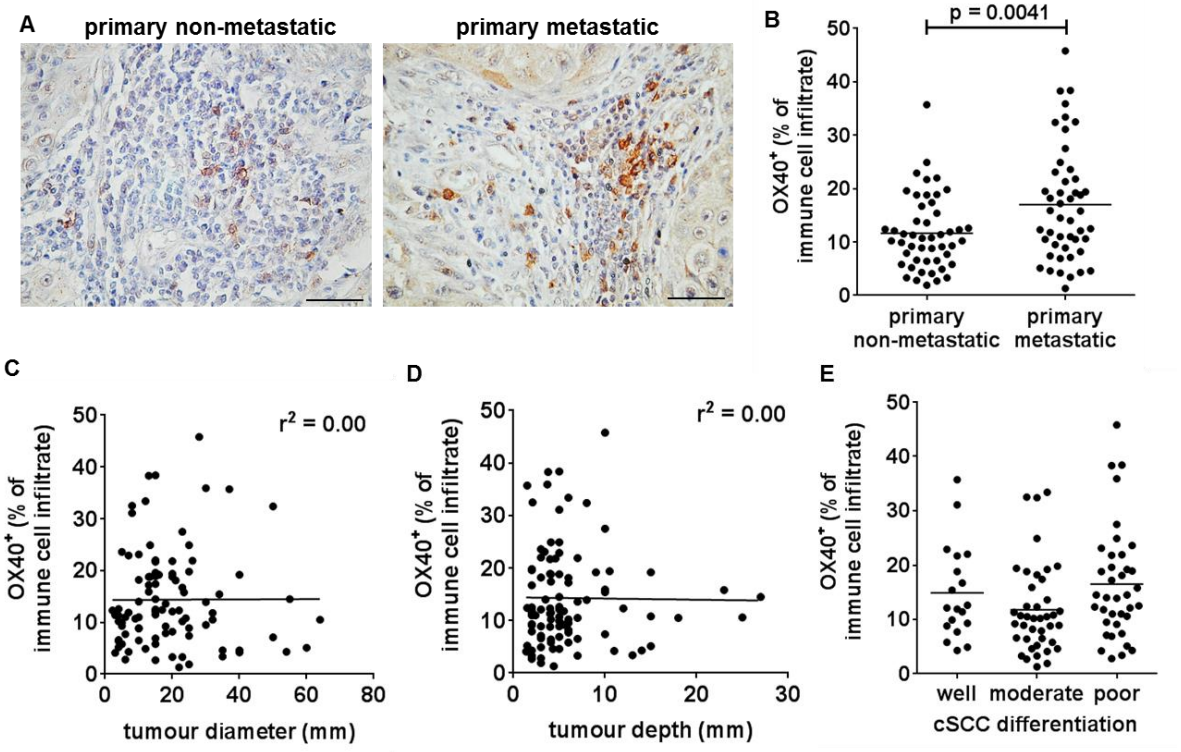

Figure 4.42 OX40 is upregulated in primary cSCCs which had metastasised.
Quantification of OX40$^+$ immune cells in 49 primary non-metastatic and 48 primary

metastatic cSCCs. (A) Representative photomicrographs, scale bars = 50 μm. (B) Graph summarising the data. (C-E) $OX40^+$ immune cell frequencies by (C) tumour diameter, (D) tumour depth and (E) histological differentiation. In (B-E), dots = mean values for each tumour from 5 high power fields, (B, E) horizontal bars = mean values for each group, t-test, (C, D) best fit line = linear regression.

4.3 Discussion

Based on the viewpoint that local cutaneous immunity plays a key role in preventing cSCC development and that dysregulation of this local immunity may allow the expansion of neoplastic keratinocytes to go unchecked, the Treg population within cSCCs was investigated in this chapter. The findings demonstrate that the cSCC tumoral immune infiltrate contains higher Treg frequencies than peripheral blood, which is in keeping with studies indicating that Tregs may accumulate in various tumours via several mechanisms and with reports that exposure of skin to UV is conducive to the generation of Tregs (Yamazaki et al., 2014). Functionally immunosuppressive Tregs have been reported in human cancer previously (Curiel et al., 2004, Gobert et al., 2009, Jie et al., 2013, Pedroza-Gonzalez et al., 2013) and this current study confirms that cSCC tumoral Tregs have the capacity to suppress tumoral effector T cell function *in vitro*, therefore highlighting Tregs as a potential mechanism by which cSCCs can avoid destruction by the skin immune system.

One of the notable features of the cSCC immune infiltrate is the predominant peritumoral distribution of the infiltrating lymphocytes. Whilst peritumoral and intratumoral infiltrating lymphocytes have previously been defined (Azzimonti et al., 2015), few studies which have examined tumour-infiltrating lymphocytes describe the distinction between the two locations of tumoral lymphocytes. In the current study, 'intratumoral' was defined as being within the clusters of neoplastic keratinocytes, 'peritumoral' as the stromal areas surrounding the tumour/tumour islands, and 'tumoral' encompassing all of the above. Whilst the current study identified that fewer immune cells were situated intratumorally than peritumorally, future investigations to examine the phenotypic differences between the intratumoral and peritumoral infiltrate and the spatial association of these immune cells (e.g. lining up against the tumour border) and characteristics of the tumour cells (e.g. those in apoptosis) would be useful.

Although Gelb et al. reported that lymphocytes infiltrating cSCC express CLA (Gelb et al., 1993), a more recent investigation recorded that T cells infiltrating

cSCCs are non-cutaneous central memory T cells which lack expression of CLA and CCR4 (Clark et al., 2008). In the current study, phenotypic characterisation of tumoral Tregs in cSCC showed that most expressed CD45RO and CLA, indicating a skin resident memory phenotype (which is the predominant T cell phenotype in skin) in cSCCs. CLA expression was confirmed on cSCC Tregs using both flow cytometry and immunofluorescence microscopy with two different anti-CLA antibodies (from BD Biosciences and Biolegend). However, the results demonstrate a high degree of variability in CLA and CCR4 expression between tumours, suggesting heterogeneous T cell responses in cSCC, possibly accounting for the differences between previous studies. In the context of the E-selectin expression by the majority of the peritumoral blood vessels, the findings from this study signify that Tregs are likely to be recruited to cSCCs via CLA on the Treg surface interacting with E-selectin on the tumoral vasculature. This is akin to T cell recruitment in inflammatory skin conditions including psoriasis (Lowes et al., 2014), atopic dermatitis (Islam and Luster, 2012) and contact dermatitis (Cavani et al., 2003) as well as in other cutaneous neoplasms such as melanoma (Gelb et al., 1993).

There has been considerable interest in developing cancer treatments that use monoclonal antibodies which act on T cell costimulatory or inhibitory pathways to augment anti-tumour immunity. Indeed, effector T cell responses can be modulated through engaging costimulatory receptors which can attenuate Treg suppressive ability (Piconese et al., 2008, Marabelle et al., 2013, Bulliard et al., 2014, Voo et al., 2013), and by blocking inhibitory receptors such as CTLA-4 on Tregs (Simpson et al., 2013, Wing et al., 2008). Whilst intracellular CTLA-4 was observed in cSCC Tregs in the current study, an anti-CTLA-4 inhibitory antibody was unable to enhance cSCC $CD4^+$ T cell proliferation *in vitro*. Other studies have similarly failed to demonstrate any effect of CTLA-4 inhibitory antibodies on Treg mediated suppression (Thornton and Shevach, 1998), which may potentially relate to the requirement in these *in vitro* assays for anti-CTLA-4 to reduce CD80 and CD86 availability for the costimulatory counterpart CD28, thereby mediating suppression in a cell extrinsic rather than intrinsic mechanism (Walker and Sansom, 2011). Despite this, the *in vitro* culture model employed in the current study was able to show enhanced tumoral $CD4^+$ T cell proliferation with the addition of agonistic anti-4-1BB and anti-OX40, suggesting costimulatory receptors may form a potential therapeutic target in cSCC.

In the current study, the tumoral Tregs were the T cell subset that expressed OX40 at the highest frequencies, consistent with observations from studies on murine tumours which used anti-OX40 antibodies to deplete intratumoral Tregs and enhance anti-tumour immunity (Piconese et al., 2008, Marabelle et al., 2013, Bulliard et al., 2014), suggesting a similar strategy could be beneficial in cSCC. OX40 has been demonstrated on $CD4^+$ tumour-infiltrating lymphocytes in melanoma and head and neck cancer (Vetto et al., 1997), and whereas the presence of OX40 expressing lymphocytes in cSCC has recently been documented (Feldmeyer et al., 2016), the current study highlights that this molecule is predominantly expressed by Tregs in this cancer. This study also found higher percentages of tumour-infiltrating lymphocytes expressing OX40 in primary metastasising cSCCs compared with primary tumours which had not metastasised. While this contrasts with some other cancers in which OX40 expression correlates with improved prognosis (Sarff et al., 2008, Petty et al., 2002, Ladanyi et al., 2004), much higher proportions of tumoral Tregs expressed OX40 than the tumoral $CD4^+FOXP3^-$ and $CD8^+$ T cells in our cSCC population. As enhanced tumoral $CD4^+$ T cell responses *in vitro* were observed with addition of an OX40 agonist, the use of an OX40 agonist approach *in vivo* may have potential benefits in patients with cSCCs at high risk of metastasising after surgical excision. Admittedly, although OX40 agonism had little effect on enhancing proliferation of tumoral $CD4^+$ effector T cells and interferon-γ production by these cells, it is unclear whether part of the effect of OX40 agonism could be mediated by the presence of $OX40^+FOXP3^-$ cells in the sorted $CD3^+CD4^+CD25^{high}CD127^{low}$ population (Figure 4.41). This is because, due to FOXP3 being an intracellular stain, it was not possible to isolate the $FOXP3^-$ fraction of the $CD3^+CD4^+CD25^{high}CD127^{low}$ population from human cSCCs and perform functional studies using this subset alone. Neither is it clear whether the effect of OX40 agonism is mediated by $OX40^+CD4^+$ effector T cells in overcoming or influencing Treg suppression, however, the results indicate that the effect of OX40 in boosting the effector T cell response is only seen in the presence of the $CD3^+CD4^+CD25^{high}CD127^{low}$ population.

In conclusion, this study demonstrates that cSCCs contain an abundance of Tregs which can suppress tumoral effector T cell function and that activation of the costimulatory receptor OX40 enhances tumoral T cell responses. Primary cSCCs that metastasise are associated with higher $OX40^+$ lymphocyte frequencies, therefore providing evidence that Tregs and OX40 play key roles in the pathogenesis of cSCC.

Chapter 5: Characterisation of effector T cell dysfunction in cSCC

5.1 Introduction

In addition to the suppressive role of Tregs, another mechanism responsible for insufficient anti-tumour responses is effector T cell hyporesponsiveness (Rabinovich et al., 2007). A key mechanism underlying T cell hyporesponsiveness in chronic viral infections is T cell exhaustion (Wherry and Kurachi, 2015), where viruses can persist despite the presence of large numbers of $CD8^+$ T cells, which lose their capacity for killing infected cells. Recent evidence indicates that T cell exhaustion may play a fundamental role in cancer (Baitsch et al., 2011, Derre et al., 2010). The induction and maintenance of T cell exhaustion is dependent on persistent antigen exposure and tumours which are more immunogenic are associated with greater degrees of $CD8^+$ T cell hyporesponsiveness (Willimsky et al., 2008). Exhausted T cells are characterised by progressive loss of production of IL-2, TNF-α and interferon-γ , followed by the inability to lyse target cells. Higher levels of inhibitory receptors are expressed by exhausted T cells, e.g. PD-1, Tim-3, BTLA, LAG-3, CD160, CD244 and TIGIT (Fourcade et al., 2010, Chauvin et al., 2015, Butler et al., 2012, Blackburn et al., 2009). Correcting T cell exhaustion offers potential for therapy, as T cell responses can be boosted independently of T cell antigen specificity (Robert et al., 2014, Topalian et al., 2012). Indeed, PD-1 inhibitors have shown promising results in certain cancers in clinical trials (Topalian et al., 2012, Hamid et al., 2013).

It has previously been shown that the TLR7 agonist imiquimod can boost T cell effector functions such as interferon-γ production in cSCC (Huang et al., 2009), demonstrating that effector T cell dysfunction in cSCC can be reversed pharmacologically. Whilst the PD-1 ligand PD-L1 has been detected in mouse models of cSCC (Cao et al., 2011) and human head and neck SCC (Strome et al., 2003), T cell exhaustion in cutaneous SCCs has not been investigated to date. As the majority of studies which have investigated T cell exhaustion in human cancer have focused on advanced tumours due to their accessibility, it is unclear whether T cell hyporesponsiveness in the early stages of cancer represents true T cell exhaustion (Baitsch et al., 2012). Therefore, the aims of this chapter are to:

1) characterise the effector T cell phenotype in cSCC,

2) determine if cSCC T cells have impaired functional capacity for cytokine production, proliferation and degranulation,

3) examine inhibitory receptor expression on T cells in cSCC, and

4) assess whether inhibiting PD-1 can enhance tumoral effector T cell function.

5.2 Results

5.2.1 CCR7 and L-selectin expression by T cells in cSCC

In the previous chapter, the majority of tumoral Tregs were found to express CLA, however, CLA was expressed by lower frequencies of $CD4^+FOXP3^-$ T cells (58.2%) and $CD8^+$ T cells (41.6%, see section 4.2.3). As it has previously been reported that cSCC T cells lack expression of skin homing markers and instead express markers characteristic of central memory T cells (Clark et al., 2008), in the current study, CCR7 and L-selectin expression on tumoral T cells was examined using flow cytometry (Figure 5.1). CCR7 was present on 17.2% ± 5.3% of Tregs, 32.9% ± 11.5% of $CD4^+FOXP3^-$ T cells and 15.5% ± 12.1% of $CD8^+$ T cells in cSCCs (n=16 tumours, Figure 5.2, page 139). CCR7 was more frequently expressed by Tregs and $CD4^+FOXP3^-$ T cells in the peripheral blood than those cells in normal skin and cSCC ($p<0.0001$ for all comparisons, Figure 5.2A, B). Although CCR7 was expressed by lower percentages of $CD8^+$ T cells in normal skin compared to blood ($p=0.0275$), there was no significant difference in CCR7 expression between $CD8^+$ T cells in blood and those in cSCC (Figure 5.2C).

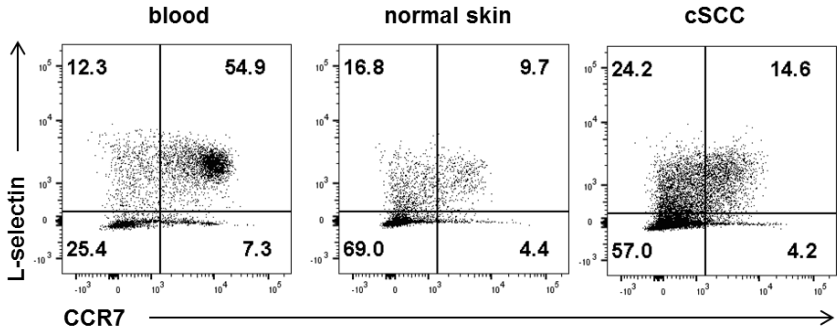

Figure 5.1 Expression of CCR7 and L-selectin by tumoral T cells.

Representative flow cytometry dot plots showing CCR7 and L-selectin expression on $CD3^+$ gated lymphocytes in blood, non-lesional skin and cSCC from the same subject. Plots representative of 12 subjects.

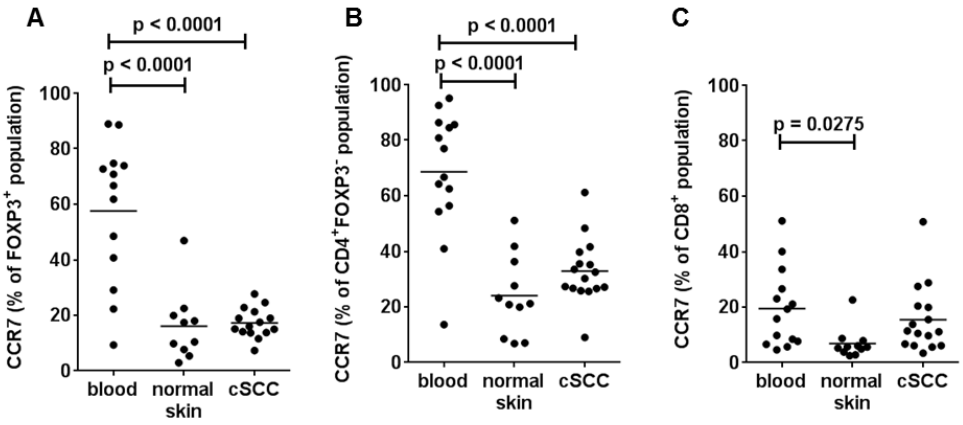

Figure 5.2 CCR7 expression by tumoral T cells.

(A-C) Graphs showing aggregate data for CCR7 expression in peripheral blood, normal skin and tumoral (A) $FOXP3^+$ Tregs, (B) $CD4^+FOXP3^-$ T cells, and (C) $CD8^+$ T cells (n=16 tumours). Horizontal bars = means, one-way ANOVA with Tukey's test for multiple comparisons.

L-selectin was expressed by 60.5% ± 20.3% of Tregs, 30.4% ± 13.8% of $CD4^+FOXP3^-$ T cells and 16.9% ± 8.5% of $CD8^+$ T cells (n=12 tumours, Figure 5.3, page 140). Similar to the CCR7 data, L-selectin was more frequently expressed by Tregs from blood than those from normal skin (p=0.0108) and cSCC (p=0.0014, Figure 5.3A). The percentage $CD4^+FOXP3^-$ cells expressing L-selectin was also higher in cSCC (p=0.0006) and normal skin (p=0.0082) compared with blood (Figure 5.3B). Higher frequencies of $CD8^+$ T cells in blood expressed L-selectin

than those from normal skin (p=0.0317), but there was no significant difference in percentage of $CD8^+$ T cells that were L-selectin$^+$ in blood and cSCC (Figure 5.3C). These results indicate that a proportion of tumoral T cells express the blood/lymph node homing markers CCR7 and L-selectin, suggesting that cSCCs contain some central memory T cells in addition to the effector memory T cells described in the previous chapter (in section 4.2.3, page 106).

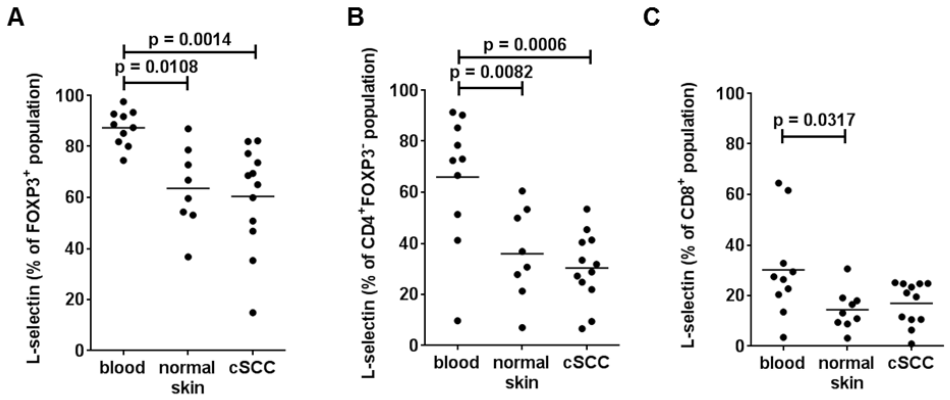

Figure 5.3 L-selectin expression by tumoral T cells.

(A-C) Graphs showing aggregate data for CCR7 expression in peripheral blood, normal skin and tumoral (A) $FOXP3^+$ Tregs, (B) $CD4^+FOXP3^-$ T cells, and (C) $CD8^+$ T cells (n=12 tumours). Horizontal bars = means, one-way ANOVA with Tukey's test for multiple comparisons.

5.2.2 Tumoral effector T cells exhibit reduced proliferative capacity

To investigate whether effector T cell dysfunction was present in cSCC, *in vitro* lymphocyte proliferation assays were conducted with effector T cells from cSCC and compared with those from corresponding blood, which were both cultured separately in the presence of accessory cells and PHA. Patient-matched non-lesional skin contained insufficient numbers of T cells for proliferation assays to be conducted. Effector $CD4^+CD25^{low}$ T cells from cSCC proliferated significantly less than those from peripheral blood (380 cpm versus 1015 cpm respectively, p=0.0005, n=23 tumours, Figure 5.4A, page 141). Similarly, proliferation was lower for tumoral $CD8^+$ T cells than peripheral blood $CD8^+$ T cells (2262 cpm versus 4032 cpm respectively, p=0.0010, n=12 tumours, Figure 5.4B). To determine whether the reduced proliferation by tumoral T cells was due to the use of collagenase during isolation of lymphocytes from skin, a single experiment

was performed using cells isolated from peripheral blood treated with collagenase in the same conditions and duration as the cells from the tumour. Collagenase treatment did not reduce proliferation of $CD4^+CD25^{low}$ effector T cells or $CD8^+$ T cells from peripheral blood down to the level of those from the tumour (data not shown). Therefore, these results suggest that tumoral effector $CD4^+$ T cells and $CD8^+$ T cells are less able to proliferate than effector T cells from blood, suggesting effector T cell dysfunctionality in cSCC.

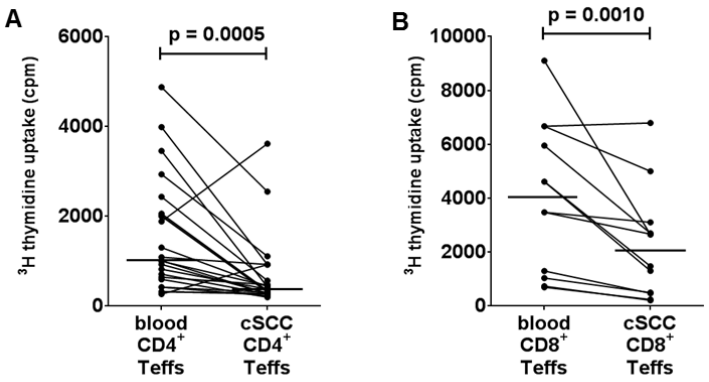

Figure 5.4 Effector T cells in cSCC proliferate less in response to stimulus compared with those from peripheral blood.

(A - B) Effector T cells from cSCC and corresponding peripheral blood were cultured with 1µg/ml PHA for 72 hours in the presence of autologous irradiated PBMCs, and tritiated thymidine uptake assays were conducted to assess cell proliferation. (A) $CD4^+CD25^{low}$ effector T cells and (B) $CD8^+$ T cells from cSCCs (n=23 and 12 tumours respectively) proliferate less than those from peripheral blood, dots = median values for each subject from triplicate well experiments, horizontal bars = median values for all subjects, paired Wilcoxon rank test.

5.2.3 Higher interferon-γ $^+$ T cell frequencies are present in cSCC than blood

Tumoral T cells were investigated to determine whether they were also dysfunctional in the ability to produce effector cytokines. Interferon-γ is secreted by TH1 and cytotoxic T cells, and is known to be protective against the development of tumours (Shankaran et al., 2001). In the current study, *ex vivo* unstimulated tumoral T cells did not produce interferon-γ , whereas when they were stimulated with PMA and ionomycin for 5 hours in the presence of Brefeldin A in the last 4 hours of culture, interferon-γ expression was detected (Figure

5.5A, page 142). Tumoral interferon-γ $^{+}$ T cells were found to contain approximately equal proportions of CD4^{+} and CD8^{+} T cells (Figure 5.5B), and were predominantly CD45RO^{+} memory T cells (Figure 5.6A).

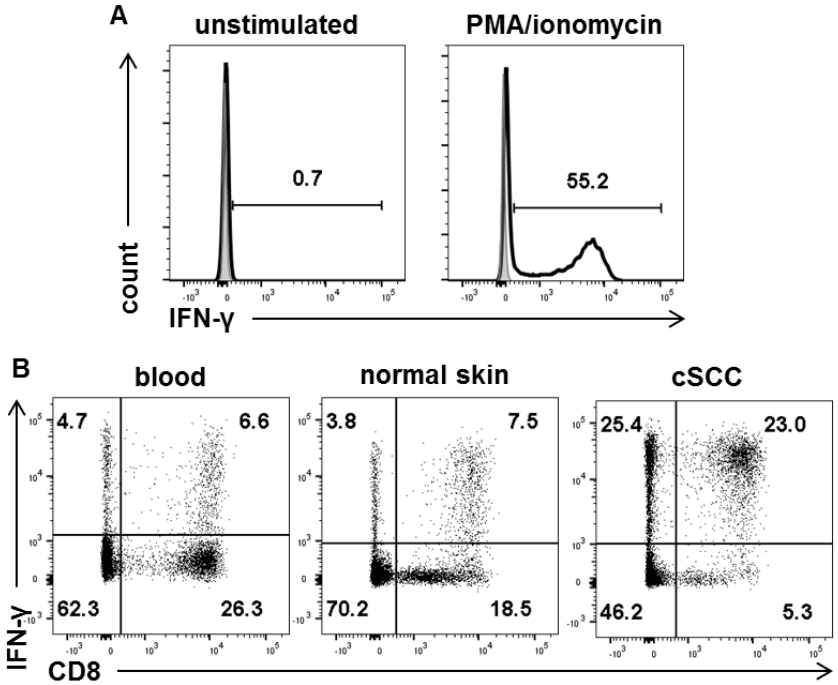

Figure 5.5 PMA and ionomycin-stimulated tumoral T cells express interferon-γ .
(A) Representative histograms demonstrating interferon-γ expression in tumoral CD3^{+} gated lymphocytes that were unstimulated or stimulated for 5 hours with PMA and ionomycin, grey shaded areas represent isotype control. (B) Representative dot plots from a separate subject showing interferon-γ and CD8 expression by PMA/ionomycin stimulated CD3^{+} gated lymphocytes from blood, normal skin and cSCC. Plots are representative of 15 tumours.

Interferon-γ was expressed by tumoral CD4^{+} and CD8^{+} T cells at higher frequencies in cSCC (17.1% ± 16.6% of CD4^{+} population, Figure 5.6B, page 143, and 32.8% ± 25.5% of CD8^{+} population, Figure 5.6C, n=15 tumours) than in peripheral blood (4.4% ± 3.6% of CD4^{+} population, p=0.0084, Figure 5.6B, and 9.2% ± 9.0% of CD8^{+} population, p=0.0077, Figure 5.6C). However, no difference in interferon-γ expression was seen between T cells from cSCC and non-lesional skin, where interferon-γ was observed in 9.4% ± 5.2% of CD4^{+} T cells and 24.2% ± 21.1% of CD8^{+} T cells. This data suggests that interferon-γ production is not impaired in effector T cells in cSCC.

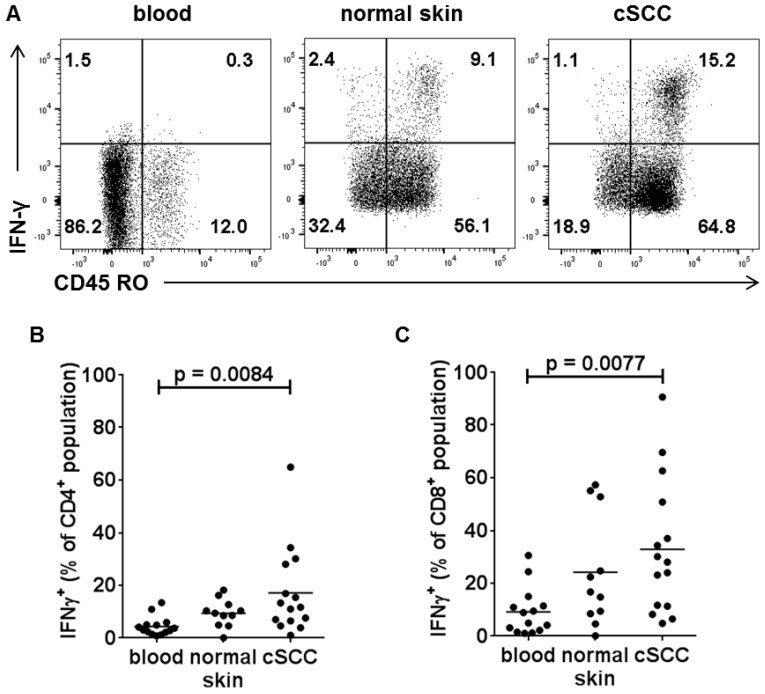

Figure 5.6 Higher interferon-γ producing frequencies of T cells are present in cSCC than peripheral blood.

(A) Representative dot plots showing interferon-γ and CD45RO expression in PMA/ionomycin stimulated $CD3^+$ gated T cells from blood, normal skin and cSCC. (B-C) Graphs showing frequencies of interferon-γ expressing (B) $CD4^+$ T cells and (C) $CD8^+$ T cells in blood, normal skin and cSCC (n=15 tumours). Horizontal bars = means, one-way ANOVA with Tukey's test for multiple comparisons.

5.2.4 Expression of TNF-α by tumoral T cells

TNF-α is another cytokine that can be produced by T cells and has been shown to be important in anti-tumour immunity (Calzascia et al., 2007), but has also more recently been implicated in promoting tumour growth (Bertrand et al., 2015). In the current study, TNF-α expression was examined in T cells from blood, normal skin and cSCC, where populations of $TNF\text{-}\alpha^+IFN\text{-}\gamma^-$ and $TNF\text{-}\alpha^+IFN\text{-}\gamma^+$ T cell populations were observed (Figure 5.7A, page 144). TNF-α was expressed by 8.7% ± 6.2% of the $CD4^+$ population in blood, 30.8% ± 22.5% of the $CD4^+$ population in normal skin, 29.2% ± 26.3% of the $CD4^+$ population in cSCC, n=11 tumours (Figure 5.7B). Although higher frequencies of $CD8^+$ T cells were $TNF\text{-}\alpha^+$ in cSCC compared with peripheral blood (49.5% ± 30.0% versus 13.7% ± 8.7%, p=0.0026, n=11 tumours), there were similar proportions of TNF-α expressing

$CD8^+$ T cells in cSCC and non-lesional skin (48.3% ± 20.4%, Figure 5.7C). This data indicates that tumoral effector T cells are not diminished in their capacity to produce TNF-α.

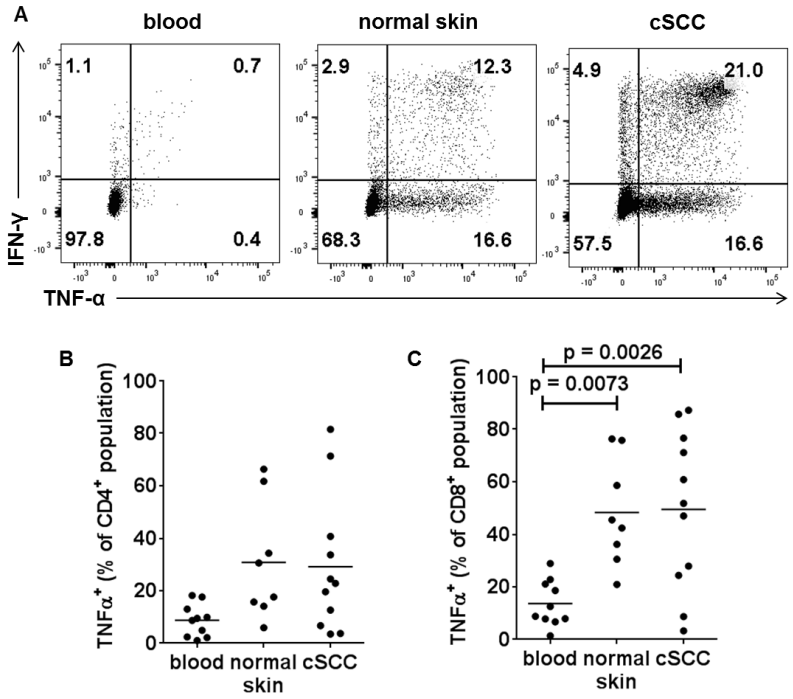

Figure 5.7 Production of TNF-α by tumoral T cells.

(A) Representative dot plots showing TNF-α and interferon-γ expression in PMA/ionomycin stimulated $CD3^+$ gated T cells from blood, normal skin and cSCC. (B-C) Graphs showing frequencies of TNF-α expressing (B) $CD4^+$ T cells and (C) $CD8^+$ T cells in blood, normal skin and cSCC (n=11 tumours). Horizontal bars = means, one-way ANOVA with Tukey's test for multiple comparisons.

5.2.5 IL-2 is expressed by lower frequencies of T cells in cSCC compared with non-lesional skin

IL-2, a cytokine produced by $CD4^+$ TH1 cells and $CD8^+$ T cells that stimulates T cell proliferation and differentiation, has shown effectiveness as a cancer immunotherapy (Rosenberg, 2014). Loss of IL-2 has been shown to be a characteristic of T cell exhaustion in cancer (Fourcade et al., 2010, Sakuishi et al., 2010). In the current study, non-lesional skin contained higher frequencies of IL-2 expressing T cells (22.8% ± 16.9% of $CD4^+$ population and 16.0% ± 11.2% of $CD8^+$ population) than corresponding blood (3.0% ± 4.1% of $CD4^+$ population,

p=0.0001, Figure 5.8B, page 145, and 1.9% ± 2.3% of CD8⁺ population, p<0.0001, Figure 5.8C) and cSCC (8.2% ± 8.7% of CD4⁺ population, p<0.0001, Figure 5.8B, and 5.3% ± 4.6% of CD8⁺ population, p<0.0001, n=14 tumours, Figure 5.8C). These results suggest that effector T cells in cSCC are less able to produce IL-2 than effector T cells from non-lesional skin, which would be consistent with the early stages of T cell exhaustion (Wherry and Kurachi, 2015).

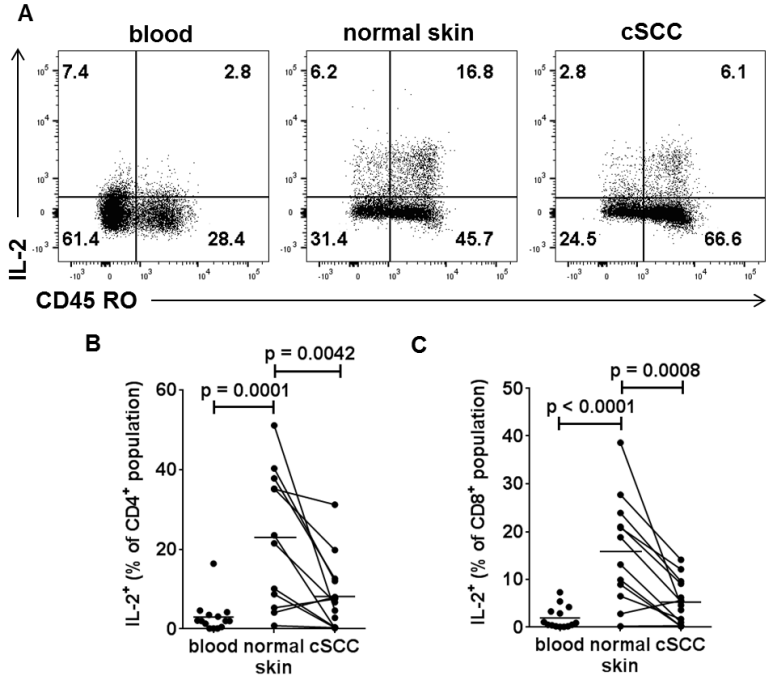

Figure 5.8 Lower frequencies of T cells express IL-2 in cSCC than normal skin.
(A) Representative dot plots showing IL-2 and CD45RO expression in PMA/ionomycin stimulated CD3⁺ gated T cells from blood, normal skin and cSCC. (B-C) Graphs showing frequencies of IL-2 expressing (B) CD4⁺ T cells and (C) CD8⁺ T cells in blood, normal skin and cSCC (n=14 tumours). In (B, C), dots represent independent experiments, paired normal skin and cSCC samples are linked to show that in most subjects, IL-2 is expressed less frequently by T cells from cSCC than those from normal skin. Horizontal bars = means, one-way ANOVA with Tukey's test for multiple comparisons.

5.2.6 IL-4, but not IL-13, is expressed by T cells at higher frequencies in the tumour compared with blood

TH2 inflammation has been implicated in promoting carcinogenesis and poorer clinical outcomes in cancer (De Monte et al., 2011). To investigate the expression of TH2 cytokines in the cSCC environment, tumoral T cell expression of IL-4 and

IL-13 was examined. IL-4 was expressed by a substantial proportion of tumoral T cells (Figure 5.9), with significantly higher frequencies of T cells in cSCC (37.4% ± 23.3% of $CD4^+$ T cell population; 15.5% ± 12.5% of $CD8^+$ T cell population, n=10 tumours) compared with blood (2.4% ± 0.9% of $CD4^+$ T cell population, p=0.0027, Figure 5.9B; 2.5% ± 1.9% of $CD8^+$ T cell population, p=0.0343, Figure 5.9C). Non-lesional skin IL-4^+ T cell frequencies (22.5% ± 21.9% of $CD4^+$ T cell population; 10.8% ± 7.5% of $CD8^+$ T cell population) were similar to those in cSCC, but significantly higher than those in peripheral blood ($p<0.05$).

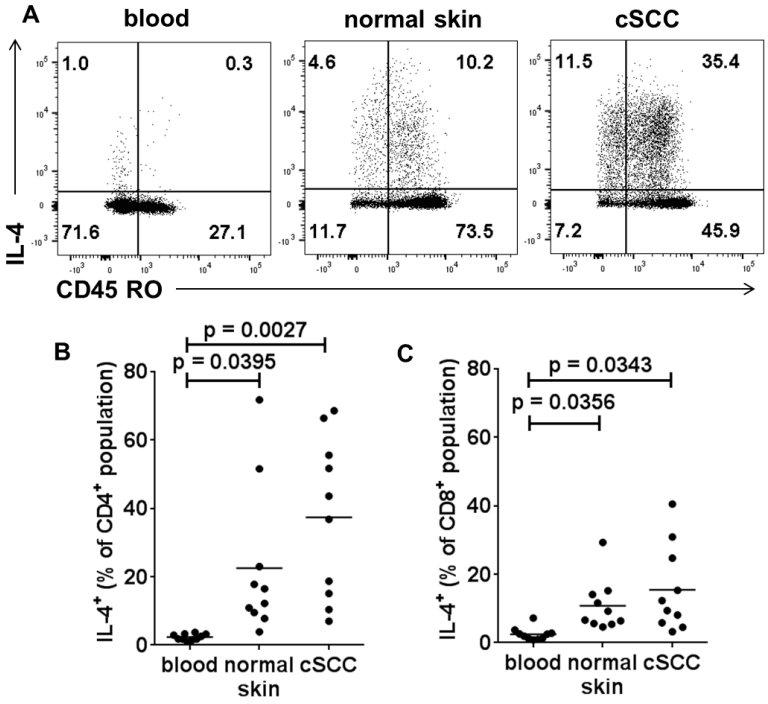

Figure 5.9 IL-4 expression is upregulated in T cells in cSCC compared with those in blood.

(A) Representative dot plots showing IL-4 and CD45RO expression in PMA/ionomycin stimulated $CD3^+$ gated T cells from blood, normal skin and cSCC. (B-C) Graphs showing frequencies of IL-4 expressing (B) $CD4^+$ T cells and (C) $CD8^+$ T cells in blood, normal skin and cSCC (n=10 tumours). Horizontal bars = means, one-way ANOVA with Tukey's test for multiple comparisons.

Analysis of IL-13 expression showed relatively low numbers of tumoral T cells expressed this cytokine in comparison to IL-4 (Figure 5.10, page 147). IL-13^+ frequencies amongst $CD4^+$ T cells in the blood, normal skin and cSCC were 0.6% ± 0.9%, 2.2% ± 2.3% and 1.2% ± 1.6% respectively, n=10 tumours (Figure 5.10B),

and in CD8⁺ T cells were 0.7% ± 0.8%, 1.3% ± 1.4% and 1.1% ± 1.0% respectively, n=10 tumours (Figure 5.10C). These results indicate that the TH2 cytokine IL-4 is expressed by a notable proportion of T cells in cSCC, but IL-13⁺ T cells are infrequent.

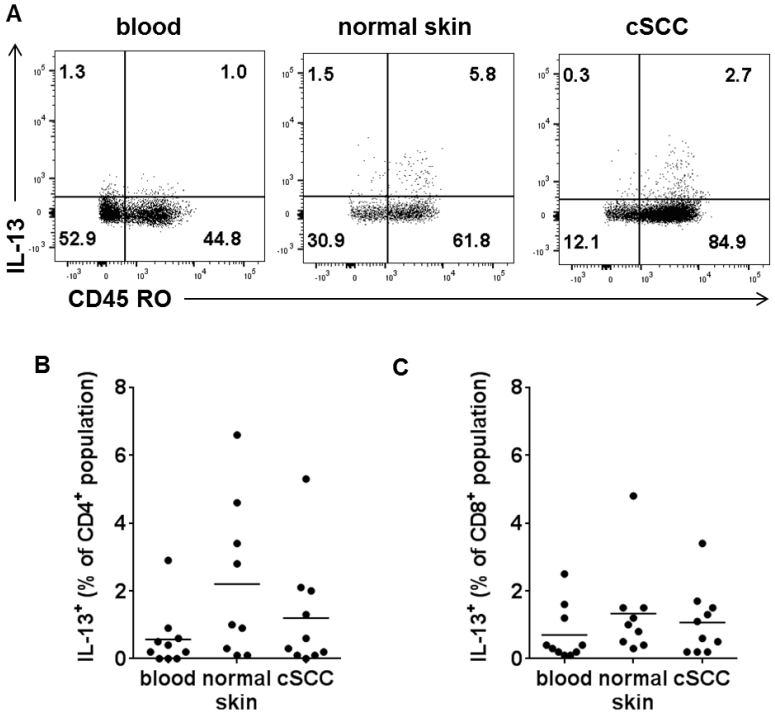

Figure 5.10 IL-13 expression by T cells in cSCC.

(A) Representative dot plots showing IL-13 and CD45RO expression in PMA/ionomycin stimulated CD3⁺ gated T cells from blood, normal skin and cSCC. (B-C) Graphs showing frequencies of IL-13 expressing (B) CD4⁺ T cells and (C) CD8⁺ T cells in blood, normal skin and cSCC (n=10 tumours). Horizontal bars = means.

5.2.7 IL-17⁺ T cells are infrequent in cSCC

TH17 cells are recognised to play an important role in certain inflammatory processes, however, their role in malignant disease remains uncertain (Maniati et al., 2010). Although some studies have demonstrated TH17 cell infiltration was associated improved clinical outcomes in human cancer (Kryczek et al., 2009), IL-17 was recently shown to enhance cSCC growth in mice (Nardinocchi et al., 2015). In the current study, IL-17 was found to be expressed by only a small fraction of tumoral T cells (Figure 5.11A, page 148), with IL-17 positivity demonstrated in 4.7% ± 9.8% of the tumoral CD4⁺ T cell population (Figure 5.11B) and 2.4% ± 5.6% of the tumoral CD8⁺ T cell population (Figure 5.11C), n=13

tumours. There were no significant differences in IL-17$^+$ T cell frequencies between cSCC and blood (0.4% ± 0.4% of CD4$^+$ T cell population, 0.3% ± 0.3% of CD8$^+$ T cell population) or normal skin (4.0% ± 4.1% of CD4$^+$ T cell population, 2.8% ± 4.1% of CD8$^+$ T cell population), but there were higher percentages of CD4$^+$ T cells that expressed IL-17 in normal skin than in blood (p=0.0352, Figure 5.11B). Overall, these results show that IL-17$^+$ T cells are infrequent in cSCC.

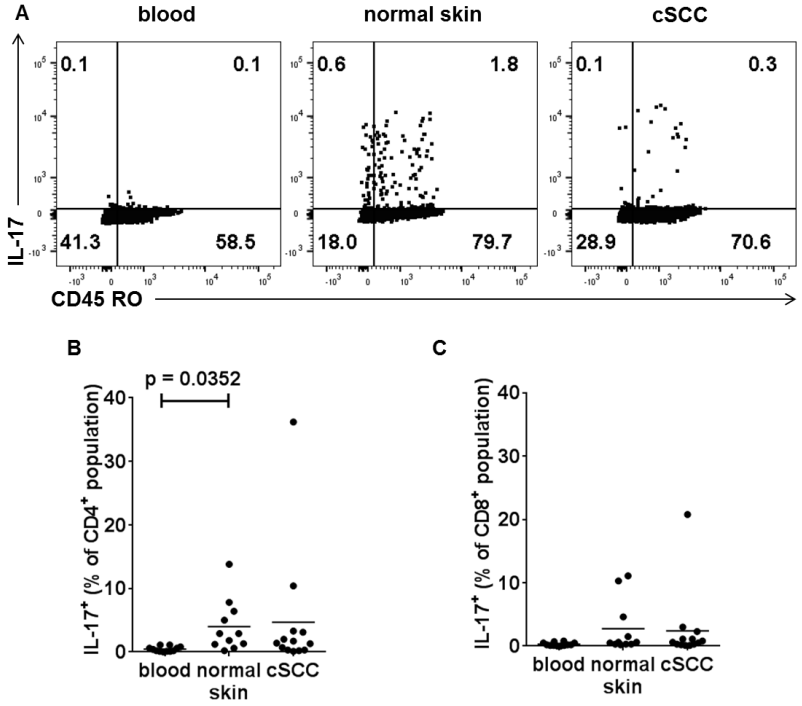

Figure 5.11 Low frequencies of IL-17$^+$ T cells are present in cSCC.

(A) Representative dot plots showing IL-17 and TNF-α expression in PMA/ionomycin stimulated CD3$^+$ gated T cells from blood, normal skin and cSCC. (B-C) Graphs showing frequencies of IL-13 expressing (B) CD4$^+$ T cells and (C) CD8$^+$ T cells in blood, normal skin and cSCC (n=13 tumours). Horizontal bars = means, one-way ANOVA with Tukey's test for multiple comparisons.

5.2.8 PD-1 is expressed on tumoral T cells

To investigate whether T cell exhaustion was responsible for effector T cell dysfunction in cSCC, inhibitory receptors were examined on tumoral T cells. PD-1 was mainly detected on CD45RO$^+$ memory T cells in the blood, non-lesional skin and cSCC (Figure 5.12A, page 150). CD4$^+$ T cells expressed PD-1 at higher frequencies in cSCC compared with in blood (19.9% ± 12.9% versus 3.1% ± 3.0% respectively, p<0.0001, n=62 tumours) and non-lesional skin (13.2% ± 9.8%, p=0.0010, Figure 5.12B). PD-1 was also expressed by greater proportions of CD8$^+$ T cells in cSCC than blood (23.7% ± 15.4% versus 3.5% ± 3.5% respectively, n=71

tumours, $p<0.0001$, Figure 5.12C), but there was no significant difference in PD-1^+ $CD8^+$ T cell percentages in cSCC and non-lesional skin (22.2% ± 15.9%). In addition, PD-1 was upregulated on both $CD4^+$ and $CD8^+$ T cell populations in non-lesional skin compared with peripheral blood ($p<0.0001$ for both comparisons). The expression of PD-1 in T cells from non-lesional skin was similar to that reported in skin from older individuals (Vukmanovic-Stejic et al., 2015). As the patient matched skin in the current study was obtained from skin sites that may have received chronic sun exposure, it is possible that chronic exposure to UVR or external antigens in aged skin could account for PD-1 expression in T cells from non-lesional skin. To investigate if UVR could upregulate PD-1 on T cells *in vitro*, flow cytometry was performed on PBMCs which had been irradiated with UVB. PD-1 expression on T cells from 5 subjects did not alter despite UVB irradiation for varying durations up to 480 s (Figure 5.12D), suggesting that acute UVR exposure *in vitro* does not lead to increased PD-1 expression on T cells.

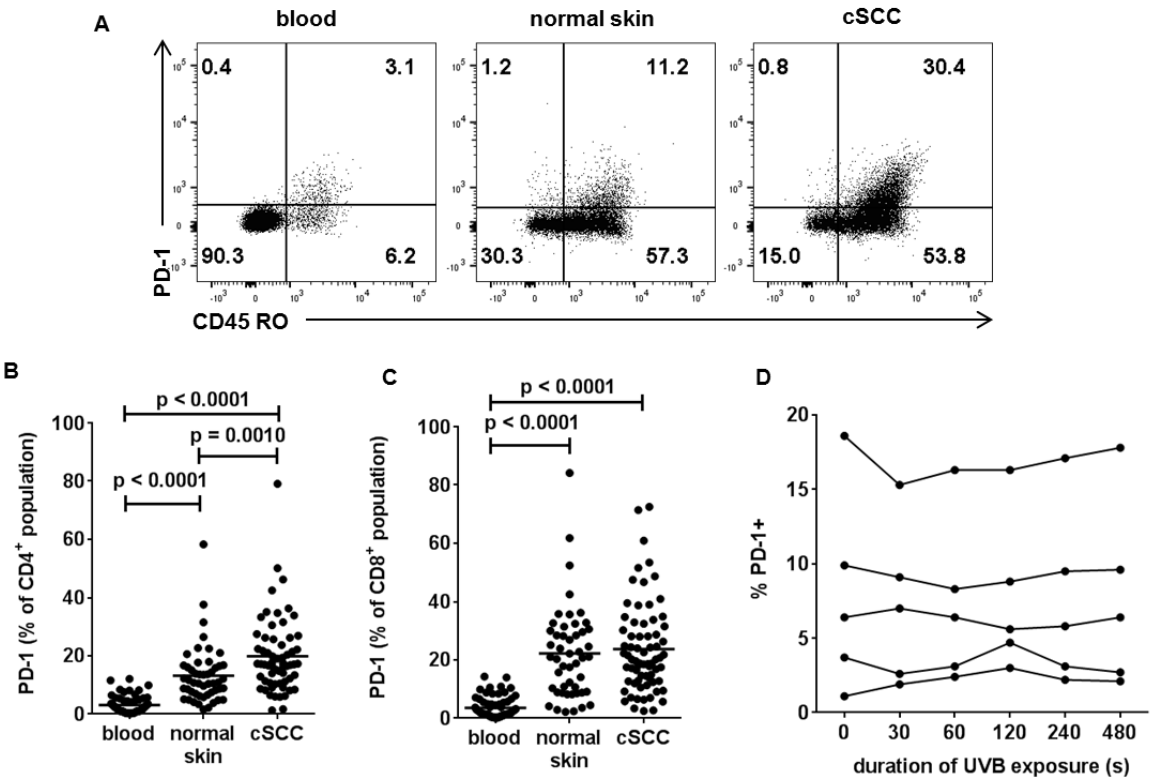

Figure 5.12 PD-1 expression by T cells in cSCC and non-lesional skin.

(A) Representative dot plots showing PD-1 and CD45RO expression in $CD3^+$ gated T cells from blood, normal skin and cSCC. (B-C) Graphs showing frequencies of PD-1 expressing (B) $CD4^+$ T cells and (C) $CD8^+$ T cells in blood, non-lesional skin and cSCC ((B) n=62 tumours, (C) n=71 tumours). Horizontal bars = means, one-way ANOVA with Tukey's test for multiple comparisons. (D) PD-1 expression on peripheral blood T cells from five subjects irradiated with varying doses of UVB. Lines connect data points from the same subject.

Although CD39 is predominantly found on Tregs and contributes to their suppressive function, CD39 has also been proposed as a marker of T cell exhaustion (Gupta et al., 2015). In the current study, PD-1 and CD39 co-expression was investigated in tumoral T cells, showing sizeable $PD\text{-}1^+CD39^+$ T cell populations in cSCC (Figure 5.13A). CD39 was upregulated in $PD\text{-}1^+$ tumoral T cells ($CD39^+$ = 37.6% ± 16.9% of $PD\text{-}1^-$ T cell population versus 55.0% ± 23.0% of $PD\text{-}1^+$ T cell population, p=0.0020, n=10 tumours, Figure 5.13B), and PD-1 expression was increased in $CD39^+$ tumoral T cells ($PD\text{-}1^+$ = 12.1% ± 9.5% of $CD39^-$ T cell population versus 25.5% ± 19.9% of $CD39^+$ T cell population, p=0.0088, Figure 5.13C). These results suggest that CD39 is highly expressed in $PD\text{-}1^+$ T cells in cSCC, which may contribute to their inhibitory phenotype.

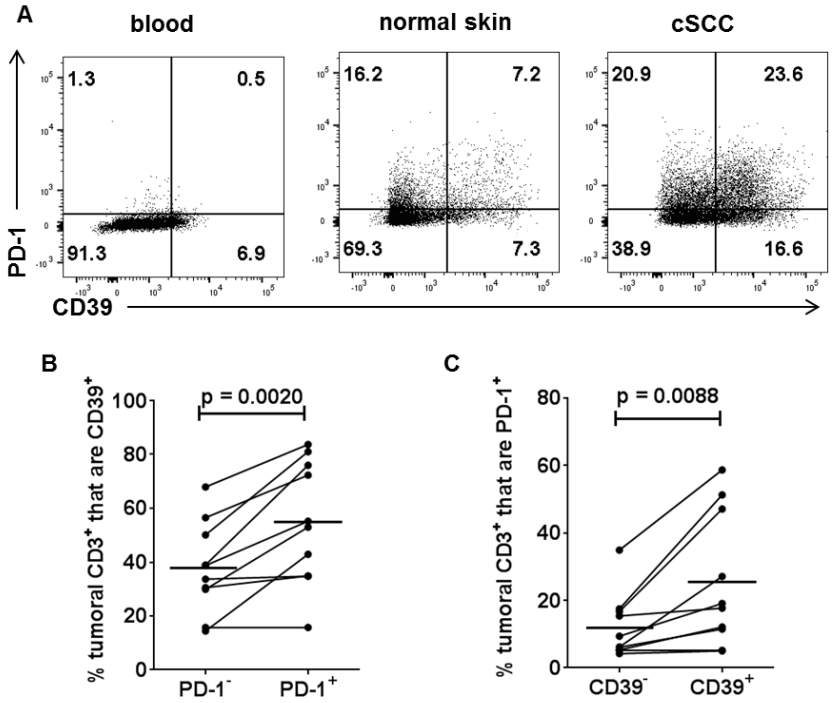

Figure 5.13 CD39 is upregulated on PD-1$^+$ tumoral T cells.

(A) Representative dot plots showing CD39 and PD-1 expression in CD3$^+$ gated T cells from blood, normal skin and cSCC. (B) CD39$^+$ expression on PD-1$^-$ and PD-1$^+$ tumoral T cells. (C) PD-1$^+$ expression on CD39$^-$ and CD39$^+$ tumoral T cells. (B, C) n=10 tumours, horizontal bars = means, paired T test.

5.2.9 **PD-L1 is expressed in cSCC**

To investigate whether PD-L1, the ligand for PD-1 was present in cSCC, confocal microscopy was performed which showed PD-L1 was expressed by cSCC keratinocytes on the cell membrane and cytoplasm, and confirmed PD-1 was expressed on the cell surface of immunocytes (Figure 5.14, page 153). Flow cytometry was also conducted to examine PD-L1 expression in immunocytes from cSCC and normal skin, as well as in corresponding PBMCs. PD-L1 was predominantly expressed by the $CD3^-$ immunocyte populations in cSCC (Figure 5.15A, page 154). PD-L1 was expressed by 10.0% ± 4.8% of live immunocytes in cSCC (n=11 tumours), which was more frequent than that in blood (2.4% ± 2.3%, p=0.0004) but similar to non-lesional skin (8.1% ± 4.0%, Figure 5.15B). PD-L1 expression was observed in 3.0% ± 3.7% of Tregs, 1.1% ± 1.0% of $CD4^+FOXP3^-$ T cells and 4.3% ± 3.4% of $CD8^+$ T cells in cSCC (n=11 tumours), and no differences in PD-$L1^+$ frequencies in the T cell subsets were found between blood, normal skin and cSCC (Figure 5.15C-E).

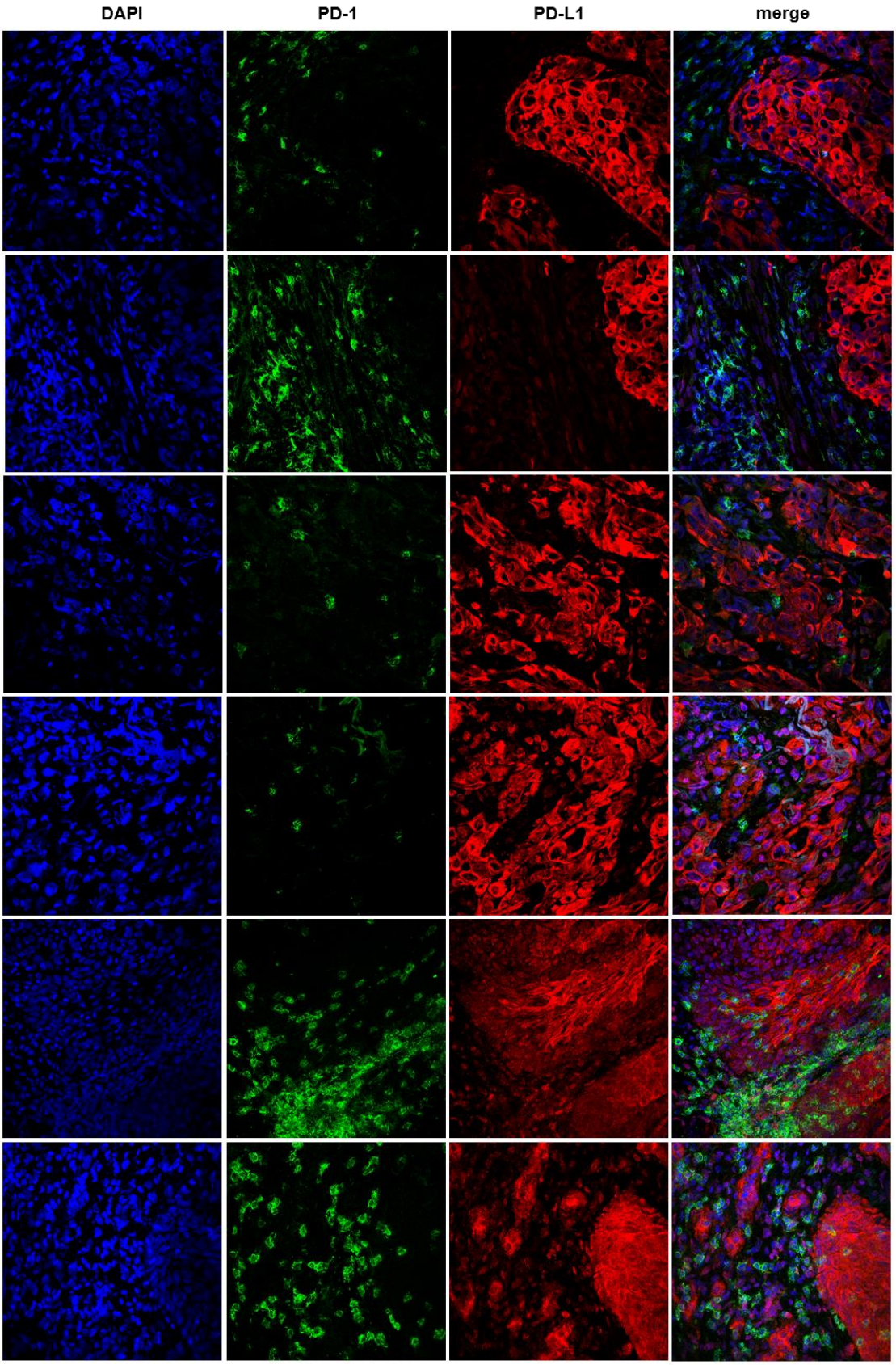

Figure 5.14 PD-L1 is expressed by cSCC tumour keratinocytes.

Representative confocal microscopy images of DAPI, PD-1, PD-L1 staining of frozen sections from 6 cSCCs. PD-1 was expressed by immunocytes whereas PD-L1 was expressed in varying intensities by tumour keratinocytes. Scale bar = 50 μm.

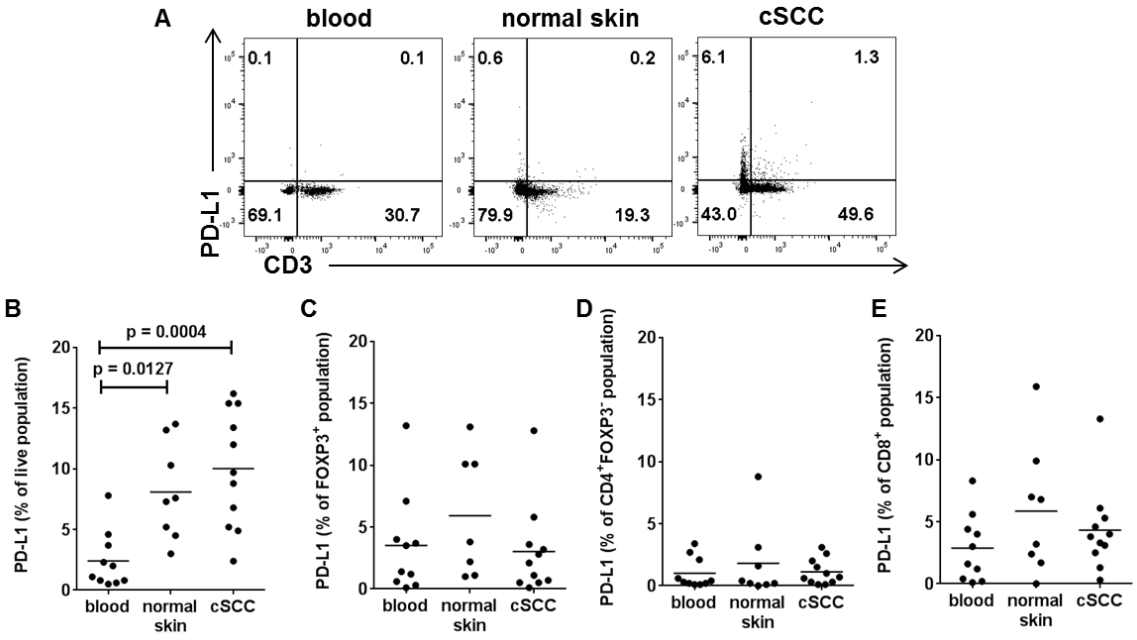

Figure 5.15 PD-L1 expression by non-T cells and T cells in cSCC.

(A) Representative dot plots showing PD-L1 and CD3 expression in live immunocytes from blood, normal skin and cSCC. (B-E) PD-L1 expression as a percentage of (B) total live immunocytes, (C) Tregs, (D) $CD4^+FOXP3^-$ T cells, and (E) $CD8^+$ T cells. Horizontal bars = means, one-way ANOVA with Tukey's test for multiple comparisons.

5.2.10 CTLA-4 is upregulated by tumoral non-regulatory T cells

In the previous chapter, the inhibitory receptor CTLA-4 was found to be highly expressed by tumoral Tregs intracellularly (section 4.2.8), and also by some $FOXP3^-$ T cells (Figure 5.16A). CTLA-4 can be expressed by exhausted effector T cells (Wherry and Kurachi, 2015), and in the current study, CTLA-4 was present in 33.4% ± 21.6% of $CD4^+FOXP3^-$ T cells and 17.6% of $CD8^+$ T cells in cSCC (n=10 tumours), which were higher than the CTLA-4^+ percentages in T cells from blood (3.3% ± 4.9% of $CD4^+FOXP3^-$ T cells, p=0.0001, and 17.6% ± 20.8% of $CD8^+$ T cells, p=0.0194) and non-lesional skin (10.0% ± 2.7% of $CD4^+FOXP3^-$ T cells, p=0.0053, and 1.3% ± 1.1% of $CD8^+$ T cells, p=0.0406, Figure 5.16B, C, page 155), indicating that CTLA-4 is upregulated by effector T cells in the tumour.

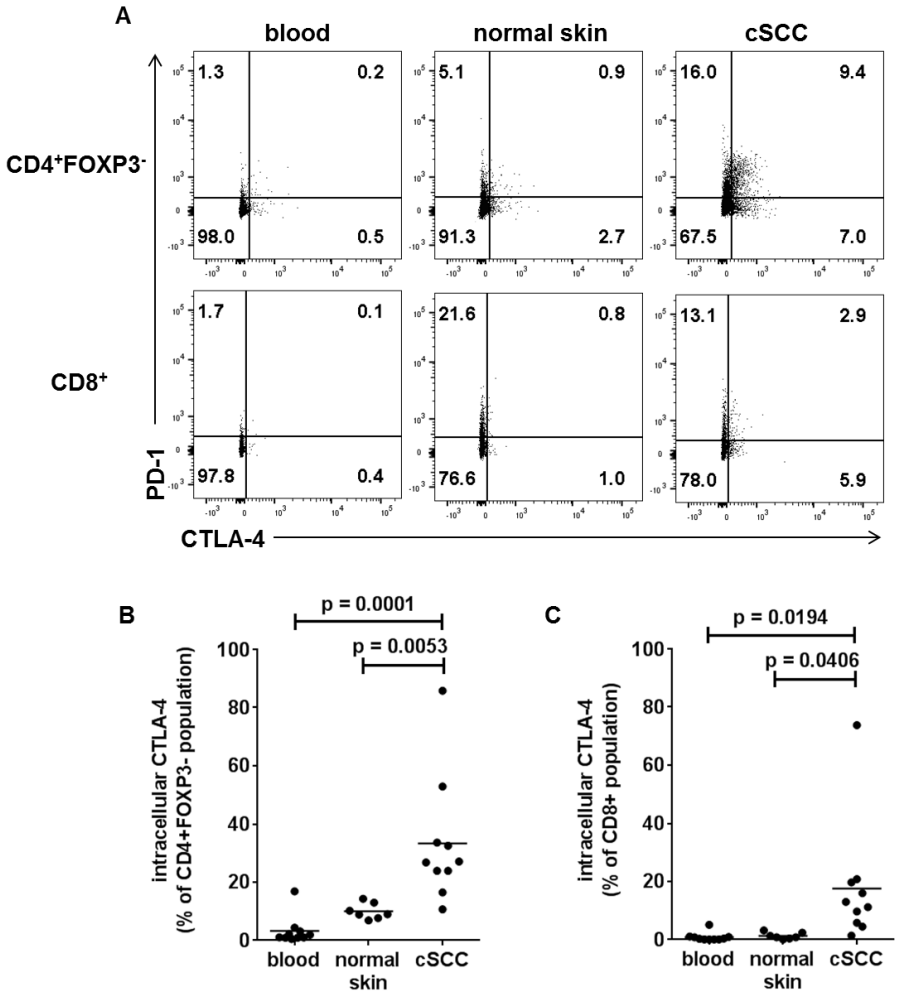

Figure 5.16 CTLA-4 is upregulated in non-regulatory T cell populations in cSCC. (A) Representative dot plots showing intracellular CTLA-4 and PD-1 expression in $CD4^+FOXP3^-$ (top row) and $CD8^+$ T cells (bottom row) from blood, normal skin and cSCC. (B-C) Intracellular CTLA-4 expression in (B) $CD4^+FOXP3^-$ T cells, and (C) $CD8^+$ T cells in blood, normal skin and cSCC. Horizontal bars = means, one-way ANOVA with Tukey's test for multiple comparisons.

5.2.11 Tim-3, BTLA, LAG-3 and CD160 are not present on tumoral T cells, but CD244 and TIGIT are detected

To investigate whether cSCC T cells expressed other inhibitory receptors characteristic of T cell exhaustion, flow cytometry was performed for Tim-3, BTLA, LAG-3, CD160, CD244 and TIGIT. Tim-3 expression was minimal in cSCC T cells despite PD-1 being present on these cells, and Tim-3 could be detected on peripheral blood T cells that had been stimulated with PHA for 72 hours for use as a positive control, demonstrating that the anti-Tim-3 antibody was working

effectively (Figure 5.17A). In *ex vivo* tumoral T cells, Tim-3 was only expressed by 0.5% ± 0.6% of $CD4^+$ T cells (Figure 5.17B) and 0.1% ± 0.1% of $CD8^+$ T cells (n=13 tumours, Figure 5.17C).

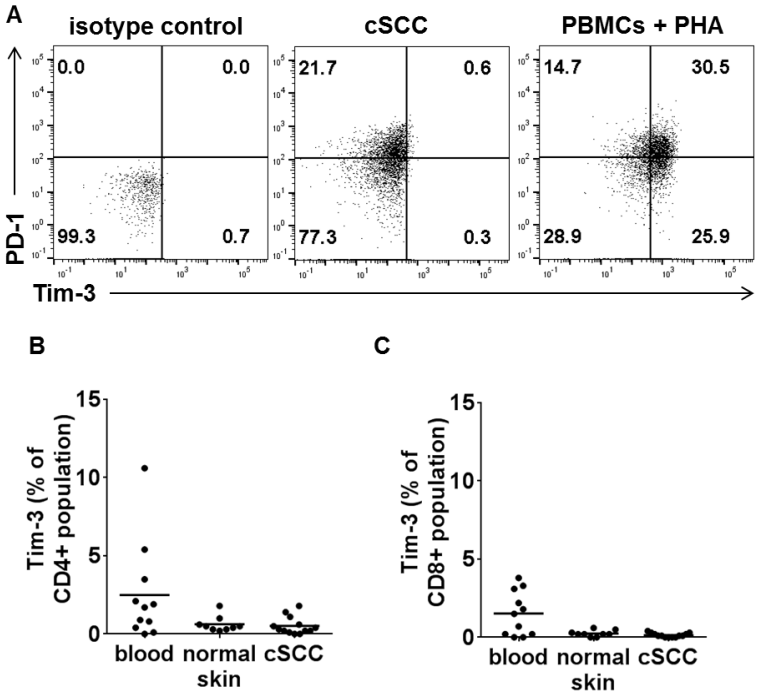

Figure 5.17 Minimal expression of Tim-3 by tumoral T cells.

(A) Representative flow cytometry dot plots showing isotype control staining of PBMCs, and staining for Tim-3 and PD-1 in *ex vivo* tumoral $CD3^+$ gated T cells and PBMCs that had been stimulated with PHA for 72 hours. (B-C) Tim-3 expression in (B) $CD4^+$ T cells, and (C) $CD8^+$ T cells in blood, normal skin and cSCC (n=13 tumours). Horizontal bars = means.

Analysis of BTLA, LAG-3 and CD160 expression showed that whilst these inhibitory receptors could be detected in small proportions of $CD3^-$ immunocyte populations from peripheral blood, their presence on $CD3^+$ T cells in blood, normal skin and cSCC was negligible (Figure 5.18A, D, G, page 157). BTLA was expressed by 0.7% ± 1.3% of $CD4^+$ T cells (Figure 5.18B) and 0.3% ± 0.4% of $CD8^+$ T cells (n=10 tumours, Figure 5.18C), LAG-3 was expressed by 0.7% ± 0.9% of $CD4^+$ T cells (Figure 5.18E) and 1.4% ± 1.6% of $CD8^+$ T cells (n=14 tumours, Figure 5.18F), and CD160 was expressed by 0.1% ± 0.1% of $CD4^+$ and 0.0% ± 0.0% of $CD8^+$ T cells (n=13 tumours, Figure 5.18H, I).

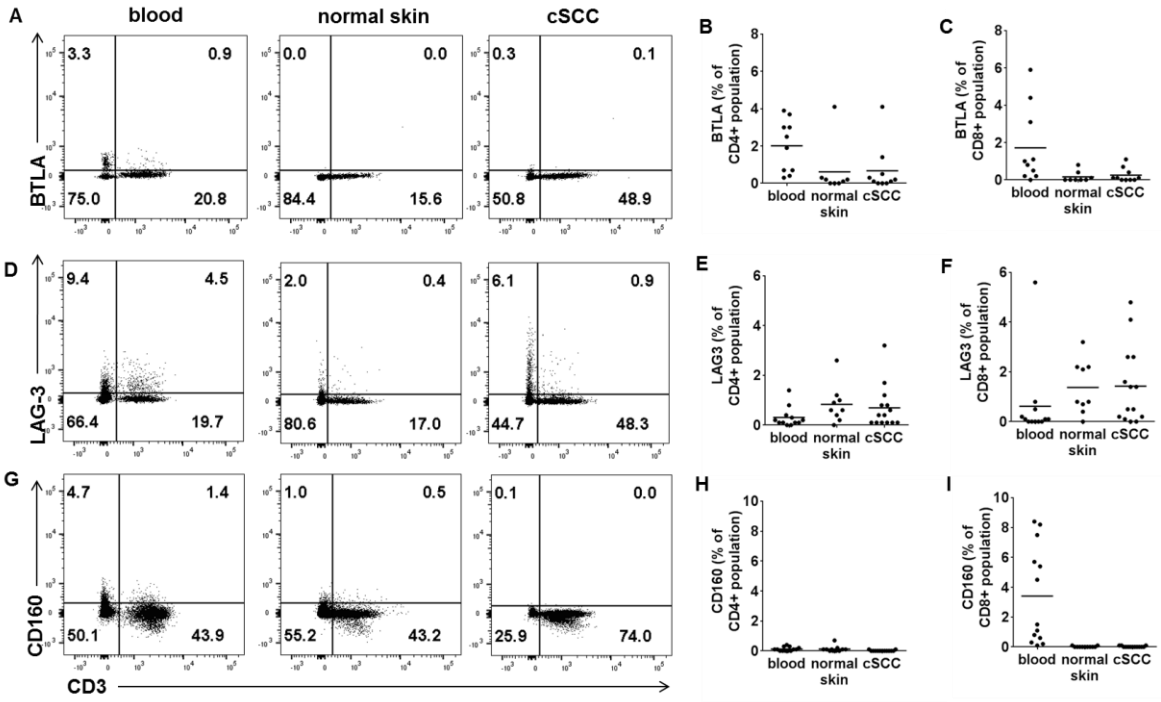

Figure 5.18 Low expression of BTLA, LAG-3 and CD160 by tumoral T cells.

(A, D, G) Representative dot plots illustrating expression of (A) BTLA, (D) LAG-3 and (G) CD160 versus CD3 in immunocytes from separate patients, from matched blood, normal skin and cSCC, demonstrating that few T cells in cSCC expressed these markers. (B, C, E, F, H, I) Expression of (B, C) BTLA, (E, F) LAG3, (H, I) CD160 on (B, E, H) $CD4^+$ T cells and (C, F, I) $CD8^+$ T cells from blood, normal skin and cSCC. (B-C) n=10 tumours, (E-F) n=14 tumours, (G, H) n=13 tumours. Horizontal bars = means.

CD244 was detected mainly on $CD8^+$ rather than $CD4^+$ T cell populations in blood, normal skin and cSCC (Figure 5.19A, page 158). No significant differences were noted in CD244 expression between T cells in blood, normal skin and cSCC; the percentages of $CD4^+$ T cells that were $CD244^+$ were 10.8% ± 14.6% in blood, 5.9% ± 4.9% in normal skin and 4.6% ± 4.5% in cSCC (n=12 tumours, Figure 5.19B), and the percentages of $CD8^+$ T cells that expressed CD244 were 65.9% ± 25.5% in blood, 44.2% ± 23.5% in normal skin and 50.7% ± 24.7% in cSCC (n=12 tumours, Figure 5.19C).

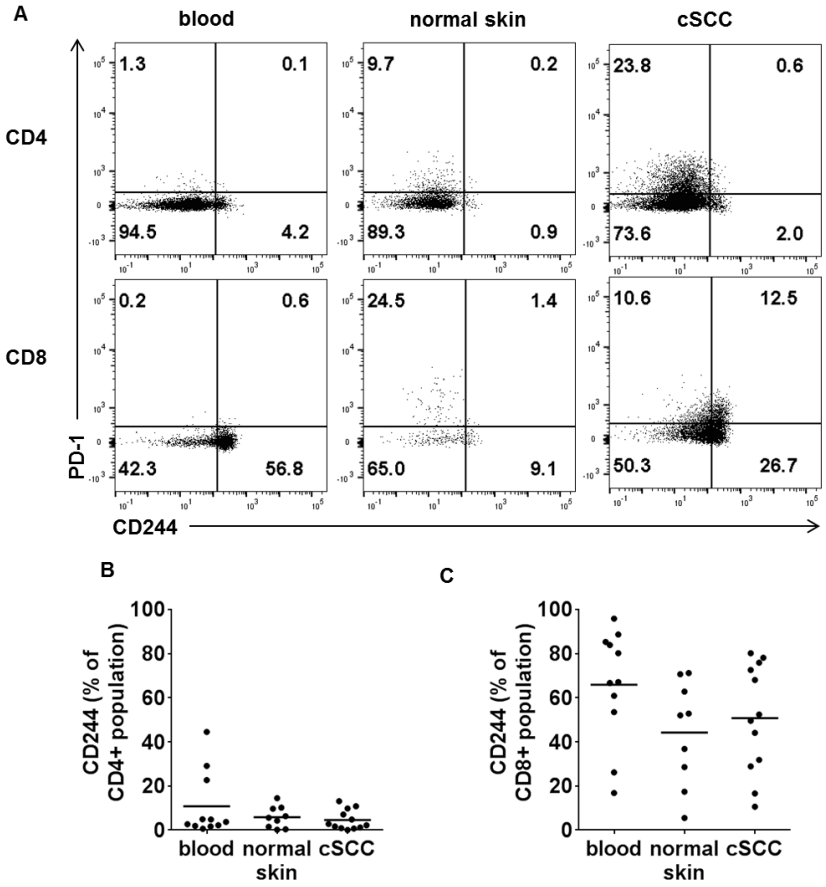

Figure 5.19 CD244 is expressed by CD8⁺ T cells in blood, non-lesional skin and cSCC.

(A) Representative flow cytometry dot plots demonstrating CD244 and PD-1 expression in CD4⁺ T cells (top row) and CD8⁺ T cells (bottom row) in blood, normal skin and cSCC. (B-C) CD244 expression by (B) CD4⁺ T cells and (C) CD8⁺ T cells in blood, normal skin and cSCC (n=12 tumours), horizontal bars = means.

TIGIT was noted to be present on many tumoral PD-1⁺ T cells (Figure 5.20A, page 160). CD4⁺ T cells expressed TIGIT at higher frequencies in cSCC compared with in peripheral blood (44.9% ± 16.2% versus 12.4% ± 5.6% respectively, $p<0.0001$, n=18 tumours, Figure 5.20B), but there was no significant difference compared with normal skin (26.0% ± 8.6%). In addition, no significant differences were observed in TIGIT expression between CD8⁺ T cells from blood (36.5% ± 22.9%), normal skin (29.6% ± 22.6%) and cSCC (40.7% ± 30.8%, n= 18 tumours, Figure 5.20C). The percentage of CD8⁺ T cells that expressed both TIGIT and PD-1 were significantly higher in normal skin and cSCC compared with blood, but TIGIT⁺PD-1⁺ frequencies were similar in CD8⁺ T cells from normal skin and cSCC (blood: 2.2% ± 2.4%, normal skin: 16.8% ± 14.1%, cSCC 16.2% ± 11.8%, blood versus

normal skin: p=0.0114, blood versus cSCC: p=0.0087, n=12 tumours, Figure 5.20D). cSCC and normal skin contained similar percentages of $CD8^+PD\text{-}1^+$ T cells that expressed TIGIT (55.1% ± 28.2%, n=12, and 46.0% ± 25.5%, n=9 respectively, Figure 5.20E), suggesting that the co-expression of TIGIT and PD-1 could not distinguish $CD8^+$ T cells from cSCC and normal skin.

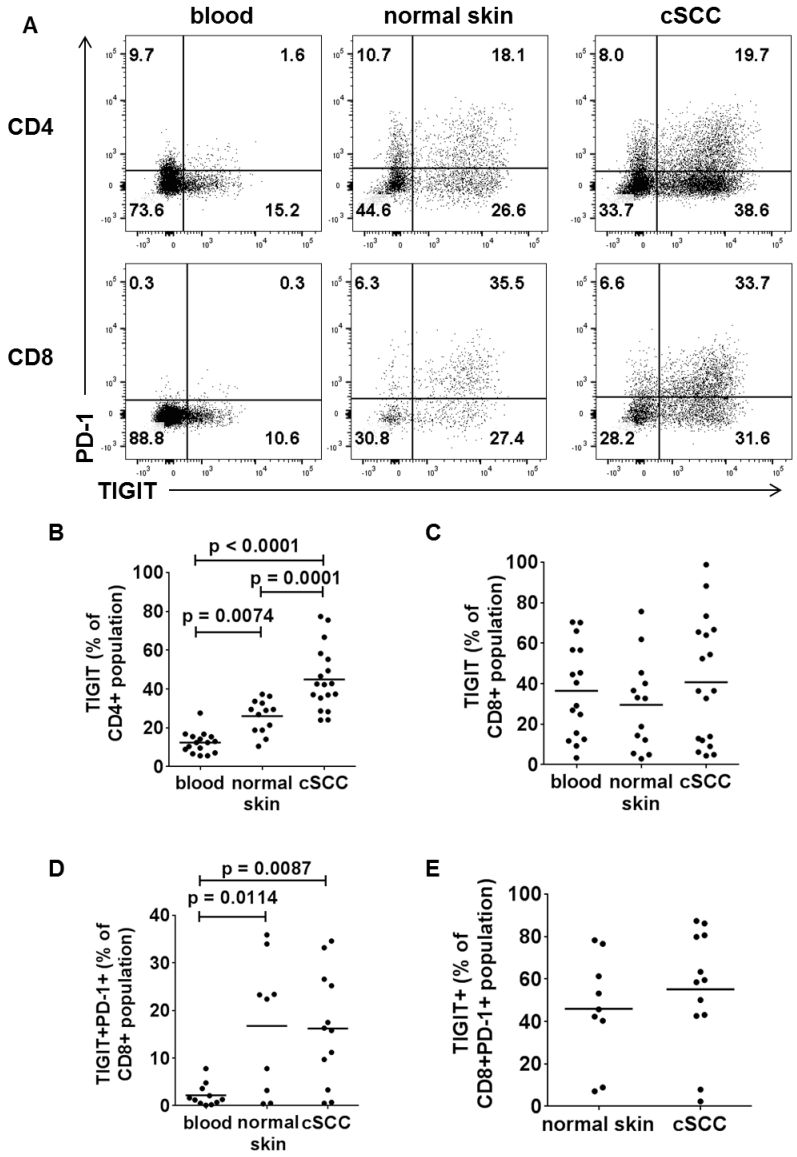

Figure 5.20 TIGIT expression by cSCC T cells.

(A) Representative dot plots showing TIGIT and PD-1 expression in $CD4^+$ (top row) and $CD8^+$ T cells (bottom row) from blood, normal skin and cSCC. (B-C) TIGIT expression in (B) $CD4^+$ T cells, and (C) $CD8^+$ T cells in blood, normal skin and cSCC (n=18 tumours). (D) $TIGIT^+PD\text{-}1^+$ frequencies in $CD8^+$ T cells in blood, normal skin and cSCC (n=12 tumours). (E) Percentage of $CD8^+PD\text{-}1^+$ T cells in normal skin (n=12) and cSCC (n=9) that are $TIGIT^+$ (there were too few $CD8^+PD\text{-}1^+$ cells from blood for this analysis). Horizontal bars = means, one-way ANOVA with Tukey's test for multiple comparisons.

5.2.12 Tumoral $PD\text{-}1^+$ T cells have higher frequencies of interferon-γ expression but lower levels of IL-2 and IL-4 expression

$CD8^+$ T cell exhaustion is characterised by the inability to produce certain T cell effector cytokines. To determine whether PD-1 expression in tumoral $CD8^+$ T cells

is a marker of T cell exhaustion and is associated with reduced expression of cytokines in cSCC, flow cytometry was used to compare the PD-1$^+$ and PD-1$^-$ gates in their expression of interferon-γ , TNF-α , IL-2 and IL-4. Interferon-γ was more frequently expressed in tumoral CD8$^+$ T cells that were PD-1$^+$ than PD-1$^-$ (59.1% ± 31.2% versus 41.8% ± 26.1% respectively, n=13 tumours, p=0.0117, Figure 5.21A, B, page 162). However, PD-1 expression was not associated with any difference in TNF-α production by tumoral CD8$^+$ T cells (TNF-α was present in 39.4% ± 28.3% of the PD-1$^+$ population and 34.6% ± 21.8% of the PD-1$^-$ population, n=8 tumours, Figure 5.21C, D). Furthermore, lower frequencies of IL-2 and IL-4 were observed in tumoral CD8$^+$ T cells that were PD-1$^+$ rather than PD-1$^-$ (IL-2$^+$ = 3.3% ± 4.3% of PD-1$^+$ population versus 5.6% ± 6.0% of PD-1$^-$ population, n=12 tumours, p=0.0069, Figure 5.21E, F; IL-4$^+$ = 7.4% ± 5.7% of PD-1$^+$ population versus 14.6% ± 13.3% of PD-1$^-$ population, n=8 tumours, p=0.0399, Figure 5.21G, H). Similar frequencies of PD-1$^+$ and PD-1$^-$ tumoral CD8$^+$ T cells expressed IL-13 (2.5% ± 2.7% of CD8$^+$PD-1$^+$ population versus 1.1% ± 1.1% of CD8$^+$PD-1$^-$ population, n=10 tumours, p=0.0858, Figure 5.21I, J) and IL-17 (1.4% ± 1.5% of CD8$^+$PD-1$^+$ population versus 0.6% ± 0.5% of CD8$^+$PD-1$^-$ population, n=9 tumours, p=0.1841, Figure 5.21K, L). This data suggests that expression of PD-1$^+$ T cells in cSCC are more able to produce interferon-γ but less able to produce IL-2 and IL-4.

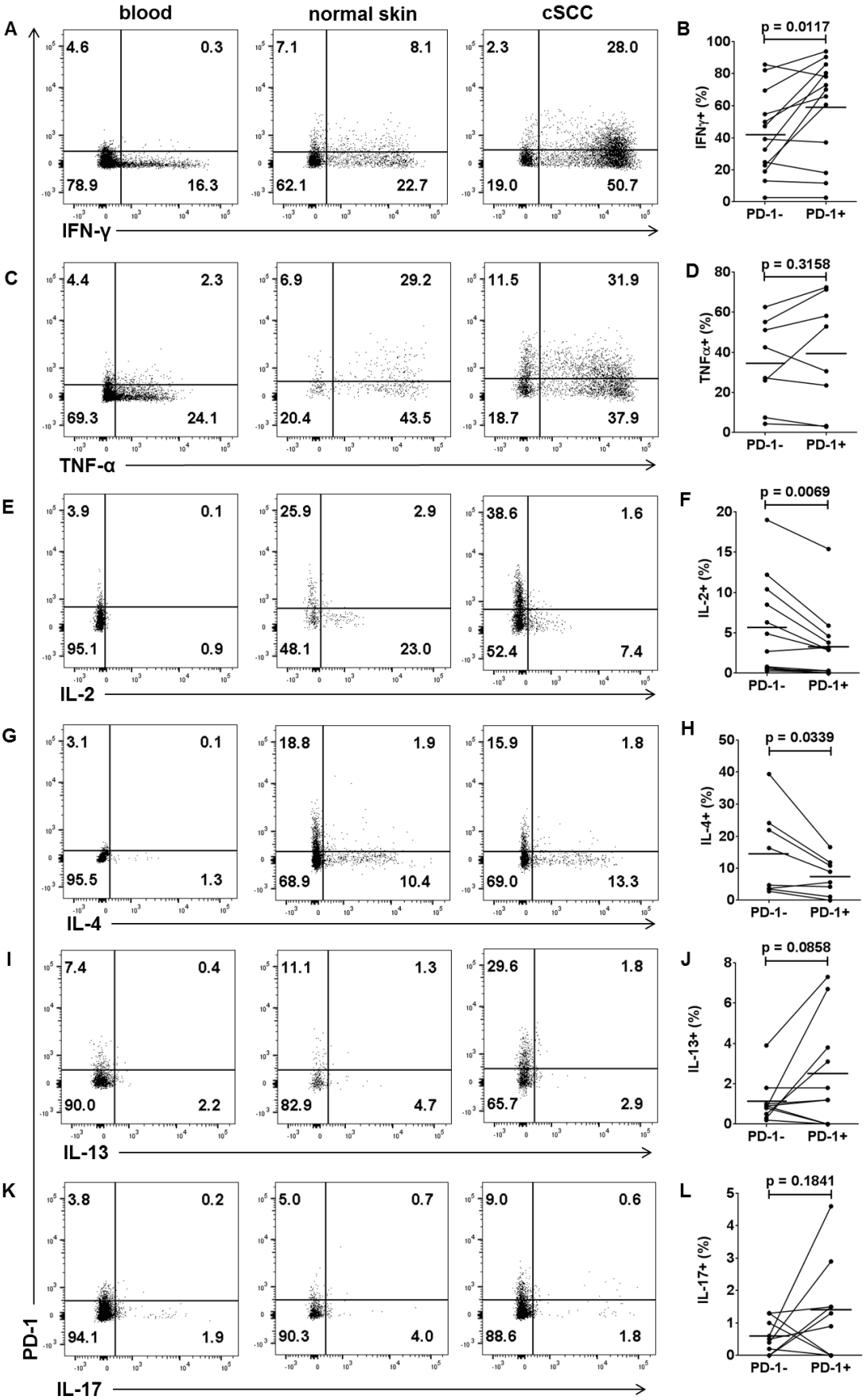

Figure 5.21 Tumoral CD8⁺ T cells that express PD-1 are more able to produce interferon-γ but less able to produce IL-2 and IL-4 than PD-1⁻ CD8⁺ T cells.

(A, C, E, G) Representative dot plots from 4 separate subjects showing expression of (A) interferon-γ , (C) TNF-α , (E) IL-2, (G) IL-4, (I) IL-13, and (K) IL-17 versus PD-1 in PMA and ionomycin stimulated $CD3^+$ gated T cells from subject matched blood, normal skin and cSCC. (B, D, F, H, J, L) Frequencies of (B) interferon-γ , (D) TNF-α , (F) IL-2 and (H) IL-4, (J) IL-13, and (L) IL-17 expressing tumoral $CD8^+$ T cell $PD\text{-}1^-$ and $PD\text{-}1^+$ subpopulations, (B) n=13 tumours, (D) n=8 tumours, (F) n=12 tumours, (H) n=8 tumours, (J) n=10 tumours, (L) n=10 tumours, horizontal bars = means, paired T test.

5.2.13 T cells in cSCC and non-lesional skin express lower frequencies of granzyme B and perforin than T cells from peripheral blood

An important function of $CD8^+$ T cells is the ability to degranulate which enables them to directly kill target cells using cytotoxic mechanisms (Shen et al., 2006). In the current study, the degranulation markers granzyme B, perforin and LAMP-1 were investigated in cSCC T cells. In the peripheral blood, granzyme B was expressed more highly by $CD8^+$ than $CD4^+$ T cells, and that granzyme B^+ cells were mainly $PD\text{-}1^-$ (Figure 5.22, page 164). In the peripheral blood, granzyme B^+ populations accounted for 5.0% ± 4.2% of unstimulated $CD4^+$ T cells, 12.4% ± 12.2% of PMA/ionomycin stimulated $CD4^+$ T cells, 31.3% ± 21.9% of unstimulated $CD8^+$ T cells and 36.5% ± 24.1% of PMA/ionomycin stimulated $CD8^+$ T cells, Figure 5.23). In comparison to peripheral blood, granzyme B was expressed less frequently by PMA/ionomycin stimulated T cells from normal skin (3.9% ± 2.5% of $CD4^+$ T cells, p=0.0111, Figure 5.23A, and 5.9% ± 5.0% of $CD8^+$ T cells, p=0.0002, Figure 5.23C) and cSCC (2.5% ± 2.7% of $CD4^+$ T cells, p=0.0006, Figure 5.23A, B, and 8.2% ± 12.3% of $CD8^+$ T cells, p=0.0003, n=13 tumours, Figure 5.23C, D).

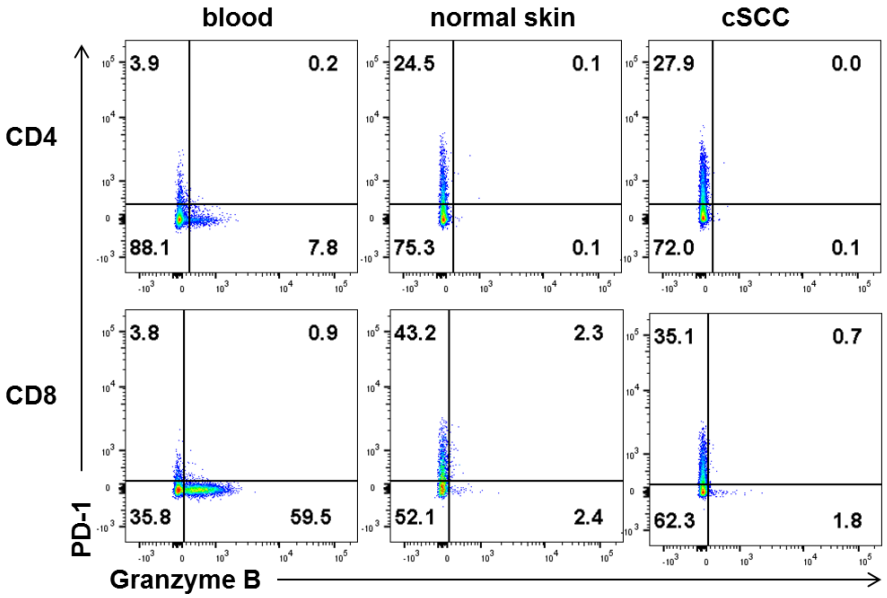

Figure 5.22 Granzyme B expression by CD4⁺ and CD8⁺ T cells from peripheral blood, non-lesional skin and cSCC.

Flow cytometry plots showing granzyme B and PD-1 expression in PMA and ionomycin stimulated CD3⁺ gated T cells from blood, normal skin and cSCC from the same subject, top row = CD4⁺ gated cells, bottom row = CD8⁺ gated cells.

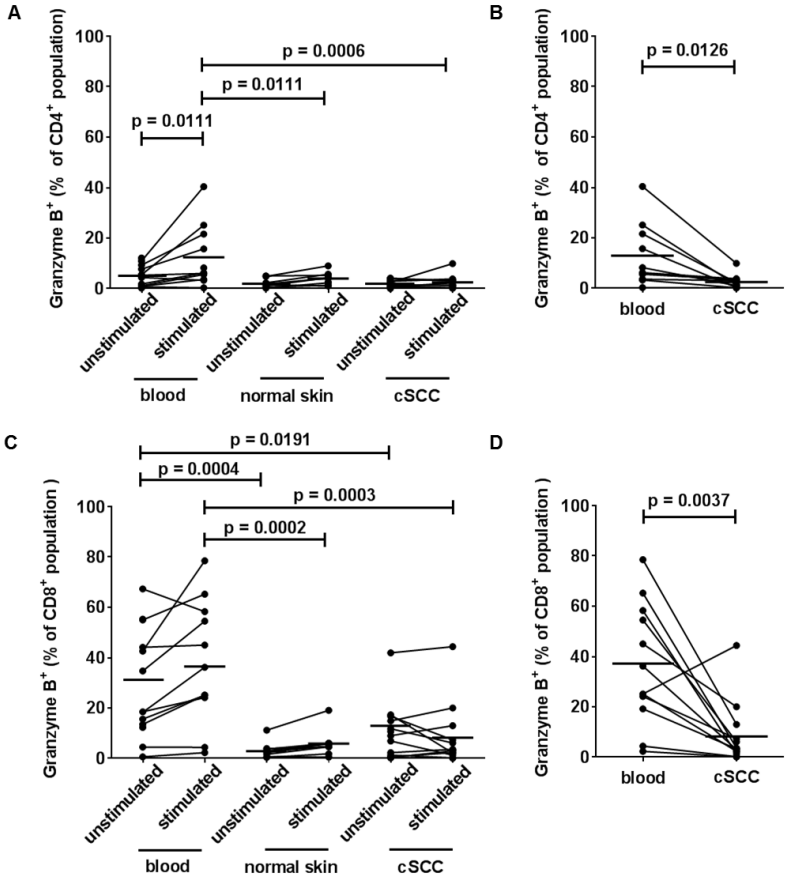

Figure 5.23 Tumoral T cells express less granzyme B than T cells from peripheral blood.

(A-D) Graphs showing flow cytometry data for granzyme B expression in (A, B) $CD4^+$ T cells and (C-D) $CD8^+$ T cells in blood, normal skin and cSCC, that were either unstimulated (n=15 tumours) or stimulated for 5 hours with PMA/ionomycin (n=13 tumours). Graphs (B) and (D) summarise data in (A) and (C) respectively, showing reduced granzyme B expression in PMA/ionomycin stimulated T cells from cSCC compared with blood. (A-D) Horizontal bars = means, (A, C) one-way ANOVA with Tukey's test for multiple comparisons, (B, D) paired T-test.

Similarly, perforin was mainly observed in peripheral blood $CD8^+$ T cells and $perforin^+$ cells were mostly $PD\text{-}1^-$ (Figure 5.24, page 166). In addition, perforin was expressed by fewer T cells in non-lesional skin (0.5% ± 0.4% of unstimulated $CD4^+$ T cells, 1.3% ± 0.9% of stimulated $CD4^+$ T cells, Figure 5.25A, 5.2% ± 4.7% of unstimulated $CD8^+$ T cells, 4.4% ± 4.6% of stimulated $CD8^+$ T cells, Figure 5.25C, page 167) and cSCC (0.9% ± 1.4% of unstimulated $CD4^+$ T cells in cSCC, 0.6% ± 0.6% of stimulated $CD4^+$ T cells in cSCC, Figure 5.25A, 6.7% ± 5.6% of unstimulated $CD8^+$ T cells in cSCC, 9.6% ± 11.6% of stimulated $CD8^+$ T cells in cSCC, n=10 tumours, Figure 5.25C) compared with blood (5.5% ± 4.6% of

unstimulated CD4⁺ T cells in blood (versus normal skin p=0.0036, versus cSCC 0.0031), 8.0% ± 3.8% of stimulated CD4⁺ T cells in blood (versus normal skin p<0.0001, versus cSCC p<0.0001, Figure 5.25A), 32.6% ± 24.3% of unstimulated CD8⁺ T cells in blood (versus normal skin p=0.0201, versus cSCC p=0.0086), 39.3% ± 24.4% of stimulated CD8⁺ T cells in blood (versus normal skin p=0.0014, versus cSCC p=0.0016, Figure 5.25C)).

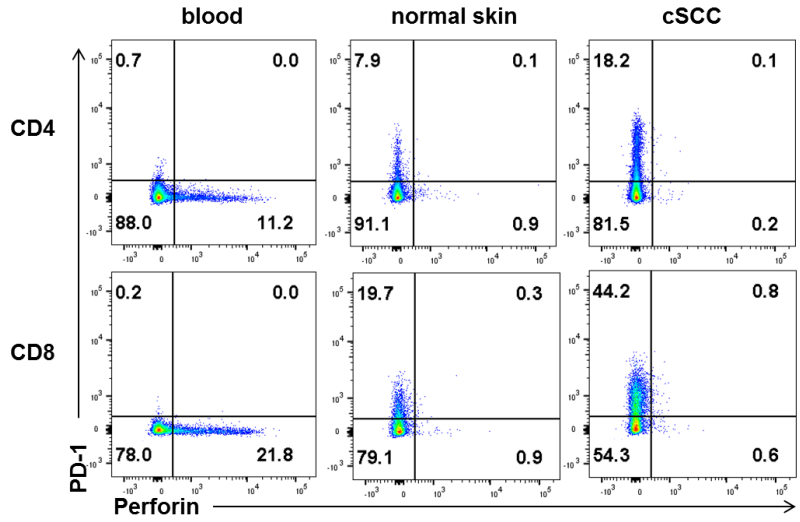

Figure 5.24 Perforin expression by CD4⁺ and CD8⁺ T cells from peripheral blood, non-lesional skin and cSCC.

Flow cytometry plots of perforin and PD-1 expression in PMA and ionomycin stimulated CD3⁺ gated lymphocytes from blood, normal skin and cSCC from the same subject, top row = CD4⁺ gated cells, bottom row = CD8⁺ gated cells.

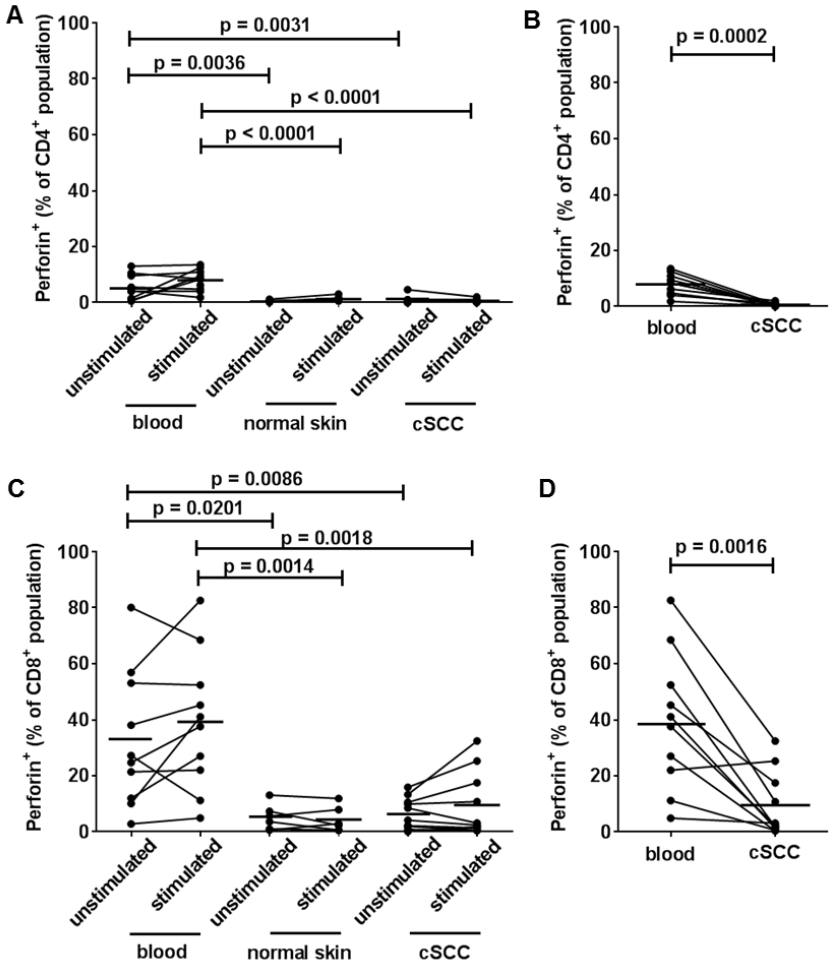

Figure 5.25 Tumoral T cells express less perforin than T cells from peripheral blood.

(A-D) Graphs demonstrating perforin expression in (A, B) $CD4^+$ T cells and (C-D) $CD8^+$ T cells in blood, normal skin and cSCC, that were either unstimulated (n=10 tumours) or stimulated for 5 hours with PMA/ionomycin (n=10 tumours). Graphs (B) and (D) summarise data in (A) and (C) respectively, showing reduced perforin expression in PMA/ionomycin stimulated T cells from cSCC compared with blood. (A-D) Horizontal bars = means, (A, C) one-way ANOVA with Tukey's test for multiple comparisons, (B, D) paired T-test.

LAMP-1 was found to be expressed on $CD4^+$ and $CD8^+$ T cells from blood normal skin and cSCC (Figure 5.26, page 168). Whilst activation with PMA and ionomycin increased LAMP-1 expression on T cells from blood, normal skin and cSCC, there were no significant differences in LAMP-1 expression between T cells from the different tissue compartments. LAMP-1 was present on 5.6% ± 4.0% of unstimulated $CD4^+$ T cells and 16.9% ± 18.7% of stimulated $CD4^+$ T cells in peripheral blood, 5.0% ± 2.8% of unstimulated $CD4^+$ T cells and 24.3% ± 19.3% of

stimulated CD4⁺ T cells in normal skin, and 8.8% ± 9.9% of unstimulated CD4⁺ T cells and 21.0% ± 20.7% of stimulated CD4⁺ T cells in cSCC, n=10 tumours (Figure 5.27A, page 169). LAMP-1 was expressed on 9.3% ± 9.4% of unstimulated and 20.1% ± 26.3% of stimulated CD8⁺ T cells from peripheral blood, 2.5% ± 3.1% of unstimulated and 22.9% ± 21.1% of stimulated CD8⁺ T cells from normal skin, and 6.9% ± 13.8% of unstimulated and 26.6% ± 23.9% of stimulated CD8⁺ T cells from cSCC, n=10 tumours (Figure 5.27B). These results suggest that whilst the production of the cytolytic molecules granzyme B and perforin is reduced in cSCC and non-lesional skin compared with peripheral blood, degranulation/LAMP-1 expression is not impaired in cSCC effector T cells.

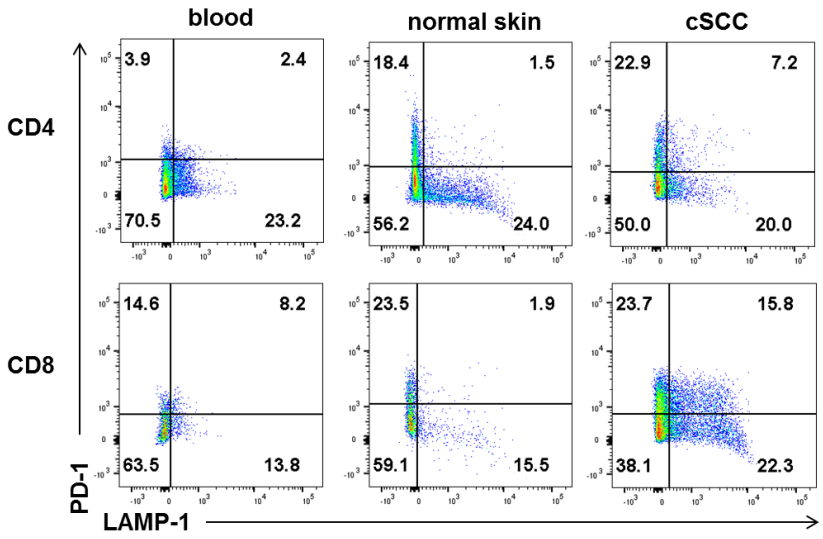

Figure 5.26 LAMP-1 expression on CD4⁺ and CD8⁺ T cells from peripheral blood, non-lesional skin and cSCC.

Flow cytometry plots of LAMP-1 and PD-1 expression in PMA and ionomycin stimulated CD3⁺ gated lymphocytes from blood, normal skin and cSCC from the same subject, top row = CD4⁺ gated cells, bottom row = CD8⁺ gated cells.

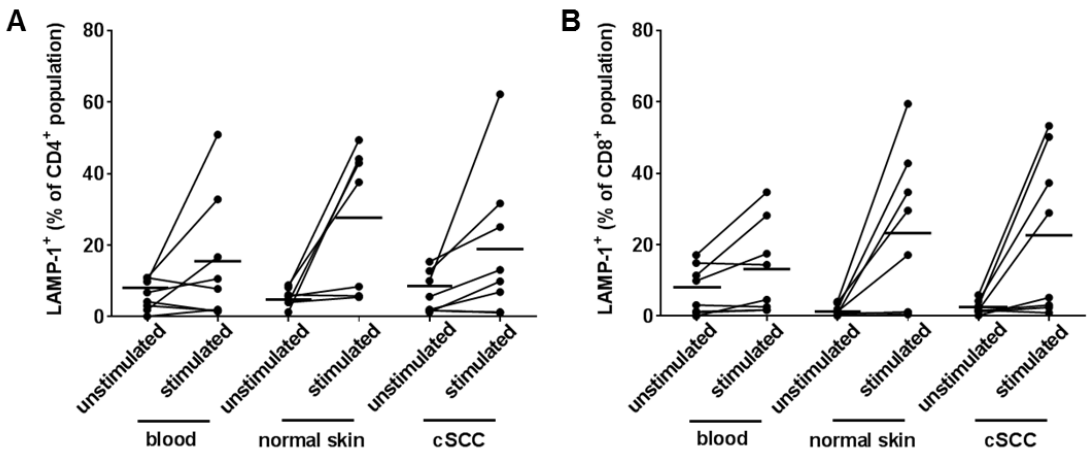

Figure 5.27 Similar levels of LAMP-1 expression on T cells in peripheral blood, normal skin and cSCC.

(A-B) Graphs showing LAMP-1 expression in unstimulated and PMA/ionomycin stimulated (A) $CD4^+$ T cells and (B) $CD8^+$ T cells in blood, normal skin and cSCC (n=10 tumours). Horizontal bars = means.

Flow cytometry gating for PD-1 expression was used to determine whether PD-1 was associated with altered ability of tumoral $CD8^+$ T cells to degranulate and express cytolytic molecules. No significant difference was detected between PD-1^+ and PD-1^- $CD8^+$ T cell populations in the expression of granzyme B (Figure 5.28A, B, page 170), perforin (Figure 5.28C, D), and LAMP-1 (Figure 5.28E, F). In cells that were unstimulated (n=10 tumours), the mean ± SD percentages expressing granzyme B were 7.2% ± 7.1% of the PD-1^+ $CD8^+$ T cell population and 9.0% ± 11.4% of the PD-1^- $CD8^+$ T cell population; the frequencies expressing perforin were 6.9% ± 6.3% of the PD-1^+ $CD8^+$ T cell population and 6.5% ± 5.6% of the PD-1^- $CD8^+$ T cell population; and LAMP-1^+ frequencies were 7.9% ± 14.5% of the PD-1^+ $CD8^+$ T cell population versus 6.1% ± 13.7% of the PD-1^- $CD8^+$ T cell population. In cells that were stimulated with PMA and ionomycin (n=10 tumours), the percentages expressing granzyme B were of the 7.6% ± 9.5% PD-1^+ $CD8^+$ T cell population and 7.5% ± 7.7% of the PD-1^- $CD8^+$ T cell population; perforin was expressed by 12.7% ± 15.9% of the PD-1^+ $CD8^+$ T cell population and 9.0% ± 8.9% of the PD-1^- $CD8^+$ T cell population; and LAMP-1 was expressed by 26.1% ± 19.0% of the PD-1^+ $CD8^+$ T cell population versus 24.4% ± 17.9% of the PD-1^- $CD8^+$ T cell population. Therefore, the data indicates that PD-1 expression is not associated with the ability of tumoral $CD8^+$ T cells in cSCC to produce cytolytic markers and degranulate.

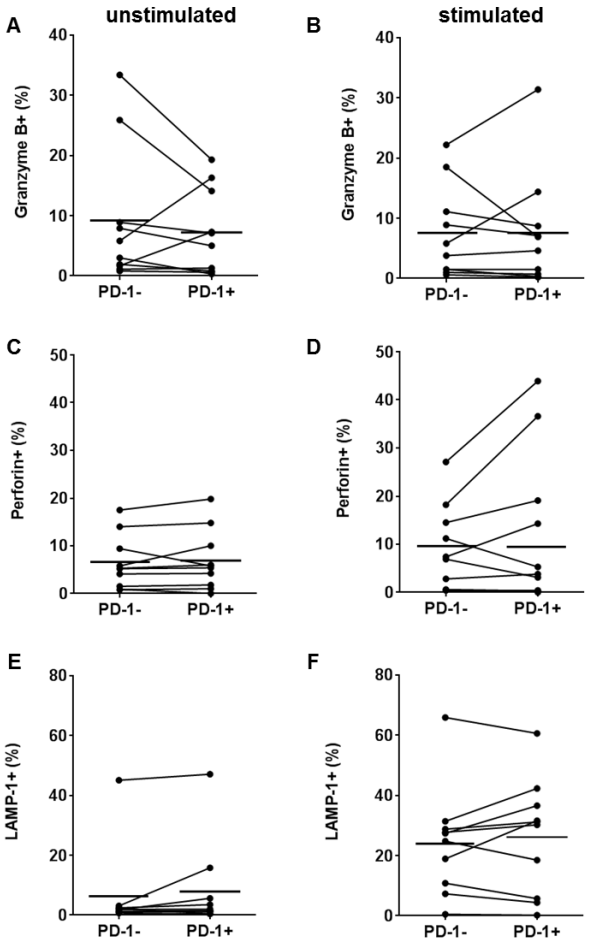

Figure 5.28 Expression of cytolytic and degranulation markers in PD-1$^+$ and PD-1$^-$ subpopulations of tumoral CD8$^+$ T cells.

(A-E) Frequencies of (A, B) granzyme B, (C-D) perforin, and (E, F) LAMP-1 expressing tumoral CD8$^+$ T cells in PD-1$^-$ and PD-1$^+$ subpopulations. In graphs (A, C, E), cells were analysed *ex vivo* without prior stimulation, whereas in (B, D, F), cells were stimulated with PMA/ionomycin for 5 hours prior to flow cytometry, n=10 tumours, horizontal bars = means.

5.2.14 Tumoral PD-1$^+$ immunocyte frequencies in primary cSCCs do not predict metastasis

To investigate whether PD-1 expression by tumoral immunocytes was associated with poorer clinical outcomes in cSCC, PD-1$^+$ immune cell frequencies were quantified in primary cSCCs which had metastasised and primary cSCCs known not to have metastasised after 5 years of follow up. Some of the

immunohistochemistry and cell quantification was performed with assistance from Dr Kimberlee Lim. PD-1 expressing lymphocytes were present in highly variable frequencies in different tumours. PD-1 expression was observed on 27.5% ± 19.2% of immunocytes in primary cSCCs which had metastasised (n=29 tumours), and in 36.4% ± 23.1% of immune cells in the non-metastatic cSCCs (n=24 tumours), with no statistically significant difference identified between the groups (p=0.1296, Figure 5.29).

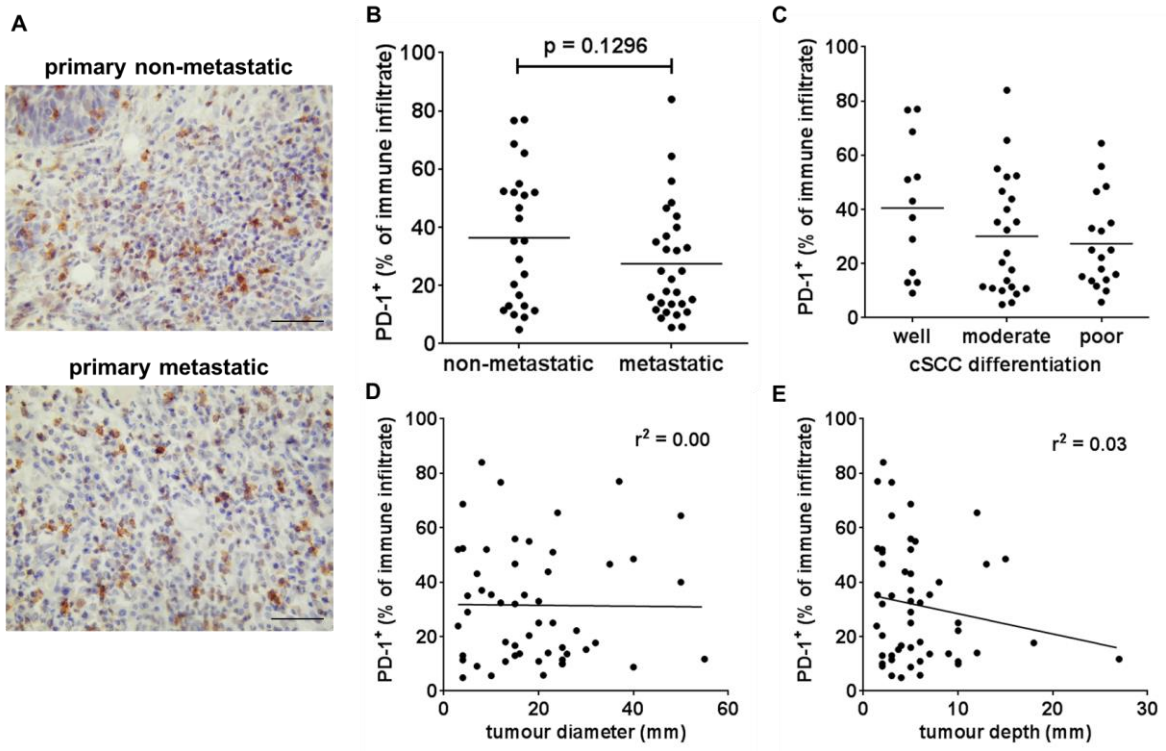

Figure 5.29 No difference in PD-1⁺ immune cell frequencies in primary cSCCs which had metastasised and primary cSCCs which had not metastasised.

(A) Representative images of immunohistochemical stains for PD-1 in a primary cSCC which had not metastasised after 5 years (top) and a primary cSCC which had metastasised (bottom), scale bars = 50 μm. (B) Quantification of PD-1⁺ immune cell frequencies in primary cSCCs which had not metastasised (n=24) and primary cSCCs which had metastasised (n=29). (C-E) PD-1⁺ immune cell frequencies by (C) histological differentiation, (D) tumour diameter and (E) tumour depth. Dots indicate mean values for each tumour from 5 high power fields, (B, C) horizontal bars represent mean values for each group, t-test, (D, E) best fit line = linear regression.

5.2.15 PD-1 inhibition enhances tumoral CD8⁺ T cell proliferation and interferon-γ production *in vitro*

To investigate whether cSCC CD8⁺ T cell function could be enhanced with PD-1 inhibition, tritiated thymidine uptake assays were conducted with tumoral CD8⁺ T cells cultured with anti-CD3 and accessory cells in the presence of an inhibitory anti-PD-1 antibody or isotype control. The addition of anti-PD-1 significantly increased anti-CD3 stimulated tumoral CD8⁺ T cell proliferation over control (median cpm 1041 versus 887 respectively, median increase in proliferation 35.3%, p=0.0039, Figure 5.30), suggesting that tumoral CD8⁺ T cell proliferation is augmented by PD-1 inhibition.

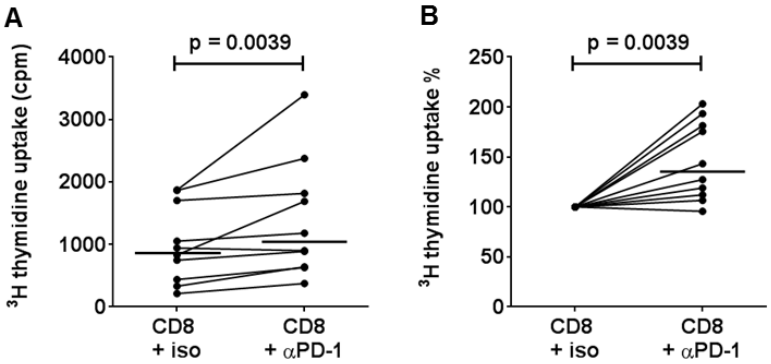

Figure 5.30 PD-1 inhibition enhances tumoral CD8⁺ T cell proliferation *in vitro*.
(A & B) Tumoral CD8⁺ T cells isolated by flow cytometry were cultured for 72 hours with anti-CD3 + autologous irradiated CD3⁺ cell depleted irradiated PBMCs ± inhibitory anti-PD-1 antibody (α PD-1) or isotype control (iso). Proliferation was assessed by tritiated thymidine uptake, results displayed in cpms in (A) and normalised to 100% without anti-PD-1 in (B), dots = median values from triplicate wells for each tumour (n=10 tumours), horizontal bar = median value from all tumours, paired Wilcoxon rank test.

Flow cytometry was conducted to assess intracellular expression of interferon-γ in tumoral CD8⁺ T cells cultured with inhibitory anti-PD-1 antibody. Interferon-γ was expressed by 51.2% ± 18.3% of tumoral CD8⁺ T cells cultured with isotype control antibody compared with 54.3% ± 17.0% of those cultured with anti-PD-1 (p=0.0383, n=14 tumours, Figure 5.31A, page 173), suggesting a small but statistically significant increase in interferon-γ production with PD-1 inhibition. The mean fluorescence intensity minus background (Δ MFI) staining for interferon-

γ was 972.5 ± 503.9 with isotype control antibody and 1173 ± 665.1 with anti-PD-1 (p=0.0103, n=14 tumours, Figure 5.31B), representing a 21.0% increase in Δ MFI (Figure 5.31C).

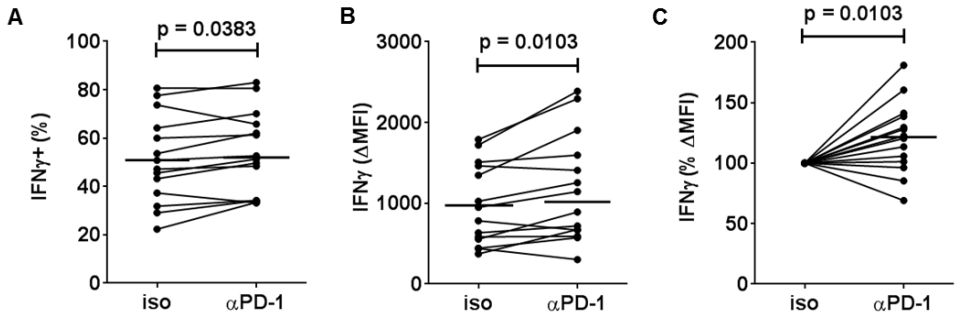

Figure 5.31 Effect of PD-1 inhibition on interferon-γ production by tumoral CD8⁺ T cells *in vitro*.

Tumoral CD8⁺ T cells isolated by flow cytometry were cultured for 72 hours with anti-CD3 + autologous irradiated CD3⁺ cell depleted irradiated PBMCs ± inhibitory anti-PD-1 antibody (α PD-1) or isotype control (iso). PMA/ionomycin was added in the last 5 hours of culture, and Brefeldin A in the last 4 hours of culture. Interferon-γ expression was determined using intracellular flow cytometry, results displayed as (A) percentage of cells that were interferon-γ ⁺, (B) Δ MFI, i.e. mean fluorescence intensity minus background fluorescence, and (C) normalised Δ MFI, with 100% representing isotype control, n=14 tumours, horizontal bars = means, paired T test.

IL-2 expression by tumoral CD8⁺ T cells did not differ significantly with culture with anti-PD-1 or isotype control antibody; the percentages of tumoral CD8⁺ T cells that were IL-2⁺ were 10.6% ± 7.9% with anti-PD-1 and 10.5% ± 7.8% with isotype control (p=0.8532, Figure 5.32A, page 174) and the Δ MFIs were 396.6 ± 208.4 with anti-PD-1 and 398.3 ± 184.3 with isotype control (p=0.9480, n=12 tumours, Figure 5.32B).

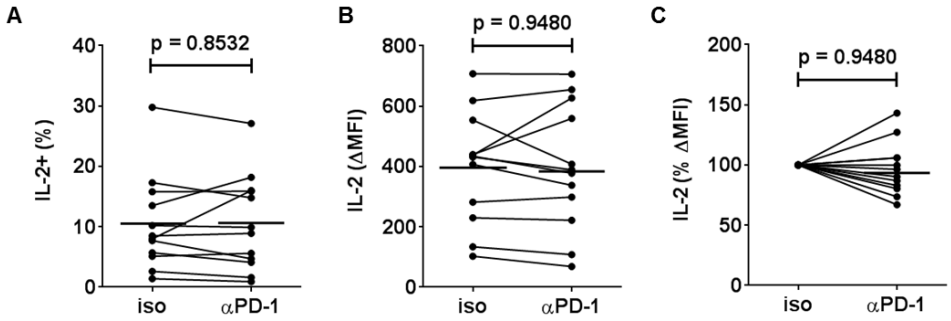

Figure 5.32 PD-1 inhibition does not affect IL-2 production by tumoral CD8⁺ T cells *in vitro*.

Tumoral CD8⁺ T cells isolated by flow cytometry were cultured for 72 hours with anti-CD3 + autologous irradiated CD3⁺ cell depleted irradiated PBMCs ± inhibitory anti-PD-1 antibody (α PD-1) or isotype control (iso). PMA/ionomycin was added in the last 5 hours of culture, and Brefeldin A in the last 4 hours of culture. IL-2 expression was determined using intracellular flow cytometry, results displayed as (A) percentage of cells that were IL-2⁺, (B) Δ MFI, and (C) normalised Δ MFI, with 100% representing isotype control. n=12 tumours, horizontal bars = means, paired T test.

Similarly, PD-1 inhibition did not affect granzyme B expression by tumoral CD8⁺ T cells; the percentages of tumoral CD8⁺ T cells that expressed granzyme B were 39.1% ± 27.6% with anti-PD-1 and 35.8% ± 25.6% with isotype control (p=0.0733, Figure 5.33A, page 175) and the Δ MFIs were 649.3 ± 582.5 with anti-PD-1 and 562.9 ± 534.4 with isotype control (p=0.0660, n=14 tumours, Figure 5.33B). These results suggest that PD-1 inhibition of tumoral CD8⁺ T cells *in vitro* does not enhance IL-2 or granzyme B production, indicating that other mechanisms may be responsible for the lack of IL-2 and granzyme B in these cells.

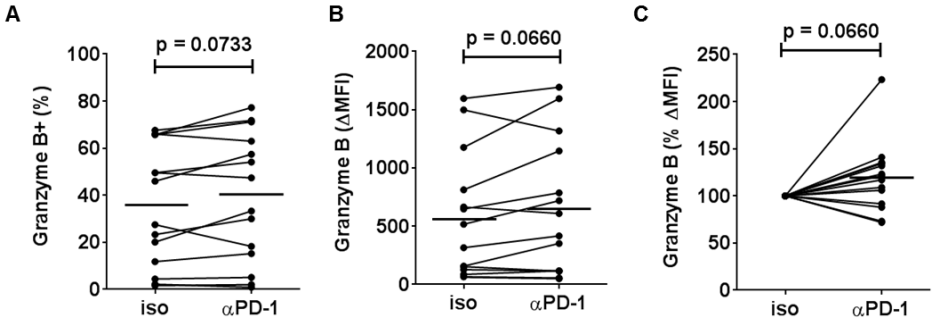

Figure 5.33 *In vitro* PD-1 inhibition does not affect granzyme B expression in tumoral CD8⁺ T cells.

Tumoral CD8⁺ T cells isolated by flow cytometry were cultured for 72 hours with anti-CD3 + autologous irradiated CD3⁺ cell depleted irradiated PBMCs ± inhibitory anti-PD-1 antibody (α PD-1) or isotype control (iso). PMA/ionomycin was added in the last 5 hours of culture. Granzyme B expression was determined using intracellular flow cytometry, results displayed as (A) percentage of cells that were granzyme B⁺, (B) Δ MFI, and (C) normalised Δ MFI, with 100% representing isotype control. n=14 tumours, horizontal bars = means, paired T test.

5.3 Discussion

Functionally deficient tumour-infiltrating T cells have been described in cancer, and may be partly responsible for the resistance of tumours to immune-mediated destruction by the host immune system (Baitsch et al., 2011, Fourcade et al., 2010, Sakuishi et al., 2010, Ahmadzadeh et al., 2009). In several advanced cancers, T cell exhaustion has been demonstrated as a key mechanism for aberrant T cell function, and targeting T cell exhaustion has been shown to be a feasible immunotherapeutic approach that can reverse tumour-specific T cell dysfunction and improve clinical outcomes in cancer (Fourcade et al., 2010, Topalian et al., 2012). As described earlier in this thesis, defective host immunity renders the skin especially vulnerable to the development of cSCC, and the data in the previous chapter support a role for Tregs in inhibiting immune responses in this tumour. However, it is unclear whether tumoral effector T cells are intrinsically functionally deficient and whether T cell exhaustion is present in cSCC.

Exhausted T cells lose effector functions in a hierarchical manner, starting with loss of IL-2 production and high proliferative capacity, followed by defects in the production of interferon-γ and TNF-α as well as in degranulation and cytotoxicity,

combined with the progressive increase in the amount and diversity of inhibitory receptors that are expressed (Wherry and Kurachi, 2015). In the present study, T cells from cSCC are less able to proliferate in response to stimulus than those from peripheral blood, and cSCC T cells produce less IL-2 than T cells from non-lesional skin. These functional differences are characteristic of T cell exhaustion, however, tumoral T cells are still able to produce interferon-γ and TNFα, suggesting that effector T cells in cSCC may be at an early stage of exhaustion compared with those in advanced melanoma, where loss of interferon-γ production has been noted (Wherry and Kurachi, 2015, Baitsch et al., 2011, Ahmadzadeh et al., 2009). In addition, analysis of tumoral T cell cytokine production in the current study demonstrated that the TH2 cytokine IL-4 is expressed by a sizeable fraction of the tumoral T cell population (roughly 40% of $CD4^+$ T cells and 20% of $CD8^+$ T cells). Whilst cSCCs have previously been reported to be associated with a TH1 bias (Clark et al., 2008), the identification of TH2 subsets in cSCC in the present study may implicate these T cells in contributing to a potentially protumorigenic inflammatory environment (De Monte et al., 2011, Demehri et al., 2014).

The inhibitory receptor PD-1 is expressed by T cells in cSCC at higher abundances than in corresponding peripheral blood, suggesting that the cSCC microenvironment can induce or maintain PD-1 on tumour-infiltrating T cells. However, although $PD\text{-}1^+CD4^+$ T cells are more frequent in cSCC than in non-lesional skin, $PD\text{-}1^+CD8^+$ T cell percentages were similar in these tissue compartments. Whilst other studies have highlighted that PD-1 expression is higher on T cells infiltrating into melanoma metastases compared to normal liver, lung and spleen tissue (Ahmadzadeh et al., 2009), it has also been reported that normal skin in healthy individuals contains higher proportions of $PD\text{-}1^+$ T cells than blood, and that PD-1 expression on T cells in skin increases with age (Vukmanovic-Stejic et al., 2015). This suggests that inhibitory signalling by T cells may regulate skin immunity in response to persistent antigen (e.g. from viruses or chronic inflammation associated with ageing), or possibly from chronic UVR resulting in non-clinically apparent changes in the skin. Indeed, the majority of subjects with cSCC in the current study were elderly, with signs of chronic UVR exposure and widespread actinic damage. UVR-induced driver gene mutations are abundant even in normal skin (Martincorena et al., 2015), and these might result in neoantigen formation (Linnemann et al., 2015), and as T cell hyporesponsiveness can be induced even in premalignant lesions, it is possible that PD-1 upregulation on T cells may occur in UVR-damaged skin at an initiating

or early stage of skin carcinogenesis. In addition, the present study showed PD-1$^+$ T cells in cSCC are less able to produce IL-2 than PD-1$^-$ T cells, consistent with T cell exhaustion in melanoma, however, PD-1 expression was not associated with any loss of interferon-γ or TNF-α production in cSCC, which is usually observed when multiple inhibitory receptors are expressed at a more advanced stage of exhaustion (Ahmadzadeh et al., 2009, Fourcade et al., 2010). The limited number of channels available for multicolour flow cytometry in the present study meant that a maximum of three cytokines could be analysed within the same panel, and future experiments using flow cytometers with extra channels would be useful to investigate the degree of polyfunctionality of the cells (e.g. whether PD-1 expression was associated with a decrease in the number of cytokines secreted). Examining other inhibitory receptors showed that whilst Tim-3, LAG-3 and BTLA were not expressed, CTLA-4, CD244 and TIGIT could be detected in some PD-1$^+$ T cells in cSCC, which could represent exhausted T cells. However, it is unclear whether the populations of T cells in cSCC that express CTLA-4, CD244 and TIGIT without PD-1 are also hyporesponsive rather than activated. Furthermore, this study demonstrates that expression of PD-1 alone on lymphocytes infiltrating primary cSCCs does not associate with metastatic potential.

Loss of cytotoxicity has been described in T cell exhaustion in cancer (Wherry and Kurachi, 2015, Wu et al., 2014). Cytotoxic T cells can lyse tumour cells using perforin which forms transmembrane pores in the target cell, and granzyme B which diffuses into the target cell cytoplasm and initiates apoptosis (Voskoboinik et al., 2015, Breart et al., 2008). Reversal of tumoral T cell exhaustion has been shown to enhance cytotoxicity and the ability of T cells to degranulate (Fourcade et al., 2014, Chauvin et al., 2015). In the current study, granzyme B and perforin expression were lower T cells in cSCC and non-lesional skin than blood, however, the expression levels of LAMP-1, a marker indicating the cells have released their cytotoxic granules, were similar in T cells in blood, normal skin and cSCC following activation, suggesting that the ability to degranulate is not lost by T cells in cSCC, whereas production of cytolytic molecules is reduced in the skin of cSCC subjects compared with in the blood. As T cell exhaustion is usually characterised by loss of the ability to degranulate before defective cytotoxicity occurs in more advanced stages (Wherry and Kurachi, 2015), the mechanism for reduced granzyme B and perforin in T cells in cSCC may be an effect of an alternative immunoregulatory process occurring in the skin of cSCC patients.

PD-1 inhibition has been shown to be an attractive strategy for improving clinical outcomes for several types of advanced cancer (Topalian et al., 2012, Hamid et al., 2013). PD-1 has been shown to identify the tumour-specific population of $CD8^+$ T cells infiltrating human tumours (Gros et al., 2014, Gubin et al., 2014), and the clinical effectiveness of PD-1 blockade requires pre-existing tumoral $CD8^+$ T cells that are negatively regulated by PD-1/PD-L1-mediated adaptive immune resistance (Tumeh et al., 2014). In the present study, PD-L1 was detected on tumour keratinocytes by confocal microscopy. It was also noted that keratinocytes in the epidermis adjacent to the cSCCs could also express PD-L1, and further experiments would be helpful to identify whether there are any patterns in PD-L1 expression by cSCC cells (e.g. any relation to features such as tumour cell death and immune cell infiltration) and whether expression levels vary between cSCC and normal epidermis, precursor skin lesions and metastatic tumours. In addition, an anti-PD-1 inhibitory antibody enhanced tumoral effector T cell proliferation and production of interferon-γ (but not IL-2 or granzyme B), suggesting that PD-1, which is upregulated by T cells in cSCC compared to blood, could play a role in inhibiting certain functions of tumoral T cells, and that some aspects of T cell hyporesponsiveness can be reversible.

In conclusion, this study has shown that effector T cells in cSCC are dysfunctional in terms of their ability to proliferate, produce IL-2 and cytotoxic molecules, and that targeting PD-1 can reverse some of these defects to enhance anti-tumoral immunity, which may constitute a potential immunotherapeutic approach for cSCC.

Chapter 6: Discussion

Skin cancer is the most common form of cancer worldwide, and due to their potential to metastasise, cSCCs constitute a large problem for global health (Lucas et al., 2006). Suppression of the immune system is associated with an increased risk of cancer development, especially of cSCC, which is the predominant type of tumour that occurs in immunosuppressed organ transplant recipients (Carroll et al., 2010, Euvrard et al., 2003). This suggests that intact cutaneous immunosurveillance is particularly important for the prevention of cSCC development, and mechanisms responsible for defective tumour immunity may be attractive immunotherapeutic targets in cSCC. Although the majority of cSCCs occur in immunocompetent individuals, as UVR exposure and old age are associated with reduced cutaneous immune responses (Vukmanovic-Stejic et al., 2015, Schwarz et al., 2010), and that cSCCs are frequently infiltrated by T cells which fail to prevent tumour growth, investigating cSCC immunity is likely to yield key pathogenic mechanisms in this cancer. Furthermore, the cSCC model offers an excellent opportunity for studying human cancer immunity because of the prevalence and ease of access to samples from human primary tumours. Immunotherapy to enhance the endogenous anti-tumour activity of tumour-specific lymphocytes is becoming increasingly recognised as a promising strategy for cancer treatment. Therefore, the aims of the current study were to investigate tumoral Tregs and effector T cell dysfunction as potential causes for the defective anti-tumour response in cSCC and to examine the effect of T cell costimulatory and inhibitory antibodies on tumoral T cell function.

The presence of Tregs in cSCC has previously been documented by Clark et al., who showed that cSCCs are characterised by aberrant T cell homing resulting in the infiltration of central memory T cells from the blood into the tumour rather than effector memory T cells due to down regulation of vascular E-selectin and the recruitment of Tregs (Clark et al., 2008). In the present study, Tregs were found to accumulate in cSCCs in higher numbers than in normal skin and peripheral blood, and that tumoral Tregs were functionally able to suppress tumoral effector T cells, suggesting that tumoral Tregs contribute to an immunosuppressive environment that permits cSCC tumour development. However, in contrast to the findings by Clark et al., Tregs were demonstrated to be predominantly effector memory T cells expressing the skin homing ligands CLA and CCR4, and E-selectin, a ligand for CLA, is expressed on the blood vessels in the stromal areas of cSCCs. A possible reason for the differences in findings

between Clark et al. and the current study is the different processing of tumoral T cells, in the former, tumoral T cells were cultured within skin explant culture matrices *in vitro* and expanded for three weeks, whereas the present study analysed tumoral T cells straight after isolation by mechanical and enzymatic digestion. Furthermore, a notable observation arising from this study is the heterogeneity in phenotype and functional responses from different tumours, suggesting that cSCC immunity is influenced by a myriad of host and environmental factors, and that investigations undertaken to investigate human tumour immunity would require sufficient sample numbers given the variability between tumours in different individuals.

Identification of tumour-specific Treg markers is important to enable suitable therapeutic targets to be determined. Characterisation of the tumoral Tregs showed that the inhibitory receptor CTLA-4 and costimulatory receptors OX40 and 4-1BB were upregulated. Whilst no effect on tumoral T cell function was seen with CTLA-4 inhibition *in vitro*, OX40 and 4-1BB agonism leads to enhanced responses by tumoral effector T cells. Although other studies have shown that costimulatory antibodies can exert anti-tumour immunity through effector T cells (Metzger et al., 2016, Linch et al., 2016), costimulatory antibodies can also inhibit suppression by tumoral Tregs (Marabelle et al., 2013, Piconese et al., 2008, Voo et al., 2013), and deplete Tregs via activating Fcγ receptors (Bulliard et al., 2014). The current study has shown that cSCC Tregs are the main T cell subset that expresses OX40 and 4-1BB, and that OX40 agonism overcomes the suppression exerted by Tregs *in vitro*. Therefore, the results in this thesis suggest that targeting costimulatory receptors can enhance anti-tumour immunity in cSCC.

As metastatic cSCC carries a poor prognosis, there is a need for effective identification of cSCCs at high risk for metastasis. An important finding in this study is that OX40 is more frequently expressed by lymphocytes in primary cSCCs which metastasise. This indicates that characteristics within the tumour immune infiltrate can provide insight into prognosis, and provides further support for the importance of immunity in the pathogenesis of cSCC. Indeed, our group has shown that increased Treg frequencies are associated with primary cSCCs which have metastasised, providing further evidence for the pathogenic role of tumoral Tregs (Lai et al., 2016). Furthermore, the results of the current study suggest that targeting OX40 could benefit the subset of cSCC patients at high risk of metastasis, although further experiments and clinical trials would be required to

investigate the potential for using OX40 agonists in patients with metastatic cSCC.

Another mechanism that results in insufficient anti-tumour immunity is T cell exhaustion. The 'exhausted' phenotype was initially observed in chronic infections, where T cells are induced that express numerous inhibitory receptors and lack normal effector T cell functions, whereas acute infections normally lead to the generation of large numbers of short-lived effector T cells and the formation of memory T cells, which are typically able to express multiple cytokines and cytotoxic effector molecules. Dysfunctional T cells with characteristics of T cell exhaustion have been described in cancer, including melanoma (Baitsch et al., 2011), ovarian cancer (Matsuzaki et al., 2010) and chronic lymphocytic leukaemia (Riches et al., 2013), where the continual presence of tumour-associated antigens leads to chronic T cell activation. It has been suggested that an 'exhausted' phenotype develops as a functional adaptation that enables a certain level of effector function to be fulfilled without causing collateral tissue damage as a result of unrestrained autoimmunity (Speiser et al., 2014). In addition, there is evidence that exhausted $CD8^+$ T cells in chronic infection and cancer may maintain certain functions, and that the infiltration of $CD8^+$ T cells is generally associated with improved clinical prognosis in various cancer types despite T cell exhaustion suggests that these tumour-infiltrating T cells retain some anti-tumour functionality (Galon et al., 2006, Fridman et al., 2012, Utzschneider et al., 2016). Indeed, recent work in our laboratory demonstrates that primary cSCCs which have not metastasised contain higher $CD8^+$ T cell frequencies in the tumour immune infiltrate than primary cSCCs that have metastasised (unpublished data), which provides support for an anti-tumour role of $CD8^+$ T cells in cSCC. That PD-1 blockade has been shown to reactivate effector T cell potential in cancer demonstrates that tumoral T cells are controlled by regulatory mechanisms that involve PD-1 signalling, and that exhausted T cells can retain the ability to mount potent effector responses, rather than being intrinsically terminally dysfunctional (Speiser et al., 2014). It has been shown that T cell exhaustion can still be observed in PD-1 knockout mice with chronic lymphocytic choriomeningitis virus infection, and that these exhausted T cells are more terminally differentiated and have reduced survival, suggesting that the role of PD-1 may be to preserve exhausted T cells from excessive activation, proliferation and terminal differentiation (Odorizzi et al., 2015).

Blockade of inhibitory receptors in preclinical models of cancer and clinical trials has demonstrated reversal of tumoral T cell exhaustion and improvement of clinical outcomes (Fourcade et al., 2010, Matsuzaki et al., 2010, Sakuishi et al., 2010, Topalian et al., 2012, Hamid et al., 2013). The advantages of targeting inhibitory receptors include their specificity for tumour-specific T cells (Gros et al., 2014), meaning that inhibitory receptor blockade can be effective across different tumours in different individuals which may express different antigens/neoantigens, and that non-tumour specific T cells are not inadvertently affected, thereby reducing adverse effects related to loss of tolerance and unrepressed immunity. Therefore, given that defective T cell immunity promotes cSCC development, it is important to determine whether T cell exhaustion forms a key mechanism for impaired anti-tumoral immune responses in this cancer.

In the current study, many T cells in cSCC were found to express the inhibitory receptor PD-1, which is upregulated on T cells in cSCC compared to blood, and can be co-expressed with CTLA-4, CD244 and TIGIT in smaller subpopulations of tumoral T cells. However, T cells that upregulate inhibitory receptors are not always dysfunctional, for example, in healthy donors, circulating PD-1^{+}CD8^{+} T cells can represent effector memory cells rather than exhausted T cells (Duraiswamy et al., 2011), and activated antigen specific T cells can upregulate PD-1 or Tim-3 depending on the T cell differentiation and activation status (Fourcade et al., 2010, Fourcade et al., 2014). Therefore, functional analysis of the cSCC T cells was required in the current study in order to confirm that they were truly dysfunctional. Indeed, cSCC effector T cells were found to have a reduced ability to proliferate, secrete IL-2 and produce the cytolytic molecules granzyme B and perforin, indicating that cSCC T cells are hyporesponsive, which may contribute to ineffective anti-tumour immunity. Although the ability to produce interferon-γ and TNF-α was maintained by tumoral T cells, the reduced capacity for proliferation and IL-2 production as well as the expression of PD-1 and other inhibitory receptors on a subset of T cells suggest that some T cells in cSCC are in an early stage of exhaustion. PD-1 blockade was able to enhance cSCC effector T cell proliferation and interferon-γ production *in vitro*, in keeping with the inhibitory role of PD-1, which contributes to tumoral effector T cell dysfunction. However, PD-1 expression was not associated with the lack of granzyme B and perforin in tumoral T cells, and PD-1 blockade did not alter granzyme B expression by tumoral CD8^{+} T cells *in vitro*, suggesting that alternative mechanisms may be responsible for the lack of cytolytic molecules in cSCC T cells.

It is notable that PD-1 is expressed by $CD8^+$ T cells in non-lesional skin in similar frequencies to those in cSCC, and in significantly higher percentages than $CD8^+$ T cells blood. T cells from the non-lesional skin were also not able to produce granzyme B and perforin, which could signify that a degree of T cell hyporesponsiveness is present in apparently normal sun-exposed skin. Hence, it is possible that T cell dysfunction may be an initiating factor in permitting cSCC development in UVR-damaged skin. Related to this, dysfunctional tumour-specific T cells can be established during the pre-malignant phase of tumorigenesis in a murine liver cancer model, with persistent antigen exposure driving this dysfunction rather than factors associated with the tumour microenvironment (Schietinger et al., 2016). It is possible that pre-malignant dysplastic cells in skin chronically exposed to ultraviolet radiation may contain antigens that activate naive T cells to undergo differentiation into a dysfunctional phenotype before the emergence of a pathologically defined malignant tumour.

Based on the findings so far, one possible aim of future investigations would be to further elucidate the contributions of different mechanisms to the dysfunctional tumoral immune response in cSCC. As cancers depend on a plethora of ways to escape immune detection and destruction, it is likely that new therapies will rely on a combination of approaches. Hence, the assessment of the relative contributions of different immunopathogenic mechanisms in cSCC, e.g. immunosuppression by Tregs and the inhibitory effect of PD-1 on effector T cells, would enable optimisation in enhancing tumour-specific immunity. In addition, Tregs themselves can promote tumoral effector T cell dysfunction through interactions via dendritic cells (Bauer et al., 2014) and IL-35 (Turnis et al., 2016), and so experiments could be performed to assess whether cSCC Tregs can induce T cell exhaustion in effector T cells. Furthermore, other inhibitory receptors can be expressed by dysfunctional effector T cells in addition to PD-1, and as strategies which target multiple inhibitory receptors may be synergistic and amplify anti-tumour immune responses over monotherapy (Pardoll, 2012, Chauvin et al., 2015), future experiments could be performed to investigate whether tumoral effector T cell function is further enhanced by targeting TIGIT, which was present on cSCC effector T cells in the current study, in combination with PD-1 blockade. Clinical trials would be required to assess safety and efficacy of inhibitory receptor blockade for the treatment of primary or metastatic cSCC. Currently, clinical trials are being conducted using PD-1 inhibition in patients with advanced or unresectable cSCC (NCT02883556 (clinicaltrials.gov, 2016a), NCT02760498 (clinicaltrials.gov, 2016b)), and a number of case reports have

indicated cSCC tumour regression with anti-PD-1 monoclonal antibody treatment (Lipson et al., 2016, Borradori et al., 2016, Winkler et al., 2016).

The current study also provides a platform for further investigations to determine the mechanisms of T cell dysfunction in cSCC. The characterisation experiments performed so far have shown that T cells can be isolated from cSCC which can be phenotypically and functionally different from those in patient-matched blood and normal skin. Gene expression profiling can be used to further determine whether cSCC T cells have the molecular signature of exhausted T cells in cancer (Baitsch et al., 2011), and identify whether other dysfunctional states are present (Schietinger and Greenberg, 2014), which could provide insight into the mechanism for reduced expression of granzyme B and perforin by cSCC T cells. Single cell RNA sequencing has shown that dysfunctional and activation statuses of tumour-infiltrating T cells can be independently silenced with gene editing technology, suggesting that this approach can be further used to identify and target specific mechanisms for tumoral T cell dysfunction (Singer et al., 2016).

The present study demonstrates that PD-1 is expressed by T cells in non-lesional skin (which was mainly from sun-exposed areas). To determine whether the presence of PD-1 on T cells relates to solar damage in skin, experiments could be performed to examine PD-1 expression in T cells from sun-protected non-lesional skin (e.g. from the buttock) compared to sun exposed skin. It is possible that defective T cell immunity is present at the initiating or early stages of cSCC development, and related to this, previous work by our group has shown that the precancerous skin lesion, actinic keratosis, contains similar frequencies of $FOXP3^+$ Tregs as in cSCC (Lai et al., 2016). Actinic keratoses and Bowen's disease could also be examined for $PD\text{-}1^+$ T cells as well as PD-L1/2 to help to ascertain whether PD-1 is relevant at the early stages of tumour development. To investigate how cSCCs can induce tumoral T cell dysfunction / PD-1 expression, T cells (from cSCC, normal skin or peripheral blood) could be cultured in the presence or absence of tumour keratinocytes (and stromal cells/supernatant); identifying mechanisms by which T cell dysfunction can be induced in cSCC/normal skin would help to uncover therapies that prevent cSCCs from developing by inhibiting T cells from becoming dysfunctional. For example, peptide vaccines which target cancer epitopes and overcome tumoral T cell dysfunction can induce tumour rejection (Williams et al., 2013, Gubin et al., 2014). Identification of antigens in cSCC would be required for the development of peptide vaccines for this cancer, and would be useful for future investigations into antigen-specific interactions in

this tumour; a number of recent publications have highlighted the great potential of tumour neoantigen discovery (Linnemann et al., 2015, McGranahan et al., 2016).

In addition to T cells and neoplastic tumour cells, the other contents of the tumour microenvironment, including cytokines, antigen presenting cells and other stromal cells are likely to contribute to cSCC development, therefore, the roles of the different cell types and mediators in the tumour microenvironment and cross-talk between them need to be further elucidated. Cytokines such as CCL22 can mediate trafficking of Tregs into tumours (Curiel et al., 2004, Klarquist et al., 2016), and so future investigations can be used to analyse chemokines in the cSCC microenvironment and determine whether the cSCC supernatant promotes migration of Tregs, as it remains unclear how these cells are directed to cSCCs. It is also not known what the relative contributions are of Tregs which have been thymically-derived and those that have been peripherally-induced from conventional $CD4^+$ T cells. In addition, the mechanisms for Treg mediated suppression in cSCC, and how these relate to OX40, still remain to be determined.

More complex experiments are likely to require more advanced models of cSCC, especially given that functional assessment of T cells from skin is limited by the relatively low numbers that can be isolated with the methods used in the current study. Moreover, *in vitro* functional experiments could be performed that enable assessment of tumour cell killing by T cells in the presence of antigenic stimulus using chromium release assays, and *in vivo* mouse models (e.g. DMBA/TPA models) could be used for functional and mechanistic analysis. The future development of cSCC models that recapitulate human immunity *in vivo* would be useful for investigating the mechanisms and potential effectiveness of new therapies. Furthermore, greater understanding of the phenotype and functional deficiencies of T cells in cSCCs could contribute to the identification of new potential targets which may ultimately enable development of new pharmacological treatments for cSCC in future years.

Overall, this study has shown that a combination of defective immune responses are present in cSCC which may play a fundamental role in the development of these tumours (see Figure 6.1, page 186). In addition, the results of this study demonstrate that *in vitro* assays using cSCC T cells allow functional assessment of antibodies that target T cell costimulation/inhibition and might be useful as a preclinical tool for investigation of anti-tumour immunotherapies.

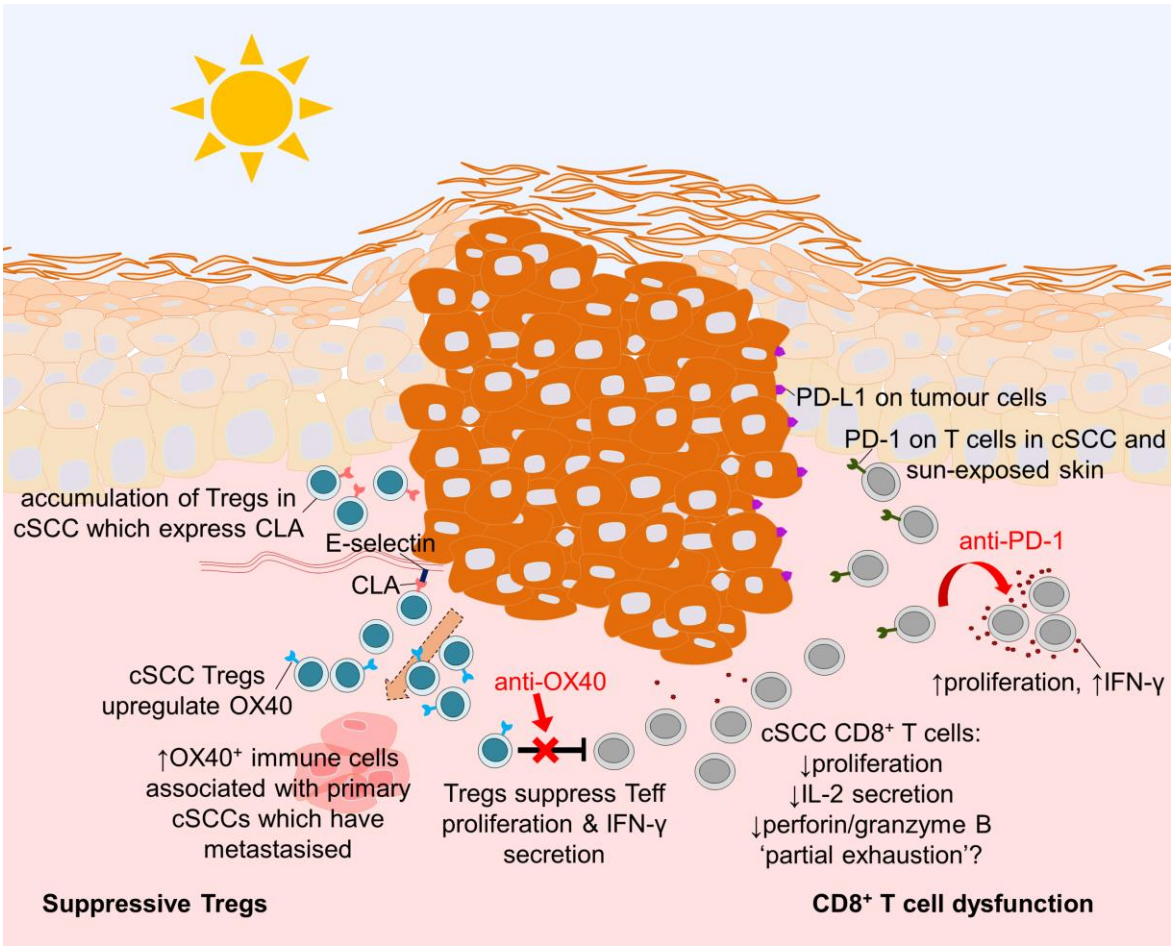

Figure 6.1 Schematic representation of key findings in this study.

A combination of mechanisms involving suppressive Tregs and dysfunctional CD8⁺ T cells contribute to ineffective anti-tumour immunity in cSCC. Tregs accumulate in cSCCs, likely via CLA on Tregs and E-selectin on cSCC blood vessels, upregulate the co-stimulatory receptor OX40, and suppress tumoral effector T cell responses. Primary cSCCs which have metastasised are associated with higher frequencies of tumoral OX40⁺ immune cells. Targeting OX40 with an agonistic antibody overcomes Treg mediated suppression and enhances tumoral effector T cell responses. CD8⁺ T cells in cSCC are less able to proliferate and produce perforin and granzyme B than CD8⁺ T cells in blood and secrete less IL-2 than those from normal skin. However, interferon-γ and TNF-α production are maintained by cSCC CD8⁺ T cells, suggesting a state of 'partial exhaustion'. The inhibitory receptor PD-1 is expressed by many T cells in cSCC and normal sun exposed skin, and PD-L1 is present on cSCC tumour cells. PD-1 inhibition augments tumoral CD8⁺ T cell proliferation and interferon-γ secretion, suggesting that CD8⁺ T cell dysfunction can be reversed. The results of this study demonstrate that defective T cell responses are present in cSCCs which may play a key role in permitting the growth and development of these tumours.

Chapter 7: References

ACHACHI, A., VOCANSON, M., BASTIEN, P., PEGUET-NAVARRO, J., GRANDE, S., GOUJON, C., BRETON, L., CASTIEL-HIGOUNENC, I., NICOLAS, J. F. & GUENICHE, A. 2015. UV radiation induces the epidermal recruitment of dendritic cells that compensate for the depletion of Langerhans cells in human skin. *J Invest Dermatol,* 135**,** 2058-67.

AFFARA, N. I., RUFFELL, B., MEDLER, T. R., GUNDERSON, A. J., JOHANSSON, M., BORNSTEIN, S., BERGSLAND, E., STEINHOFF, M., LI, Y., GONG, Q., MA, Y., WIESEN, J. F., WONG, M. H., KULESZ-MARTIN, M., IRVING, B. & COUSSENS, L. M. 2014. B cells regulate macrophage phenotype and response to chemotherapy in squamous carcinomas. *Cancer Cell,* 25**,** 809-21.

AGIUS, E., LACY, K. E., VUKMANOVIC-STEJIC, M., JAGGER, A. L., PAPAGEORGIOU, A. P., HALL, S., REED, J. R., CURNOW, S. J., FUENTES-DUCULAN, J., BUCKLEY, C. D., SALMON, M., TAAMS, L. S., KRUEGER, J., GREENWOOD, J., KLEIN, N., RUSTIN, M. H. & AKBAR, A. N. 2009. Decreased TNF-alpha synthesis by macrophages restricts cutaneous immunosurveillance by memory CD4+ T cells during aging. *J Exp Med,* 206**,** 1929-40.

AHMADZADEH, M., JOHNSON, L. A., HEEMSKERK, B., WUNDERLICH, J. R., DUDLEY, M. E., WHITE, D. E. & ROSENBERG, S. A. 2009. Tumor antigen-specific CD8 T cells infiltrating the tumor express high levels of PD-1 and are functionally impaired. *Blood,* 114**,** 1537-44.

AKHMETZYANOVA, I., ZELINSKYY, G., LITTWITZ-SALOMON, E., MALYSHKINA, A., DIETZE, K. K., STREECK, H., BRANDAU, S. & DITTMER, U. 2016. CD137 agonist therapy can reprogram regulatory T cells into cytotoxic CD4+ T cells with antitumor activity. *J Immunol,* 196**,** 484-92.

ALAM, M. & RATNER, D. 2001. Cutaneous squamous-cell carcinoma. *N Engl J Med,* 344**,** 975-83.

ALAMEDA, J. P., MORENO-MALDONADO, R., NAVARRO, M., BRAVO, A., RAMIREZ, A., PAGE, A., JORCANO, J. L., FERNANDEZ-ACENERO, M. J. & CASANOVA, M. L. 2010. An inactivating CYLD mutation promotes skin tumor progression by conferring enhanced proliferative, survival and angiogenic properties to epidermal cancer cells. *Oncogene,* 29**,** 6522-32.

ALITALO, A. K., PROULX, S. T., KARAMAN, S., AEBISCHER, D., MARTINO, S., JOST, M., SCHNEIDER, N., BRY, M. & DETMAR, M. 2013. VEGF-C and VEGF-D blockade inhibits inflammatory skin carcinogenesis. *Cancer Res,* 73**,** 4212-21.

ALL PARTY PARLIAMENTARY GROUP ON SKIN 2008. Skin cancer - improving prevention, treatment and care. A report of the All Party Parliamentary Group on Skin. London.

ALT-HOLLAND, A., SOWALSKY, A. G., SZWEC-LEVIN, Y., SHAMIS, Y., HATCH, H., FEIG, L. A. & GARLICK, J. A. 2011. Suppression of E-cadherin function drives the early stages of Ras-induced squamous cell carcinoma through upregulation of FAK and Src. *J Invest Dermatol,* 131**,** 2306-15.

ALTER, B. P., GIRI, N., SAVAGE, S. A. & ROSENBERG, P. S. 2009. Cancer in dyskeratosis congenita. *Blood,* 113**,** 6549-57.

AMERICAN CANCER SOCIETY. 2015. *Skin cancer - basal and squamous cell* [Online]. Available: http://www.cancer.org/cancer/skincancer-basalandsquamouscell/detailedguide/skin-cancer-basal-and-squamous-cell-key-statistics [Accessed 5/01 2016].

ANDREU, P., JOHANSSON, M., AFFARA, N. I., PUCCI, F., TAN, T., JUNANKAR, S., KORETS, L., LAM, J., TAWFIK, D., DENARDO, D. G., NALDINI, L., DE VISSER, K. E., DE PALMA, M. & COUSSENS, L. M. 2010. FcRgamma activation regulates inflammation-associated squamous carcinogenesis. *Cancer Cell,* 17**,** 121-34.

ANTSIFEROVA, M., HUBER, M., MEYER, M., PIWKO-CZUCHRA, A., RAMADAN, T., MACLEOD, A. S., HAVRAN, W. L., DUMMER, R., HOHL, D. & WERNER, S. 2011. Activin enhances skin tumourigenesis and malignant progression by inducing a pro-tumourigenic immune cell response. *Nat Commun,* 2**,** 576.

ARIOTTI, S., HOGENBIRK, M. A., DIJKGRAAF, F. E., VISSER, L. L., HOEKSTRA, M. E., SONG, J. Y., JACOBS, H., HAANEN, J. B. & SCHUMACHER, T. N. 2014. T cell memory. Skin-resident memory CD8(+) T cells trigger a state of tissue-wide pathogen alert. *Science,* 346**,** 101-5.

ARRON, S. T., RUBY, J. G., DYBBRO, E., GANEM, D. & DERISI, J. L. 2011. Transcriptome sequencing demonstrates that human papillomavirus is not active in cutaneous squamous cell carcinoma. *J Invest Dermatol,* 131**,** 1745-53.

ATKINS, M. B., LOTZE, M. T., DUTCHER, J. P., FISHER, R. I., WEISS, G., MARGOLIN, K., ABRAMS, J., SZNOL, M., PARKINSON, D., HAWKINS, M., PARADISE, C., KUNKEL, L. & ROSENBERG, S. A. 1999. High-dose recombinant interleukin 2 therapy for patients with metastatic melanoma: analysis of 270 patients treated between 1985 and 1993. *J Clin Oncol,* 17**,** 2105-16.

AZZIMONTI, B., ZAVATTARO, E., PROVASI, M., VIDALI, M., CONCA, A., CATALANO, E., RIMONDINI, L., COLOMBO, E. & VALENTE, G. 2015. Intense Foxp3+ CD25+ regulatory T-cell infiltration is associated with high-grade cutaneous squamous cell carcinoma and counterbalanced by CD8+/Foxp3+ CD25+ ratio. *Br J Dermatol,* 172**,** 64-73.

BAITSCH, L., BAUMGAERTNER, P., DEVEVRE, E., RAGHAV, S. K., LEGAT, A., BARBA, L., WIECKOWSKI, S., BOUZOURENE, H., DEPLANCKE, B., ROMERO, P., RUFER, N. & SPEISER, D. E. 2011. Exhaustion of tumor-specific CD8(+) T cells in metastases from melanoma patients. *J Clin Invest,* 121**,** 2350-60.

BAITSCH, L., FUERTES-MARRACO, S. A., LEGAT, A., MEYER, C. & SPEISER, D. E. 2012. The three main stumbling blocks for anticancer T cells. *Trends Immunol,* 33**,** 364-72.

BARTKOWIAK, T., SINGH, S., YANG, G., GALVAN, G., HARIA, D., AI, M., ALLISON, J. P., SASTRY, K. J. & CURRAN, M. A. 2015. Unique potential of 4-1BB agonist antibody to promote durable regression of HPV+ tumors when combined with an E6/E7 peptide vaccine. *Proc Natl Acad Sci U S A,* 112**,** E5290-9.

BASTIAENS, M. T., TER HUURNE, J. A., KIELICH, C., GRUIS, N. A., WESTENDORP, R. G., VERMEER, B. J., BAVINCK, J. N. & LEIDEN SKIN CANCER STUDY, T. 2001. Melanocortin-1 receptor gene variants determine the risk of nonmelanoma skin cancer independently of fair skin and red hair. *Am J Hum Genet,* 68**,** 884-94.

BASTID, J., COTTALORDA-REGAIRAZ, A., ALBERICI, G., BONNEFOY, N., ELIAOU, J. F. & BENSUSSAN, A. 2013. ENTPD1/CD39 is a promising therapeutic target in oncology. *Oncogene,* 32**,** 1743-51.

BATES, G. J., FOX, S. B., HAN, C., LEEK, R. D., GARCIA, J. F., HARRIS, A. L. & BANHAM, A. H. 2006. Quantification of regulatory T cells enables the identification of high-risk breast cancer patients and those at risk of late relapse. *J Clin Oncol,* 24**,** 5373-80.

BATH-HEXTALL, F. J., MATIN, R. N., WILKINSON, D. & LEONARDI-BEE, J. 2013. Interventions for cutaneous Bowen's disease. *Cochrane Database Syst Rev,* 6**,** CD007281.

BATINAC, T., ZAMOLO, G., HADZISEJDIC, I. & ZAUHAR, G. 2006. A comparative study of granzyme B expression in keratoacanthoma and squamous cell carcinoma. *J Dermatol Sci,* 44**,** 109-12.

BAUER, C. A., KIM, E. Y., MARANGONI, F., CARRIZOSA, E., CLAUDIO, N. M. & MEMPEL, T. R. 2014. Dynamic Treg interactions with intratumoral APCs promote local CTL dysfunction. *J Clin Invest,* 124**,** 2425-40.

BELKAID, Y. & OLDENHOVE, G. 2008. Tuning microenvironments: induction of regulatory T cells by dendritic cells. *Immunity,* 29**,** 362-71.

BELKAID, Y., PICCIRILLO, C. A., MENDEZ, S., SHEVACH, E. M. & SACKS, D. L. 2002. CD4+CD25+ regulatory T cells control Leishmania major persistence and immunity. *Nature,* 420**,** 502-7.

BELKIN, D. A., CHEN, J., MO, J. L., ROSOFF, J. S., GOLDENBERG, S., POPPAS, D. P., KRUEGER, J. G., HERSCHMAN, M., MITSUI, H., FELSEN, D. & CARUCCI, J. A. 2013. An animal explant model for the study of human cutaneous squamous cell carcinoma. *PLoS One,* 8**,** e76156.

BERHANE, T., HALLIDAY, G. M., COOKE, B. & BARNETSON, R. S. 2002. Inflammation is associated with progression of actinic keratoses to squamous cell carcinomas in humans. *Br J Dermatol,* 146**,** 810-5.

BERTRAND, F., ROCHOTTE, J., COLACIOS, C., MONTFORT, A., TILKIN-MARIAME, A. F., TOURIOL, C., ROCHAIX, P., LAJOIE-MAZENC, I., ANDRIEU-ABADIE, N., LEVADE, T., BENOIST, H. & SEGUI, B. 2015. Blocking tumor necrosis factor alpha enhances CD8 T-cell-dependent immunity in experimental melanoma. *Cancer Res,* 75**,** 2619-28.

BICKERS, D. R., LIM, H. W., MARGOLIS, D., WEINSTOCK, M. A., GOODMAN, C., FAULKNER, E., GOULD, C., GEMMEN, E., DALL, T., AMERICAN ACADEMY OF DERMATOLOGY, A. & SOCIETY FOR INVESTIGATIVE, D. 2006. The burden of skin diseases: 2004 a joint project of the American Academy of Dermatology Association and the Society for Investigative Dermatology. *J Am Acad Dermatol,* 55**,** 490-500.

BILATE, A. M. & LAFAILLE, J. J. 2012. Induced CD4+Foxp3+ regulatory T cells in immune tolerance. *Annu Rev Immunol,* 30**,** 733-58.

BISWAS, A., RICHARDS, J. E., MASSARO, J. & MAHALINGAM, M. 2014. Mast cells in cutaneous tumors: innocent bystander or maestro conductor? *Int J Dermatol,* 53**,** 806-11.

BLACK, A. P., BAILEY, A., JONES, L., TURNER, R. J., HOLLOWOOD, K. & OGG, G. S. 2005. p53-specific CD8+ T-cell responses in individuals with cutaneous squamous cell carcinoma. *Br J Dermatol,* 153**,** 987-91.

BLACKBURN, S. D., SHIN, H., HAINING, W. N., ZOU, T., WORKMAN, C. J., POLLEY, A., BETTS, M. R., FREEMAN, G. J., VIGNALI, D. A. & WHERRY, E. J. 2009. Coregulation of CD8+ T cell exhaustion by multiple inhibitory receptors during chronic viral infection. *Nat Immunol,* 10**,** 29-37.

BLUTH, M. J., ZABA, L. C., MOUSSAI, D., SUAREZ-FARINAS, M., KAPORIS, H., FAN, L., PIERSON, K. C., WHITE, T. R., PITTS-KIEFER, A., FUENTES-DUCULAN, J., GUTTMAN-YASSKY, E., KRUEGER, J. G., LOWES, M. A. & CARUCCI, J. A. 2009. Myeloid dendritic cells from human cutaneous squamous cell carcinoma are poor stimulators of T-cell proliferation. *J Invest Dermatol,* 129**,** 2451-62.

BOHM, M., WOLFF, I., SCHOLZEN, T. E., ROBINSON, S. J., HEALY, E., LUGER, T. A., SCHWARZ, T. & SCHWARZ, A. 2005. alpha-Melanocyte-stimulating hormone protects from ultraviolet radiation-induced apoptosis and DNA damage. *J Biol Chem,* 280**,** 5795-802.

BOISSONNAS, A., SCHOLER-DAHIREL, A., SIMON-BLANCAL, V., PACE, L., VALET, F., KISSENPFENNIG, A., SPARWASSER, T., MALISSEN, B., FETLER, L. & AMIGORENA, S. 2010. Foxp3+ T cells induce perforin-dependent dendritic cell death in tumor-draining lymph nodes. *Immunity,* 32**,** 266-78.

BOOTH, N. J., MCQUAID, A. J., SOBANDE, T., KISSANE, S., AGIUS, E., JACKSON, S. E., SALMON, M., FALCIANI, F., YONG, K., RUSTIN, M. H., AKBAR, A. N. & VUKMANOVIC-STEJIC, M. 2010. Different proliferative potential and migratory characteristics of human CD4+ regulatory T cells that express either CD45RA or CD45RO. *J Immunol,* 184**,** 4317-26.

BOPP, T., BECKER, C., KLEIN, M., KLEIN-HESSLING, S., PALMETSHOFER, A., SERFLING, E., HEIB, V., BECKER, M., KUBACH, J., SCHMITT, S., STOLL, S., SCHILD, H., STAEGE, M. S., STASSEN, M., JONULEIT, H. & SCHMITT, E. 2007. Cyclic adenosine monophosphate is a key component of regulatory T cell-mediated suppression. *J Exp Med,* 204**,** 1303-10.

BORGHAEI, H., PAZ-ARES, L., HORN, L., SPIGEL, D. R., STEINS, M., READY, N. E., CHOW, L. Q., VOKES, E. E., FELIP, E., HOLGADO, E., BARLESI, F., KOHLHAUFL, M., ARRIETA, O., BURGIO, M. A., FAYETTE, J., LENA, H., PODDUBSKAYA, E., GERBER, D. E., GETTINGER, S. N., RUDIN, C. M., RIZVI, N., CRINO, L., BLUMENSCHEIN, G. R., JR., ANTONIA, S. J., DORANGE, C., HARBISON, C. T., GRAF FINCKENSTEIN, F. & BRAHMER, J. R. 2015. Nivolumab versus docetaxel in advanced nonsquamous non-small-cell lung cancer. *N Engl J Med,* 373**,** 1627-39.

BORRADORI, L., SUTTON, B., SHAYESTEH, P. & DANIELS, G. A. 2016. Rescue therapy with anti-programmed cell death protein 1 inhibitors of advanced cutaneous squamous cell carcinoma and basosquamous carcinoma: preliminary experience in five cases. *Br J Dermatol*.

BOTTI, E., SPALLONE, G., MORETTI, F., MARINARI, B., PINETTI, V., GALANTI, S., DE MEO, P. D., DE NICOLA, F., GANCI, F., CASTRIGNANO, T., PESOLE, G., CHIMENTI, S., GUERRINI, L., FANCIULLI, M., BLANDINO, G., KARIN, M. & COSTANZO, A. 2011. Developmental factor IRF6 exhibits tumor suppressor activity in squamous cell carcinomas. *Proc Natl Acad Sci U S A,* 108**,** 13710-5.

BOUWES BAVINCK, J. N., NEALE, R. E., ABENI, D., EUVRARD, S., GREEN, A. C., HARWOOD, C. A., DE KONING, M. N., NALDI, L., NINDL, I., PAWLITA, M., PFISTER, H., PROBY, C. M., QUINT, W. G., TER SCHEGGET, J., WATERBOER, T., WEISSENBORN, S., FELTKAMP, M. C. & GROUP, E.-H.-U.-C. 2010. Multicenter study of the association between betapapillomavirus infection and cutaneous squamous cell carcinoma. *Cancer Res,* 70**,** 9777-86.

BOX, N. F., DUFFY, D. L., IRVING, R. E., RUSSELL, A., CHEN, W., GRIFFYTHS, L. R., PARSONS, P. G., GREEN, A. C. & STURM, R. A. 2001. Melanocortin-1 receptor genotype is a risk factor for basal and squamous cell carcinoma. *J Invest Dermatol,* 116**,** 224-9.

BRADFORD, P. T., GOLDSTEIN, A. M., TAMURA, D., KHAN, S. G., UEDA, T., BOYLE, J., OH, K. S., IMOTO, K., INUI, H., MORIWAKI, S., EMMERT, S., PIKE, K. M., RAZIUDDIN, A., PLONA, T. M., DIGIOVANNA, J. J., TUCKER, M. A. & KRAEMER, K. H. 2011. Cancer and neurologic degeneration in xeroderma pigmentosum: long term follow-up characterises the role of DNA repair. *J Med Genet,* 48**,** 168-76.

BRAHMER, J., RECKAMP, K. L., BAAS, P., CRINO, L., EBERHARDT, W. E., PODDUBSKAYA, E., ANTONIA, S., PLUZANSKI, A., VOKES, E. E., HOLGADO, E., WATERHOUSE, D., READY, N., GAINOR, J., AREN FRONTERA, O., HAVEL, L., STEINS, M., GARASSINO, M. C., AERTS, J. G., DOMINE, M., PAZ-ARES, L., RECK, M., BAUDELET, C., HARBISON, C. T., LESTINI, B. & SPIGEL, D. R. 2015. Nivolumab versus docetaxel in advanced squamous-cell non-small-cell lung cancer. *N Engl J Med,* 373**,** 123-35.

BRANTSCH, K. D., MEISNER, C., SCHONFISCH, B., TRILLING, B., WEHNER-CAROLI, J., ROCKEN, M. & BREUNINGER, H. 2008. Analysis of risk factors determining prognosis of cutaneous squamous-cell carcinoma: a prospective study. *Lancet Oncol,* 9**,** 713-20.

BRASH, D. E., RUDOLPH, J. A., SIMON, J. A., LIN, A., MCKENNA, G. J., BADEN, H. P., HALPERIN, A. J. & PONTEN, J. 1991. A role for sunlight in skin cancer: UV-induced p53 mutations in squamous cell carcinoma. *Proc Natl Acad Sci U S A,* 88**,** 10124-8.

BREART, B., LEMAITRE, F., CELLI, S. & BOUSSO, P. 2008. Two-photon imaging of intratumoral CD8+ T cell cytotoxic activity during adoptive T cell therapy in mice. *J Clin Invest,* 118**,** 1390-7.

BRINCKS, E. L., ROBERTS, A. D., COOKENHAM, T., SELL, S., KOHLMEIER, J. E., BLACKMAN, M. A. & WOODLAND, D. L. 2013. Antigen-specific memory regulatory CD4+Foxp3+ T cells control memory responses to influenza virus infection. *J Immunol,* 190**,** 3438-46.

BROWN, L., WASEEM, A., CRUZ, I. N., SZARY, J., GUNIC, E., MANNAN, T., UNADKAT, M., YANG, M., VALDERRAMA, F., O'TOOLE, E. A. & WAN, H. 2014. Desmoglein 3 promotes cancer cell migration and invasion by regulating activator protein 1 and protein kinase C-dependent-Ezrin activation. *Oncogene,* 33**,** 2363-74.

BULLIARD, Y., JOLICOEUR, R., ZHANG, J., DRANOFF, G., WILSON, N. S. & BROGDON, J. L. 2014. OX40 engagement depletes intratumoral Tregs via activating FcgammaRs, leading to antitumor efficacy. *Immunol Cell Biol,* 92**,** 475-80.

BUTLER, N. S., MOEBIUS, J., PEWE, L. L., TRAORE, B., DOUMBO, O. K., TYGRETT, L. T., WALDSCHMIDT, T. J., CROMPTON, P. D. & HARTY, J. T. 2012.

Therapeutic blockade of PD-L1 and LAG-3 rapidly clears established blood-stage Plasmodium infection. *Nat Immunol,* 13**,** 188-95.

BYRNE, S. N., BEAUGIE, C., O'SULLIVAN, C., LEIGHTON, S. & HALLIDAY, G. M. 2011. The immune-modulating cytokine and endogenous Alarmin interleukin-33 is upregulated in skin exposed to inflammatory UVB radiation. *Am J Pathol,* 179**,** 211-22.

CALZASCIA, T., PELLEGRINI, M., HALL, H., SABBAGH, L., ONO, N., ELFORD, A. R., MAK, T. W. & OHASHI, P. S. 2007. TNF-alpha is critical for antitumor but not antiviral T cell immunity in mice. *J Clin Invest,* 117**,** 3833-45.

CAMPBELL, J. J., HARALDSEN, G., PAN, J., ROTTMAN, J., QIN, S., PONATH, P., ANDREW, D. P., WARNKE, R., RUFFING, N., KASSAM, N., WU, L. & BUTCHER, E. C. 1999. The chemokine receptor CCR4 in vascular recognition by cutaneous but not intestinal memory T cells. *Nature,* 400**,** 776-80.

CAMPBELL, J. J., MURPHY, K. E., KUNKEL, E. J., BRIGHTLING, C. E., SOLER, D., SHEN, Z., BOISVERT, J., GREENBERG, H. B., VIERRA, M. A., GOODMAN, S. B., GENOVESE, M. C., WARDLAW, A. J., BUTCHER, E. C. & WU, L. 2001. CCR7 expression and memory T cell diversity in humans. *J Immunol,* 166**,** 877-84.

CANCER COUNCIL AUSTRALIA. 2015. *Skin cancer statistics and issues* [Online]. Sydney: Cancer Council Australia. Available: http://www.cancer.org.au/about-cancer/types-of-cancer/skin-cancer.html [Accessed 7 Jul 2015].

CANCER GENOME ATLAS NETWORK 2015. Genomic classification of cutaneous melanoma. *Cell,* 161**,** 1681-96.

CANCER RESEARCH UK. 2015. *Skin cancer incidence statistics* [Online]. Available: http://www.cancerresearchuk.org/health-professional/skin-cancer-incidence-statistics [Accessed 23 Dec 2015].

CANTWELL, M. M., MURRAY, L. J., CATNEY, D., DONNELLY, D., AUTIER, P., BONIOL, M., FOX, C., MIDDLETON, R. J., DOLAN, O. M. & GAVIN, A. T. 2009. Second primary cancers in patients with skin cancer: a population-based study in Northern Ireland. *Br J Cancer,* 100**,** 174-7.

CAO, Y., ZHANG, L., KAMIMURA, Y., RITPRAJAK, P., HASHIGUCHI, M., HIROSE, S. & AZUMA, M. 2011. B7-H1 overexpression regulates epithelial-mesenchymal transition and accelerates carcinogenesis in skin. *Cancer Res,* 71**,** 1235-43.

CARRETERO, R., SEKTIOGLU, I. M., GARBI, N., SALGADO, O. C., BECKHOVE, P. & HAMMERLING, G. J. 2015. Eosinophils orchestrate cancer rejection by normalizing tumor vessels and enhancing infiltration of CD8(+) T cells. *Nat Immunol,* 16**,** 609-17.

CARROLL, R. P., SEGUNDO, D. S., HOLLOWOOD, K., MARAFIOTI, T., CLARK, T. G., HARDEN, P. N. & WOOD, K. J. 2010. Immune phenotype predicts risk for posttransplantation squamous cell carcinoma. *J Am Soc Nephrol,* 21**,** 713-22.

CAVANI, A., NASORRI, F., OTTAVIANI, C., SEBASTIANI, S., DE PITA, O. & GIROLOMONI, G. 2003. Human CD25+ regulatory T cells maintain immune tolerance to nickel in healthy, nonallergic individuals. *J Immunol,* 171**,** 5760-8.

CEBULA, A., SEWERYN, M., REMPALA, G. A., PABLA, S. S., MCINDOE, R. A., DENNING, T. L., BRY, L., KRAJ, P., KISIELOW, P. & IGNATOWICZ, L. 2013. Thymus-derived regulatory T cells contribute to tolerance to commensal microbiota. *Nature,* 497**,** 258-62.

CHACON-SALINAS, R., LIMON-FLORES, A. Y., CHAVEZ-BLANCO, A. D., GONZALEZ-ESTRADA, A. & ULLRICH, S. E. 2011. Mast cell-derived IL-10 suppresses germinal center formation by affecting T follicular helper cell function. *J Immunol,* 186**,** 25-31.

CHACON, J. A., WU, R. C., SUKHUMALCHANDRA, P., MOLLDREM, J. J., SARNAIK, A., PILON-THOMAS, S., WEBER, J., HWU, P. & RADVANYI, L. 2013. Co-stimulation through 4-1BB/CD137 improves the expansion and function of CD8(+) melanoma tumor-infiltrating lymphocytes for adoptive T-cell therapy. *PLoS One,* 8**,** e60031.

CHANG, C. H., QIU, J., O'SULLIVAN, D., BUCK, M. D., NOGUCHI, T., CURTIS, J. D., CHEN, Q., GINDIN, M., GUBIN, M. M., VAN DER WINDT, G. J., TONC, E., SCHREIBER, R. D., PEARCE, E. J. & PEARCE, E. L. 2015. Metabolic competition in the tumor microenvironment is a driver of cancer progression. *Cell,* 162**,** 1229-41.

CHANG, J. H., XIAO, Y., HU, H., JIN, J., YU, J., ZHOU, X., WU, X., JOHNSON, H. M., AKIRA, S., PASPARAKIS, M., CHENG, X. & SUN, S. C. 2012. Ubc13 maintains the suppressive function of regulatory T cells and prevents their conversion into effector-like T cells. *Nat Immunol,* 13**,** 481-90.

CHANG, J. T., WHERRY, E. J. & GOLDRATH, A. W. 2014. Molecular regulation of effector and memory T cell differentiation. *Nat Immunol,* 15**,** 1104-15.

CHATZINASIOU, F., LILL, C. M., KYPREOU, K., STEFANAKI, I., NICOLAOU, V., SPYROU, G., EVANGELOU, E., ROEHR, J. T., KODELA, E., KATSAMBAS, A., TSAO, H., IOANNIDIS, J. P., BERTRAM, L. & STRATIGOS, A. J. 2011. Comprehensive field synopsis and systematic meta-analyses of genetic association studies in cutaneous melanoma. *J Natl Cancer Inst,* 103**,** 1227-35.

CHAUDHRY, A., RUDRA, D., TREUTING, P., SAMSTEIN, R. M., LIANG, Y., KAS, A. & RUDENSKY, A. Y. 2009. CD4+ regulatory T cells control TH17 responses in a Stat3-dependent manner. *Science,* 326**,** 986-91.

CHAUVIN, J. M., PAGLIANO, O., FOURCADE, J., SUN, Z., WANG, H., SANDER, C., KIRKWOOD, J. M., CHEN, T. H., MAURER, M., KORMAN, A. J. & ZAROUR, H. M. 2015. TIGIT and PD-1 impair tumor antigen-specific CD8(+) T cells in melanoma patients. *J Clin Invest,* 125**,** 2046-58.

CHEN, A. C., MARTIN, A. J., CHOY, B., FERNANDEZ-PENAS, P., DALZIELL, R. A., MCKENZIE, C. A., SCOLYER, R. A., DHILLON, H. M., VARDY, J. L., KRICKER, A., ST GEORGE, G., CHINNIAH, N., HALLIDAY, G. M. & DAMIAN, D. L. 2015. A phase 3 randomized trial of nicotinamide for skin-cancer chemoprevention. *N Engl J Med,* 373**,** 1618-26.

CHEN, J., RUCZINSKI, I., JORGENSEN, T. J., YENOKYAN, G., YAO, Y., ALANI, R., LIEGEOIS, N. J., HOFFMAN, S. C., HOFFMAN-BOLTON, J., STRICKLAND, P. T., HELZLSOUER, K. J. & ALBERG, A. J. 2008. Nonmelanoma skin cancer and risk for subsequent malignancy. *J Natl Cancer Inst,* 100**,** 1215-22.

CHEN, L. & FLIES, D. B. 2013. Molecular mechanisms of T cell co-stimulation and co-inhibition. *Nat Rev Immunol,* 13**,** 227-42.

CHEN, W., JIN, W., HARDEGEN, N., LEI, K. J., LI, L., MARINOS, N., MCGRADY, G. & WAHL, S. M. 2003. Conversion of peripheral CD4+CD25- naive T cells to CD4+CD25+ regulatory T cells by TGF-beta induction of transcription factor Foxp3. *J Exp Med,* 198**,** 1875-86.

CHEN, Z., BARBI, J., BU, S., YANG, H. Y., LI, Z., GAO, Y., JINASENA, D., FU, J., LIN, F., CHEN, C., ZHANG, J., YU, N., LI, X., SHAN, Z., NIE, J., GAO, Z., TIAN, H., LI, Y., YAO, Z., ZHENG, Y., PARK, B. V., PAN, Z., ZHANG, J., DANG, E., LI, Z., WANG, H., LUO, W., LI, L., SEMENZA, G. L., ZHENG, S. G., LOSER, K., TSUN, A., GREENE, M. I., PARDOLL, D. M., PAN, F. & LI, B. 2013. The ubiquitin ligase Stub1 negatively modulates regulatory T cell suppressive activity by promoting degradation of the transcription factor Foxp3. *Immunity,* 39**,** 272-85.

CHITSAZZADEH, V., COARFA, C., DRUMMOND, J. A., NGUYEN, T., JOSEPH, A., CHILUKURI, S., CHARPIOT, E., ADELMANN, C. H., CHING, G., NGUYEN, T. N., NICHOLAS, C., THOMAS, V. D., MIGDEN, M., MACFARLANE, D., THOMPSON, E., SHEN, J., TAKATA, Y., MCNIECE, K., POLANSKY, M. A., ABBAS, H. A., RAJAPAKSHE, K., GOWER, A., SPIRA, A., COVINGTON, K. R., XIAO, W., GUNARATNE, P., PICKERING, C., FREDERICK, M., MYERS, J. N., SHEN, L., YAO, H., SU, X., RAPINI, R. P., WHEELER, D. A., HAWK, E. T., FLORES, E. R. & TSAI, K. Y. 2016. Cross-species identification of genomic drivers of squamous cell carcinoma development across preneoplastic intermediates. *Nat Commun,* 7**,** 12601.

CHOA, R., RAYATT, S. & MAHTANI, K. 2015. Marjolin's ulcer. *BMJ,* 351**,** h3997.

CHOI, B. K., BAE, J. S., CHOI, E. M., KANG, W. J., SAKAGUCHI, S., VINAY, D. S. & KWON, B. S. 2004. 4-1BB-dependent inhibition of immunosuppression by activated CD4+CD25+ T cells. *J Leukoc Biol,* 75**,** 785-91.

CHREN, M. M., LINOS, E., TORRES, J. S., STUART, S. E., PARVATANENI, R. & BOSCARDIN, W. J. 2013. Tumor recurrence 5 years after treatment of cutaneous basal cell carcinoma and squamous cell carcinoma. *J Invest Dermatol,* 133**,** 1188-96.

CHRISTIAN, J. B., LAPANE, K. L., HUME, A. L., EATON, C. B., WEINSTOCK, M. A. & TRIAL, V. 2008. Association of ACE inhibitors and angiotensin receptor blockers with keratinocyte cancer prevention in the randomized VATTC trial. *J Natl Cancer Inst,* 100**,** 1223-32.

CHU, C. C., ALI, N., KARAGIANNIS, P., DI MEGLIO, P., SKOWERA, A., NAPOLITANO, L., BARINAGA, G., GRYS, K., SHARIF-PAGHALEH, E., KARAGIANNIS, S. N., PEAKMAN, M., LOMBARDI, G. & NESTLE, F. O. 2012. Resident CD141 (BDCA3)+ dendritic cells in human skin produce IL-10 and induce regulatory T cells that suppress skin inflammation. *J Exp Med,* 209**,** 935-45.

CICHON, M. A., SZENTPETERY, Z., CALEY, M. P., PAPADAKIS, E. S., MACKENZIE, I. C., BRENNAN, C. H. & O'TOOLE, E. A. 2014. The receptor tyrosine kinase Axl regulates cell-cell adhesion and stemness in cutaneous squamous cell carcinoma. *Oncogene,* 33**,** 4185-92.

CLARK, R. A., CHONG, B., MIRCHANDANI, N., BRINSTER, N. K., YAMANAKA, K., DOWGIERT, R. K. & KUPPER, T. S. 2006a. The vast majority of CLA+ T cells are resident in normal skin. *J Immunol,* 176**,** 4431-9.

CLARK, R. A., CHONG, B. F., MIRCHANDANI, N., YAMANAKA, K., MURPHY, G. F., DOWGIERT, R. K. & KUPPER, T. S. 2006b. A novel method for the isolation of skin resident T cells from normal and diseased human skin. *J Invest Dermatol,* 126**,** 1059-70.

CLARK, R. A., HUANG, S. J., MURPHY, G. F., MOLLET, I. G., HIJNEN, D., MUTHUKURU, M., SCHANBACHER, C. F., EDWARDS, V., MILLER, D. M., KIM, J. E., LAMBERT, J. & KUPPER, T. S. 2008. Human squamous cell carcinomas evade the immune response by down-regulation of vascular E-selectin and recruitment of regulatory T cells. *J Exp Med,* 205**,** 2221-34.

CLARK, R. A. & KUPPER, T. S. 2007. IL-15 and dermal fibroblasts induce proliferation of natural regulatory T cells isolated from human skin. *Blood,* 109**,** 194-202.

CLAYMAN, G. L., LEE, J. J., HOLSINGER, F. C., ZHOU, X., DUVIC, M., EL-NAGGAR, A. K., PRIETO, V. G., ALTAMIRANO, E., TUCKER, S. L., STROM, S. S., KRIPKE, M. L. & LIPPMAN, S. M. 2005. Mortality risk from squamous cell skin cancer. *J Clin Oncol,* 23**,** 759-65.

CLAYTON, A., MITCHELL, J. P., COURT, J., MASON, M. D. & TABI, Z. 2007. Human tumor-derived exosomes selectively impair lymphocyte responses to interleukin-2. *Cancer Res,* 67**,** 7458-66.

CLINICALTRIALS.GOV. 2016a. *NCT02760498. Study of Pembrolizumab as first line therapy in patients with unresectable squamous cell carcinoma of the skin (CARSKIN).* [Online]. Available: https://www.clinicaltrials.gov/ct2/show/NCT02883556?term=NCT02883556&rank=1 [Accessed 1/10/2016].

CLINICALTRIALS.GOV. 2016b. *NCT02760498. Study of REGN2810 in patients with advanced cutaneous squamous cell carcinoma.* [Online]. Available: https://www.clinicaltrials.gov/ct2/show/NCT02760498?term=NCT02760498&rank=1 [Accessed 1/10/2016].

COHNEN, A., CHIANG, S. C., STOJANOVIC, A., SCHMIDT, H., CLAUS, M., SAFTIG, P., JANSSEN, O., CERWENKA, A., BRYCESON, Y. T. & WATZL, C. 2013. Surface CD107a/LAMP-1 protects natural killer cells from degranulation-associated damage. *Blood,* 122**,** 1411-8.

COLEY, W. B. 1891. II. Contribution to the knowledge of sarcoma. *Ann Surg,* 14**,** 199-220.

COLLISON, L. W., WORKMAN, C. J., KUO, T. T., BOYD, K., WANG, Y., VIGNALI, K. M., CROSS, R., SEHY, D., BLUMBERG, R. S. & VIGNALI, D. A. 2007. The inhibitory cytokine IL-35 contributes to regulatory T-cell function. *Nature,* 450**,** 566-9.

COMMANDEUR, S., DE GRUIJL, F. R., WILLEMZE, R., TENSEN, C. P. & EL GHALBZOURI, A. 2009. An in vitro three-dimensional model of primary human cutaneous squamous cell carcinoma. *Exp Dermatol,* 18**,** 849-56.

COMMANDEUR, S., HO, S. H., DE GRUIJL, F. R., WILLEMZE, R., TENSEN, C. P. & EL GHALBZOURI, A. 2011. Functional characterization of cancer-associated fibroblasts of human cutaneous squamous cell carcinoma. *Exp Dermatol,* 20**,** 737-42.

COOMBES, J. L., SIDDIQUI, K. R., ARANCIBIA-CARCAMO, C. V., HALL, J., SUN, C. M., BELKAID, Y. & POWRIE, F. 2007. A functionally specialized population of mucosal CD103+ DCs induces Foxp3+ regulatory T cells via a TGF-beta and retinoic acid-dependent mechanism. *J Exp Med,* 204**,** 1757-64.

COOPER, H. L., COOK, I. S., THEAKER, J. M., MALLIPEDDI, R., MCGRATH, J., FRIEDMANN, P. & HEALY, E. 2004. Expression and glycosylation of MUC1 in epidermolysis bullosa-associated and sporadic cutaneous squamous cell carcinomas. *Br J Dermatol,* 151**,** 540-5.

CRABBE, L., JAUCH, A., NAEGER, C. M., HOLTGREVE-GREZ, H. & KARLSEDER, J. 2007. Telomere dysfunction as a cause of genomic instability in Werner syndrome. *Proc Natl Acad Sci U S A,* 104**,** 2205-10.

CRISCIONE, V. D., WEINSTOCK, M. A., NAYLOR, M. F., LUQUE, C., EIDE, M. J., BINGHAM, S. F. & DEPARTMENT OF VETERAN AFFAIRS TOPICAL TRETINOIN CHEMOPREVENTION TRIAL, G. 2009. Actinic keratoses: Natural history and risk of malignant transformation in the Veterans Affairs Topical Tretinoin Chemoprevention Trial. *Cancer,* 115**,** 2523-30.

CURIEL, T. J., COUKOS, G., ZOU, L., ALVAREZ, X., CHENG, P., MOTTRAM, P., EVDEMON-HOGAN, M., CONEJO-GARCIA, J. R., ZHANG, L., BUROW, M., ZHU, Y., WEI, S., KRYCZEK, I., DANIEL, B., GORDON, A., MYERS, L., LACKNER, A., DISIS, M. L., KNUTSON, K. L., CHEN, L. & ZOU, W. 2004. Specific recruitment of regulatory T cells in ovarian carcinoma fosters immune privilege and predicts reduced survival. *Nat Med,* 10**,** 942-9.

CUROTTO DE LAFAILLE, M. A. & LAFAILLE, J. J. 2009. Natural and adaptive foxp3+ regulatory T cells: more of the same or a division of labor? *Immunity,* 30**,** 626-35.

CURRAN, M. A., GEIGER, T. L., MONTALVO, W., KIM, M., REINER, S. L., AL-SHAMKHANI, A., SUN, J. C. & ALLISON, J. P. 2013. Systemic 4-1BB activation induces a novel T cell phenotype driven by high expression of Eomesodermin. *J Exp Med,* 210**,** 743-55.

CURRAN, M. A., KIM, M., MONTALVO, W., AL-SHAMKHANI, A. & ALLISON, J. P. 2011. Combination CTLA-4 blockade and 4-1BB activation enhances tumor rejection by increasing T-cell infiltration, proliferation, and cytokine production. *PLoS One,* 6**,** e19499.

CURTI, B. D., KOVACSOVICS-BANKOWSKI, M., MORRIS, N., WALKER, E., CHISHOLM, L., FLOYD, K., WALKER, J., GONZALEZ, I., MEEUWSEN, T., FOX, B. A., MOUDGIL, T., MILLER, W., HALEY, D., COFFEY, T., FISHER, B., DELANTY-MILLER, L., RYMARCHYK, N., KELLY, T., CROCENZI, T., BERNSTEIN, E., SANBORN, R., URBA, W. J. & WEINBERG, A. D. 2013. OX40 is a potent immune-stimulating target in late-stage cancer patients. *Cancer Res,* 73**,** 7189-98.

CZARNECKI, D., MEEHAN, C. J., BRUCE, F. & CULJAK, G. 2002. The majority of cutaneous squamous cell carcinomas arise in actinic keratoses. *J Cutan Med Surg,* 6**,** 207-9.

DAHAN, R., SEGA, E., ENGELHARDT, J., SELBY, M., KORMAN, A. J. & RAVETCH, J. V. 2015. FcgammaRs Modulate the Anti-tumor Activity of Antibodies Targeting the PD-1/PD-L1 Axis. *Cancer Cell,* 28**,** 285-95.

DAJEE, M., LAZAROV, M., ZHANG, J. Y., CAI, T., GREEN, C. L., RUSSELL, A. J., MARINKOVICH, M. P., TAO, S., LIN, Q., KUBO, Y. & KHAVARI, P. A. 2003. NF-kappaB blockade and oncogenic Ras trigger invasive human epidermal neoplasia. *Nature,* 421**,** 639-43.

DANIEL, D., MEYER-MORSE, N., BERGSLAND, E. K., DEHNE, K., COUSSENS, L. M. & HANAHAN, D. 2003. Immune enhancement of skin carcinogenesis by CD4+ T cells. *J Exp Med,* 197**,** 1017-28.

DARWICHE, N., RYSCAVAGE, A., PEREZ-LORENZO, R., WRIGHT, L., BAE, D. S., HENNINGS, H., YUSPA, S. H. & GLICK, A. B. 2007. Expression profile of skin papillomas with high cancer risk displays a unique genetic signature that clusters with squamous cell carcinomas and predicts risk for malignant conversion. *Oncogene,* 26**,** 6885-95.

DE BERKER, D., IBBOTSON, S., SIMPSON, N. B., MATTHEWS, J. N., IDLE, J. R. & REES, J. L. 1995. Reduced experimental contact sensitivity in squamous cell but not basal cell carcinomas of skin. *Lancet,* 345**,** 425-6.

DE HERTOG, S. A., WENSVEEN, C. A., BASTIAENS, M. T., KIELICH, C. J., BERKHOUT, M. J., WESTENDORP, R. G., VERMEER, B. J., BOUWES BAVINCK, J. N. & LEIDEN SKIN CANCER, S. 2001. Relation between smoking and skin cancer. *J Clin Oncol,* 19**,** 231-8.

DE MONTE, L., RENI, M., TASSI, E., CLAVENNA, D., PAPA, I., RECALDE, H., BRAGA, M., DI CARLO, V., DOGLIONI, C. & PROTTI, M. P. 2011. Intratumor T helper type 2 cell infiltrate correlates with cancer-associated fibroblast thymic stromal lymphopoietin production and reduced survival in pancreatic cancer. *J Exp Med,* 208**,** 469-78.

DE VISSER, K. E., KORETS, L. V. & COUSSENS, L. M. 2005. De novo carcinogenesis promoted by chronic inflammation is B lymphocyte dependent. *Cancer Cell,* 7**,** 411-23.

DEAGLIO, S., DWYER, K. M., GAO, W., FRIEDMAN, D., USHEVA, A., ERAT, A., CHEN, J. F., ENJYOJI, K., LINDEN, J., OUKKA, M., KUCHROO, V. K., STROM, T. B. & ROBSON, S. C. 2007. Adenosine generation catalyzed by CD39 and CD73 expressed on regulatory T cells mediates immune suppression. *J Exp Med,* 204**,** 1257-65.

DEBES, G. F., ARNOLD, C. N., YOUNG, A. J., KRAUTWALD, S., LIPP, M., HAY, J. B. & BUTCHER, E. C. 2005. Chemokine receptor CCR7 required for T lymphocyte exit from peripheral tissues. *Nat Immunol,* 6**,** 889-94.

DELEEUW, R. J., KOST, S. E., KAKAL, J. A. & NELSON, B. H. 2012. The prognostic value of FoxP3+ tumor-infiltrating lymphocytes in cancer: a critical review of the literature. *Clin Cancer Res,* 18**,** 3022-9.

DELGOFFE, G. M., WOO, S. R., TURNIS, M. E., GRAVANO, D. M., GUY, C., OVERACRE, A. E., BETTINI, M. L., VOGEL, P., FINKELSTEIN, D., BONNEVIER, J., WORKMAN, C. J. & VIGNALI, D. A. 2013. Stability and function of regulatory T cells is maintained by a neuropilin-1-semaphorin-4a axis. *Nature,* 501**,** 252-6.

DEMEHRI, S., CUNNINGHAM, T. J., HURST, E. A., SCHAFFER, A., SHEINBEIN, D. M. & YOKOYAMA, W. M. 2014. Chronic allergic contact dermatitis promotes skin cancer. *J Clin Invest,* 124**,** 5037-41.

DENG, L., ZHANG, H., LUAN, Y., ZHANG, J., XING, Q., DONG, S., WU, X., LIU, M. & WANG, S. 2010. Accumulation of Foxp3+ T regulatory cells in draining lymph nodes correlates with disease progression and immune suppression in colorectal cancer patients. *Clin Cancer Res,* 16**,** 4105-12.

DERRE, L., RIVALS, J. P., JANDUS, C., PASTOR, S., RIMOLDI, D., ROMERO, P., MICHIELIN, O., OLIVE, D. & SPEISER, D. E. 2010. BTLA mediates inhibition of human tumor-specific CD8+ T cells that can be partially reversed by vaccination. *J Clin Invest,* 120**,** 157-67.

DI MEGLIO, P., PERERA, G. K. & NESTLE, F. O. 2011. The multitasking organ: recent insights into skin immune function. *Immunity,* 35**,** 857-69.

DIFFEY, B. L. & LANGTRY, J. A. 2005. Skin cancer incidence and the ageing population. *Br J Dermatol,* 153**,** 679-80.

DIMON, M. T., WOOD, H. M., RABBITTS, P. H., LIAO, W., CHO, R. J. & ARRON, S. T. 2014. No evidence for integrated viral DNA in the genome sequence of cutaneous squamous cell carcinoma. *J Invest Dermatol,* 134**,** 2055-7.

DONG, H., STROME, S. E., SALOMAO, D. R., TAMURA, H., HIRANO, F., FLIES, D. B., ROCHE, P. C., LU, J., ZHU, G., TAMADA, K., LENNON, V. A., CELIS, E. & CHEN, L. 2002. Tumor-associated B7-H1 promotes T-cell apoptosis: a potential mechanism of immune evasion. *Nat Med,* 8**,** 793-800.

DOTTO, G. P. 2014. Multifocal epithelial tumors and field cancerization: stroma as a primary determinant. *J Clin Invest,* 124**,** 1446-53.

DURAISWAMY, J., FREEMAN, G. J. & COUKOS, G. 2013. Therapeutic PD-1 pathway blockade augments with other modalities of immunotherapy T-cell function to prevent immune decline in ovarian cancer. *Cancer Res,* 73**,** 6900-12.

DURAISWAMY, J., IBEGBU, C. C., MASOPUST, D., MILLER, J. D., ARAKI, K., DOHO, G. H., TATA, P., GUPTA, S., ZILLIOX, M. J., NAKAYA, H. I., PULENDRAN, B., HAINING, W. N., FREEMAN, G. J. & AHMED, R. 2011. Phenotype, function, and gene expression profiles of programmed death-1(hi) CD8 T cells in healthy human adults. *J Immunol,* 186**,** 4200-12.

DURINCK, S., HO, C., WANG, N. J., LIAO, W., JAKKULA, L. R., COLLISSON, E. A., PONS, J., CHAN, S. W., LAM, E. T., CHU, C., PARK, K., HONG, S. W., HUR, J. S., HUH, N., NEUHAUS, I. M., YU, S. S., GREKIN, R. C., MAURO, T. M., CLEAVER, J. E., KWOK, P. Y., LEBOIT, P. E., GETZ, G., CIBULSKIS, K., ASTER, J. C., HUANG, H., PURDOM, E., LI, J., BOLUND, L., ARRON, S. T., GRAY, J. W., SPELLMAN, P. T. & CHO, R. J. 2011. Temporal dissection of tumorigenesis in primary cancers. *Cancer Discov,* 1**,** 137-43.

DUSTIN, M. L. & DEPOIL, D. 2011. New insights into the T cell synapse from single molecule techniques. *Nat Rev Immunol,* 11**,** 672-84.

DZIUNYCZ, P., IOTZOVA-WEISS, G., ELORANTA, J. J., LAUCHLI, S., HAFNER, J., FRENCH, L. E. & HOFBAUER, G. F. 2010. Squamous cell carcinoma of the skin shows a distinct microRNA profile modulated by UV radiation. *J Invest Dermatol,* 130**,** 2686-9.

EGAWA, G. & KABASHIMA, K. 2011. Skin as a peripheral lymphoid organ: revisiting the concept of skin-associated lymphoid tissues. *J Invest Dermatol,* 131**,** 2178-85.

ELLIS, N. A., GRODEN, J., YE, T. Z., STRAUGHEN, J., LENNON, D. J., CIOCCI, S., PROYTCHEVA, M. & GERMAN, J. 1995. The Bloom's syndrome gene product is homologous to RecQ helicases. *Cell,* 83**,** 655-66.

ELPEK, K. G., YOLCU, E. S., FRANKE, D. D., LACELLE, C., SCHABOWSKY, R. H. & SHIRWAN, H. 2007. Ex vivo expansion of CD4+CD25+FoxP3+ T regulatory cells based on synergy between IL-2 and 4-1BB signaling. *J Immunol,* 179**,** 7295-304.

ENGLISH, D. R., ARMSTRONG, B. K., KRICKER, A., WINTER, M. G., HEENAN, P. J. & RANDELL, P. L. 1998. Demographic characteristics, pigmentary and cutaneous risk factors for squamous cell carcinoma of the skin: a case-control study. *Int J Cancer,* 76**,** 628-34.

EUVRARD, S., KANITAKIS, J. & CLAUDY, A. 2003. Skin cancers after organ transplantation. *N Engl J Med,* 348**,** 1681-91.

FACCIABENE, A., PENG, X., HAGEMANN, I. S., BALINT, K., BARCHETTI, A., WANG, L. P., GIMOTTY, P. A., GILKS, C. B., LAL, P., ZHANG, L. & COUKOS, G. 2011. Tumour hypoxia promotes tolerance and angiogenesis via CCL28 and T(reg) cells. *Nature,* 475**,** 226-30.

FALLARINO, F., GROHMANN, U., HWANG, K. W., ORABONA, C., VACCA, C., BIANCHI, R., BELLADONNA, M. L., FIORETTI, M. C., ALEGRE, M. L. & PUCCETTI, P. 2003. Modulation of tryptophan catabolism by regulatory T cells. *Nat Immunol,* 4**,** 1206-12.

FARSHCHIAN, M., NISSINEN, L., SILJAMAKI, E., RIIHILA, P., TORISEVA, M., KIVISAARI, A., ALA-AHO, R., KALLAJOKI, M., VERAJANKORVA, E., HONKANEN, H. K., HELJASVAARA, R., PIHLAJANIEMI, T., GRENMAN, R., PELTONEN, J., PELTONEN, S. & KAHARI, V. M. 2015. EphB2 promotes progression of cutaneous squamous cell carcinoma. *J Invest Dermatol,* 135**,** 1882-92.

FELDMEYER, L., CHING, G., VIN, H., MA, W., BANSAL, V., CHITSAZZADEH, V., JAHAN-TIGH, R., CHU, E. Y., FULLER, P., MAITI, S., DAVIS, R. E., COOPER, L. J. & TSAI, K. Y. 2016. Differential T-cell subset representation in cutaneous squamous cell carcinoma arising in immunosuppressed versus immunocompetent individuals. *Exp Dermatol,* 25**,** 245-7.

FINDLAY, G. M. 1928. Ultraviolet light and skin cancer. *Lancet,* 212**,** 1070-1073.

FITZHUGH, D. J., NAIK, S., CAUGHMAN, S. W. & HWANG, S. T. 2000. Cutting edge: C-C chemokine receptor 6 is essential for arrest of a subset of memory T cells on activated dermal microvascular endothelial cells under physiologic flow conditions in vitro. *J Immunol,* 165**,** 6677-81.

FOURCADE, J., SUN, Z., BENALLAOUA, M., GUILLAUME, P., LUESCHER, I. F., SANDER, C., KIRKWOOD, J. M., KUCHROO, V. & ZAROUR, H. M. 2010. Upregulation of Tim-3 and PD-1 expression is associated with tumor antigen-specific CD8+ T cell dysfunction in melanoma patients. *J Exp Med,* 207**,** 2175-86.

FOURCADE, J., SUN, Z., PAGLIANO, O., CHAUVIN, J. M., SANDER, C., JANJIC, B., TARHINI, A. A., TAWBI, H. A., KIRKWOOD, J. M., MOSCHOS, S., WANG, H., GUILLAUME, P., LUESCHER, I. F., KRIEG, A., ANDERSON, A. C., KUCHROO, V. K. & ZAROUR, H. M. 2014. PD-1 and Tim-3 regulate the expansion of tumor

antigen-specific CD8(+) T cells induced by melanoma vaccines. *Cancer Res,* 74**,** 1045-55.

FOURCADE, J., SUN, Z., PAGLIANO, O., GUILLAUME, P., LUESCHER, I. F., SANDER, C., KIRKWOOD, J. M., OLIVE, D., KUCHROO, V. & ZAROUR, H. M. 2012. CD8(+) T cells specific for tumor antigens can be rendered dysfunctional by the tumor microenvironment through upregulation of the inhibitory receptors BTLA and PD-1. *Cancer Res,* 72**,** 887-96.

FRANCISCO, L. M., SALINAS, V. H., BROWN, K. E., VANGURI, V. K., FREEMAN, G. J., KUCHROO, V. K. & SHARPE, A. H. 2009. PD-L1 regulates the development, maintenance, and function of induced regulatory T cells. *J Exp Med,* 206**,** 3015-29.

FRANSEN, M., KARAHALIOS, A., SHARMA, N., ENGLISH, D. R., GILES, G. G. & SINCLAIR, R. D. 2012. Non-melanoma skin cancer in Australia. *Med J Aust,* 197**,** 565-8.

FREEMAN, A., BRIDGE, J. A., MARUTHAYANAR, P., OVERGAARD, N. H., JUNG, J. W., SIMPSON, F., PROW, T. W., SOYER, H. P., FRAZER, I. H., FREEMAN, M. & WELLS, J. W. 2014. Comparative immune phenotypic analysis of cutaneous squamous cell carcinoma and intraepidermal carcinoma in immune-competent individuals: proportional representation of CD8+ T-cells but not FoxP3+ regulatory T-cells is associated with disease stage. *PLoS One,* 9**,** e110928.

FRIDMAN, W. H., PAGES, F., SAUTES-FRIDMAN, C. & GALON, J. 2012. The immune contexture in human tumours: impact on clinical outcome. *Nat Rev Cancer,* 12**,** 298-306.

FUHLBRIGGE, R. C., KIEFFER, J. D., ARMERDING, D. & KUPPER, T. S. 1997. Cutaneous lymphocyte antigen is a specialized form of PSGL-1 expressed on skin-homing T cells. *Nature,* 389**,** 978-81.

FUJITA, H., SUAREZ-FARINAS, M., MITSUI, H., GONZALEZ, J., BLUTH, M. J., ZHANG, S., FELSEN, D., KRUEGER, J. G. & CARUCCI, J. A. 2012. Langerhans cells from human cutaneous squamous cell carcinoma induce strong type 1 immunity. *J Invest Dermatol,* 132**,** 1645-55.

FURUDATE, S., FUJIMURA, T., KAMBAYASHI, Y., HAGA, T., HASHIMOTO, A. & AIBA, S. 2014. Immunosuppressive and cytotoxic cells in invasive vs. non-invasive Bowen's disease. *Acta Derm Venereol,* 94**,** 337-9.

GADDAMEEDHI, S., SELBY, C. P., KAUFMANN, W. K., SMART, R. C. & SANCAR, A. 2011. Control of skin cancer by the circadian rhythm. *Proc Natl Acad Sci U S A,* 108**,** 18790-5.

GAIDE, O., EMERSON, R. O., JIANG, X., GULATI, N., NIZZA, S., DESMARAIS, C., ROBINS, H., KRUEGER, J. G., CLARK, R. A. & KUPPER, T. S. 2015. Common clonal origin of central and resident memory T cells following skin immunization. *Nat Med,* 21**,** 647-53.

GALON, J., COSTES, A., SANCHEZ-CABO, F., KIRILOVSKY, A., MLECNIK, B., LAGORCE-PAGES, C., TOSOLINI, M., CAMUS, M., BERGER, A., WIND, P., ZINZINDOHOUE, F., BRUNEVAL, P., CUGNENC, P. H., TRAJANOSKI, Z., FRIDMAN, W. H. & PAGES, F. 2006. Type, density, and location of immune cells within human colorectal tumors predict clinical outcome. *Science,* 313**,** 1960-4.

GEBHARDT, T., WAKIM, L. M., EIDSMO, L., READING, P. C., HEATH, W. R. & CARBONE, F. R. 2009. Memory T cells in nonlymphoid tissue that provide enhanced local immunity during infection with herpes simplex virus. *Nat Immunol,* 10**,** 524-30.

GEBHARDT, T., WHITNEY, P. G., ZAID, A., MACKAY, L. K., BROOKS, A. G., HEATH, W. R., CARBONE, F. R. & MUELLER, S. N. 2011. Different patterns of peripheral migration by memory CD4+ and CD8+ T cells. *Nature,* 477**,** 216-9.

GEHAD, A. E., LICHTMAN, M. K., SCHMULTS, C. D., TEAGUE, J. E., CALARESE, A. W., JIANG, Y., WATANABE, R. & CLARK, R. A. 2012. Nitric oxide-producing myeloid-derived suppressor cells inhibit vascular E-selectin expression in human squamous cell carcinomas. *J Invest Dermatol,* 132**,** 2642-51.

GELB, A. B., SMOLLER, B. R., WARNKE, R. A. & PICKER, L. J. 1993. Lymphocytes infiltrating primary cutaneous neoplasms selectively express the cutaneous lymphocyte-associated antigen (CLA). *Am J Pathol,* 142**,** 1556-64.

GIORDANO, M., RONCAGALLI, R., BOURDELY, P., CHASSON, L., BUFERNE, M., YAMASAKI, S., BEYAERT, R., VAN LOO, G., AUPHAN-ANEZIN, N., SCHMITT-VERHULST, A. M. & VERDEIL, G. 2014. The tumor necrosis factor alpha-induced protein 3 (TNFAIP3, A20) imposes a brake on antitumor activity of CD8 T cells. *Proc Natl Acad Sci U S A,* 111**,** 11115-20.

GIRARDI, M., OPPENHEIM, D. E., STEELE, C. R., LEWIS, J. M., GLUSAC, E., FILLER, R., HOBBY, P., SUTTON, B., TIGELAAR, R. E. & HAYDAY, A. C. 2001. Regulation of cutaneous malignancy by gammadelta T cells. *Science,* 294**,** 605-9.

GOBERT, M., TREILLEUX, I., BENDRISS-VERMARE, N., BACHELOT, T., GODDARD-LEON, S., ARFI, V., BIOTA, C., DOFFIN, A. C., DURAND, I., OLIVE, D., PEREZ, S., PASQUAL, N., FAURE, C., RAY-COQUARD, I., PUISIEUX, A., CAUX, C., BLAY, J. Y. & MENETRIER-CAUX, C. 2009. Regulatory T cells recruited through CCL22/CCR4 are selectively activated in lymphoid infiltrates surrounding primary breast tumors and lead to an adverse clinical outcome. *Cancer Res,* 69**,** 2000-9.

GOLDIE, S. J., MULDER, K. W., TAN, D. W., LYONS, S. K., SIMS, A. H. & WATT, F. M. 2012. FRMD4A upregulation in human squamous cell carcinoma promotes tumor growth and metastasis and is associated with poor prognosis. *Cancer Res,* 72**,** 3424-36.

GOON, P. K., GREENBERG, D. C., IGALI, L. & LEVELL, N. J. 2015. Squamous cell carcinoma of the skin has more than doubled over the last decade in the UK. *Acta Derm Venereol,* DOI 10.2340/00015555-2310. Epub ahead of print.

GOTTSCHALK, R. A., CORSE, E. & ALLISON, J. P. 2012. Expression of Helios in peripherally induced Foxp3+ regulatory T cells. *J Immunol,* 188**,** 976-80.

GOUDIE, D. R., D'ALESSANDRO, M., MERRIMAN, B., LEE, H., SZEVERENYI, I., AVERY, S., O'CONNOR, B. D., NELSON, S. F., COATS, S. E., STEWART, A., CHRISTIE, L., PICHERT, G., FRIEDEL, J., HAYES, I., BURROWS, N., WHITTAKER, S., GERDES, A. M., BROESBY-OLSEN, S., FERGUSON-SMITH, M. A., VERMA, C., LUNNY, D. P., REVERSADE, B. & LANE, E. B. 2011. Multiple self-healing squamous epithelioma is caused by a disease-specific spectrum of mutations in TGFBR1. *Nat Genet,* 43**,** 365-9.

GRABBE, S., BRUVERS, S., GALLO, R. L., KNISELY, T. L., NAZARENO, R. & GRANSTEIN, R. D. 1991. Tumor antigen presentation by murine epidermal cells. *J Immunol,* 146**,** 3656-61.

GRATZ, I. K., TRUONG, H. A., YANG, S. H., MAURANO, M. M., LEE, K., ABBAS, A. K. & ROSENBLUM, M. D. 2013. Cutting Edge: memory regulatory t cells require IL-7 and not IL-2 for their maintenance in peripheral tissues. *J Immunol,* 190**,** 4483-7.

GRAY, S. E., KAY, E., LEADER, M. & MABRUK, M. 2006. Analysis of p16 expression and allelic imbalance / loss of heterozygosity of 9p21 in cutaneous squamous cell carcinomas. *J Cell Mol Med,* 10**,** 778-88.

GREEN, A., WILLIAMS, G., NEALE, R., HART, V., LESLIE, D., PARSONS, P., MARKS, G. C., GAFFNEY, P., BATTISTUTTA, D., FROST, C., LANG, C. & RUSSELL, A. 1999. Daily sunscreen application and betacarotene supplementation in prevention of basal-cell and squamous-cell carcinomas of the skin: a randomised controlled trial. *Lancet,* 354**,** 723-9.

GREENE, M. I., SY, M. S., KRIPKE, M. & BENACERRAF, B. 1979. Impairment of antigen-presenting cell function by ultraviolet radiation. *Proc Natl Acad Sci U S A,* 76**,** 6591-5.

GRIFFITHS, S. J., RIDDELL, N. E., MASTERS, J., LIBRI, V., HENSON, S. M., WERTHEIMER, A., WALLACE, D., SIMS, S., RIVINO, L., LARBI, A., KEMENY, D. M., NIKOLICH-ZUGICH, J., KERN, F., KLENERMAN, P., EMERY, V. C. & AKBAR, A. N. 2013. Age-associated increase of low-avidity cytomegalovirus-specific CD8+ T cells that re-express CD45RA. *J Immunol,* 190**,** 5363-72.

GRIMBALDESTON, M. A., SKOV, L., BAADSGAARD, O., SKOV, B. G., MARSHMAN, G., FINLAY-JONES, J. J. & HART, P. H. 2000. Communications: high dermal mast cell prevalence is a predisposing factor for basal cell carcinoma in humans. *J Invest Dermatol,* 115**,** 317-20.

GRIMBALDESTON, M. A., SKOV, L., FINLAY-JONES, J. J. & HART, P. H. 2002. Squamous cell carcinoma is not associated with high dermal mast cell prevalence in humans. *J Invest Dermatol,* 119**,** 1204-6.

GRIVENNIKOV, S. I., GRETEN, F. R. & KARIN, M. 2010. Immunity, inflammation, and cancer. *Cell,* 140**,** 883-99.

GROS, A., ROBBINS, P. F., YAO, X., LI, Y. F., TURCOTTE, S., TRAN, E., WUNDERLICH, J. R., MIXON, A., FARID, S., DUDLEY, M. E., HANADA, K., ALMEIDA, J. R., DARKO, S., DOUEK, D. C., YANG, J. C. & ROSENBERG, S. A. 2014. PD-1 identifies the patient-specific CD8(+) tumor-reactive repertoire infiltrating human tumors. *J Clin Invest,* 124**,** 2246-59.

GROSSMAN, W. J., VERBSKY, J. W., BARCHET, W., COLONNA, M., ATKINSON, J. P. & LEY, T. J. 2004. Human T regulatory cells can use the perforin pathway to cause autologous target cell death. *Immunity,* 21**,** 589-601.

GUBIN, M. M., ZHANG, X., SCHUSTER, H., CARON, E., WARD, J. P., NOGUCHI, T., IVANOVA, Y., HUNDAL, J., ARTHUR, C. D., KREBBER, W. J., MULDER, G. E., TOEBES, M., VESELY, M. D., LAM, S. S., KORMAN, A. J., ALLISON, J. P., FREEMAN, G. J., SHARPE, A. H., PEARCE, E. L., SCHUMACHER, T. N., AEBERSOLD, R., RAMMENSEE, H. G., MELIEF, C. J., MARDIS, E. R., GILLANDERS, W. E., ARTYOMOV, M. N. & SCHREIBER, R. D. 2014.

Checkpoint blockade cancer immunotherapy targets tumour-specific mutant antigens. *Nature,* 515**,** 577-81.

GUINEA-VINIEGRA, J., ZENZ, R., SCHEUCH, H., JIMENEZ, M., BAKIRI, L., PETZELBAUER, P. & WAGNER, E. F. 2012. Differentiation-induced skin cancer suppression by FOS, p53, and TACE/ADAM17. *J Clin Invest,* 122**,** 2898-910.

GUNDESTRUP, M. & STORM, H. H. 1999. Radiation-induced acute myeloid leukaemia and other cancers in commercial jet cockpit crew: a population-based cohort study. *Lancet,* 354**,** 2029-31.

GUPTA, P. K., GODEC, J., WOLSKI, D., ADLAND, E., YATES, K., PAUKEN, K. E., COSGROVE, C., LEDDEROSE, C., JUNGER, W. G., ROBSON, S. C., WHERRY, E. J., ALTER, G., GOULDER, P. J., KLENERMAN, P., SHARPE, A. H., LAUER, G. M. & HAINING, W. N. 2015. CD39 expression identifies terminally exhausted CD8+ T Cells. *PLoS Pathog,* 11**,** e1005177.

HADDADEEN, C., LAI, C., CHO, S. Y. & HEALY, E. 2015. Variants of the melanocortin-1 receptor: do they matter clinically? *Exp Dermatol,* 24**,** 5-9.

HAIDER, A. S., PETERS, S. B., KAPORIS, H., CARDINALE, I., FEI, J., OTT, J., BLUMENBERG, M., BOWCOCK, A. M., KRUEGER, J. G. & CARUCCI, J. A. 2006. Genomic analysis defines a cancer-specific gene expression signature for human squamous cell carcinoma and distinguishes malignant hyperproliferation from benign hyperplasia. *J Invest Dermatol,* 126**,** 869-81.

HAMANISHI, J., MANDAI, M., IWASAKI, M., OKAZAKI, T., TANAKA, Y., YAMAGUCHI, K., HIGUCHI, T., YAGI, H., TAKAKURA, K., MINATO, N., HONJO, T. & FUJII, S. 2007. Programmed cell death 1 ligand 1 and tumor-infiltrating CD8+ T lymphocytes are prognostic factors of human ovarian cancer. *Proc Natl Acad Sci U S A,* 104**,** 3360-5.

HAMID, O., ROBERT, C., DAUD, A., HODI, F. S., HWU, W. J., KEFFORD, R., WOLCHOK, J. D., HERSEY, P., JOSEPH, R. W., WEBER, J. S., DRONCA, R., GANGADHAR, T. C., PATNAIK, A., ZAROUR, H., JOSHUA, A. M., GERGICH, K., ELASSAISS-SCHAAP, J., ALGAZI, A., MATEUS, C., BOASBERG, P., TUMEH, P. C., CHMIELOWSKI, B., EBBINGHAUS, S. W., LI, X. N., KANG, S. P. & RIBAS, A. 2013. Safety and tumor responses with lambrolizumab (anti-PD-1) in melanoma. *N Engl J Med,* 369**,** 134-44.

HAN, J., QURESHI, A. A., NAN, H., ZHANG, J., SONG, Y., GUO, Q. & HUNTER, D. J. 2011. A germline variant in the interferon regulatory factor 4 gene as a novel skin cancer risk locus. *Cancer Res,* 71**,** 1533-9.

HANAHAN, D. & WEINBERG, R. A. 2011. Hallmarks of cancer: the next generation. *Cell,* 144**,** 646-74.

HANIFFA, M., SHIN, A., BIGLEY, V., MCGOVERN, N., TEO, P., SEE, P., WASAN, P. S., WANG, X. N., MALINARICH, F., MALLERET, B., LARBI, A., TAN, P., ZHAO, H., POIDINGER, M., PAGAN, S., COOKSON, S., DICKINSON, R., DIMMICK, I., JARRETT, R. F., RENIA, L., TAM, J., SONG, C., CONNOLLY, J., CHAN, J. K., GEHRING, A., BERTOLETTI, A., COLLIN, M. & GINHOUX, F. 2012. Human tissues contain CD141hi cross-presenting dendritic cells with functional homology to mouse CD103+ nonlymphoid dendritic cells. *Immunity,* 37**,** 60-73.

HANKS, B. A., HOLTZHAUSEN, A., EVANS, K. S., JAMIESON, R., GIMPEL, P., CAMPBELL, O. M., HECTOR-GREENE, M., SUN, L., TEWARI, A., GEORGE, A., STARR, M., NIXON, A., AUGUSTINE, C., BEASLEY, G., TYLER, D. S., OSADA, T., MORSE, M. A., LING, L., LYERLY, H. K. & BLOBE, G. C. 2013. Type III TGF-beta receptor downregulation generates an immunotolerant tumor microenvironment. *J Clin Invest,* 123**,** 3925-40.

HARIBHAI, D., WILLIAMS, J. B., JIA, S., NICKERSON, D., SCHMITT, E. G., EDWARDS, B., ZIEGELBAUER, J., YASSAI, M., LI, S. H., RELLAND, L. M., WISE, P. M., CHEN, A., ZHENG, Y. Q., SIMPSON, P. M., GORSKI, J., SALZMAN, N. H., HESSNER, M. J., CHATILA, T. A. & WILLIAMS, C. B. 2011. A requisite role for induced regulatory T cells in tolerance based on expanding antigen receptor diversity. *Immunity,* 35**,** 109-22.

HART, R. W., SETLOW, R. B. & WOODHEAD, A. D. 1977. Evidence that pyrimidine dimers in DNA can give rise to tumors. *Proc Natl Acad Sci U S A,* 74**,** 5574-8.

HARTEVELT, M. M., BAVINCK, J. N., KOOTTE, A. M., VERMEER, B. J. & VANDENBROUCKE, J. P. 1990. Incidence of skin cancer after renal transplantation in The Netherlands. *Transplantation,* 49**,** 506-9.

HATTON, J. L., PARENT, A., TOBER, K. L., HOPPES, T., WULFF, B. C., DUNCAN, F. J., KUSEWITT, D. F., VANBUSKIRK, A. M. & OBERYSZYN, T. M. 2007. Depletion of CD4+ cells exacerbates the cutaneous response to acute and chronic UVB exposure. *J Invest Dermatol,* 127**,** 1507-15.

HAYDAY, A. C. 2009. Gammadelta T cells and the lymphoid stress-surveillance response. *Immunity,* 31**,** 184-96.

HEAL, C. F., RAASCH, B. A., BUETTNER, P. G. & WEEDON, D. 2008. Accuracy of clinical diagnosis of skin lesions. *Br J Dermatol,* 159**,** 661-8.

HEALY, E., BROWN, S. J., LANGAN, S. M., NICHOLLS, S. G., SHAMS, K., REYNOLDS, N. J. & UK, T. 2015. Identification of translational dermatology research priorities in the U.K.: results of an electronic Delphi exercise. *Br J Dermatol,* 173**,** 1191-8.

HEALY, E., FLANNAGAN, N., RAY, A., TODD, C., JACKSON, I. J., MATTHEWS, J. N., BIRCH-MACHIN, M. A. & REES, J. L. 2000. Melanocortin-1-receptor gene and sun sensitivity in individuals without red hair. *Lancet,* 355**,** 1072-3.

HEATH, W. R. & CARBONE, F. R. 2013. The skin-resident and migratory immune system in steady state and memory: innate lymphocytes, dendritic cells and T cells. *Nat Immunol,* 14**,** 978-85.

HERBST, R. S., SORIA, J. C., KOWANETZ, M., FINE, G. D., HAMID, O., GORDON, M. S., SOSMAN, J. A., MCDERMOTT, D. F., POWDERLY, J. D., GETTINGER, S. N., KOHRT, H. E., HORN, L., LAWRENCE, D. P., ROST, S., LEABMAN, M., XIAO, Y., MOKATRIN, A., KOEPPEN, H., HEGDE, P. S., MELLMAN, I., CHEN, D. S. & HODI, F. S. 2014. Predictive correlates of response to the anti-PD-L1 antibody MPDL3280A in cancer patients. *Nature,* 515**,** 563-7.

HINDLEY, J. P., FERREIRA, C., JONES, E., LAUDER, S. N., LADELL, K., WYNN, K. K., BETTS, G. J., SINGH, Y., PRICE, D. A., GODKIN, A. J., DYSON, J. & GALLIMORE, A. 2011. Analysis of the T-cell receptor repertoires of tumor-infiltrating conventional and regulatory T cells reveals no evidence for conversion in carcinogen-induced tumors. *Cancer Res,* 71**,** 736-46.

HINO, R., KABASHIMA, K., KATO, Y., YAGI, H., NAKAMURA, M., HONJO, T., OKAZAKI, T. & TOKURA, Y. 2010. Tumor cell expression of programmed cell death-1 ligand 1 is a prognostic factor for malignant melanoma. *Cancer,* 116**,** 1757-66.

HIRAHARA, K., LIU, L., CLARK, R. A., YAMANAKA, K., FUHLBRIGGE, R. C. & KUPPER, T. S. 2006. The majority of human peripheral blood CD4+CD25highFoxp3+ regulatory T cells bear functional skin-homing receptors. *J Immunol,* 177**,** 4488-94.

HIRAKAWA, S., BROWN, L. F., KODAMA, S., PAAVONEN, K., ALITALO, K. & DETMAR, M. 2007. VEGF-C-induced lymphangiogenesis in sentinel lymph nodes promotes tumor metastasis to distant sites. *Blood,* 109**,** 1010-7.

HIRAOKA, N., ONOZATO, K., KOSUGE, T. & HIROHASHI, S. 2006. Prevalence of FOXP3+ regulatory T cells increases during the progression of pancreatic ductal adenocarcinoma and its premalignant lesions. *Clin Cancer Res,* 12**,** 5423-34.

HODI, F. S., O'DAY, S. J., MCDERMOTT, D. F., WEBER, R. W., SOSMAN, J. A., HAANEN, J. B., GONZALEZ, R., ROBERT, C., SCHADENDORF, D., HASSEL, J. C., AKERLEY, W., VAN DEN EERTWEGH, A. J., LUTZKY, J., LORIGAN, P., VAUBEL, J. M., LINETTE, G. P., HOGG, D., OTTENSMEIER, C. H., LEBBE, C., PESCHEL, C., QUIRT, I., CLARK, J. I., WOLCHOK, J. D., WEBER, J. S., TIAN, J., YELLIN, M. J., NICHOL, G. M., HOOS, A. & URBA, W. J. 2010. Improved survival with ipilimumab in patients with metastatic melanoma. *N Engl J Med,* 363**,** 711-23.

HOLDERFIELD, M., LORENZANA, E., WEISBURD, B., LOMOVASKY, L., BOUSSEMART, L., LACROIX, L., TOMASIC, G., FAVRE, M., VAGNER, S., ROBERT, C., GHODDUSI, M., DANIEL, D., PRYER, N., MCCORMICK, F. & STUART, D. 2014. Vemurafenib cooperates with HPV to promote initiation of cutaneous tumors. *Cancer Res,* 74**,** 2238-45.

HOLICK, M. F. 2008. Deficiency of sunlight and vitamin D. *BMJ,* 336**,** 1318-9.

HOUSMAN, T. S., FELDMAN, S. R., WILLIFORD, P. M., FLEISCHER, A. B., JR., GOLDMAN, N. D., ACOSTAMADIEDO, J. M. & CHEN, G. J. 2003. Skin cancer is among the most costly of all cancers to treat for the Medicare population. *J Am Acad Dermatol,* 48**,** 425-9.

HSIEH, C. S., LEE, H. M. & LIO, C. W. 2012. Selection of regulatory T cells in the thymus. *Nat Rev Immunol,* 12**,** 157-67.

HU, B., CASTILLO, E., HAREWOOD, L., OSTANO, P., REYMOND, A., DUMMER, R., RAFFOUL, W., HOETZENECKER, W., HOFBAUER, G. F. & DOTTO, G. P. 2012. Multifocal epithelial tumors and field cancerization from loss of mesenchymal CSL signaling. *Cell,* 149**,** 1207-20.

HUANG, C. T., WORKMAN, C. J., FLIES, D., PAN, X., MARSON, A. L., ZHOU, G., HIPKISS, E. L., RAVI, S., KOWALSKI, J., LEVITSKY, H. I., POWELL, J. D., PARDOLL, D. M., DRAKE, C. G. & VIGNALI, D. A. 2004. Role of LAG-3 in regulatory T cells. *Immunity,* 21**,** 503-13.

HUANG, S. J., HIJNEN, D., MURPHY, G. F., KUPPER, T. S., CALARESE, A. W., MOLLET, I. G., SCHANBACHER, C. F., MILLER, D. M., SCHMULTS, C. D. & CLARK, R. A. 2009. Imiquimod enhances IFN-gamma production and effector function of

T cells infiltrating human squamous cell carcinomas of the skin. *J Invest Dermatol,* 129**,** 2676-85.

HUSSAIN, S. K., SUNDQUIST, J. & HEMMINKI, K. 2009. The effect of having an affected parent or sibling on invasive and in situ skin cancer risk in Sweden. *J Invest Dermatol,* 129**,** 2142-7.

ICHIHARA, F., KONO, K., TAKAHASHI, A., KAWAIDA, H., SUGAI, H. & FUJII, H. 2003. Increased populations of regulatory T cells in peripheral blood and tumor-infiltrating lymphocytes in patients with gastric and esophageal cancers. *Clin Cancer Res,* 9**,** 4404-8.

INTLEKOFER, A. M., TAKEMOTO, N., WHERRY, E. J., LONGWORTH, S. A., NORTHRUP, J. T., PALANIVEL, V. R., MULLEN, A. C., GASINK, C. R., KAECH, S. M., MILLER, J. D., GAPIN, L., RYAN, K., RUSS, A. P., LINDSTEN, T., ORANGE, J. S., GOLDRATH, A. W., AHMED, R. & REINER, S. L. 2005. Effector and memory CD8+ T cell fate coupled by T-bet and eomesodermin. *Nat Immunol,* 6**,** 1236-44.

ISLAM, S. A., CHANG, D. S., COLVIN, R. A., BYRNE, M. H., MCCULLY, M. L., MOSER, B., LIRA, S. A., CHARO, I. F. & LUSTER, A. D. 2011. Mouse CCL8, a CCR8 agonist, promotes atopic dermatitis by recruiting IL-5+ T(H)2 cells. *Nat Immunol,* 12**,** 167-77.

ISLAM, S. A. & LUSTER, A. D. 2012. T cell homing to epithelial barriers in allergic disease. *Nat Med,* 18**,** 705-15.

JAMIESON, A. M., DIEFENBACH, A., MCMAHON, C. W., XIONG, N., CARLYLE, J. R. & RAULET, D. H. 2002. The role of the NKG2D immunoreceptor in immune cell activation and natural killing. *Immunity,* 17**,** 19-29.

JANG, T. J. 2008. Prevalence of Foxp3 positive T regulatory cells is increased during progression of cutaneous squamous tumors. *Yonsei Med J,* 49**,** 942-8.

JIANG, W., ANANTHASWAMY, H. N., MULLER, H. K. & KRIPKE, M. L. 1999. p53 protects against skin cancer induction by UV-B radiation. *Oncogene,* 18**,** 4247-53.

JIANG, X., CLARK, R. A., LIU, L., WAGERS, A. J., FUHLBRIGGE, R. C. & KUPPER, T. S. 2012. Skin infection generates non-migratory memory CD8+ T(RM) cells providing global skin immunity. *Nature,* 483**,** 227-31.

JIE, H. B., GILDENER-LEAPMAN, N., LI, J., SRIVASTAVA, R. M., GIBSON, S. P., WHITESIDE, T. L. & FERRIS, R. L. 2013. Intratumoral regulatory T cells upregulate immunosuppressive molecules in head and neck cancer patients. *Br J Cancer,* 109**,** 2629-35.

JONASON, A. S., KUNALA, S., PRICE, G. J., RESTIFO, R. J., SPINELLI, H. M., PERSING, J. A., LEFFELL, D. J., TARONE, R. E. & BRASH, D. E. 1996. Frequent clones of p53-mutated keratinocytes in normal human skin. *Proc Natl Acad Sci U S A,* 93**,** 14025-9.

JOSEFOWICZ, S. Z., NIEC, R. E., KIM, H. Y., TREUTING, P., CHINEN, T., ZHENG, Y., UMETSU, D. T. & RUDENSKY, A. Y. 2012. Extrathymically generated regulatory T cells control mucosal TH2 inflammation. *Nature,* 482**,** 395-9.

JOSHI, N. S., CUI, W., CHANDELE, A., LEE, H. K., URSO, D. R., HAGMAN, J., GAPIN, L. & KAECH, S. M. 2007. Inflammation directs memory precursor and short-

lived effector CD8(+) T cell fates via the graded expression of T-bet transcription factor. *Immunity,* 27**,** 281-95.

KAECH, S. M. & CUI, W. 2012. Transcriptional control of effector and memory CD8+ T cell differentiation. *Nat Rev Immunol,* 12**,** 749-61.

KAMBAYASHI, Y., FUJIMURA, T. & AIBA, S. 2013. Comparison of immunosuppressive and immunomodulatory cells in keratoacanthoma and cutaneous squamous cell carcinoma. *Acta Derm Venereol,* 93**,** 663-8.

KAO, C., OESTREICH, K. J., PALEY, M. A., CRAWFORD, A., ANGELOSANTO, J. M., ALI, M. A., INTLEKOFER, A. M., BOSS, J. M., REINER, S. L., WEINMANN, A. S. & WHERRY, E. J. 2011. Transcription factor T-bet represses expression of the inhibitory receptor PD-1 and sustains virus-specific CD8+ T cell responses during chronic infection. *Nat Immunol,* 12**,** 663-71.

KARAGAS, M. R., MCDONALD, J. A., GREENBERG, E. R., STUKEL, T. A., WEISS, J. E., BARON, J. A. & STEVENS, M. M. 1996. Risk of basal cell and squamous cell skin cancers after ionizing radiation therapy. For The Skin Cancer Prevention Study Group. *J Natl Cancer Inst,* 88**,** 1848-53.

KARAGAS, M. R., STUKEL, T. A., MORRIS, J. S., TOSTESON, T. D., WEISS, J. E., SPENCER, S. K. & GREENBERG, E. R. 2001. Skin cancer risk in relation to toenail arsenic concentrations in a US population-based case-control study. *Am J Epidemiol,* 153**,** 559-65.

KARAGAS, M. R., WATERBOER, T., LI, Z., NELSON, H. H., MICHAEL, K. M., BAVINCK, J. N., PERRY, A. E., SPENCER, S. K., DALING, J., GREEN, A. C., PAWLITA, M. & NEW HAMPSHIRE SKIN CANCER STUDY, G. 2010. Genus beta human papillomaviruses and incidence of basal cell and squamous cell carcinomas of skin: population based case-control study. *BMJ,* 341**,** c2986.

KARIA, P. S., JAMBUSARIA-PAHLAJANI, A., HARRINGTON, D. P., MURPHY, G. F., QURESHI, A. A. & SCHMULTS, C. D. 2014. Evaluation of American Joint Committee on Cancer, International Union Against Cancer, and Brigham and Women's Hospital tumor staging for cutaneous squamous cell carcinoma. *J Clin Oncol,* 32**,** 327-34.

KEIR, M. E., BUTTE, M. J., FREEMAN, G. J. & SHARPE, A. H. 2008. PD-1 and its ligands in tolerance and immunity. *Annu Rev Immunol,* 26**,** 677-704.

KENNEDY, C., TER HUURNE, J., BERKHOUT, M., GRUIS, N., BASTIAENS, M., BERGMAN, W., WILLEMZE, R. & BAVINCK, J. N. 2001. Melanocortin 1 receptor (MC1R) gene variants are associated with an increased risk for cutaneous melanoma which is largely independent of skin type and hair color. *J Invest Dermatol,* 117**,** 294-300.

KERR, C. 2002. 'Rub on' treatment for basal-cell carcinoma. *Lancet Oncol,* 3**,** 201.

KHACHIGIAN, L. M., CAI, H., MOLONEY, F. J., PARISH, C. R., CHONG, B. H., STOCKER, R., BARNETSON, R. S. & HALLIDAY, G. M. 2012. Destroying c-jun messenger: new insights into biological mechanisms of DNAzyme function. *Oncotarget,* 3**,** 594-5.

KIM, J. H., CHOI, Y. J., LEE, B. H., SONG, M. Y., BAN, C. Y., KIM, J., PARK, J., KIM, S. E., KIM, T. G., PARK, S. H., KIM, H. P., SUNG, Y. C., KIM, S. C. & SHIN, E. C. 2016. Programmed cell death ligand 1 alleviates psoriatic inflammation by

suppressing IL-17A production from programmed cell death 1-high T cells. *J Allergy Clin Immunol,* 137**,** 1466-1476 e3.

KLARQUIST, J., TOBIN, K., FARHANGI OSKUEI, P., HENNING, S. W., FERNANDEZ, M. F., DELLACECCA, E. R., NAVARRO, F. C., EBY, J. M., CHATTERJEE, S., MEHROTRA, S., CLARK, J. I. & LE POOLE, I. C. 2016. Ccl22 diverts T regulatory cells and controls the growth of melanoma. *Cancer Res.*

KLEIN, L., KYEWSKI, B., ALLEN, P. M. & HOGQUIST, K. A. 2014. Positive and negative selection of the T cell repertoire: what thymocytes see (and don't see). *Nat Rev Immunol,* 14**,** 377-91.

KOBAYASHI, N., NAKAGAWA, A., MURAMATSU, T., YAMASHINA, Y., SHIRAI, T., HASHIMOTO, M. W., ISHIGAKI, Y., OHNISHI, T. & MORI, T. 1998. Supranuclear melanin caps reduce ultraviolet induced DNA photoproducts in human epidermis. *J Invest Dermatol,* 110**,** 806-10.

KOCH, M. A., TUCKER-HEARD, G., PERDUE, N. R., KILLEBREW, J. R., URDAHL, K. B. & CAMPBELL, D. J. 2009. The transcription factor T-bet controls regulatory T cell homeostasis and function during type 1 inflammation. *Nat Immunol,* 10**,** 595-602.

KOHRT, H. E., COLEVAS, A. D., HOUOT, R., WEISKOPF, K., GOLDSTEIN, M. J., LUND, P., MUELLER, A., SAGIV-BARFI, I., MARABELLE, A., LIRA, R., TROUTNER, E., RICHARDS, L., RAJAPASKA, A., HEBB, J., CHESTER, C., WALLER, E., OSTASHKO, A., WENG, W. K., CHEN, L., CZERWINSKI, D., FU, Y. X., SUNWOO, J. & LEVY, R. 2014. Targeting CD137 enhances the efficacy of cetuximab. *J Clin Invest,* 124**,** 2668-82.

KOLEV, V., MANDINOVA, A., GUINEA-VINIEGRA, J., HU, B., LEFORT, K., LAMBERTINI, C., NEEL, V., DUMMER, R., WAGNER, E. F. & DOTTO, G. P. 2008. EGFR signalling as a negative regulator of Notch1 gene transcription and function in proliferating keratinocytes and cancer. *Nat Cell Biol,* 10**,** 902-11.

KRIPKE, M. L., COX, P. A., ALAS, L. G. & YAROSH, D. B. 1992. Pyrimidine dimers in DNA initiate systemic immunosuppression in UV-irradiated mice. *Proc Natl Acad Sci U S A,* 89**,** 7516-20.

KRYCZEK, I., BANERJEE, M., CHENG, P., VATAN, L., SZELIGA, W., WEI, S., HUANG, E., FINLAYSON, E., SIMEONE, D., WELLING, T. H., CHANG, A., COUKOS, G., LIU, R. & ZOU, W. 2009. Phenotype, distribution, generation, and functional and clinical relevance of Th17 cells in the human tumor environments. *Blood,* 114**,** 1141-9.

KRYNITZ, B., LUNDH ROZELL, B. & LINDELOF, B. 2010. Differences in the peritumoural inflammatory skin infiltrate between squamous cell carcinomas in organ transplant recipients and immunocompetent patients. *Acta Derm Venereol,* 90**,** 379-85.

KRZEWSKI, K., GIL-KRZEWSKA, A., NGUYEN, V., PERUZZI, G. & COLIGAN, J. E. 2013. LAMP1/CD107a is required for efficient perforin delivery to lytic granules and NK-cell cytotoxicity. *Blood,* 121**,** 4672-83.

KUBO, A., NAGAO, K., YOKOUCHI, M., SASAKI, H. & AMAGAI, M. 2009. External antigen uptake by Langerhans cells with reorganization of epidermal tight junction barriers. *J Exp Med,* 206**,** 2937-46.

KUEHN, H. S., OUYANG, W., LO, B., DEENICK, E. K., NIEMELA, J. E., AVERY, D. T., SCHICKEL, J. N., TRAN, D. Q., STODDARD, J., ZHANG, Y., FRUCHT, D. M., DUMITRIU, B., SCHEINBERG, P., FOLIO, L. R., FREIN, C. A., PRICE, S., KOH, C., HELLER, T., SEROOGY, C. M., HUTTENLOCHER, A., RAO, V. K., SU, H. C., KLEINER, D., NOTARANGELO, L. D., RAMPERTAAP, Y., OLIVIER, K. N., MCELWEE, J., HUGHES, J., PITTALUGA, S., OLIVEIRA, J. B., MEFFRE, E., FLEISHER, T. A., HOLLAND, S. M., LENARDO, M. J., TANGYE, S. G. & UZEL, G. 2014. Immune dysregulation in human subjects with heterozygous germline mutations in CTLA4. *Science,* 345**,** 1623-7.

KYRIAKAKIS, E., MASLOVA, K., PHILIPPOVA, M., PFAFF, D., JOSHI, M. B., BUECHNER, S. A., ERNE, P. & RESINK, T. J. 2012. T-Cadherin is an auxiliary negative regulator of EGFR pathway activity in cutaneous squamous cell carcinoma: impact on cell motility. *J Invest Dermatol,* 132**,** 2275-85.

LADANYI, A., SOMLAI, B., GILDE, K., FEJOS, Z., GAUDI, I. & TIMAR, J. 2004. T-cell activation marker expression on tumor-infiltrating lymphocytes as prognostic factor in cutaneous malignant melanoma. *Clin Cancer Res,* 10**,** 521-30.

LAI, C., AUGUST, S., ALBIBAS, A., BEHAR, R., CHO, S. Y., POLAK, M. E., THEAKER, J., MACLEOD, A. S., FRENCH, R. R., GLENNIE, M. J., AL-SHAMKHANI, A. & HEALY, E. 2016. OX40+ regulatory T cells in cutaneous squamous cell carcinoma suppress effector T-cell responses and associate with metastatic potential. *Clin Cancer Res,* 22**,** 4236-48.

LAMBERT, S. R., MLADKOVA, N., GULATI, A., HAMOUDI, R., PURDIE, K., CERIO, R., LEIGH, I., PROBY, C. & HARWOOD, C. A. 2014. Key differences identified between actinic keratosis and cutaneous squamous cell carcinoma by transcriptome profiling. *Br J Cancer,* 110**,** 520-9.

LANSBURY, L., BATH-HEXTALL, F., PERKINS, W., STANTON, W. & LEONARDI-BEE, J. 2013. Interventions for non-metastatic squamous cell carcinoma of the skin: systematic review and pooled analysis of observational studies. *BMJ,* 347**,** f6153.

LAPOUGE, G., YOUSSEF, K. K., VOKAER, B., ACHOURI, Y., MICHAUX, C., SOTIROPOULOU, P. A. & BLANPAIN, C. 2011. Identifying the cellular origin of squamous skin tumors. *Proc Natl Acad Sci U S A,* 108**,** 7431-6.

LARKIN, J., CHIARION-SILENI, V., GONZALEZ, R., GROB, J. J., COWEY, C. L., LAO, C. D., SCHADENDORF, D., DUMMER, R., SMYLIE, M., RUTKOWSKI, P., FERRUCCI, P. F., HILL, A., WAGSTAFF, J., CARLINO, M. S., HAANEN, J. B., MAIO, M., MARQUEZ-RODAS, I., MCARTHUR, G. A., ASCIERTO, P. A., LONG, G. V., CALLAHAN, M. K., POSTOW, M. A., GROSSMANN, K., SZNOL, M., DRENO, B., BASTHOLT, L., YANG, A., ROLLIN, L. M., HORAK, C., HODI, F. S. & WOLCHOK, J. D. 2015. Combined nivolumab and ipilimumab or monotherapy in untreated melanoma. *N Engl J Med,* 373**,** 23-34.

LAZAROV, M., KUBO, Y., CAI, T., DAJEE, M., TARUTANI, M., LIN, Q., FANG, M., TAO, S., GREEN, C. L. & KHAVARI, P. A. 2002. CDK4 coexpression with Ras generates malignant human epidermal tumorigenesis. *Nat Med,* 8**,** 1105-14.

LE, D. T., URAM, J. N., WANG, H., BARTLETT, B. R., KEMBERLING, H., EYRING, A. D., SKORA, A. D., LUBER, B. S., AZAD, N. S., LAHERU, D., BIEDRZYCKI, B., DONEHOWER, R. C., ZAHEER, A., FISHER, G. A., CROCENZI, T. S., LEE, J. J., DUFFY, S. M., GOLDBERG, R. M., DE LA CHAPELLE, A., KOSHIJI, M., BHAIJEE,

F., HUEBNER, T., HRUBAN, R. H., WOOD, L. D., CUKA, N., PARDOLL, D. M., PAPADOPOULOS, N., KINZLER, K. W., ZHOU, S., CORNISH, T. C., TAUBE, J. M., ANDERS, R. A., ESHLEMAN, J. R., VOGELSTEIN, B. & DIAZ, L. A., JR. 2015. PD-1 blockade in tumors with mismatch-repair deficiency. *N Engl J Med,* 372**,** 2509-20.

LE MIRE, L., HOLLOWOOD, K., GRAY, D., BORDEA, C. & WOJNAROWSKA, F. 2006. Melanomas in renal transplant recipients. *Br J Dermatol,* 154**,** 472-7.

LEE, C. S., BHADURI, A., MAH, A., JOHNSON, W. L., UNGEWICKELL, A., AROS, C. J., NGUYEN, C. B., RIOS, E. J., SIPRASHVILI, Z., STRAIGHT, A., KIM, J., AASI, S. Z. & KHAVARI, P. A. 2014. Recurrent point mutations in the kinetochore gene KNSTRN in cutaneous squamous cell carcinoma. *Nat Genet,* 46**,** 1060-2.

LEVELL, N. J., IGALI, L., WRIGHT, K. A. & GREENBERG, D. C. 2013. Basal cell carcinoma epidemiology in the UK: the elephant in the room. *Clin Exp Dermatol,* 38**,** 367-9.

LI, J., WANG, K., GAO, F., JENSEN, T. D., LI, S. T., DEANGELIS, P. M., KOLVRAA, S., PROBY, C., FORSLUND, O., BOLUND, L. & CLAUSEN, O. P. 2012. Array comparative genomic hybridization of keratoacanthomas and squamous cell carcinomas: different patterns of genetic aberrations suggest two distinct entities. *J Invest Dermatol,* 132**,** 2060-6.

LI, Y. Y., HANNA, G. J., LAGA, A. C., HADDAD, R. I., LORCH, J. H. & HAMMERMAN, P. S. 2015. Genomic analysis of metastatic cutaneous squamous cell carcinoma. *Clin Cancer Res,* 21**,** 1447-56.

LINCH, S. N., KASIEWICZ, M. J., MCNAMARA, M. J., HILGART-MARTISZUS, I. F., FARHAD, M. & REDMOND, W. L. 2016. Combination OX40 agonism/CTLA-4 blockade with HER2 vaccination reverses T-cell anergy and promotes survival in tumor-bearing mice. *Proc Natl Acad Sci U S A,* 113**,** E319-27.

LINNEMANN, C., VAN BUUREN, M. M., BIES, L., VERDEGAAL, E. M., SCHOTTE, R., CALIS, J. J., BEHJATI, S., VELDS, A., HILKMANN, H., ATMIOUI, D. E., VISSER, M., STRATTON, M. R., HAANEN, J. B., SPITS, H., VAN DER BURG, S. H. & SCHUMACHER, T. N. 2015. High-throughput epitope discovery reveals frequent recognition of neo-antigens by CD4+ T cells in human melanoma. *Nat Med,* 21**,** 81-5.

LIPSON, E. J., BAGNASCO, S. M., MOORE, J., JR., JANG, S., PATEL, M. J., ZACHARY, A. A., PARDOLL, D. M., TAUBE, J. M. & DRAKE, C. G. 2016. Tumor regression and allograft rejection after administration of anti-PD-1. *N Engl J Med,* 374**,** 896-8.

LISTON, A. & GRAY, D. H. 2014. Homeostatic control of regulatory T cell diversity. *Nat Rev Immunol,* 14**,** 154-65.

LIU, D., FERNANDEZ, B. O., HAMILTON, A., LANG, N. N., GALLAGHER, J. M., NEWBY, D. E., FEELISCH, M. & WELLER, R. B. 2014. UVA irradiation of human skin vasodilates arterial vasculature and lowers blood pressure independently of nitric oxide synthase. *J Invest Dermatol,* 134**,** 1839-46.

LIU, V. C., WONG, L. Y., JANG, T., SHAH, A. H., PARK, I., YANG, X., ZHANG, Q., LONNING, S., TEICHER, B. A. & LEE, C. 2007. Tumor evasion of the immune system by converting CD4+CD25- T cells into CD4+CD25+ T regulatory cells: role of tumor-derived TGF-beta. *J Immunol,* 178**,** 2883-92.

LOMAS, A., LEONARDI-BEE, J. & BATH-HEXTALL, F. 2012. A systematic review of worldwide incidence of nonmelanoma skin cancer. *Br J Dermatol,* 166**,** 1069-80.

LOSER, K., APELT, J., VOSKORT, M., MOHAUPT, M., BALKOW, S., SCHWARZ, T., GRABBE, S. & BEISSERT, S. 2007. IL-10 controls ultraviolet-induced carcinogenesis in mice. *J Immunol,* 179**,** 365-71.

LOWES, M. A., BISHOP, G. A., COOKE, B. E., BARNETSON, R. S. & HALLIDAY, G. M. 1999. Keratoacanthomas have an immunosuppressive cytokine environment of increased IL-10 and decreased GM-CSF compared to squamous cell carcinomas. *Br J Cancer,* 80**,** 1501-5.

LOWES, M. A., SUAREZ-FARINAS, M. & KRUEGER, J. G. 2014. Immunology of psoriasis. *Annu Rev Immunol,* 32**,** 227-55.

LUCAS, R., MCMICHAEL, T., SMITH, W. & ARMSTRONG, B. 2006. Solar ultraviolet radiation: Global burden of disease from solar ultraviolet radiation. *In:* PRÜSS-ÜSTÜN, A., ZEEB, H., MATHERS, C. & REPACHOLI, M. (eds.) *Environmental Burden of Disease Series.* Geneva: World Health Organization Public Health and the Environment.

MABULA, J. B., CHALYA, P. L., MCHEMBE, M. D., JAKA, H., GIITI, G., RAMBAU, P., MASALU, N., KAMUGISHA, E., ROBERT, S. & GILYOMA, J. M. 2012. Skin cancers among albinos at a university teaching hospital in Northwestern Tanzania: a retrospective review of 64 cases. *BMC Dermatol,* 12**,** 5.

MACKAY, L. K., RAHIMPOUR, A., MA, J. Z., COLLINS, N., STOCK, A. T., HAFON, M. L., VEGA-RAMOS, J., LAUZURICA, P., MUELLER, S. N., STEFANOVIC, T., TSCHARKE, D. C., HEATH, W. R., INOUYE, M., CARBONE, F. R. & GEBHARDT, T. 2013. The developmental pathway for CD103(+)CD8+ tissue-resident memory T cells of skin. *Nat Immunol,* 14**,** 1294-301.

MACKIE, R. M., REID, R. & JUNOR, B. 2003. Fatal melanoma transferred in a donated kidney 16 years after melanoma surgery. *N Engl J Med,* 348**,** 567-8.

MACKINTOSH, L. J., GEDDES, C. C. & HERD, R. M. 2013. Skin tumours in the West of Scotland renal transplant population. *Br J Dermatol,* 168**,** 1047-53.

MACLEOD, A. S., RUDOLPH, R., CORRIDEN, R., YE, I., GARIJO, O. & HAVRAN, W. L. 2014. Skin-resident T cells sense ultraviolet radiation-induced injury and contribute to DNA repair. *J Immunol,* 192**,** 5695-702.

MADAN, V., LEAR, J. T. & SZEIMIES, R. M. 2010. Non-melanoma skin cancer. *Lancet,* 375**,** 673-85.

MADIREDDI, S., EUN, S. Y., LEE, S. W., NEMCOVICOVA, I., MEHTA, A. K., ZAJONC, D. M., NISHI, N., NIKI, T., HIRASHIMA, M. & CROFT, M. 2014. Galectin-9 controls the therapeutic activity of 4-1BB-targeting antibodies. *J Exp Med,* 211**,** 1433-48.

MAN, K. & KALLIES, A. 2015. Synchronizing transcriptional control of T cell metabolism and function. *Nat Rev Immunol,* 15**,** 574-84.

MANDAPATHIL, M., SZCZEPANSKI, M. J., SZAJNIK, M., REN, J., LENZNER, D. E., JACKSON, E. K., GORELIK, E., LANG, S., JOHNSON, J. T. & WHITESIDE, T. L. 2009. Increased ectonucleotidase expression and activity in regulatory T cells of patients with head and neck cancer. *Clin Cancer Res,* 15**,** 6348-57.

MANIATI, E., SOPER, R. & HAGEMANN, T. 2010. Up for mischief? IL-17/Th17 in the tumour microenvironment. *Oncogene,* 29**,** 5653-62.

MARABELLE, A., KOHRT, H., SAGIV-BARFI, I., AJAMI, B., AXTELL, R. C., ZHOU, G., RAJAPAKSA, R., GREEN, M. R., TORCHIA, J., BRODY, J., LUONG, R., ROSENBLUM, M. D., STEINMAN, L., LEVITSKY, H. I., TSE, V. & LEVY, R. 2013. Depleting tumor-specific Tregs at a single site eradicates disseminated tumors. *J Clin Invest,* 123**,** 2447-63.

MARCIL, I. & STERN, R. S. 2000. Risk of developing a subsequent nonmelanoma skin cancer in patients with a history of nonmelanoma skin cancer: a critical review of the literature and meta-analysis. *Arch Dermatol,* 136**,** 1524-30.

MARKS, R., RENNIE, G. & SELWOOD, T. S. 1988. Malignant transformation of solar keratoses to squamous cell carcinoma. *Lancet,* 1**,** 795-7.

MARTINCORENA, I., ROSHAN, A., GERSTUNG, M., ELLIS, P., VAN LOO, P., MCLAREN, S., WEDGE, D. C., FULLAM, A., ALEXANDROV, L. B., TUBIO, J. M., STEBBINGS, L., MENZIES, A., WIDAA, S., STRATTON, M. R., JONES, P. H. & CAMPBELL, P. J. 2015. Tumor evolution. High burden and pervasive positive selection of somatic mutations in normal human skin. *Science,* 348**,** 880-6.

MASOPUST, D. & SCHENKEL, J. M. 2013. The integration of T cell migration, differentiation and function. *Nat Rev Immunol,* 13**,** 309-20.

MATSUSHITA, H., VESELY, M. D., KOBOLDT, D. C., RICKERT, C. G., UPPALURI, R., MAGRINI, V. J., ARTHUR, C. D., WHITE, J. M., CHEN, Y. S., SHEA, L. K., HUNDAL, J., WENDL, M. C., DEMETER, R., WYLIE, T., ALLISON, J. P., SMYTH, M. J., OLD, L. J., MARDIS, E. R. & SCHREIBER, R. D. 2012. Cancer exome analysis reveals a T-cell-dependent mechanism of cancer immunoediting. *Nature,* 482**,** 400-4.

MATSUZAKI, J., GNJATIC, S., MHAWECH-FAUCEGLIA, P., BECK, A., MILLER, A., TSUJI, T., EPPOLITO, C., QIAN, F., LELE, S., SHRIKANT, P., OLD, L. J. & ODUNSI, K. 2010. Tumor-infiltrating NY-ESO-1-specific CD8+ T cells are negatively regulated by LAG-3 and PD-1 in human ovarian cancer. *Proc Natl Acad Sci U S A,* 107**,** 7875-80.

MCCULLY, M. L., LADELL, K., HAKOBYAN, S., MANSEL, R. E., PRICE, D. A. & MOSER, B. 2012. Epidermis instructs skin homing receptor expression in human T cells. *Blood,* 120**,** 4591-8.

MCGRANAHAN, N., FURNESS, A. J., ROSENTHAL, R., RAMSKOV, S., LYNGAA, R., SAINI, S. K., JAMAL-HANJANI, M., WILSON, G. A., BIRKBAK, N. J., HILEY, C. T., WATKINS, T. B., SHAFI, S., MURUGAESU, N., MITTER, R., AKARCA, A. U., LINARES, J., MARAFIOTI, T., HENRY, J. Y., VAN ALLEN, E. M., MIAO, D., SCHILLING, B., SCHADENDORF, D., GARRAWAY, L. A., MAKAROV, V., RIZVI, N. A., SNYDER, A., HELLMANN, M. D., MERGHOUB, T., WOLCHOK, J. D., SHUKLA, S. A., WU, C. J., PEGGS, K. S., CHAN, T. A., HADRUP, S. R., QUEZADA, S. A. & SWANTON, C. 2016. Clonal neoantigens elicit T cell immunoreactivity and sensitivity to immune checkpoint blockade. *Science,* 351**,** 1463-9.

MCKINNEY, E. F., LEE, J. C., JAYNE, D. R., LYONS, P. A. & SMITH, K. G. 2015. T-cell exhaustion, co-stimulation and clinical outcome in autoimmunity and infection. *Nature,* 523**,** 612-6.

MCLOONE, P., SIMICS, E., BARTON, A., NORVAL, M. & GIBBS, N. K. 2005. An action spectrum for the production of cis-urocanic acid in human skin in vivo. *J Invest Dermatol,* 124**,** 1071-4.

MELERO, I., SHUFORD, W. W., NEWBY, S. A., ARUFFO, A., LEDBETTER, J. A., HELLSTROM, K. E., MITTLER, R. S. & CHEN, L. 1997. Monoclonal antibodies against the 4-1BB T-cell activation molecule eradicate established tumors. *Nat Med,* 3**,** 682-5.

METZGER, T. C., LONG, H., POTLURI, S., PERTEL, T., BAILEY-BUCKTROUT, S. L., LIN, J. C., FU, T., SHARMA, P., ALLISON, J. P. & FELDMAN, R. M. 2016. ICOS promotes the function of CD4+ effector T cells during anti-OX40-mediated tumor rejection. *Cancer Res,* 76**,** 3684-9.

MILPIED, P., RENAND, A., BRUNEAU, J., MENDES-DA-CRUZ, D. A., JACQUELIN, S., ASNAFI, V., RUBIO, M. T., MACINTYRE, E., LEPELLETIER, Y. & HERMINE, O. 2009. Neuropilin-1 is not a marker of human Foxp3+ Treg. *Eur J Immunol,* 39**,** 1466-71.

MITSUI, H., SUAREZ-FARINAS, M., GULATI, N., SHAH, K. R., CANNIZZARO, M. V., COATS, I., FELSEN, D., KRUEGER, J. G. & CARUCCI, J. A. 2014. Gene expression profiling of the leading edge of cutaneous squamous cell carcinoma: IL-24-driven MMP-7. *J Invest Dermatol,* 134**,** 1418-27.

MITTELBRONN, M. A., MULLINS, D. L., RAMOS-CARO, F. A. & FLOWERS, F. P. 1998. Frequency of pre-existing actinic keratosis in cutaneous squamous cell carcinoma. *Int J Dermatol,* 37**,** 677-81.

MIYARA, M., YOSHIOKA, Y., KITOH, A., SHIMA, T., WING, K., NIWA, A., PARIZOT, C., TAFLIN, C., HEIKE, T., VALEYRE, D., MATHIAN, A., NAKAHATA, T., YAMAGUCHI, T., NOMURA, T., ONO, M., AMOURA, Z., GOROCHOV, G. & SAKAGUCHI, S. 2009. Functional delineation and differentiation dynamics of human CD4+ T cells expressing the FoxP3 transcription factor. *Immunity,* 30**,** 899-911.

MODI, B. G., NEUSTADTER, J., BINDA, E., LEWIS, J., FILLER, R. B., ROBERTS, S. J., KWONG, B. Y., REDDY, S., OVERTON, J. D., GALAN, A., TIGELAAR, R., CAI, L., FU, P., SHLOMCHIK, M., KAPLAN, D. H., HAYDAY, A. & GIRARDI, M. 2012. Langerhans cells facilitate epithelial DNA damage and squamous cell carcinoma. *Science,* 335**,** 104-8.

MORRIS, G. P. & ALLEN, P. M. 2012. How the TCR balances sensitivity and specificity for the recognition of self and pathogens. *Nat Immunol,* 13**,** 121-8.

MOTZ, G. T., SANTORO, S. P., WANG, L. P., GARRABRANT, T., LASTRA, R. R., HAGEMANN, I. S., LAL, P., FELDMAN, M. D., BENENCIA, F. & COUKOS, G. 2014. Tumor endothelium FasL establishes a selective immune barrier promoting tolerance in tumors. *Nat Med,* 20**,** 607-15.

MOTZER, R. J., ESCUDIER, B., MCDERMOTT, D. F., GEORGE, S., HAMMERS, H. J., SRINIVAS, S., TYKODI, S. S., SOSMAN, J. A., PROCOPIO, G., PLIMACK, E. R., CASTELLANO, D., CHOUEIRI, T. K., GURNEY, H., DONSKOV, F., BONO, P., WAGSTAFF, J., GAULER, T. C., UEDA, T., TOMITA, Y., SCHUTZ, F. A., KOLLMANNSBERGER, C., LARKIN, J., RAVAUD, A., SIMON, J. S., XU, L. A., WAXMAN, I. M., SHARMA, P. & CHECKMATE, I. 2015. Nivolumab versus everolimus in advanced renal-cell carcinoma. *N Engl J Med,* 373**,** 1803-13.

MOUSSAI, D., MITSUI, H., PETTERSEN, J. S., PIERSON, K. C., SHAH, K. R., SUAREZ-FARINAS, M., CARDINALE, I. R., BLUTH, M. J., KRUEGER, J. G. & CARUCCI, J. A. 2011. The human cutaneous squamous cell carcinoma microenvironment is characterized by increased lymphatic density and enhanced expression of macrophage-derived VEGF-C. *J Invest Dermatol,* 131**,** 229-36.

MUELLER, S. N., GEBHARDT, T., CARBONE, F. R. & HEATH, W. R. 2013. Memory T cell subsets, migration patterns, and tissue residence. *Annu Rev Immunol,* 31**,** 137-61.

MUHLEISEN, B., PETROV, I., GACHTER, T., KURRER, M., SCHARER, L., DUMMER, R., FRENCH, L. E. & HOFBAUER, G. F. 2009. Progression of cutaneous squamous cell carcinoma in immunosuppressed patients is associated with reduced CD123+ and FOXP3+ cells in the perineoplastic inflammatory infiltrate. *Histopathology,* 55**,** 67-76.

MURANUSHI, C., OLSEN, C. M., PANDEYA, N. & GREEN, A. C. 2015. Aspirin and nonsteroidal anti-inflammatory drugs can prevent cutaneous squamous cell carcinoma: a systematic review and meta-analysis. *J Invest Dermatol,* 135**,** 975-83.

NAGARAJ, S., SCHRUM, A. G., CHO, H. I., CELIS, E. & GABRILOVICH, D. I. 2010. Mechanism of T cell tolerance induced by myeloid-derived suppressor cells. *J Immunol,* 184**,** 3106-16.

NAKAMURA, K., KITANI, A. & STROBER, W. 2001. Cell contact-dependent immunosuppression by CD4(+)CD25(+) regulatory T cells is mediated by cell surface-bound transforming growth factor beta. *J Exp Med,* 194**,** 629-44.

NAN, H., XU, M., KRAFT, P., QURESHI, A. A., CHEN, C., GUO, Q., HU, F. B., CURHAN, G., AMOS, C. I., WANG, L. E., LEE, J. E., WEI, Q., HUNTER, D. J. & HAN, J. 2011. Genome-wide association study identifies novel alleles associated with risk of cutaneous basal cell carcinoma and squamous cell carcinoma. *Hum Mol Genet,* 20**,** 3718-24.

NARDINOCCHI, L., SONEGO, G., PASSARELLI, F., AVITABILE, S., SCARPONI, C., FAILLA, C. M., SIMONI, S., ALBANESI, C. & CAVANI, A. 2015. Interleukin-17 and interleukin-22 promote tumor progression in human nonmelanoma skin cancer. *Eur J Immunol,* 45**,** 922-31.

NASSAR, D., LATIL, M., BOECKX, B., LAMBRECHTS, D. & BLANPAIN, C. 2015. Genomic landscape of carcinogen-induced and genetically induced mouse skin squamous cell carcinoma. *Nat Med,* 21**,** 946-54.

NATIONAL CANCER INSTITUTE. 2016. *PDQ® Genetics of skin cancer.* [Online]. Bethesda, MD: National Cancer Institute. Available: http://www.cancer.gov/types/skin/hp/skin-genetics-pdq [Accessed 11/02 2016].

NATSUAKI, Y., EGAWA, G., NAKAMIZO, S., ONO, S., HANAKAWA, S., OKADA, T., KUSUBA, N., OTSUKA, A., KITOH, A., HONDA, T., NAKAJIMA, S., TSUCHIYA, S., SUGIMOTO, Y., ISHII, K. J., TSUTSUI, H., YAGITA, H., IWAKURA, Y., KUBO, M., NG, L., HASHIMOTO, T., FUENTES, J., GUTTMAN-YASSKY, E., MIYACHI, Y. & KABASHIMA, K. 2014. Perivascular leukocyte clusters are essential for efficient activation of effector T cells in the skin. *Nat Immunol,* 15**,** 1064-9.

NAVID, F., BRUHS, A., SCHULLER, W., FRITSCHE, E., KRUTMANN, J., SCHWARZ, T. & SCHWARZ, A. 2013. The Aryl hydrocarbon receptor is involved in UVR-induced immunosuppression. *J Invest Dermatol,* 133**,** 2763-70.

NESTLE, F. O., DI MEGLIO, P., QIN, J. Z. & NICKOLOFF, B. J. 2009. Skin immune sentinels in health and disease. *Nat Rev Immunol,* 9**,** 679-91.

NG, Y. Z., POURREYRON, C., SALAS-ALANIS, J. C., DAYAL, J. H., CEPEDA-VALDES, R., YAN, W., WRIGHT, S., CHEN, M., FINE, J. D., HOGG, F. J., MCGRATH, J. A., MURRELL, D. F., LEIGH, I. M., LANE, E. B. & SOUTH, A. P. 2012. Fibroblast-derived dermal matrix drives development of aggressive cutaneous squamous cell carcinoma in patients with recessive dystrophic epidermolysis bullosa. *Cancer Res,* 72**,** 3522-34.

NICOLAS, M., WOLFER, A., RAJ, K., KUMMER, J. A., MILL, P., VAN NOORT, M., HUI, C. C., CLEVERS, H., DOTTO, G. P. & RADTKE, F. 2003. Notch1 functions as a tumor suppressor in mouse skin. *Nat Genet,* 33**,** 416-21.

NIJSTEN, T. E. & STERN, R. S. 2003. The increased risk of skin cancer is persistent after discontinuation of psoralen+ultraviolet A: a cohort study. *J Invest Dermatol,* 121**,** 252-8.

NORVAL, M., LUCAS, R. M., CULLEN, A. P., DE GRUIJL, F. R., LONGSTRETH, J., TAKIZAWA, Y. & VAN DER LEUN, J. C. 2011. The human health effects of ozone depletion and interactions with climate change. *Photochem Photobiol Sci,* 10**,** 199-225.

O'BRYAN, K., SHERMAN, W., NIEDT, G. W., TABACK, B., MANOLIDIS, S., WANG, A. & RATNER, D. 2013. An evolving paradigm for the workup and management of high-risk cutaneous squamous cell carcinoma. *J Am Acad Dermatol,* 69**,** 595-602 e1.

O'DONOVAN, P., PERRETT, C. M., ZHANG, X., MONTANER, B., XU, Y. Z., HARWOOD, C. A., MCGREGOR, J. M., WALKER, S. L., HANAOKA, F. & KARRAN, P. 2005. Azathioprine and UVA light generate mutagenic oxidative DNA damage. *Science,* 309**,** 1871-4.

O'SHEA, J. J. & PAUL, W. E. 2010. Mechanisms underlying lineage commitment and plasticity of helper CD4+ T cells. *Science,* 327**,** 1098-102.

ODORIZZI, P. M., PAUKEN, K. E., PALEY, M. A., SHARPE, A. & WHERRY, E. J. 2015. Genetic absence of PD-1 promotes accumulation of terminally differentiated exhausted CD8+ T cells. *J Exp Med,* 212**,** 1125-37.

OERTLI, M., SUNDQUIST, M., HITZLER, I., ENGLER, D. B., ARNOLD, I. C., REUTER, S., MAXEINER, J., HANSSON, M., TAUBE, C., QUIDING-JARBRINK, M. & MULLER, A. 2012. DC-derived IL-18 drives Treg differentiation, murine Helicobacter pylori-specific immune tolerance, and asthma protection. *J Clin Invest,* 122**,** 1082-96.

OESTREICH, K. J., YOON, H., AHMED, R. & BOSS, J. M. 2008. NFATc1 regulates PD-1 expression upon T cell activation. *J Immunol,* 181**,** 4832-9.

OPPENHEIM, D. E., ROBERTS, S. J., CLARKE, S. L., FILLER, R., LEWIS, J. M., TIGELAAR, R. E., GIRARDI, M. & HAYDAY, A. C. 2005. Sustained localized expression of ligand for the activating NKG2D receptor impairs natural cytotoxicity in vivo and reduces tumor immunosurveillance. *Nat Immunol,* 6**,** 928-37.

ORTIZ-URDA, S., GARCIA, J., GREEN, C. L., CHEN, L., LIN, Q., VEITCH, D. P., SAKAI, L. Y., LEE, H., MARINKOVICH, M. P. & KHAVARI, P. A. 2005. Type VII collagen is required for Ras-driven human epidermal tumorigenesis. *Science,* 307**,** 1773-6.

PACIFICO, A., GOLDBERG, L. H., PERIS, K., CHIMENTI, S., LEONE, G. & ANANTHASWAMY, H. N. 2008. Loss of CDKN2A and p14ARF expression occurs frequently in human nonmelanoma skin cancers. *Br J Dermatol,* 158**,** 291-7.

PAGES, F., BERGER, A., CAMUS, M., SANCHEZ-CABO, F., COSTES, A., MOLIDOR, R., MLECNIK, B., KIRILOVSKY, A., NILSSON, M., DAMOTTE, D., MEATCHI, T., BRUNEVAL, P., CUGNENC, P. H., TRAJANOSKI, Z., FRIDMAN, W. H. & GALON, J. 2005. Effector memory T cells, early metastasis, and survival in colorectal cancer. *N Engl J Med,* 353**,** 2654-66.

PALAZON, A., MARTINEZ-FORERO, I., TEIJEIRA, A., MORALES-KASTRESANA, A., ALFARO, C., SANMAMED, M. F., PEREZ-GRACIA, J. L., PENUELAS, I., HERVAS-STUBBS, S., ROUZAUT, A., DE LANDAZURI, M. O., JURE-KUNKEL, M., ARAGONES, J. & MELERO, I. 2012. The HIF-1alpha hypoxia response in tumor-infiltrating T lymphocytes induces functional CD137 (4-1BB) for immunotherapy. *Cancer Discov,* 2**,** 608-23.

PARDOLL, D. M. 2012. The blockade of immune checkpoints in cancer immunotherapy. *Nat Rev Cancer,* 12**,** 252-64.

PARK, Y. W., YOUNES, M. N., JASSER, S. A., YIGITBASI, O. G., ZHOU, G., BUCANA, C. D., BEKELE, B. N. & MYERS, J. N. 2005. AEE788, a dual tyrosine kinase receptor inhibitor, induces endothelial cell apoptosis in human cutaneous squamous cell carcinoma xenografts in nude mice. *Clin Cancer Res,* 11**,** 1963-73.

PARSA, A. T., WALDRON, J. S., PANNER, A., CRANE, C. A., PARNEY, I. F., BARRY, J. J., CACHOLA, K. E., MURRAY, J. C., TIHAN, T., JENSEN, M. C., MISCHEL, P. S., STOKOE, D. & PIEPER, R. O. 2007. Loss of tumor suppressor PTEN function increases B7-H1 expression and immunoresistance in glioma. *Nat Med,* 13**,** 84-8.

PATEL, A. S., KARAGAS, M. R., PAWLITA, M., WATERBOER, T. & NELSON, H. H. 2008. Cutaneous human papillomavirus infection, the EVER2 gene and incidence of squamous cell carcinoma: a case-control study. *Int J Cancer,* 122**,** 2377-9.

PATSOUKIS, N., BROWN, J., PETKOVA, V., LIU, F., LI, L. & BOUSSIOTIS, V. A. 2012. Selective effects of PD-1 on Akt and Ras pathways regulate molecular components of the cell cycle and inhibit T cell proliferation. *Sci Signal,* 5**,** ra46.

PEDROZA-GONZALEZ, A., VERHOEF, C., IJZERMANS, J. N., PEPPELENBOSCH, M. P., KWEKKEBOOM, J., VERHEIJ, J., JANSSEN, H. L. & SPRENGERS, D. 2013. Activated tumor-infiltrating CD4+ regulatory T cells restrain antitumor immunity in patients with primary or metastatic liver cancer. *Hepatology,* 57**,** 183-94.

PEGGS, K. S., QUEZADA, S. A., CHAMBERS, C. A., KORMAN, A. J. & ALLISON, J. P. 2009. Blockade of CTLA-4 on both effector and regulatory T cell compartments contributes to the antitumor activity of anti-CTLA-4 antibodies. *J Exp Med,* 206**,** 1717-25.

PENTCHEVA-HOANG, T., EGEN, J. G., WOJNOONSKI, K. & ALLISON, J. P. 2004. B7-1 and B7-2 selectively recruit CTLA-4 and CD28 to the immunological synapse. *Immunity,* 21**,** 401-13.

PETKOVIC, M., DIETSCHY, T., FREIRE, R., JIAO, R. & STAGLJAR, I. 2005. The human Rothmund-Thomson syndrome gene product, RECQL4, localizes to distinct nuclear foci that coincide with proteins involved in the maintenance of genome stability. *J Cell Sci,* 118**,** 4261-9.

PETTERSEN, J. S., FUENTES-DUCULAN, J., SUAREZ-FARINAS, M., PIERSON, K. C., PITTS-KIEFER, A., FAN, L., BELKIN, D. A., WANG, C. Q., BHUVANENDRAN, S., JOHNSON-HUANG, L. M., BLUTH, M. J., KRUEGER, J. G., LOWES, M. A. & CARUCCI, J. A. 2011. Tumor-associated macrophages in the cutaneous SCC microenvironment are heterogeneously activated. *J Invest Dermatol,* 131**,** 1322-30.

PETTY, J. K., HE, K., CORLESS, C. L., VETTO, J. T. & WEINBERG, A. D. 2002. Survival in human colorectal cancer correlates with expression of the T-cell costimulatory molecule OX-40 (CD134). *Am J Surg,* 183**,** 512-8.

PICKERING, C. R., ZHOU, J. H., LEE, J. J., DRUMMOND, J. A., PENG, S. A., SAADE, R. E., TSAI, K. Y., CURRY, J. L., TETZLAFF, M. T., LAI, S. Y., YU, J., MUZNY, D. M., DODDAPANENI, H., SHINBROT, E., COVINGTON, K. R., ZHANG, J., SETH, S., CAULIN, C., CLAYMAN, G. L., EL-NAGGAR, A. K., GIBBS, R. A., WEBER, R. S., MYERS, J. N., WHEELER, D. A. & FREDERICK, M. J. 2014. Mutational landscape of aggressive cutaneous squamous cell carcinoma. *Clin Cancer Res,* 20**,** 6582-92.

PICONESE, S., VALZASINA, B. & COLOMBO, M. P. 2008. OX40 triggering blocks suppression by regulatory T cells and facilitates tumor rejection. *J Exp Med,* 205**,** 825-39.

PLITAS, G., KONOPACKI, C., WU, K., BOS, P. D., MORROW, M., PUTINTSEVA, E. V., CHUDAKOV, D. M. & RUDENSKY, A. Y. 2016. Regulatory T Cells Exhibit Distinct Features in Human Breast Cancer. *Immunity,* 45**,** 1122-1134.

POLAK, M. E. 2011. Isolation of inflammatory cells from human tumours. *In:* CREE, I. A. (ed.) *Cancer Cell Culture: Methods and Protocols.* 2nd ed. New York: Humana Press, Springer Science.

POWLES, T., EDER, J. P., FINE, G. D., BRAITEH, F. S., LORIOT, Y., CRUZ, C., BELLMUNT, J., BURRIS, H. A., PETRYLAK, D. P., TENG, S. L., SHEN, X., BOYD, Z., HEGDE, P. S., CHEN, D. S. & VOGELZANG, N. J. 2014. MPDL3280A (anti-PD-L1) treatment leads to clinical activity in metastatic bladder cancer. *Nature,* 515**,** 558-62.

PRIOR, S. L., GRIFFITHS, A. P. & LEWIS, P. D. 2009. A study of mitochondrial DNA D-loop mutations and p53 status in nonmelanoma skin cancer. *Br J Dermatol,* 161**,** 1067-71.

PURDIE, K. J., POURREYRON, C., SOUTH, A.P. 2011. Isolation and culture of squamous cell carcinoma lines. *In:* CREE, I. A. (ed.) *Cancer Cell Culture: Methods and Protocols.* 2nd ed. New York: Humana Press, Springer Science.

QUEZADA, S. A., PEGGS, K. S., CURRAN, M. A. & ALLISON, J. P. 2006. CTLA4 blockade and GM-CSF combination immunotherapy alters the intratumor balance of effector and regulatory T cells. *J Clin Invest,* 116**,** 1935-45.

QUIGLEY, M., PEREYRA, F., NILSSON, B., PORICHIS, F., FONSECA, C., EICHBAUM, Q., JULG, B., JESNECK, J. L., BROSNAHAN, K., IMAM, S., RUSSELL, K., TOTH, I., PIECHOCKA-TROCHA, A., DOLFI, D., ANGELOSANTO, J., CRAWFORD, A., SHIN, H., KWON, D. S., ZUPKOSKY, J., FRANCISCO, L., FREEMAN, G. J., WHERRY, E. J., KAUFMANN, D. E., WALKER, B. D., EBERT, B. & HAINING, W. N. 2010. Transcriptional analysis of HIV-specific CD8+ T cells shows that PD-1 inhibits T cell function by upregulating BATF. *Nat Med,* 16**,** 1147-51.

RABINOVICH, G. A., GABRILOVICH, D. & SOTOMAYOR, E. M. 2007. Immunosuppressive strategies that are mediated by tumor cells. *Annu Rev Immunol,* 25**,** 267-96.

RAMSEY, M. R., HE, L., FORSTER, N., ORY, B. & ELLISEN, L. W. 2011. Physical association of HDAC1 and HDAC2 with p63 mediates transcriptional repression and tumor maintenance in squamous cell carcinoma. *Cancer Res,* 71**,** 4373-9.

RAMSEY, M. R., WILSON, C., ORY, B., ROTHENBERG, S. M., FAQUIN, W., MILLS, A. A. & ELLISEN, L. W. 2013. FGFR2 signaling underlies p63 oncogenic function in squamous cell carcinoma. *J Clin Invest,* 123**,** 3525-38.

RATUSHNY, V., GOBER, M. D., HICK, R., RIDKY, T. W. & SEYKORA, J. T. 2012. From keratinocyte to cancer: the pathogenesis and modeling of cutaneous squamous cell carcinoma. *J Clin Invest,* 122**,** 464-72.

REBEL, H., KRAM, N., WESTERMAN, A., BANUS, S., VAN KRANEN, H. J. & DE GRUIJL, F. R. 2005. Relationship between UV-induced mutant p53 patches and skin tumours, analysed by mutation spectra and by induction kinetics in various DNA-repair-deficient mice. *Carcinogenesis,* 26**,** 2123-30.

REILLY, G. D., MUHLEMANN, M., LAI, C., VERNE, J., IVES, A., SOUTHALL, P. J., GOULDING, H. & HEALY, E. 2013. High incidence of skin cancer in the Channel Islands. *Clin Exp Dermatol,* 38**,** 239-43.

RICE, S. A., CARPENTER, M., FITYAN, A., VEARNCOMBE, L. M., ARDERN-JONES, M., JACKSON, A. A., COOPER, C., BAIRD, J. & HEALY, E. 2015. Limited exposure to ambient ultraviolet radiation and 25-hydroxyvitamin D levels: a systematic review. *Br J Dermatol,* 172**,** 652-61.

RICHES, J. C., DAVIES, J. K., MCCLANAHAN, F., FATAH, R., IQBAL, S., AGRAWAL, S., RAMSAY, A. G. & GRIBBEN, J. G. 2013. T cells from CLL patients exhibit features of T-cell exhaustion but retain capacity for cytokine production. *Blood,* 121**,** 1612-21.

RIDKY, T. W., CHOW, J. M., WONG, D. J. & KHAVARI, P. A. 2010. Invasive three-dimensional organotypic neoplasia from multiple normal human epithelia. *Nat Med,* 16**,** 1450-5.

RIIHILA, P., NISSINEN, L., FARSHCHIAN, M., KIVISAARI, A., ALA-AHO, R., KALLAJOKI, M., GRENMAN, R., MERI, S., PELTONEN, S., PELTONEN, J. & KAHARI, V. M. 2015. Complement factor I promotes progression of cutaneous squamous cell carcinoma. *J Invest Dermatol,* 135**,** 579-88.

RIIHILA, P. M., NISSINEN, L. M., ALA-AHO, R., KALLAJOKI, M., GRENMAN, R., MERI, S., PELTONEN, S., PELTONEN, J. & KAHARI, V. M. 2014. Complement factor H: a biomarker for progression of cutaneous squamous cell carcinoma. *J Invest Dermatol,* 134**,** 498-506.

RITPRAJAK, P., HASHIGUCHI, M., TSUSHIMA, F., CHALERMSARP, N. & AZUMA, M. 2010. Keratinocyte-associated B7-H1 directly regulates cutaneous effector CD8+ T cell responses. *J Immunol,* 184**,** 4918-25.

RIZVI, N. A., HELLMANN, M. D., SNYDER, A., KVISTBORG, P., MAKAROV, V., HAVEL, J. J., LEE, W., YUAN, J., WONG, P., HO, T. S., MILLER, M. L., REKHTMAN, N., MOREIRA, A. L., IBRAHIM, F., BRUGGEMAN, C., GASMI, B., ZAPPASODI, R., MAEDA, Y., SANDER, C., GARON, E. B., MERGHOUB, T., WOLCHOK, J. D., SCHUMACHER, T. N. & CHAN, T. A. 2015. Cancer immunology. Mutational landscape determines sensitivity to PD-1 blockade in non-small cell lung cancer. *Science,* 348**,** 124-8.

ROBERT, C., SCHACHTER, J., LONG, G. V., ARANCE, A., GROB, J. J., MORTIER, L., DAUD, A., CARLINO, M. S., MCNEIL, C., LOTEM, M., LARKIN, J., LORIGAN, P., NEYNS, B., BLANK, C. U., HAMID, O., MATEUS, C., SHAPIRA-FROMMER, R., KOSH, M., ZHOU, H., IBRAHIM, N., EBBINGHAUS, S., RIBAS, A. & INVESTIGATORS, K.-. 2015. Pembrolizumab versus ipilimumab in advanced melanoma. *N Engl J Med,* 372**,** 2521-32.

ROBERT, C., THOMAS, L., BONDARENKO, I., O'DAY, S., WEBER, J., GARBE, C., LEBBE, C., BAURAIN, J. F., TESTORI, A., GROB, J. J., DAVIDSON, N., RICHARDS, J., MAIO, M., HAUSCHILD, A., MILLER, W. H., JR., GASCON, P., LOTEM, M., HARMANKAYA, K., IBRAHIM, R., FRANCIS, S., CHEN, T. T., HUMPHREY, R., HOOS, A. & WOLCHOK, J. D. 2011. Ipilimumab plus dacarbazine for previously untreated metastatic melanoma. *N Engl J Med,* 364**,** 2517-26.

ROBERT, L., TSOI, J., WANG, X., EMERSON, R., HOMET, B., CHODON, T., MOK, S., HUANG, R. R., COCHRAN, A. J., COMIN-ANDUIX, B., KOYA, R. C., GRAEBER, T. G., ROBINS, H. & RIBAS, A. 2014. CTLA4 blockade broadens the peripheral T-cell receptor repertoire. *Clin Cancer Res,* 20**,** 2424-32.

ROBINSON, S., DIXON, S., AUGUST, S., DIFFEY, B., WAKAMATSU, K., ITO, S., FRIEDMANN, P. S. & HEALY, E. 2010. Protection against UVR involves MC1R-mediated non-pigmentary and pigmentary mechanisms in vivo. *J Invest Dermatol,* 130**,** 1904-13.

ROBINSON, S. N., ZENS, M. S., PERRY, A. E., SPENCER, S. K., DUELL, E. J. & KARAGAS, M. R. 2013. Photosensitizing agents and the risk of non-melanoma skin cancer: a population-based case-control study. *J Invest Dermatol,* 133**,** 1950-5.

ROGERS, L. M., RIORDAN, J. D., SWICK, B. L., MEYERHOLZ, D. K. & DUPUY, A. J. 2013. Ectopic expression of Zmiz1 induces cutaneous squamous cell malignancies in a mouse model of cancer. *J Invest Dermatol,* 133**,** 1863-9.

ROMANO, E., KUSIO-KOBIALKA, M., FOUKAS, P. G., BAUMGAERTNER, P., MEYER, C., BALLABENI, P., MICHIELIN, O., WEIDE, B., ROMERO, P. & SPEISER, D. E. 2015. Ipilimumab-dependent cell-mediated cytotoxicity of regulatory T cells ex vivo by nonclassical monocytes in melanoma patients. *Proc Natl Acad Sci U S A,* 112**,** 6140-5.

ROSE, R. F., BOON, A., FORMAN, D., MERCHANT, W., BISHOP, R. & NEWTON-BISHOP, J. A. 2013. An exploration of reported mortality from cutaneous squamous cell carcinoma using death certification and cancer registry data. *Br J Dermatol,* 169**,** 682-6.

ROSENBERG, S. A. 2014. IL-2: the first effective immunotherapy for human cancer. *J Immunol,* 192**,** 5451-8.

ROSENBERG, S. A., SPIESS, P. & LAFRENIERE, R. 1986. A new approach to the adoptive immunotherapy of cancer with tumor-infiltrating lymphocytes. *Science,* 233**,** 1318-21.

ROSENBLUM, M. D., GRATZ, I. K., PAW, J. S., LEE, K., MARSHAK-ROTHSTEIN, A. & ABBAS, A. K. 2011. Response to self antigen imprints regulatory memory in tissues. *Nature,* 480**,** 538-42.

ROSSO, S., ZANETTI, R., MARTINEZ, C., TORMO, M. J., SCHRAUB, S., SANCHO-GARNIER, H., FRANCESCHI, S., GAFA, L., PEREA, E., NAVARRO, C., LAURENT, R., SCHRAMECK, C., TALAMINI, R., TUMINO, R. & WECHSLER, J. 1996. The multicentre south European study 'Helios'. II: Different sun exposure patterns in the aetiology of basal cell and squamous cell carcinomas of the skin. *Br J Cancer,* 73**,** 1447-54.

ROWE, D. E., CARROLL, R. J. & DAY, C. L., JR. 1992. Prognostic factors for local recurrence, metastasis, and survival rates in squamous cell carcinoma of the skin, ear, and lip. Implications for treatment modality selection. *J Am Acad Dermatol,* 26**,** 976-90.

ROYCHOUDHURI, R., HIRAHARA, K., MOUSAVI, K., CLEVER, D., KLEBANOFF, C. A., BONELLI, M., SCIUME, G., ZARE, H., VAHEDI, G., DEMA, B., YU, Z., LIU, H., TAKAHASHI, H., RAO, M., MURANSKI, P., CROMPTON, J. G., PUNKOSDY, G., BEDOGNETTI, D., WANG, E., HOFFMANN, V., RIVERA, J., MARINCOLA, F. M., NAKAMURA, A., SARTORELLI, V., KANNO, Y., GATTINONI, L., MUTO, A., IGARASHI, K., O'SHEA, J. J. & RESTIFO, N. P. 2013. BACH2 represses effector programs to stabilize T(reg)-mediated immune homeostasis. *Nature,* 498**,** 506-10.

RUBTSOV, Y. P., NIEC, R. E., JOSEFOWICZ, S., LI, L., DARCE, J., MATHIS, D., BENOIST, C. & RUDENSKY, A. Y. 2010. Stability of the regulatory T cell lineage in vivo. *Science,* 329**,** 1667-71.

RUBTSOV, Y. P., RASMUSSEN, J. P., CHI, E. Y., FONTENOT, J., CASTELLI, L., YE, X., TREUTING, P., SIEWE, L., ROERS, A., HENDERSON, W. R., JR., MULLER, W. & RUDENSKY, A. Y. 2008. Regulatory T cell-derived interleukin-10 limits inflammation at environmental interfaces. *Immunity,* 28**,** 546-58.

SAITO, T., NISHIKAWA, H., WADA, H., NAGANO, Y., SUGIYAMA, D., ATARASHI, K., MAEDA, Y., HAMAGUCHI, M., OHKURA, N., SATO, E., NAGASE, H., NISHIMURA, J., YAMAMOTO, H., TAKIGUCHI, S., TANOUE, T., SUDA, W., MORITA, H., HATTORI, M., HONDA, K., MORI, M., DOKI, Y. & SAKAGUCHI, S. 2016. Two FOXP3(+)CD4(+) T cell subpopulations distinctly control the prognosis of colorectal cancers. *Nat Med,* 22**,** 679-84.

SAKAGUCHI, S., MIYARA, M., COSTANTINO, C. M. & HAFLER, D. A. 2010. FOXP3+ regulatory T cells in the human immune system. *Nat Rev Immunol,* 10**,** 490-500.

SAKAGUCHI, S., SAKAGUCHI, N., ASANO, M., ITOH, M. & TODA, M. 1995. Immunologic self-tolerance maintained by activated T cells expressing IL-2 receptor alpha-chains (CD25). Breakdown of a single mechanism of self-tolerance causes various autoimmune diseases. *J Immunol,* 155**,** 1151-64.

SAKAGUCHI, S., VIGNALI, D. A., RUDENSKY, A. Y., NIEC, R. E. & WALDMANN, H. 2013. The plasticity and stability of regulatory T cells. *Nat Rev Immunol,* 13**,** 461-7.

SAKUISHI, K., APETOH, L., SULLIVAN, J. M., BLAZAR, B. R., KUCHROO, V. K. & ANDERSON, A. C. 2010. Targeting Tim-3 and PD-1 pathways to reverse T cell exhaustion and restore anti-tumor immunity. *J Exp Med,* 207**,** 2187-94.

SALAMA, P., PHILLIPS, M., GRIEU, F., MORRIS, M., ZEPS, N., JOSEPH, D., PLATELL, C. & IACOPETTA, B. 2009. Tumor-infiltrating FOXP3+ T regulatory cells show strong prognostic significance in colorectal cancer. *J Clin Oncol,* 27**,** 186-92.

SALLUSTO, F., LENIG, D., FORSTER, R., LIPP, M. & LANZAVECCHIA, A. 1999. Two subsets of memory T lymphocytes with distinct homing potentials and effector functions. *Nature,* 401**,** 708-12.

SAMSTEIN, R. M., ARVEY, A., JOSEFOWICZ, S. Z., PENG, X., REYNOLDS, A., SANDSTROM, R., NEPH, S., SABO, P., KIM, J. M., LIAO, W., LI, M. O., LESLIE, C., STAMATOYANNOPOULOS, J. A. & RUDENSKY, A. Y. 2012a. Foxp3 exploits a pre-existent enhancer landscape for regulatory T cell lineage specification. *Cell,* 151**,** 153-66.

SAMSTEIN, R. M., JOSEFOWICZ, S. Z., ARVEY, A., TREUTING, P. M. & RUDENSKY, A. Y. 2012b. Extrathymic generation of regulatory T cells in placental mammals mitigates maternal-fetal conflict. *Cell,* 150**,** 29-38.

SARCHIO, S. N., SCOLYER, R. A., BEAUGIE, C., MCDONALD, D., MARSH-WAKEFIELD, F., HALLIDAY, G. M. & BYRNE, S. N. 2014. Pharmacologically antagonizing the CXCR4-CXCL12 chemokine pathway with AMD3100 inhibits sunlight-induced skin cancer. *J Invest Dermatol,* 134**,** 1091-100.

SARFF, M., EDWARDS, D., DHUNGEL, B., WEGMANN, K. W., CORLESS, C., WEINBERG, A. D. & VETTO, J. T. 2008. OX40 (CD134) expression in sentinel lymph nodes correlates with prognostic features of primary melanomas. *Am J Surg,* 195**,** 621-5.

SATCHELL, A. C., BARNETSON, R. S. & HALLIDAY, G. M. 2004. Increased Fas ligand expression by T cells and tumour cells in the progression of actinic keratosis to squamous cell carcinoma. *Br J Dermatol,* 151**,** 42-9.

SATHER, B. D., TREUTING, P., PERDUE, N., MIAZGOWICZ, M., FONTENOT, J. D., RUDENSKY, A. Y. & CAMPBELL, D. J. 2007. Altering the distribution of Foxp3(+) regulatory T cells results in tissue-specific inflammatory disease. *J Exp Med,* 204**,** 1335-47.

SATO, E., OLSON, S. H., AHN, J., BUNDY, B., NISHIKAWA, H., QIAN, F., JUNGBLUTH, A. A., FROSINA, D., GNJATIC, S., AMBROSONE, C., KEPNER, J., ODUNSI, T., RITTER, G., LELE, S., CHEN, Y. T., OHTANI, H., OLD, L. J. & ODUNSI, K. 2005. Intraepithelial CD8+ tumor-infiltrating lymphocytes and a high CD8+/regulatory T cell ratio are associated with favorable prognosis in ovarian cancer. *Proc Natl Acad Sci U S A,* 102**,** 18538-43.

SCHAERLI, P., EBERT, L., WILLIMANN, K., BLASER, A., ROOS, R. S., LOETSCHER, P. & MOSER, B. 2004. A skin-selective homing mechanism for human immune surveillance T cells. *J Exp Med,* 199**,** 1265-75.

SCHAERLI, P., EBERT, L. M. & MOSER, B. 2006. Comment on "The vast majority of CLA+ T cells are resident in normal skin". *J Immunol,* 177**,** 1375-6; author reply 1376-7.

SCHARSCHMIDT, T. C., VASQUEZ, K. S., TRUONG, H. A., GEARTY, S. V., PAULI, M. L., NOSBAUM, A., GRATZ, I. K., OTTO, M., MOON, J. J., LIESE, J., ABBAS, A. K., FISCHBACH, M. A. & ROSENBLUM, M. D. 2015. A wave of regulatory T cells into neonatal skin mediates tolerance to commensal microbes. *Immunity,* 43**,** 1011-21.

SCHENKEL, J. M., FRASER, K. A., BEURA, L. K., PAUKEN, K. E., VEZYS, V. & MASOPUST, D. 2014. T cell memory. Resident memory CD8 T cells trigger protective innate and adaptive immune responses. *Science,* 346**,** 98-101.

SCHIETINGER, A. & GREENBERG, P. D. 2014. Tolerance and exhaustion: defining mechanisms of T cell dysfunction. *Trends Immunol,* 35**,** 51-60.

SCHIETINGER, A., PHILIP, M., KRISNAWAN, V. E., CHIU, E. Y., DELROW, J. J., BASOM, R. S., LAUER, P., BROCKSTEDT, D. G., KNOBLAUGH, S. E., HAMMERLING, G. J., SCHELL, T. D., GARBI, N. & GREENBERG, P. D. 2016. Tumor-Specific T Cell Dysfunction Is a Dynamic Antigen-Driven Differentiation Program Initiated Early during Tumorigenesis. *Immunity,* 45**,** 389-401.

SCHIOPPA, T., MOORE, R., THOMPSON, R. G., ROSSER, E. C., KULBE, H., NEDOSPASOV, S., MAURI, C., COUSSENS, L. M. & BALKWILL, F. R. 2011. B regulatory cells and the tumor-promoting actions of TNF-alpha during squamous carcinogenesis. *Proc Natl Acad Sci U S A,* 108**,** 10662-7.

SCHIPMANN, S., WERMKER, K., SCHULZE, H. J., KLEINHEINZ, J. & BRUNNER, G. 2014. Cutaneous and oral squamous cell carcinoma-dual immunosuppression via recruitment of FOXP3+ regulatory T cells and endogenous tumour FOXP3 expression? *J Craniomaxillofac Surg,* 42**,** 1827-33.

SCHMITT, D. A., OWEN-SCHAUB, L. & ULLRICH, S. E. 1995. Effect of IL-12 on immune suppression and suppressor cell induction by ultraviolet radiation. *J Immunol,* 154**,** 5114-20.

SCHMITT, J., SEIDLER, A., DIEPGEN, T. L. & BAUER, A. 2011. Occupational ultraviolet light exposure increases the risk for the development of cutaneous squamous cell carcinoma: a systematic review and meta-analysis. *Br J Dermatol,* 164**,** 291-307.

SCHREIBER, R. D., OLD, L. J. & SMYTH, M. J. 2011. Cancer immunoediting: integrating immunity's roles in cancer suppression and promotion. *Science,* 331**,** 1565-70.

SCHUBERT, D., BODE, C., KENEFECK, R., HOU, T. Z., WING, J. B., KENNEDY, A., BULASHEVSKA, A., PETERSEN, B. S., SCHAFFER, A. A., GRUNING, B. A., UNGER, S., FREDE, N., BAUMANN, U., WITTE, T., SCHMIDT, R. E., DUECKERS, G., NIEHUES, T., SENEVIRATNE, S., KANARIOU, M., SPECKMANN, C., EHL, S., RENSING-EHL, A., WARNATZ, K., RAKHMANOV, M., THIMME, R., HASSELBLATT, P., EMMERICH, F., CATHOMEN, T., BACKOFEN, R., FISCH, P., SEIDL, M., MAY, A., SCHMITT-GRAEFF, A., IKEMIZU, S., SALZER, U., FRANKE, A., SAKAGUCHI, S., WALKER, L. S., SANSOM, D. M. & GRIMBACHER, B. 2014. Autosomal dominant immune dysregulation syndrome in humans with CTLA4 mutations. *Nat Med,* 20**,** 1410-6.

SCHUMACHER, T. N. & SCHREIBER, R. D. 2015. Neoantigens in cancer immunotherapy. *Science,* 348**,** 69-74.

SCHWARZ, A., MAEDA, A., STANDER, S., VAN STEEG, H. & SCHWARZ, T. 2006. IL-18 reduces ultraviolet radiation-induced DNA damage and thereby affects photoimmunosuppression. *J Immunol,* 176**,** 2896-901.

SCHWARZ, A., MAEDA, A., WILD, M. K., KERNEBECK, K., GROSS, N., ARAGANE, Y., BEISSERT, S., VESTWEBER, D. & SCHWARZ, T. 2004. Ultraviolet radiation-induced regulatory T cells not only inhibit the induction but can suppress the effector phase of contact hypersensitivity. *J Immunol,* 172**,** 1036-43.

SCHWARZ, A., NOORDEGRAAF, M., MAEDA, A., TORII, K., CLAUSEN, B. E. & SCHWARZ, T. 2010. Langerhans cells are required for UVR-induced immunosuppression. *J Invest Dermatol,* 130**,** 1419-27.

SEDDIKI, N., SANTNER-NANAN, B., MARTINSON, J., ZAUNDERS, J., SASSON, S., LANDAY, A., SOLOMON, M., SELBY, W., ALEXANDER, S. I., NANAN, R., KELLEHER, A. & FAZEKAS DE ST GROTH, B. 2006. Expression of interleukin (IL)-2 and IL-7 receptors discriminates between human regulatory and activated T cells. *J Exp Med,* 203**,** 1693-700.

SENESCHAL, J., CLARK, R. A., GEHAD, A., BAECHER-ALLAN, C. M. & KUPPER, T. S. 2012. Human epidermal Langerhans cells maintain immune homeostasis in skin by activating skin resident regulatory T cells. *Immunity,* 36**,** 873-84.

SERRELS, A., LUND, T., SERRELS, B., BYRON, A., MCPHERSON, R. C., VON KRIEGSHEIM, A., GOMEZ-CUADRADO, L., CANEL, M., MUIR, M., RING, J. E., MANIATI, E., SIMS, A. H., PACHTER, J. A., BRUNTON, V. G., GILBERT, N., ANDERTON, S. M., NIBBS, R. J. & FRAME, M. C. 2015. Nuclear FAK controls chemokine transcription, Tregs, and evasion of anti-tumor immunity. *Cell,* 163**,** 160-73.

SETLOW, R. B. & CARRIER, W. L. 1964. The disappearance of thymine dimers from DNA: an error-correcting mechanism. *Proc Natl Acad Sci U S A,* 51**,** 226-31.

SETLOW, R. B., REGAN, J. D., GERMAN, J. & CARRIER, W. L. 1969. Evidence that xeroderma pigmentosum cells do not perform the first step in the repair of ultraviolet damage to their DNA. *Proc Natl Acad Sci U S A,* 64**,** 1035-41.

SETLOW, R. B. & SETLOW, J. K. 1962. Evidence that ultraviolet-induced thymine dimers in DNA cause biological damage. *Proc Natl Acad Sci U S A,* 48**,** 1250-7.

SHANKARAN, V., IKEDA, H., BRUCE, A. T., WHITE, J. M., SWANSON, P. E., OLD, L. J. & SCHREIBER, R. D. 2001. IFNgamma and lymphocytes prevent primary tumour development and shape tumour immunogenicity. *Nature,* 410**,** 1107-11.

SHARMA, M. D., HUANG, L., CHOI, J. H., LEE, E. J., WILSON, J. M., LEMOS, H., PAN, F., BLAZAR, B. R., PARDOLL, D. M., MELLOR, A. L., SHI, H. & MUNN, D. H. 2013. An inherently bifunctional subset of Foxp3+ T helper cells is controlled by the transcription factor eos. *Immunity,* 38**,** 998-1012.

SHEN, D. T., MA, J. S., MATHER, J., VUKMANOVIC, S. & RADOJA, S. 2006. Activation of primary T lymphocytes results in lysosome development and polarized granule exocytosis in CD4+ and CD8+ subsets, whereas expression of lytic molecules confers cytotoxicity to CD8+ T cells. *J Leukoc Biol,* 80**,** 827-37.

SHIMIZU, J., YAMAZAKI, S. & SAKAGUCHI, S. 1999. Induction of tumor immunity by removing CD25+CD4+ T cells: a common basis between tumor immunity and autoimmunity. *J Immunol,* 163**,** 5211-8.

SHIN, H., BLACKBURN, S. D., INTLEKOFER, A. M., KAO, C., ANGELOSANTO, J. M., REINER, S. L. & WHERRY, E. J. 2009. A role for the transcriptional repressor Blimp-1 in CD8(+) T cell exhaustion during chronic viral infection. *Immunity,* 31**,** 309-20.

SHIOW, L. R., ROSEN, D. B., BRDICKOVA, N., XU, Y., AN, J., LANIER, L. L., CYSTER, J. G. & MATLOUBIAN, M. 2006. CD69 acts downstream of interferon-alpha/beta to inhibit S1P1 and lymphocyte egress from lymphoid organs. *Nature,* 440**,** 540-4.

SHREEDHAR, V. K., PRIDE, M. W., SUN, Y., KRIPKE, M. L. & STRICKLAND, F. M. 1998. Origin and characteristics of ultraviolet-B radiation-induced suppressor T lymphocytes. *J Immunol,* 161**,** 1327-35.

SIEGLE, J. M., BASIN, A., SASTRE-PERONA, A., YONEKUBO, Y., BROWN, J., SENNETT, R., RENDL, M., TSIRIGOS, A., CARUCCI, J. A. & SCHOBER, M. 2014. SOX2 is a cancer-specific regulator of tumour initiating potential in cutaneous squamous cell carcinoma. *Nat Commun,* 5**,** 4511.

SILVERBERG, M. J., LEYDEN, W., WARTON, E. M., QUESENBERRY, C. P., JR., ENGELS, E. A. & ASGARI, M. M. 2013. HIV infection status, immunodeficiency, and the incidence of non-melanoma skin cancer. *J Natl Cancer Inst,* 105**,** 350-60.

SIMPSON, T. R., LI, F., MONTALVO-ORTIZ, W., SEPULVEDA, M. A., BERGERHOFF, K., ARCE, F., RODDIE, C., HENRY, J. Y., YAGITA, H., WOLCHOK, J. D., PEGGS, K. S., RAVETCH, J. V., ALLISON, J. P. & QUEZADA, S. A. 2013. Fc-dependent depletion of tumor-infiltrating regulatory T cells co-defines the efficacy of anti-CTLA-4 therapy against melanoma. *J Exp Med,* 210**,** 1695-710.

SINGER, M., WANG, C., CONG, L., MARJANOVIC, N. D., KOWALCZYK, M. S., ZHANG, H., NYMAN, J., SAKUISHI, K., KURTULUS, S., GENNERT, D., XIA, J., KWON, J. Y., NEVIN, J., HERBST, R. H., YANAI, I., ROZENBLATT-ROSEN, O., KUCHROO, V. K., REGEV, A. & ANDERSON, A. C. 2016. A Distinct Gene Module for Dysfunction Uncoupled from Activation in Tumor-Infiltrating T Cells. *Cell,* 166**,** 1500-1511 e9.

SINGH, A., SINGH, A., SAND, J. M., BAUER, S. J., HAFEEZ, B. B., MESKE, L. & VERMA, A. K. 2015. Topically applied Hsp90 inhibitor 17AAG inhibits UVR-induced cutaneous squamous cell carcinomas. *J Invest Dermatol,* 135**,** 1098-107.

SKON, C. N., LEE, J. Y., ANDERSON, K. G., MASOPUST, D., HOGQUIST, K. A. & JAMESON, S. C. 2013. Transcriptional downregulation of S1pr1 is required for the establishment of resident memory CD8+ T cells. *Nat Immunol,* 14**,** 1285-93.

SNYDER, A., MAKAROV, V., MERGHOUB, T., YUAN, J., ZARETSKY, J. M., DESRICHARD, A., WALSH, L. A., POSTOW, M. A., WONG, P., HO, T. S., HOLLMANN, T. J., BRUGGEMAN, C., KANNAN, K., LI, Y., ELIPENAHLI, C., LIU, C., HARBISON, C. T., WANG, L., RIBAS, A., WOLCHOK, J. D. & CHAN, T. A. 2014. Genetic basis for clinical response to CTLA-4 blockade in melanoma. *N Engl J Med,* 371**,** 2189-99.

SOUTH, A. P., PURDIE, K. J., WATT, S. A., HALDENBY, S., DEN BREEMS, N. Y., DIMON, M., ARRON, S. T., KLUK, M. J., ASTER, J. C., MCHUGH, A., XUE, D. J., DAYAL, J. H., ROBINSON, K. S., RIZVI, S. M., PROBY, C. M., HARWOOD, C. A. & LEIGH, I. M. 2014. NOTCH1 mutations occur early during cutaneous squamous cell carcinogenesis. *J Invest Dermatol,* 134**,** 2630-8.

SPEISER, D. E., UTZSCHNEIDER, D. T., OBERLE, S. G., MUNZ, C., ROMERO, P. & ZEHN, D. 2014. T cell differentiation in chronic infection and cancer: functional adaptation or exhaustion? *Nat Rev Immunol,* 14**,** 768-74.

SPRANGER, S., BAO, R. & GAJEWSKI, T. F. 2015. Melanoma-intrinsic beta-catenin signalling prevents anti-tumour immunity. *Nature,* 523**,** 231-5.

STACEY, S. N., SULEM, P., MASSON, G., GUDJONSSON, S. A., THORLEIFSSON, G., JAKOBSDOTTIR, M., SIGURDSSON, A., GUDBJARTSSON, D. F., SIGURGEIRSSON, B., BENEDIKTSDOTTIR, K. R., THORISDOTTIR, K., RAGNARSSON, R., SCHERER, D., HEMMINKI, K., RUDNAI, P., GURZAU, E., KOPPOVA, K., BOTELLA-ESTRADA, R., SORIANO, V., JUBERIAS, P., SAEZ, B., GILABERTE, Y., FUENTELSAZ, V., CORREDERA, C., GRASA, M., HOIOM, V., LINDBLOM, A., BONENKAMP, J. J., VAN ROSSUM, M. M., ABEN, K. K., DE VRIES, E., SANTINAMI, M., DI MAURO, M. G., MAURICHI, A., WENDT, J., HOCHLEITNER, P., PEHAMBERGER, H., GUDMUNDSSON, J., MAGNUSDOTTIR, D. N., GRETARSDOTTIR, S., HOLM, H., STEINTHORSDOTTIR, V., FRIGGE, M. L., BLONDAL, T., SAEMUNDSDOTTIR, J., BJARNASON, H., KRISTJANSSON, K., BJORNSDOTTIR, G., OKAMOTO, I., RIVOLTINI, L., RODOLFO, M., KIEMENEY, L. A., HANSSON, J., NAGORE, E., MAYORDOMO, J. I., KUMAR, R., KARAGAS, M. R., NELSON, H. H., GULCHER, J. R., RAFNAR, T., THORSTEINSDOTTIR, U., OLAFSSON, J. H., KONG, A. & STEFANSSON, K. 2009. New common variants affecting susceptibility to basal cell carcinoma. *Nat Genet,* 41**,** 909-14.

STARON, M. M., GRAY, S. M., MARSHALL, H. D., PARISH, I. A., CHEN, J. H., PERRY, C. J., CUI, G., LI, M. O. & KAECH, S. M. 2014. The transcription factor FoxO1 sustains expression of the inhibitory receptor PD-1 and survival of antiviral CD8(+) T cells during chronic infection. *Immunity,* 41**,** 802-14.

STEIN, P., RECHTSTEINER, G., WARGER, T., BOPP, T., FUHR, T., PRUFER, S., PROBST, H. C., STASSEN, M., LANGGUTH, P., SCHILD, H. & RADSAK, M. P. 2011. UV exposure boosts transcutaneous immunization and improves tumor immunity: cytotoxic T-cell priming through the skin. *J Invest Dermatol,* 131**,** 211-9.

STEMBERGER, C., HUSTER, K. M., KOFFLER, M., ANDERL, F., SCHIEMANN, M., WAGNER, H. & BUSCH, D. H. 2007. A single naive CD8+ T cell precursor can develop into diverse effector and memory subsets. *Immunity,* 27**,** 985-97.

STRAUSS, G. H., BRIDGES, B. A., GREAVES, M., HALL-SMITH, P., PRICE, M. & VELLA-BRIFFA, D. 1980. Inhibition of delayed hypersensitivity reaction in skin (DNCB test) by 8-methoxypsoralen photochemotherapy. Possible basis for pseudo-promoting action in skin carcinogenesis? *Lancet,* 2**,** 556-9.

STRAUSS, L., BERGMANN, C., SZCZEPANSKI, M., GOODING, W., JOHNSON, J. T. & WHITESIDE, T. L. 2007. A unique subset of CD4+CD25highFoxp3+ T cells secreting interleukin-10 and transforming growth factor-beta1 mediates suppression in the tumor microenvironment. *Clin Cancer Res,* 13**,** 4345-54.

STRID, J., ROBERTS, S. J., FILLER, R. B., LEWIS, J. M., KWONG, B. Y., SCHPERO, W., KAPLAN, D. H., HAYDAY, A. C. & GIRARDI, M. 2008. Acute upregulation of an NKG2D ligand promotes rapid reorganization of a local immune

compartment with pleiotropic effects on carcinogenesis. *Nat Immunol,* 9**,** 146-54.

STROME, S. E., DONG, H., TAMURA, H., VOSS, S. G., FLIES, D. B., TAMADA, K., SALOMAO, D., CHEVILLE, J., HIRANO, F., LIN, W., KASPERBAUER, J. L., BALLMAN, K. V. & CHEN, L. 2003. B7-H1 blockade augments adoptive T-cell immunotherapy for squamous cell carcinoma. *Cancer Res,* 63**,** 6501-5.

STUMPFOVA, M., RATNER, D., DESCIAK, E. B., ELIEZRI, Y. D. & OWENS, D. M. 2010. The immunosuppressive surface ligand CD200 augments the metastatic capacity of squamous cell carcinoma. *Cancer Res,* 70**,** 2962-72.

SU, F., VIROS, A., MILAGRE, C., TRUNZER, K., BOLLAG, G., SPLEISS, O., REIS-FILHO, J. S., KONG, X., KOYA, R. C., FLAHERTY, K. T., CHAPMAN, P. B., KIM, M. J., HAYWARD, R., MARTIN, M., YANG, H., WANG, Q., HILTON, H., HANG, J. S., NOE, J., LAMBROS, M., GEYER, F., DHOMEN, N., NICULESCU-DUVAZ, I., ZAMBON, A., NICULESCU-DUVAZ, D., PREECE, N., ROBERT, L., OTTE, N. J., MOK, S., KEE, D., MA, Y., ZHANG, C., HABETS, G., BURTON, E. A., WONG, B., NGUYEN, H., KOCKX, M., ANDRIES, L., LESTINI, B., NOLOP, K. B., LEE, R. J., JOE, A. K., TROY, J. L., GONZALEZ, R., HUTSON, T. E., PUZANOV, I., CHMIELOWSKI, B., SPRINGER, C. J., MCARTHUR, G. A., SOSMAN, J. A., LO, R. S., RIBAS, A. & MARAIS, R. 2012. RAS mutations in cutaneous squamous-cell carcinomas in patients treated with BRAF inhibitors. *N Engl J Med,* 366**,** 207-15.

SUGIYAMA, D., NISHIKAWA, H., MAEDA, Y., NISHIOKA, M., TANEMURA, A., KATAYAMA, I., EZOE, S., KANAKURA, Y., SATO, E., FUKUMORI, Y., KARBACH, J., JAGER, E. & SAKAGUCHI, S. 2013. Anti-CCR4 mAb selectively depletes effector-type FoxP3+CD4+ regulatory T cells, evoking antitumor immune responses in humans. *Proc Natl Acad Sci U S A,* 110**,** 17945-50.

TAN, W., ZHANG, W., STRASNER, A., GRIVENNIKOV, S., CHENG, J. Q., HOFFMAN, R. M. & KARIN, M. 2011. Tumour-infiltrating regulatory T cells stimulate mammary cancer metastasis through RANKL-RANK signalling. *Nature,* 470**,** 548-53.

TANG, Q., ADAMS, J. Y., TOOLEY, A. J., BI, M., FIFE, B. T., SERRA, P., SANTAMARIA, P., LOCKSLEY, R. M., KRUMMEL, M. F. & BLUESTONE, J. A. 2006. Visualizing regulatory T cell control of autoimmune responses in nonobese diabetic mice. *Nat Immunol,* 7**,** 83-92.

TANG, X., ZHU, Y., HAN, L., KIM, A. L., KOPELOVICH, L., BICKERS, D. R. & ATHAR, M. 2007. CP-31398 restores mutant p53 tumor suppressor function and inhibits UVB-induced skin carcinogenesis in mice. *J Clin Invest,* 117**,** 3753-64.

TARABAN, V. Y., ROWLEY, T. F., O'BRIEN, L., CHAN, H. T., HASWELL, L. E., GREEN, M. H., TUTT, A. L., GLENNIE, M. J. & AL-SHAMKHANI, A. 2002. Expression and costimulatory effects of the TNF receptor superfamily members CD134 (OX40) and CD137 (4-1BB), and their role in the generation of anti-tumor immune responses. *Eur J Immunol,* 32**,** 3617-27.

THOMPSON, S. C., JOLLEY, D. & MARKS, R. 1993. Reduction of solar keratoses by regular sunscreen use. *N Engl J Med,* 329**,** 1147-51.

THORNTON, A. M., KORTY, P. E., TRAN, D. Q., WOHLFERT, E. A., MURRAY, P. E., BELKAID, Y. & SHEVACH, E. M. 2010. Expression of Helios, an Ikaros

transcription factor family member, differentiates thymic-derived from peripherally induced Foxp3+ T regulatory cells. *J Immunol,* 184**,** 3433-41.

THORNTON, A. M. & SHEVACH, E. M. 1998. CD4+CD25+ immunoregulatory T cells suppress polyclonal T cell activation in vitro by inhibiting interleukin 2 production. *J Exp Med,* 188**,** 287-96.

TOEWS, G. B., BERGSTRESSER, P. R. & STREILEIN, J. W. 1980. Epidermal Langerhans cell density determines whether contact hypersensitivity or unresponsiveness follows skin painting with DNFB. *J Immunol,* 124**,** 445-53.

TOICHI, E., LU, K. Q., SWICK, A. R., MCCORMICK, T. S. & COOPER, K. D. 2008. Skin-infiltrating monocytes/macrophages migrate to draining lymph nodes and produce IL-10 after contact sensitizer exposure to UV-irradiated skin. *J Invest Dermatol,* 128**,** 2705-15.

TOPALIAN, S. L., HODI, F. S., BRAHMER, J. R., GETTINGER, S. N., SMITH, D. C., MCDERMOTT, D. F., POWDERLY, J. D., CARVAJAL, R. D., SOSMAN, J. A., ATKINS, M. B., LEMING, P. D., SPIGEL, D. R., ANTONIA, S. J., HORN, L., DRAKE, C. G., PARDOLL, D. M., CHEN, L., SHARFMAN, W. H., ANDERS, R. A., TAUBE, J. M., MCMILLER, T. L., XU, H., KORMAN, A. J., JURE-KUNKEL, M., AGRAWAL, S., MCDONALD, D., KOLLIA, G. D., GUPTA, A., WIGGINTON, J. M. & SZNOL, M. 2012. Safety, activity, and immune correlates of anti-PD-1 antibody in cancer. *N Engl J Med,* 366**,** 2443-54.

TORO, J., TURNER, M. & GAHL, W. A. 1999. Dermatologic manifestations of Hermansky-Pudlak syndrome in patients with and without a 16-base pair duplication in the HPS1 gene. *Arch Dermatol,* 135**,** 774-80.

TUMEH, P. C., HARVIEW, C. L., YEARLEY, J. H., SHINTAKU, I. P., TAYLOR, E. J., ROBERT, L., CHMIELOWSKI, B., SPASIC, M., HENRY, G., CIOBANU, V., WEST, A. N., CARMONA, M., KIVORK, C., SEJA, E., CHERRY, G., GUTIERREZ, A. J., GROGAN, T. R., MATEUS, C., TOMASIC, G., GLASPY, J. A., EMERSON, R. O., ROBINS, H., PIERCE, R. H., ELASHOFF, D. A., ROBERT, C. & RIBAS, A. 2014. PD-1 blockade induces responses by inhibiting adaptive immune resistance. *Nature,* 515**,** 568-71.

TURNIS, M. E., SAWANT, D. V., SZYMCZAK-WORKMAN, A. L., ANDREWS, L. P., DELGOFFE, G. M., YANO, H., BERES, A. J., VOGEL, P., WORKMAN, C. J. & VIGNALI, D. A. 2016. Interleukin-35 Limits Anti-Tumor Immunity. *Immunity,* 44**,** 316-29.

ULLRICH, S. E. 1994. Mechanism involved in the systemic suppression of antigen-presenting cell function by UV irradiation. Keratinocyte-derived IL-10 modulates antigen-presenting cell function of splenic adherent cells. *J Immunol,* 152**,** 3410-6.

UTZSCHNEIDER, D. T., ALFEI, F., ROELLI, P., BARRAS, D., CHENNUPATI, V., DARBRE, S., DELORENZI, M., PINSCHEWER, D. D. & ZEHN, D. 2016. High antigen levels induce an exhausted phenotype in a chronic infection without impairing T cell expansion and survival. *J Exp Med,* 213**,** 1819-34.

VAJDIC, C. M., MCDONALD, S. P., MCCREDIE, M. R., VAN LEEUWEN, M. T., STEWART, J. H., LAW, M., CHAPMAN, J. R., WEBSTER, A. C., KALDOR, J. M. & GRULICH, A. E. 2006. Cancer incidence before and after kidney transplantation. *JAMA,* 296**,** 2823-31.

VALLEJO-TORRES, L., MORRIS, S., KINGE, J. M., POIRIER, V. & VERNE, J. 2014. Measuring current and future cost of skin cancer in England. *J Public Health (Oxf),* 36**,** 140-8.

VALVERDE, P., HEALY, E., JACKSON, I., REES, J. L. & THODY, A. J. 1995. Variants of the melanocyte-stimulating hormone receptor gene are associated with red hair and fair skin in humans. *Nat Genet,* 11**,** 328-30.

VALVERDE, P., HEALY, E., SIKKINK, S., HALDANE, F., THODY, A. J., CAROTHERS, A., JACKSON, I. J. & REES, J. L. 1996. The Asp84Glu variant of the melanocortin 1 receptor (MC1R) is associated with melanoma. *Hum Mol Genet,* 5**,** 1663-6.

VALZASINA, B., PICONESE, S., GUIDUCCI, C. & COLOMBO, M. P. 2006. Tumor-induced expansion of regulatory T cells by conversion of CD4+CD25- lymphocytes is thymus and proliferation independent. *Cancer Res,* 66**,** 4488-95.

VAN ALLEN, E. M., MIAO, D., SCHILLING, B., SHUKLA, S. A., BLANK, C., ZIMMER, L., SUCKER, A., HILLEN, U., FOPPEN, M. H., GOLDINGER, S. M., UTIKAL, J., HASSEL, J. C., WEIDE, B., KAEHLER, K. C., LOQUAI, C., MOHR, P., GUTZMER, R., DUMMER, R., GABRIEL, S., WU, C. J., SCHADENDORF, D. & GARRAWAY, L. A. 2015. Genomic correlates of response to CTLA-4 blockade in metastatic melanoma. *Science,* 350**,** 207-11.

VAN DER POLS, J. C., RUSSELL, A., BAUER, U., NEALE, R. E., KIMLIN, M. G. & GREEN, A. C. 2013. Vitamin D status and skin cancer risk independent of time outdoors: 11-year prospective study in an Australian community. *J Invest Dermatol,* 133**,** 637-41.

VAN DER POLS, J. C., WILLIAMS, G. M., PANDEYA, N., LOGAN, V. & GREEN, A. C. 2006. Prolonged prevention of squamous cell carcinoma of the skin by regular sunscreen use. *Cancer Epidemiol Biomarkers Prev,* 15**,** 2546-8.

VANDERGRIFF, T. W. B., P.R. 2012. Overview of basic science. *In:* BOLOGNIA, J. L. J., J.L.; SCHAFFER, J.V. (ed.) *Dermatology.* 3rd edition ed.: Elsevier.

VARGHESE, A. J. & WANG, S. Y. 1967. Ultraviolet irradiation of DNA in vitro and in vivo produces a 3d thymine-derived product. *Science,* 156**,** 955-7.

VENZA, I., VISALLI, M., TRIPODO, B., DE GRAZIA, G., LODDO, S., TETI, D. & VENZA, M. 2010a. FOXE1 is a target for aberrant methylation in cutaneous squamous cell carcinoma. *Br J Dermatol,* 162**,** 1093-7.

VENZA, M., CATALANO, T., VISALLI, M., VENZA, I., LENTINI, M., CURIA, M. C., MARIANI-COSTANTINI, R. & TETI, D. 2010b. Association of the DSS1 c.143G>A polymorphism with skin squamous cell carcinoma. *J Invest Dermatol,* 130**,** 1719-25.

VETTO, J. T., LUM, S., MORRIS, A., SICOTTE, M., DAVIS, J., LEMON, M. & WEINBERG, A. 1997. Presence of the T-cell activation marker OX-40 on tumor infiltrating lymphocytes and draining lymph node cells from patients with melanoma and head and neck cancers. *Am J Surg,* 174**,** 258-65.

VIGNALI, D. A., COLLISON, L. W. & WORKMAN, C. J. 2008. How regulatory T cells work. *Nat Rev Immunol,* 8**,** 523-32.

VOGELSTEIN, B., PAPADOPOULOS, N., VELCULESCU, V. E., ZHOU, S., DIAZ, L. A., JR. & KINZLER, K. W. 2013. Cancer genome landscapes. *Science,* 339**,** 1546-58.

VOLKER, M., MONE, M. J., KARMAKAR, P., VAN HOFFEN, A., SCHUL, W., VERMEULEN, W., HOEIJMAKERS, J. H., VAN DRIEL, R., VAN ZEELAND, A. A. & MULLENDERS, L. H. 2001. Sequential assembly of the nucleotide excision repair factors in vivo. *Mol Cell,* 8**,** 213-24.

VOO, K. S., BOVER, L., HARLINE, M. L., VIEN, L. T., FACCHINETTI, V., ARIMA, K., KWAK, L. W. & LIU, Y. J. 2013. Antibodies targeting human OX40 expand effector T cells and block inducible and natural regulatory T cell function. *J Immunol,* 191**,** 3641-50.

VOSKOBOINIK, I., WHISSTOCK, J. C. & TRAPANI, J. A. 2015. Perforin and granzymes: function, dysfunction and human pathology. *Nat Rev Immunol,* 15**,** 388-400.

VUKMANOVIC-STEJIC, M., AGIUS, E., BOOTH, N., DUNNE, P. J., LACY, K. E., REED, J. R., SOBANDE, T. O., KISSANE, S., SALMON, M., RUSTIN, M. H. & AKBAR, A. N. 2008. The kinetics of CD4+Foxp3+ T cell accumulation during a human cutaneous antigen-specific memory response in vivo. *J Clin Invest,* 118**,** 3639-50.

VUKMANOVIC-STEJIC, M., SANDHU, D., SEIDEL, J. A., PATEL, N., SOBANDE, T. O., AGIUS, E., JACKSON, S. E., FUENTES-DUCULAN, J., SUAREZ-FARINAS, M., MABBOTT, N. A., LACY, K. E., OGG, G., NESTLE, F. O., KRUEGER, J. G., RUSTIN, M. H. & AKBAR, A. N. 2015. The characterization of varicella zoster virus-specific T cells in skin and blood during aging. *J Invest Dermatol,* 135**,** 1752-62.

VUKMANOVIC-STEJIC, M., ZHANG, Y., COOK, J. E., FLETCHER, J. M., MCQUAID, A., MASTERS, J. E., RUSTIN, M. H., TAAMS, L. S., BEVERLEY, P. C., MACALLAN, D. C. & AKBAR, A. N. 2006. Human CD4+ CD25hi Foxp3+ regulatory T cells are derived by rapid turnover of memory populations in vivo. *J Clin Invest,* 116**,** 2423-33.

WAKITA, D., CHAMOTO, K., OHKURI, T., NARITA, Y., ASHINO, S., SUMIDA, K., NISHIKAWA, H., SHIKU, H., TOGASHI, Y., KITAMURA, H. & NISHIMURA, T. 2009. IFN-gamma-dependent type 1 immunity is crucial for immunosurveillance against squamous cell carcinoma in a novel mouse carcinogenesis model. *Carcinogenesis,* 30**,** 1408-15.

WALKER, L. S. & SANSOM, D. M. 2011. The emerging role of CTLA4 as a cell-extrinsic regulator of T cell responses. *Nat Rev Immunol,* 11**,** 852-63.

WALTER, A., BARYSCH, M. J., BEHNKE, S., DZIUNYCZ, P., SCHMID, B., RITTER, E., GNJATIC, S., KRISTIANSEN, G., MOCH, H., KNUTH, A., DUMMER, R. & VAN DEN BROEK, M. 2010. Cancer-testis antigens and immunosurveillance in human cutaneous squamous cell and basal cell carcinomas. *Clin Cancer Res,* 16**,** 3562-70.

WANG, L., JAMESON, S. C. & HOGQUIST, K. A. 2009. Epidermal Langerhans cells are not required for UV-induced immunosuppression. *J Immunol,* 183**,** 5548-53.

WANG, L., PINO-LAGOS, K., DE VRIES, V. C., GULERIA, I., SAYEGH, M. H. & NOELLE, R. J. 2008. Programmed death 1 ligand signaling regulates the generation of adaptive Foxp3+CD4+ regulatory T cells. *Proc Natl Acad Sci U S A,* 105**,** 9331-6.

WANG, N. J., SANBORN, Z., ARNETT, K. L., BAYSTON, L. J., LIAO, W., PROBY, C. M., LEIGH, I. M., COLLISSON, E. A., GORDON, P. B., JAKKULA, L., PENNYPACKER, S., ZOU, Y., SHARMA, M., NORTH, J. P., VEMULA, S. S., MAURO, T. M., NEUHAUS, I. M., LEBOIT, P. E., HUR, J. S., PARK, K., HUH, N., KWOK, P. Y., ARRON, S. T., MASSION, P. P., BALE, A. E., HAUSSLER, D., CLEAVER, J. E., GRAY, J. W., SPELLMAN, P. T., SOUTH, A. P., ASTER, J. C., BLACKLOW, S. C. & CHO, R. J. 2011. Loss-of-function mutations in Notch receptors in cutaneous and lung squamous cell carcinoma. *Proc Natl Acad Sci U S A,* 108**,** 17761-6.

WATT, S. A., PURDIE, K. J., DEN BREEMS, N. Y., DIMON, M., ARRON, S. T., MCHUGH, A. T., XUE, D. J., DAYAL, J. H., PROBY, C. M., HARWOOD, C. A., LEIGH, I. M. & SOUTH, A. P. 2015. Novel CARD11 mutations in human cutaneous squamous cell carcinoma lead to aberrant NF-kappaB regulation. *Am J Pathol,* 185**,** 2354-63.

WEHNER, M. R., SHIVE, M. L., CHREN, M. M., HAN, J., QURESHI, A. A. & LINOS, E. 2012. Indoor tanning and non-melanoma skin cancer: systematic review and meta-analysis. *BMJ,* 345**,** e5909.

WELSH, M. M., KARAGAS, M. R., KURIGER, J. K., HOUSEMAN, A., SPENCER, S. K., PERRY, A. E. & NELSON, H. H. 2011. Genetic determinants of UV-susceptibility in non-melanoma skin cancer. *PLoS One,* 6**,** e20019.

WERNER, R. N., SAMMAIN, A., ERDMANN, R., HARTMANN, V., STOCKFLETH, E. & NAST, A. 2013. The natural history of actinic keratosis: a systematic review. *Br J Dermatol,* 169**,** 502-18.

WESTERS-ATTEMA, A., JOOSTEN, V. M., ROOZEBOOM, M. H., NELEMANS, P. J., LOHMAN, B. G., BOTTERWECK, A. A., STEIJLEN, P. M., VAN MARION, A. M. & KELLENERS-SMEETS, N. W. 2015. Correlation between histological findings on punch biopsy specimens and subsequent excision specimens in cutaneous squamous cell carcinoma. *Acta Derm Venereol,* 95**,** 181-5.

WHERRY, E. J. & KURACHI, M. 2015. Molecular and cellular insights into T cell exhaustion. *Nat Rev Immunol,* 15**,** 486-99.

WHITE, A. C., KHUU, J. K., DANG, C. Y., HU, J., TRAN, K. V., LIU, A., GOMEZ, S., ZHANG, Z., YI, R., SCUMPIA, P., GRIGORIAN, M. & LOWRY, W. E. 2014. Stem cell quiescence acts as a tumour suppressor in squamous tumours. *Nat Cell Biol,* 16**,** 99-107.

WHITE, R. A., NEIMAN, J. M., REDDI, A., HAN, G., BIRLEA, S., MITRA, D., DIONNE, L., FERNANDEZ, P., MURAO, K., BIAN, L., KEYSAR, S. B., GOLDSTEIN, N. B., SONG, N., BORNSTEIN, S., HAN, Z., LU, X., WISELL, J., LI, F., SONG, J., LU, S. L., JIMENO, A., ROOP, D. R. & WANG, X. J. 2013. Epithelial stem cell mutations that promote squamous cell carcinoma metastasis. *J Clin Invest,* 123**,** 4390-404.

WILLIAMS, E. L., DUNN, S. N., JAMES, S., JOHNSON, P. W., CRAGG, M. S., GLENNIE, M. J. & GRAY, J. C. 2013. Immunomodulatory monoclonal antibodies combined with peptide vaccination provide potent immunotherapy in an aggressive murine neuroblastoma model. *Clin Cancer Res,* 19**,** 3545-55.

WILLIMSKY, G., CZEH, M., LODDENKEMPER, C., GELLERMANN, J., SCHMIDT, K., WUST, P., STEIN, H. & BLANKENSTEIN, T. 2008. Immunogenicity of premalignant lesions is the primary cause of general cytotoxic T lymphocyte unresponsiveness. *J Exp Med,* 205**,** 1687-700.

WILLOUGHBY, J. E., KERR, J. P., ROGEL, A., TARABAN, V. Y., BUCHAN, S. L., JOHNSON, P. W. & AL-SHAMKHANI, A. 2014. Differential impact of CD27 and 4-1BB costimulation on effector and memory CD8 T cell generation following peptide immunization. *J Immunol,* 193**,** 244-51.

WILSON, N. J., BONIFACE, K., CHAN, J. R., MCKENZIE, B. S., BLUMENSCHEIN, W. M., MATTSON, J. D., BASHAM, B., SMITH, K., CHEN, T., MOREL, F., LECRON, J. C., KASTELEIN, R. A., CUA, D. J., MCCLANAHAN, T. K., BOWMAN, E. P. & DE WAAL MALEFYT, R. 2007. Development, cytokine profile and function of human interleukin 17-producing helper T cells. *Nat Immunol,* 8**,** 950-7.

WING, K., ONISHI, Y., PRIETO-MARTIN, P., YAMAGUCHI, T., MIYARA, M., FEHERVARI, Z., NOMURA, T. & SAKAGUCHI, S. 2008. CTLA-4 control over Foxp3+ regulatory T cell function. *Science,* 322**,** 271-5.

WINKLER, A. E., BROTMAN, J. J., PITTMAN, M. E., JUDD, N. P., LEWIS, J. S., JR., SCHREIBER, R. D. & UPPALURI, R. 2011. CXCR3 enhances a T-cell-dependent epidermal proliferative response and promotes skin tumorigenesis. *Cancer Res,* 71**,** 5707-16.

WINKLER, J. K., SCHNEIDERBAUER, R., BENDER, C., SEDLACZEK, O., FROHLING, S., PENZEL, R., ENK, A. & HASSEL, J. C. 2016. Anti-programmed cell death-1 therapy in nonmelanoma skin cancer. *Br J Dermatol*.

WORLD HEALTH ORGANIZATION. 2015. *Ultraviolet radiation and the INTERSUN Programme; Skin cancers: How common is skin cancer?* [Online]. Available: http://www.who.int/uv/faq/skincancer/en/index1.html [Accessed 24 Aug 2015].

WU, X., ZHANG, H., XING, Q., CUI, J., LI, J., LI, Y., TAN, Y. & WANG, S. 2014. PD-1(+) CD8(+) T cells are exhausted in tumours and functional in draining lymph nodes of colorectal cancer patients. *Br J Cancer,* 111**,** 1391-9.

XIANG, F., LUCAS, R., HALES, S. & NEALE, R. 2014. Incidence of nonmelanoma skin cancer in relation to ambient UV radiation in white populations, 1978-2012: empirical relationships. *JAMA Dermatol,* 150**,** 1063-71.

XIONG, M. Y., RIZZO, A. E., COHEN, T. S., DYER, R. K., KORGAVKAR, K., BINGHAM, S. F., WEINSTOCK, M. A. & VETERANS AFFAIRS TOPICAL TRETINOIN CHEMOPREVENTION TRIAL, G. 2013. Predictors of squamous cell carcinoma in high-risk patients in the VATTC trial. *J Invest Dermatol,* 133**,** 1521-32.

YAMANE, H. & PAUL, W. E. 2012. Cytokines of the gamma(c) family control CD4+ T cell differentiation and function. *Nat Immunol,* 13**,** 1037-44.

YAMAZAKI, S., NISHIOKA, A., KASUYA, S., OHKURA, N., HEMMI, H., KAISHO, T., TAGUCHI, O., SAKAGUCHI, S. & MORITA, A. 2014. Homeostasis of thymus-derived Foxp3+ regulatory T cells is controlled by ultraviolet B exposure in the skin. *J Immunol,* 193**,** 5488-97.

YE, Q., SONG, D. G., POUSSIN, M., YAMAMOTO, T., BEST, A., LI, C., COUKOS, G. & POWELL, D. J., JR. 2014. CD137 accurately identifies and enriches for naturally occurring tumor-reactive T cells in tumor. *Clin Cancer Res,* 20**,** 44-55.

YIASEMIDES, E., SIVAPIRABU, G., HALLIDAY, G. M., PARK, J. & DAMIAN, D. L. 2009. Oral nicotinamide protects against ultraviolet radiation-induced immunosuppression in humans. *Carcinogenesis,* 30**,** 101-5.

YOKOSUKA, T., TAKAMATSU, M., KOBAYASHI-IMANISHI, W., HASHIMOTO-TANE, A., AZUMA, M. & SAITO, T. 2012. Programmed cell death 1 forms negative costimulatory microclusters that directly inhibit T cell receptor signaling by recruiting phosphatase SHP2. *J Exp Med,* 209**,** 1201-17.

YOUNGBLOOD, B., OESTREICH, K. J., HA, S. J., DURAISWAMY, J., AKONDY, R. S., WEST, E. E., WEI, Z., LU, P., AUSTIN, J. W., RILEY, J. L., BOSS, J. M. & AHMED, R. 2011. Chronic virus infection enforces demethylation of the locus that encodes PD-1 in antigen-specific CD8(+) T cells. *Immunity,* 35**,** 400-12.

YOUSSEF, K. K., VAN KEYMEULEN, A., LAPOUGE, G., BECK, B., MICHAUX, C., ACHOURI, Y., SOTIROPOULOU, P. A. & BLANPAIN, C. 2010. Identification of the cell lineage at the origin of basal cell carcinoma. *Nat Cell Biol,* 12**,** 299-305.

ZABA, L. C., KRUEGER, J. G. & LOWES, M. A. 2009. Resident and "inflammatory" dendritic cells in human skin. *J Invest Dermatol,* 129**,** 302-8.

ZELENAY, S., VAN DER VEEN, A. G., BOTTCHER, J. P., SNELGROVE, K. J., ROGERS, N., ACTON, S. E., CHAKRAVARTY, P., GIROTTI, M. R., MARAIS, R., QUEZADA, S. A., SAHAI, E. & REIS E SOUSA, C. 2015. Cyclooxygenase-dependent tumor growth through evasion of immunity. *Cell,* 162**,** 1257-70.

ZHANG, S., FUJITA, H., MITSUI, H., YANOFSKY, V. R., FUENTES-DUCULAN, J., PETTERSEN, J. S., SUAREZ-FARINAS, M., GONZALEZ, J., WANG, C. Q., KRUEGER, J. G., FELSEN, D. & CARUCCI, J. A. 2013. Increased Tc22 and Treg/CD8 ratio contribute to aggressive growth of transplant associated squamous cell carcinoma. *PLoS One,* 8**,** e62154.

ZHAO, L., LI, W., MARSHALL, C., GRIFFIN, T., HANSON, M., HICK, R., DENTCHEV, T., WILLIAMS, E., WERTH, A., MILLER, C., BASHIR, H., PEAR, W. & SEYKORA, J. T. 2009. Srcasm inhibits Fyn-induced cutaneous carcinogenesis with modulation of Notch1 and p53. *Cancer Res,* 69**,** 9439-47.

ZHENG, Y., CHAUDHRY, A., KAS, A., DEROOS, P., KIM, J. M., CHU, T. T., CORCORAN, L., TREUTING, P., KLEIN, U. & RUDENSKY, A. Y. 2009. Regulatory T-cell suppressor program co-opts transcription factor IRF4 to control T(H)2 responses. *Nature,* 458**,** 351-6.

ZHENG, Y., JOSEFOWICZ, S., CHAUDHRY, A., PENG, X. P., FORBUSH, K. & RUDENSKY, A. Y. 2010. Role of conserved non-coding DNA elements in the Foxp3 gene in regulatory T-cell fate. *Nature,* 463**,** 808-12.

ZHOU, G. & LEVITSKY, H. I. 2007. Natural regulatory T cells and de novo-induced regulatory T cells contribute independently to tumor-specific tolerance. *J Immunol,* 178**,** 2155-62.

ZHOU, L., CHONG, M. M. & LITTMAN, D. R. 2009. Plasticity of CD4+ T cell lineage differentiation. *Immunity,* 30**,** 646-55.

ZHOU, L., LOPES, J. E., CHONG, M. M., IVANOV, II, MIN, R., VICTORA, G. D., SHEN, Y., DU, J., RUBTSOV, Y. P., RUDENSKY, A. Y., ZIEGLER, S. F. & LITTMAN, D. R. 2008. TGF-beta-induced Foxp3 inhibits T(H)17 cell differentiation by antagonizing RORgammat function. *Nature,* 453**,** 236-40.

ZHU, J., PENG, T., JOHNSTON, C., PHASOUK, K., KASK, A. S., KLOCK, A., JIN, L., DIEM, K., KOELLE, D. M., WALD, A., ROBINS, H. & COREY, L. 2013. Immune surveillance by CD8alphaalpha+ skin-resident T cells in human herpes virus infection. *Nature,* 497**,** 494-7.

ZIEGLER, A., JONASON, A. S., LEFFELL, D. J., SIMON, J. A., SHARMA, H. W., KIMMELMAN, J., REMINGTON, L., JACKS, T. & BRASH, D. E. 1994. Sunburn and p53 in the onset of skin cancer. *Nature,* 372**,** 773-6.

ZINSELMEYER, B. H., HEYDARI, S., SACRISTAN, C., NAYAK, D., CAMMER, M., HERZ, J., CHENG, X., DAVIS, S. J., DUSTIN, M. L. & MCGAVERN, D. B. 2013. PD-1 promotes immune exhaustion by inducing antiviral T cell motility paralysis. *J Exp Med,* 210**,** 757-74.

ZOU, X. Y., DING, D., ZHAN, N., LIU, X. M., PAN, C. & XIA, Y. M. 2015. Glyoxalase I is differentially expressed in cutaneous neoplasms and contributes to the progression of squamous cell carcinoma. *J Invest Dermatol,* 135**,** 589-98.

Appendix A Details of cSCCs used in the study

Table 7.1 List of cSCCs excised by the author for the purpose of this study.

	sex	age	immuno-suppressed	maximum diameter (mm)	site	differentiation	maximum depth of invasion (mm)	perineural invasion	complete excision
1	m	88	no	10	R cheek	moderate	2		complete
2	m	87	no	20	scalp	moderate	4		complete
3	m	94	no	18	R forehead	moderate	6		complete
4	m	77	no	21	L forehead	moderate	5		complete
5	m	78	yes	28	R temple	poor	6		complete
6	m	72	no	22	R hand	moderate	4.5		complete
7	m	76	yes	15	R hand	well	2		complete
8	f	81	no	15	R hand	well	4		complete
9	m	60	no	15	L temple	moderate	5		complete
10	f	84	no	15	R cheek	well	2.9		complete
11	f	83	no	15	R upper leg	moderate	4		complete
12	m	52	no	15	behind L ear	well	3.2		complete
13	m	84	no	17	scalp	moderate	3.5		complete
14	f	86	no	20	L hand	well	5		complete
15	f	79	no	12	scalp	moderate	4.5		complete
16	f	77	no	14	R cheek	poor	2.1		complete
17	m	92	no	27	scalp	poor	5		complete
18	m	77	yes	15	R scalp	moderate	4.2	yes	complete
19	f	88	no	11	L calf	well	2.2		complete
20	f	85	yes	29	R forehead	moderate	9	yes	complete
21		75	no	12	L temple	moderate	6		complete
22	m	79	no	23	R hand	poor	3.8		complete
23	m	70	no	20	L ant scalp	mod	4.2		complete
24	f	89	no	23	L lower leg	poor	2.6		complete
25	m	82	no	25	R temple	poor	3.5		complete
26	m	75	no	20	L shin	well	4.6		complete
27	f	85	no	25	L shin	moderate	3.1		complete
28	m	81	no	22	scalp	moderate	4.5		complete
29	f	95	no	17	R lower leg superior	poor	1		complete
30	f	95	no	24	R lower leg inferior	well	1		complete
31	f	81	no	12	L lower leg	well	1.6		complete
32	f	88	no	17	R hand	well	7		complete
33	f	88	no	13	L shin	moderate	5		complete
34	m	72	no	23	R ear	well			complete
35	m	87	no	22	central forehead	moderate	8		complete
36	f	87	no	20	R shin	well	2.5		complete
37	m	91	no	17	R frontal scalp	poor	3		complete

	sex	age	immuno-suppressed	maximum diameter (mm)	site	differentiation	maximum depth of invasion (mm)	perineural invasion	complete excision
38	m	91	no	13	occipital scalp	moderate	4		complete
39	f	81	no	8	R lower leg	well	1.9		complete
42	m	95	no	19	scalp	poor	3.2		complete
43	f	68	no	16	back	well	2		complete
44	f	68	no	12	R arm	well	4		complete
45	f	78	no	15	R jawline	moderate	2		complete
46	f	90	no	17	L lower leg	moderate	3.5		complete
47	m	84	no	8	R hand	well	2.5		complete
48	f	87	no	10	R lower leg	moderate	3		complete
49	m	68	no	19	R hand	well	7.5		complete
50	f	82	no	21	R lower leg	poor	2.2		complete
51	m	86	no	18	R hand	well	3.5		complete
52	m	73	no	17	frontal scalp	well	5		complete
53	m	79	no	11	R temple	well	2.4		complete
54	m	79	no	18	frontal scalp	poor	3		complete
55	m	70	no	14	L wrist	poor	1.1		complete
56	m	79	no	9	R hand	moderate	2.8		complete
57	f	83	no	24	R temple	moderate	6	yes	present at deep margin
58	m	79	no	12	L hand	moderate	3		complete
59	m	78	no	20	R lower leg	well	2		complete
60	f	79	no	28	R cheek	moderate	5		complete
61	m	89	no	30	R upper arm	moderate	4		complete
62	m	51	no	20	L thigh	well	4.5		complete
63	f	94	no	20	L neck	poor	5		complete
64	f	94	no	15	scalp	moderate	6	yes	complete
65	m	80	no	15	L cheek	moderate	2		complete
66	m	88	no	35	L frontal scalp	moderate	9		complete
67	m	95	no	12	L cheek	moderate	3		complete
68	m	88	no	10	L neck	poor	7		complete
69	f	90	no	28	L forearm	poor	2.5		complete
70	m	80	no	17	R scalp	poor	2.5		complete
71	f	93	no	11	L shin	well	3.5		complete
72	f	88	no	19	L foot	poor	5.8		complete
73	m	87	no	18	R cheek	moderate	2		complete
74	m	87	no	25	L hand	well	1		complete
75	m	74	yes	9	L hand	well	1.5		complete
76	m	79	no	27	L shin	well	4		complete
77	m	66	no	22	L temple	moderate	5.2		present at deep margin
78	f	64	no	14	L hand	well	3		complete
79	f	87	no	19	R shin	moderate	1.9		complete
80	f	86	no	27	L forehead	moderate	13		complete

	sex	age	immuno-suppressed	maximum diameter (mm)	site	differentiation	maximum depth of invasion (mm)	perineural invasion	complete excision
81	m	84	no	9	L hand	moderate	3		complete
82	m	87	no	23	L forearm	poor	6.6		complete
83	m	78	no	17	scalp	poor	3		complete
84	m	57	no	27	R upper back	moderate	3		complete
85	m	77	yes	10	R forearm	moderate	4		complete
86	m	64	no	14	L cheek	moderate	4.5		complete
87	m	86	yes	17	L wrist	well	3.5		complete
88	f	87	no	15	L lower leg	poor	3.5		complete
89	f	85	no	30	L shin	well	2		complete
90	f	94	no	11	L hand	well	4		complete
91	m	78	yes	10	R hand	moderate	1		complete
92	m	73	no	10	R temple	moderate	4.3		complete
93	f	89	no	10	L cheek	moderate	6		complete
94	m	90	yes	15	R temple	poor	6	yes	complete
95	m	78	no	12	R temple	well	0.4		complete
96	m	74	no	18	R hand	well	3.7		complete
97	m	87	no	12	R neck	moderate	1.5		complete
98	m	61	no	20	chest	moderate	4.5		complete
99	m	83	no	8	R scalp	moderate	1.2		complete
100	m	81	no	11	R ear	well	2.6		complete
101	f	83	no	15	R lower leg	well	3		complete
102	m	92	no	10	R ear	well	1		complete
103	m	78	no	14	R shin	moderate	2.5		complete
104	m	63	no	14	L shoulder	well	2.8		complete
105	f	86	no	13	L lower leg	well	2.5		complete
106	m	68	no	13	R ear	moderate	1.5		complete
107	m	84	no	17	L temple	moderate	2.5		complete
108	m	80	no	18	posterior scalp	moderate	2.4		complete
109	m	88	yes	12	R forehead	moderate	3.5		complete
110	f	81	no	16	L lower leg	moderate	2.5		complete
111	f	60	no	24	L hand	moderate	3		complete
112	m	88	no	15	R forearm	well	5		complete
113	f	89	no	15	R lower leg	well	4.5		complete
114	m	69	yes	20	L scapular region	moderate	1		complete
115	m	71	no	16	L hand	moderate	2.5		complete
116	m	81	no	19	L forearm	moderate	3.5		complete
117	m	76	no	12	L ear	poor	7		complete
118	m	79	no	23	scalp	moderate	4.5		complete
119	m	89	no	12	scalp	moderate	4.8		present at deep margin
120	m	79	yes	9	scalp	moderate	1.5		complete
121	m	79	no	25	scalp	moderate	3.5		complete

	sex	age	immuno-suppressed	maximum diameter (mm)	site	differentiation	maximum depth of invasion (mm)	perineural invasion	complete excision
122	f	87	yes	12	R forehead	moderate	4		complete
123	m	81	no	17	chest	moderate	1.3		complete
124	f	86	no	15	L cheek	moderate	2.5		complete
125	m	82	no	22	scalp	moderate	3.7		complete
126	m	72	no	15	R temple	moderate	4		complete
127	m	76	no	13	R shin	moderate	3.5		complete
128	m	91	no	8	R ear	moderate	4		complete
129	f	73	no	13	L upper lip	moderate	5.5		complete
130	m	90	no	11	L ear	moderate	2.5		complete
131	f	83	no	13	L temple	moderate	3.5		complete
132	m	86	no	12	L parietal scalp	poor	4.8		complete
133	m	85	no	40	scalp	moderate	10		complete
134	m	79	yes	9	R lower leg	well	0.9		complete
135	m	82	no	21	scalp	moderate	3		complete
136	f	80	no	15	R hand	moderate	1.9		complete
137	f	92	yes	14	R forearm	moderate	1		complete
138	m	70	yes	10	scalp	moderate	3.5	yes	complete
139	f	85	no	10	R wrist	moderate	4		complete
140	m	72	no	12	R hand	well	1.7		complete
141	m	77	no	12	posterior scalp	moderate	4.1		complete
142	m	71	no	22	chest	moderate	9.5		complete
143	f	79	no	12	L upper forehead	well	1.9		complete
144	m	53	no	23	R forearm	moderate	3.5		complete
145	m	87	yes	30	L scalp	moderate	3		complete
146	m	85	no	36	R forehead	moderate	9		complete
147	f	86	no	11	L forehead	moderate	4.5		complete
148	m	90	no	18	R cheek	moderate	10		present at deep margin
149	m	78	no	11	L scalp	poor	2.3		complete
150	m	71	no	18	L scalp	moderate	5.5		complete
151	f	71	no	20	R foot	moderate	5.9		complete
152	m	90	no	20	R hand	moderate	2		complete
153	m	46	yes	10	R hand	moderate	1.5		complete
154	m	71	no	10	L chest	well	2		complete
155	m	68	no	11	frontal scalp	moderate	3.1		complete
156	m	81	no	18	R scalp	moderate	5		complete
157	m	83	no	13	L upper arm	well	5		complete
158	m	70	no	12	R hand	well	0.4		complete
159	f	100	no	19	R upper arm	poor	4		complete
160	m	76	no	26	L scalp	moderate	7		complete
161	m	82	no	11	L temple	poor	2		complete
162	m	51	no	45	R forearm	moderate	4		complete

	sex	age	immuno-suppressed	maximum diameter (mm)	site	differentiation	maximum depth of invasion (mm)	perineural invasion	complete excision
163	m	79	no	12	L ear	moderate	3		complete
164	m	65	no	14	scalp vertex	moderate	3.4		complete
165	f	99	no	20	L hand	moderate	2.5		complete
166	m	95	no	20	L upper back	poor	4.4		complete
167	m	82	yes	10	L upper chest	poor	3.1		complete
168	m	82	yes	8	R upper chest	moderate	1.1		complete
169	m	90	no	40	R chest	poor	12		complete
170	m	72	yes	10	right cheek	poor	2.2		complete
171	m	94	no	18	scalp vertex	moderate	6		complete
172	f	90	no	12	L mid upper leg	well	1.6		complete
173	f	90	no	12	R mid lower leg	well	2		complete
174	m	68	no	11	R cheek	moderate	4.5		complete
175	m	83	no	18	scalp vertex	moderate	1		complete
176	f	91	no	15	L shin	moderate	4.2		complete
177	m	84	yes	18	L forehead	poor	3	yes	complete
178	m	84	no	14	R lateral eye	moderate	4		complete
179	f	87	no	9	L foot	moderate	2		complete
180	m	72	yes	13	R forehead	moderate	5	yes	complete
181	m	79	no	11	L ear	moderate	2.5	yes	complete
182	f	61	yes	10	L hand	moderate	1.8		complete
183	f	92	no	32	L shin	well	6		complete
184	f	92	no	23	R medial lower leg	well	5		complete
185	m	85	no	12	R parietal scalp	moderate	3		complete
186	f	77	yes	14	L ear	well	1.4		complete
187	f	77	yes	7	R upper chest	well	1.4		complete
188	m	76	yes	14	L cheek	well	1.4		complete
189	m	93	no	34	L scalp	poor	10		present at deep margin
190	m	94	no	14	L ear lobe	poor	5		complete
191	f	86	no	10	L ankle	well	2.5		complete
192	m	86	no	10	R chest	moderate	3.2	yes	complete
193	f	85	no	15	L lower leg	well	2.5		complete
194	m	87	no	11	R wrist	moderate	2.7		complete
195	f	86	no	18	L forearm	moderate	3.7		complete
196	f	79	yes	25	L lower leg	well	4		complete
197	m	76	no	25	scalp vertex	poor	5.6	yes	complete
198	m	72	no	10	L forehead	moderate	2.3		complete
199	f	90	no	12	upper L calf	moderate	1.3		complete
200	f	90	no	16	lower L calf	poor	2.5		complete

Appendix B Flow cytometry panels

Table 7.2 Flow cytometry panels used in this study.

Fluorophore	FITC	PE	PerCP Cy5.5	PE Cy7	APC	APC Cy7	BV421	Aqua
Laser	green	green	green	green	red	red	violet	violet
Excitation (nm)	488	488	488	488	633	633	405	405
Emission (nm)	519	575	690	785	668	760	421	526
Detector ± filter (nm)	530 ± 30	576 ± 26	695 ± 40	780 ± 60	660 ± 20	780 ± 30	450 ± 50	530 ± 30
Panel 1	CD4	CD25		CD8	FOXP3	CD3	CD127	Live/dead
Panel 2	CD25	OX40	CD4	CD8	FOXP3	CD3	CD127	Live/dead
Panel 3	CD4	4-1BB		CD8	FOXP3	CD3	OX40	Live/dead
Panel 4	CD4		Helios	CD8	FOXP3	CD3	OX40	Live/dead
Panel 5	CD4	CTLA-4	PD-1	CD8	FOXP3	CD3	OX40	Live/dead
Panel 6	CD4	CD45RO	PD-1	CD8	FOXP3	CD3	PD-L1	Live/dead
Panel 7	CD4	CD39	CD45RO	CD8	FOXP3	CD3	CLA	Live/dead
Panel 8	CD4	CD39	PD-1	CD8	FOXP3	CD3	CD73	Live/dead
Panel 9	CD4	CD39	CCR4	CD8	FOXP3	CD3	CLA	Live/dead
Panel 10	CCR4	CD39	CD4	CD8	FOXP3	CD3	CLA	Live/dead
Panel 11	CLA	CCR7	CD4	CD8	FOXP3	CD3	L-selectin	Live/dead
Panel 12	CD4	LAG-3	PD-1	CD8		CD3	PD-L1	Live/dead
Panel 13	CD4	Tim-3	PD-1	CD8	BTLA	CD3		Live/dead
Panel 14	CD4	CD160	PD-1	CD8		CD3		Live/dead
Panel 15	CD4	CD244	PD-1	CD8		CD3		Live/dead
Panel 16	CD4	TIGIT	PD-1	CD8		CD3		Live/dead
Panel 17	CD4	CD25	IFN-γ	CD127	FOXP3	CD3	OX40	Live/dead
Panel 18	CD4	IFN-γ	TNF-α	CD8	PD-1	CD3	IL-2	Live/dead
Panel 19	CD4	IFN-γ	CD45RO	CD8	PD-1	CD3	IL-2	Live/dead
Panel 20	CD4	IL-4	CD45RO	CD8	PD-1	CD3		Live/dead
Panel 21	CD4	IL-13	CD45RO	CD8	PD-1	CD3		Live/dead
Panel 22	CD4	IL-17	CD45RO	CD8	PD-1	CD3		Live/dead
Panel 23	Granzyme B	Perforin	CD4	CD8	PD-1	CD3	LAMP-1	Live/dead
Panel 24	NKG2D	γ δ TCR	CD45		CD19	Live/dead		

Fluorophore	FITC	PE	PerCP Cy5.5	PE Cy7	APC	APC Cy7	BV421	Aqua
Panel 25		CD15	CD45	CD16	CD11c	Live/dead		CD14
Panel 26	Fcε RI	2D7	CD45	CD203c	CD117	Live/dead		
Panel 27					CD56	CD3		Live/dead
Panel 28	CD68			CD11c	CD1a	CD14		Live/dead
Panel 29	DC-SIGN			CD11c	DC-LAMP	CD14		Live/dead
Panel 30	CD123	CD141		CD11c		CD14		Live/dead

Appendix C Supplementary figures

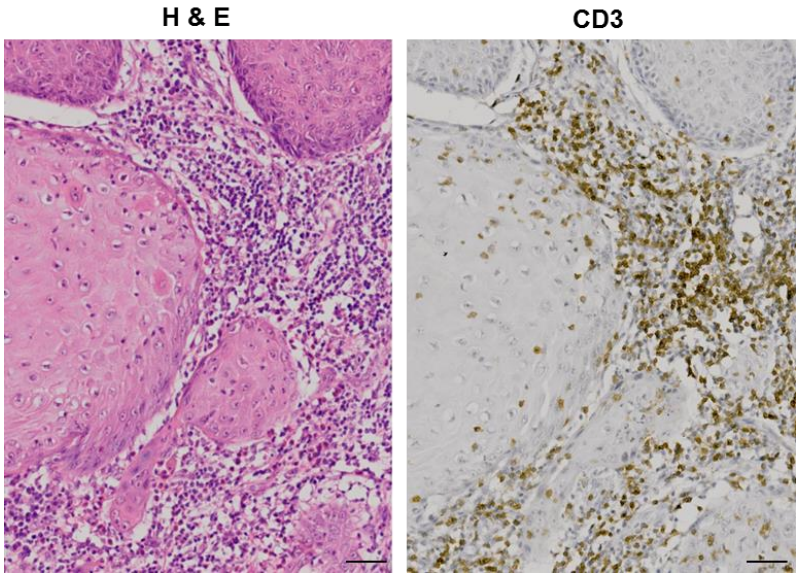

Figure 7.1 Predominant peritumoral location of T cells in cSCC.

Representative images of sequential cSCC sections showing H & E stain (left) and immunohistochemistry for $CD3^+$ T cells (right). Scale bars = 50 μm.

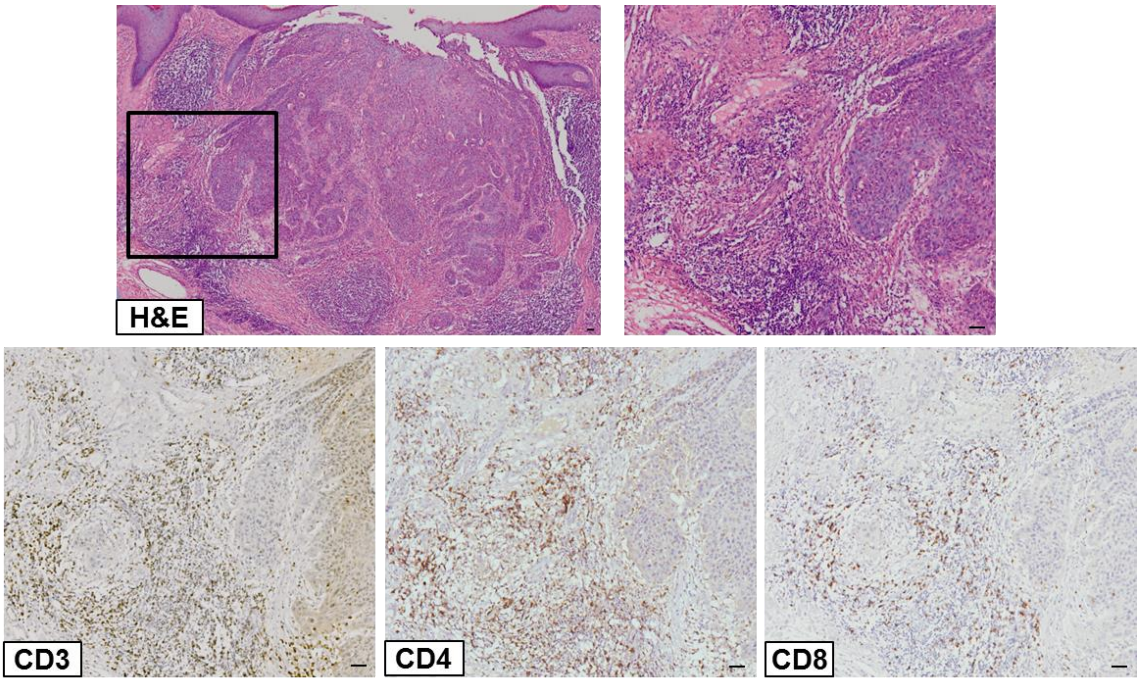

Figure 7.2 T cell subsets in the cSCC peritumoral infiltrate.

Representative H & E and CD3, CD4 and CD8 immunostains in sequential cSCC sections. Scale bars = 50 μm.

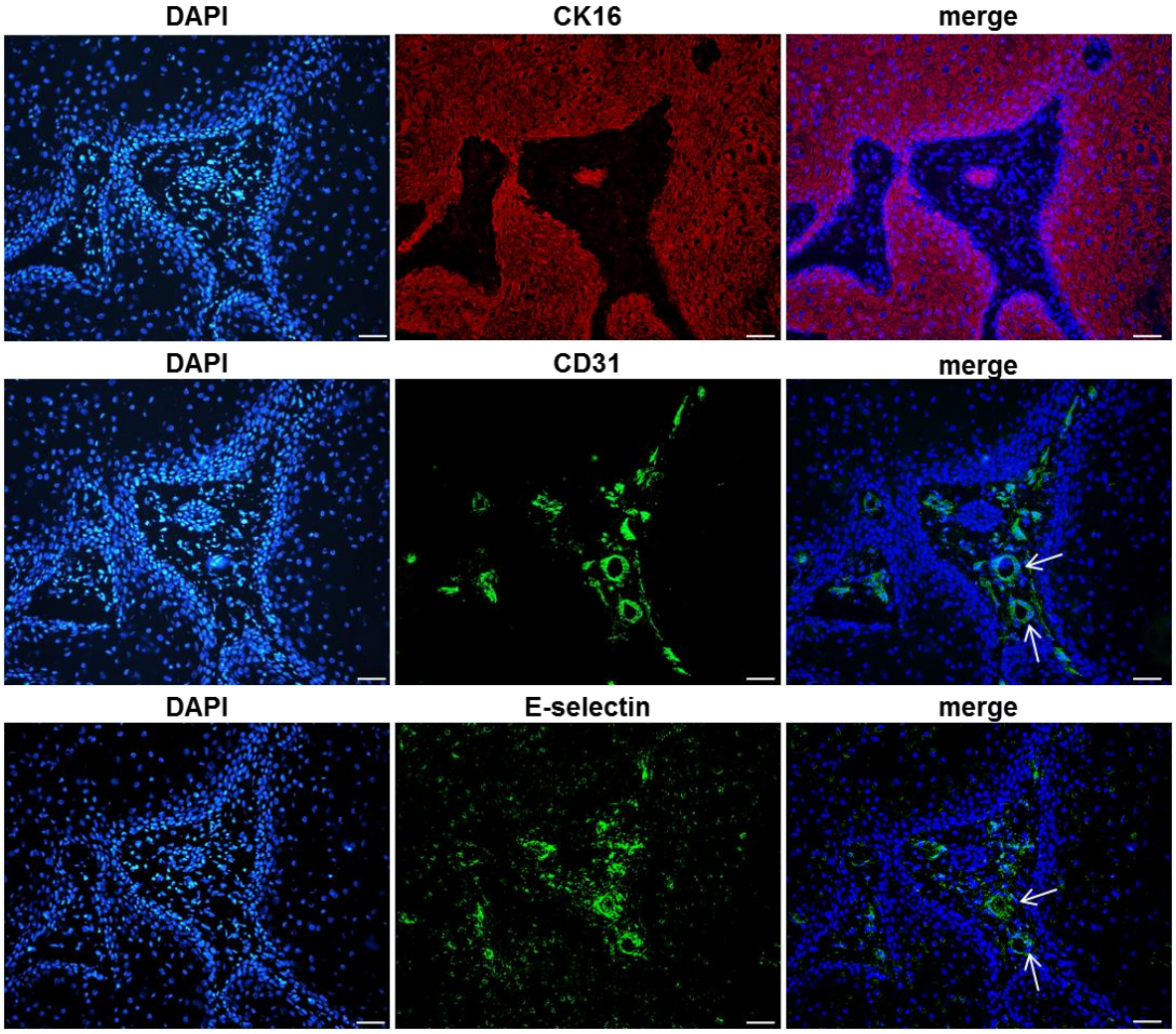

Figure 7.3 cSCC blood vessels express E-selectin.

Immunofluorescence microscopy of sequential cSCC sections demonstrating $CD31^+$ blood vessels expressing e-selectin in peritumoral/stromal areas of cSCC. Arrows denote the same vascular structures on sequential sections, images representative of 5 cSCCs, scale bars = 50 μm.